Technical Report CHL-99-20
October 1999

US Army Corps of Engineers
Engineer Research and Development Center

Los Angeles and Long Beach Harbors Model Enhancement Program: Long Waves and Harbor Resonance Analysis

by William C. Seabergh, Leonette J. Thomas

Prepared for U.S. Army Engineer District, Los Angeles
Port of Los Angeles
and Port of Long Beach

Technical Report CHL-99-20
October 1999

Los Angeles and Long Beach Harbors Model Enhancement Program: Long Waves and Harbor Resonance Analysis

by William C. Seabergh, Leonette J. Thomas

U.S. Army Engineer Research and Development Center
Waterways Experiment Station
3909 Halls Ferry Road
Vicksburg, MS 39180-6199

Final report

Approved for public release; distribution is unlimited

Prepared for U.S. Army Engineer District, Los Angeles
Los Angeles, CA 90053-2325

Port of Los Angeles
San Pedro, CA 90733-0151

Port of Long Beach
Long Beach, CA 90801-0570

Engineer Research and Development Center Cataloging-in-Publication Data

Seabergh, William C.
Los Angeles and Long Beach Harbors Model Enhancement Program : long waves and harbor resonance analysis / by William C. Seabergh, Leonette J. Thomas ; prepared for U.S. Army Engineer District, Los Angeles, Port of Los Angeles, Port of Long Beach.
131 p. : ill. ; 28 cm. — (Technical report ; CHL-99-20)
Includes bibliographic references.
1. Water waves — California — Mathematical models. 2. Long Beach Harbor (Calif.) 3. Los Angeles Harbor (Calif.) I. Thomas, Leonette J. II. United States. Army. Corps of Engineers. Los Angeles District. III. U.S. Army Engineer Research and Development Center. IV. Coastal and Hydraulics Laboratory (U.S.) V. Port of Los Angeles. VI. Port of Long Beach. VII. Title. VIII. Title: Long waves and harbor resonance analysis. IX. Series: Technical report CHL ; 99-20.
TA7 W34 no.CHL-99-20

Contents

List of Figures

Preface

This report was prepared by the U.S. Army Engineer Research and Development Center (ERDC) Coastal and Hydraulics Laboratory (CHL) and is a product of the Los Angeles and Long Beach Harbors Model Enhancement (HME) Program. The HME Program was conducted jointly by the Ports of Los Angeles and Long Beach (LA/LB); the U.S. Army Engineer District, Los Angeles; and ERDC. The purpose of the HME Program has been to provide state-of-the-art engineering tools to aid in port development. In response to the expansion of oceanborne world commerce, the Ports of LA/LB are conducting planning studies for harbor development in coordination with the Los Angeles District. Ports are a natural resource, and enhanced port capacity is vital to the Nation's economic well-being. In a feasibility study being conducted by the Los Angeles District, the Ports of LA/LB are proposing a well-defined and necessary expansion to accommodate predicted needs in the near future. The Corps of Engineers will be charged with responsibility for providing deeper channels and determining effects of this construction on the local environment. This includes changes in harbor resonance caused by expansion and channel deepening.

This investigation was conducted during the period June 1987 through September 1991 by personnel of the Wave Processes Branch (WPB), now the Harbors and Entrances Branch (HEB), Wave Dynamics Division, now Navigation and Harbors Division (NHD). WPB personnel involved in the study were Mr. William C. Seabergh and Ms. Leonette J. Thomas under the direct supervision of Mr. Douglas Outlaw, former Chief, WPB, and Mr. Dennis G. Markle, current Chief, HEB, and Mr. C. E. Chatham, Chief, NHD. Mr. Seabergh and Ms. Thomas prepared the report. Ms. Debbie Fulcher, NHD, and Ms. Debra Katzenmeyer, formerly WPB, assisted in preparation of the final report. Messrs. Jay Rosati, Pat McKinney, and Sam Corson, Prototype and Measurement Analysis Branch, Coastal Sedimentation and Engineering Division, provided prototype data. Overall CHL management of the HME Program was furnished by Messrs. Outlaw and Seabergh, and this study was conducted under the general supervision of Dr. James R. Houston, Director, CHL, and Mr. Charles C. Calhoun, Jr. (retired), Assistant Director, CHL.

During the course of the study, significant liaison was maintained between ERDC, the Los Angeles District, and the Ports. Mr. Dan Muslin, followed by Mr. Angel P. Fuertes, Mr. Mike Piszker, and then Ms. Jane Grandon, were Los Angeles District points of contact. Mr. John Warwar, Mr. Dick Wittkop, and Ms. Lillian Kawasaki, Port of Los Angeles, and Mr. Michael Burke, followed by Mr. Angel Fuertes and Dr. Geraldine Knatz, Port of Long Beach, were Ports of LA/LB points of contact and provided invaluable assistance.

At the time of publication of this report, Dr. Lewis E. Link was Acting Director of ERDC, and COL Robin R. Cababa, EN, was Commander.

Conversion Factors, Non-SI to SI Units Of Measurement

Non-SI units of measurement used in this report can be converted to SI units as follows:

Multiply	By	To Obtain
acres	4,046.873	square meters
fathoms	1.828	meters
feet	0.3048	meters
inches	2.54	centimeters
square feet	0.09290304	square meters

1 Introduction

Background and Purpose of Study

New channel and basin configurations and depths will be designed for Los Angeles and Long Beach harbors (Figures 1, 2, and 3) because of harbor expansion and the effect on harbor resonance for both existing berths, and new berth locations must be determined. Long-period waves (25 to 400 sec and greater) constantly invade the harbors and can create resonant oscillations that may cause ship-mooring and/or ship-loading/unloading problems. In order to provide greater understanding of the harbors' and ships' response to these wave conditions, this study examined, in some detail, the analyzed long-period prototype wave data acquired by the

Figure 1. Photograph of Los Angeles and Long Beach harbors, 1992

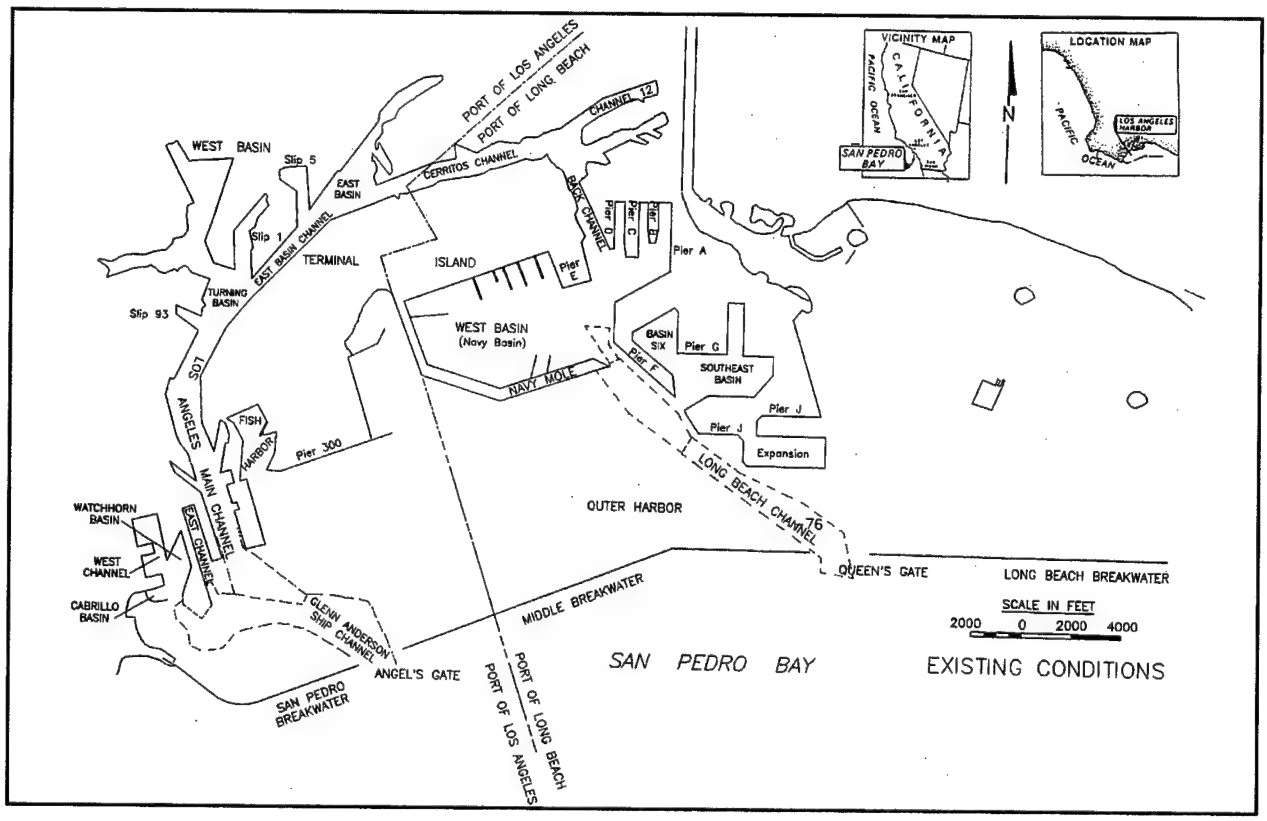

Figure 2. Los Angeles and Long Beach harbors layout

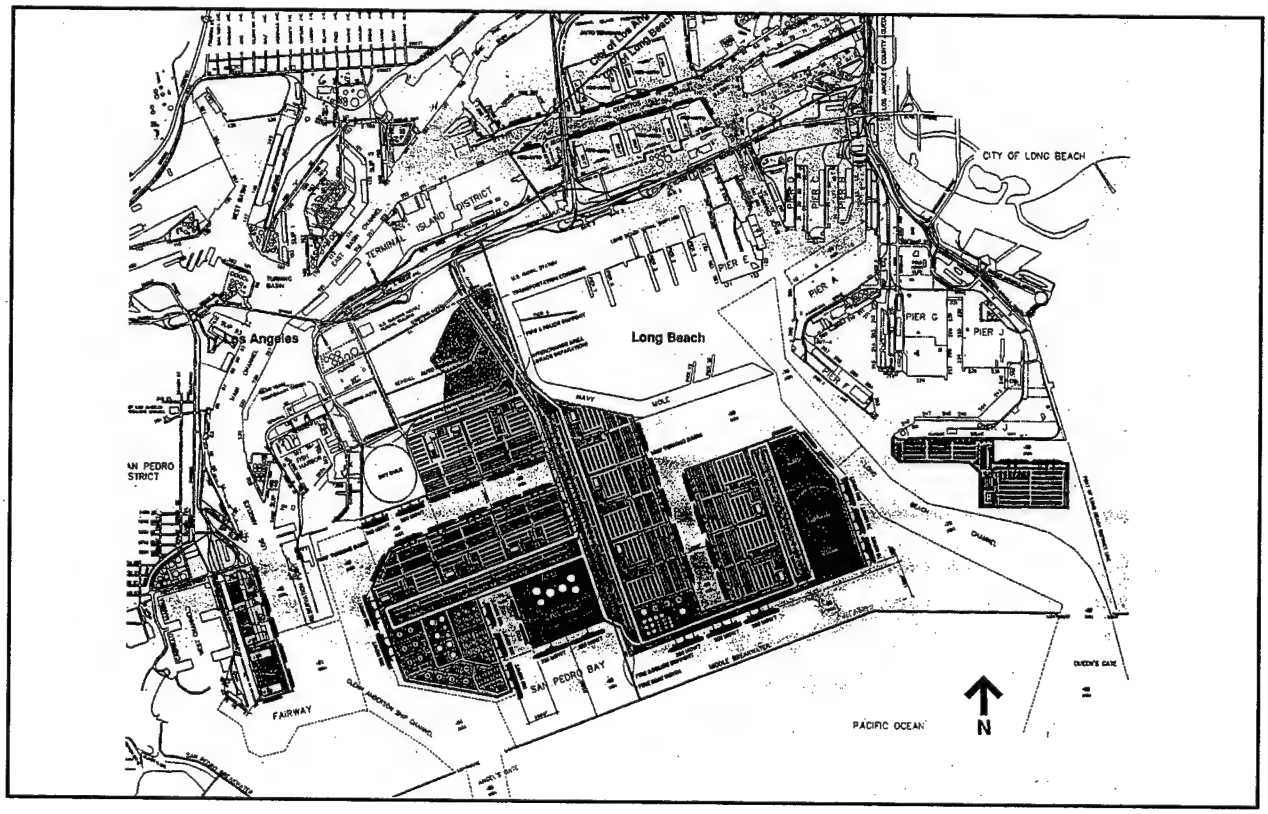

Figure 3. Example of a Los Angeles-Long Beach harbors potential plan - OFI Scheme B

Coastal Engineering Research Center in Los Angeles and Long Beach harbors. The data are presented in a Harbors Model Enhancement Program report by Rosati, McKinney, and Puckette (1998).

A physical model of Los Angeles and Long Beach harbors was constructed at the U.S. Army Engineer Research and Development Center (ERDC) in 1973. This 1:400 horizontal, 1:100 vertical scale model was designed to reproduce tides and waves. Since 1973, the model has been used to examine the effects of harbor expansion projects on tidal currents and harbor resonance. More recently, it has been used exclusively for performing harbor resonance tests with simulation of long-period waves. In the past, these tests have involved the construction of proposed projects in the model and subjecting them to a series of over 200 monochromatic wave tests, with wave periods ranging from 30 to 400 sec. Wave data are usually collected at 50 or more locations throughout the harbors at existing and proposed berths (see Seabergh (1985) for example). Using prototype long-period wave data collected offshore of the harbors, it was possible to develop long-period wave spectra that could be input to the computer-controlled model wave generators (Seabergh and Thomas 1993). This approach permits the simultaneous reproduction of a broad range of frequencies (periods) during a single test. These results can be used to pinpoint troublesome wave-period ranges, which create harbor surge conditions that may lead to difficult loading/unloading conditions and possible ship damage. These harbor amplifications may then be related to ocean statistics for long-wave-period waves to provide information on energy levels to be expected at a particular berth. This information may then be used in conjunction with a moored-ship motion model to determine if troublesome conditions exist so that changes to the plan and/or mooring arrangements can be made to minimize problem conditions.

Model Enhancement Program

The Ports of Los Angeles and Long Beach are conducting planning studies for harbor development in coordination with the U.S. Army Engineer District, Los Angeles. The Ports, in order to meet the forecast demand for berthing space resulting from increased Pacific Rim trade, will need deeper and wider channels and up to 2,400 acres of new landfill. Figure 1 shows a photograph of the existing harbor configuration (1992); Figure 2 identifies the various basins; and Figure 3 shows an example of a proposed plan. The Los Angeles District has determined that there is a Federal interest in construction and maintenance of new navigation channels to meet projected cargo growth. In order to provide up-to-date modeling technology to help design the proposed plans, the Los Angeles-Long Beach Harbors Model Enhancement (HME) Program was developed. Major elements of the program included three-dimensional numerical modeling of tidal circulation and water quality, a numerical moored-ship motion model, and work to model long-period spectral waves in the physical model. In conjunction with the modeling efforts, field data were collected and included tidal

velocities and elevation, water quality data, winds, moored-ship movements and mooring forces, and long-period wave data. This report presents an examination of some of the long-period wave data collected.

The HME Program was separated into two major parts. Part A was concerned with harbor resonance and moored-ship motion resulting from the action of short- and long-period waves (under 25-sec and over 25-sec period, respectively). Very little was known about the origin and frequency of occurrence of the long-period waves, but their existence was evident in difficult loading and unloading conditions occasionally encountered at various berths in the harbors. This part of the program provided prototype wave data, a moored-ship motion model, and an upgraded testing capability for the physical model.

Part B of the HME Program provided improved tidal-circulation modeling capability with a more advanced and efficient numerical tidal-circulation model system that coupled a three-dimensional hydrodynamic model to a water quality model.

The HME Program areas concerned with harbor resonance were as follows:

Task A.1 Wave-Data Acquisition

This task consisted of making long-term measurements of harbor long-period wave (surge) events and the forcing functions external to the harbor that generate those events.

Task A.2 Wave-Data Analysis

This task consisted of completing work on the software needed to reduce, analyze, and check the quality of measurements made by the automated surge measurement system, then performing these tasks and associated activities for the period of surge data collection. Monthly data reports were compiled, distributed, and then summarized (Rosati, McKinney, and Puckette 1998).

Task A.3 Harbors Resonance Analysis

This is the task area described in this report.

Task A.4 Ship-Motion Data Acquisition and Analysis

This task consisted of the development and application of a system to measure vessel motion and mooring-line forces during harbor surge events at the Ports and the reduction and summarization of data collected by the

system (McGehee 1991). Measurements allowed determination of vessel motion in each of six degrees of freedom (surge, sway, heave, pitch, yaw, and roll) and mooring loads in up to eight mooring lines simultaneously. Data collection took place over a 4-month period during the time of highest probability of harbor-surge events. Depending upon vessel availability, ship-motion data acquisition and analysis were performed at berthing locations at each port and included dry bulk and container ships.

Task A.5 Ship-Motion Model Development, Calibration, and Verification

A ship-motion model was developed to provide a method to evaluate the recurrence interval for adverse moored-ship motion. The moored-ship response model considered all six degrees of freedom of the vessel. The resonant interaction between the ship, mooring system, and frequency of oscillation is modeled incorporating both sidewall effects and shallow-depth effect. The model was calibrated and verified initially using observed data from a container ship harbor in Iceland. After initial verification with this data set, ship-model calibration and verification were completed using data from Task A.4 (Sargent, in preparation). The model may now be used for analysis of mooring conditions at any harbor berthing facility and for commercial ship types projected to use the harbors.

Task A.6 Improved Physical Model Harbor Resonance Methodology

This task examined the transfer of measured prototype long-period wave spectra to physical model testing of harbor resonance. Previously, monochromatic waves were used for testing, and 200 individual tests were performed. Spectral testing can aid in reducing the number of tests required to be performed in the physical model because of the reproduction of all frequencies in the 25- to 400-sec period range. Spectra were selected from two storms that had significant impact on the San Pedro Bay region. The storms of 2 February 1986 and the Martin Luther King Day storm of 17 January 1988 were selected for model testing. A third spectrum selected represented more typical conditions (Seabergh and Thomas 1993).

2 Terminology and Los Angeles and Long Beach Harbors Previous Studies

Description

The Los Angeles and Long Beach harbors have evolved since development started in the 1870s by a sequence of landfills, which includes a variety of sizes and shapes of basins as shown in Figure 1 and some of which are identified in Figure 2. This in turn permits a wide variety of possible resonant wave conditions (defined below). Also, the intertwining nature of the harbors permits intrabasin interaction with regard to long-period waves as they are reflected and diffracted within the harbors. Future plans call for the addition of new channels and landfills as shown in a possible design presented in Figure 3.

Definition of Terms

Waves with periods longer than short wind waves (wind waves typically include wave periods from 3 to 25 sec) are called long waves. This term derives from the "long" wavelength water waves can have with periods greater than 25 sec and typically extends through tidal waves, which have major constituents with periods of about 12 hr. For the purposes of this report, long waves in the period range of 25–500 sec will be examined because of the association of problems of moored ships with this period range and also since wavelengths of shallow-water waves in this period range are of the magnitude of slip sizes in a major port such as Los Angeles and Long Beach harbors. This "fitting" of wavelength in a slip or berth can lead to resonant conditions (also called seiching) in a basin, which will mean an amplification of wave height in the basin. In recent years, waves with periods in the 25- to 500-sec range have been called infragravity waves. They may also be referred to as low-frequency waves. Another reason for the 25- to 500-sec period range as a subset of long waves relates to

wave-generating mechanisms for this range, which appear to be distinct from that for other period ranges. This will be discussed later.

Waves are typically thought of in terms of height, but another manner of measurement is energy, which derives from the analysis techniques that are used to extract information from measurements that typically are of a complex variation of the water surface. Usually, wave fields are made up of many different waves that have many periods and heights that are superimposed on each other. Long-period waves are difficult to measure directly because of their combined presence with regular wind waves that are much larger. A technique typically used is spectral analysis, which determines how much energy is in a certain range of wave periods. If all the individual energy period "bands" are added together, a total energy is determined and can be related to wave height by the relationship:

$$H = 4\sqrt{E} \tag{1}$$

where

H = wave height

E = total energy contained in the period range of interest

Harbor resonance is caused by reflection of an incoming wave off a boundary such as a wooden or concrete bulkhead or a sloped rock revetment. The adding together (or superposition) of the incoming (or incident) wave and the reflected wave leads to formation of a standing wave, where the adding together of water-particle velocities will have both canceling effects and reinforcing effects. This creates a wave system that has nodes (fixed locations where there is no vertical movement but strong horizontal velocity) and antinodes (where there is no horizontal movement of the water particle but strong vertical movement, see Figure 4). Note that there is an antinode at the reflecting wall, and the location of the node is dependent on wavelength, which in turn can be dependent on water depth. If the length of the wave "fits" the basin, or some integral number of waves, or fraction of wavelength, which positions a node at the basin entrance, the possibility of resonance occurs if there is not sufficient frictional effects to dampen out energy. This effect is strengthened as waves become longer and lower and they tend not to break and lose energy as shorter steep waves will. Long waves (periods greater than 25 sec) are typically less than 15 cm high and have wavelengths greater than 300 m. Even-sloped revetments will fully reflect a long wave. The analogy of a mechanical mass-spring system is frequently used to explain the resonance phenomenon (Wilson 1972). In a more obvious analogy, the forced sloshing of a tub of water at a certain frequency that causes the water to overtop the edge is a resonant wave condition.

The phenomenon of harbor resonance produces strong horizontal currents. A ship-mooring system has its own resonant frequencies, dependent on mooring-line configuration, type of lines, and ship characteristics.

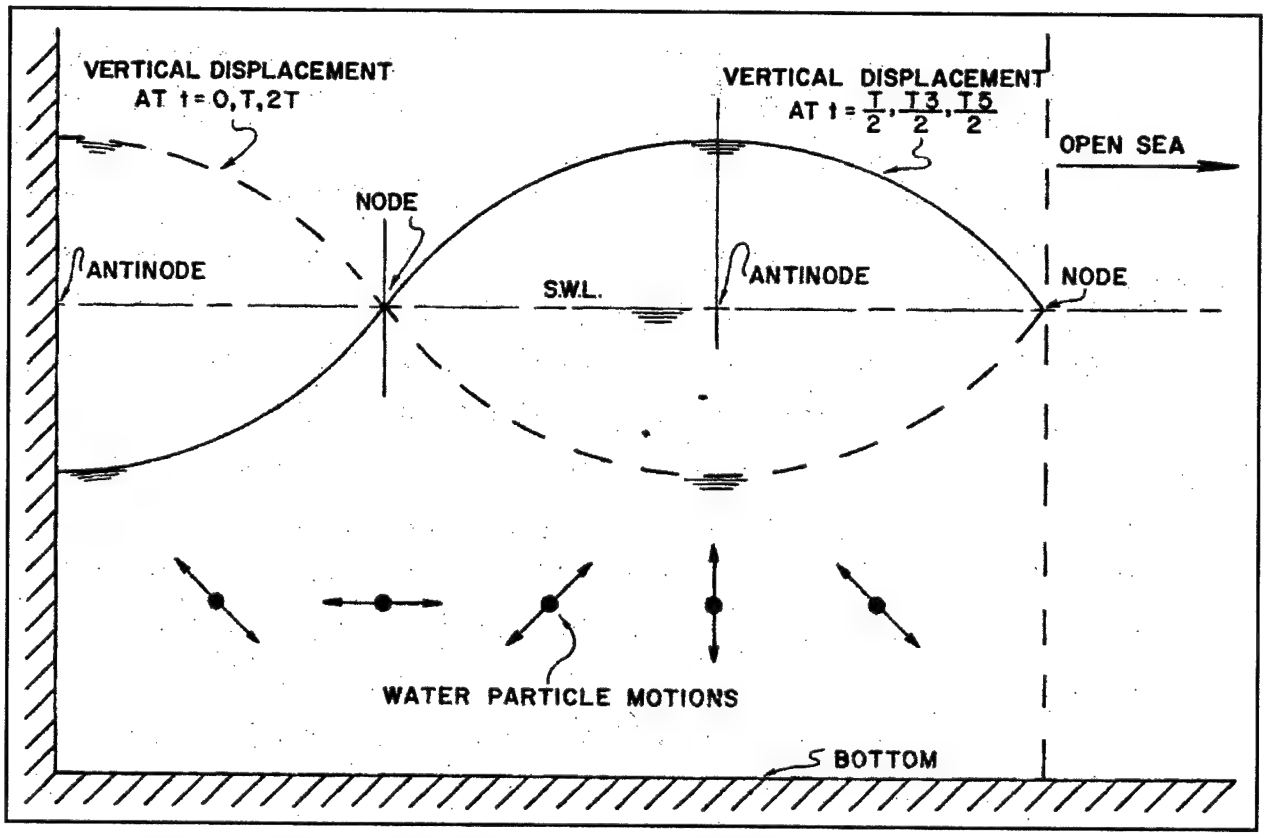

Figure 4. Node, antinode, and water-particle motions in a rectangular channel open to the sea with a node at the channel entrance

Moored ships can move in six ways or have "six degrees of freedom." Figure 5 shows the axes along which movement translates or rotates. The terms in Figure 5 are defined as follows:

a. **Surge** indicates a fore and aft movement parallel to the wharf.

b. **Sway** is a transverse or sideways movement perpendicular to the wharf.

c. **Heave** is a vertical or up and down movement.

d. **Roll** is a rolling or rotational displacement about the ship's longitudinal axis.

e. **Yaw** is a rotational displacement about the vertical axis through the ship's center of gravity (CG). Sometimes it is called "fishtail," when other motions combine to create a "figure eight" movement.

f. **Pitch** is a rotational displacement about a horizontal axis through the CG, perpendicular to the ship's longitudinal axis.

Surge is usually the most significant motion with regard to long waves and creation of large tension values in mooring lines. Roll can be troublesome, especially with regard to loading/unloading containerships, but is

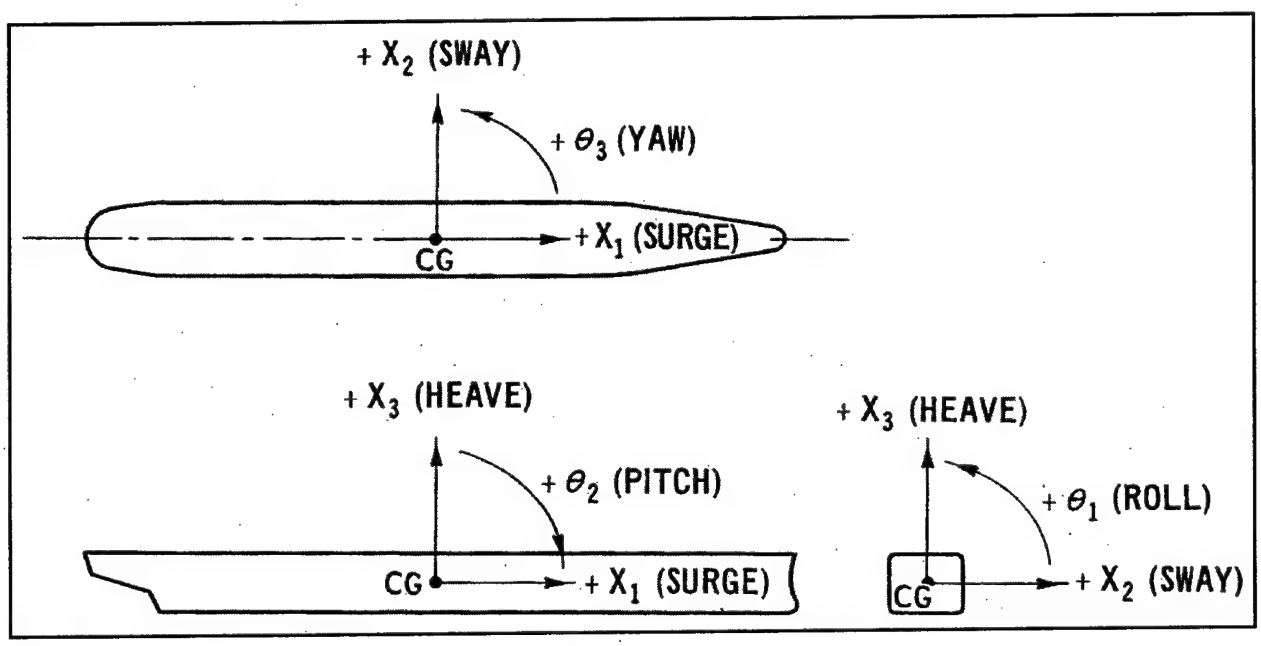

Figure 5. Coordinate system for motion of a ship

usually associated with short-period waves. Sway can also be a significant factor if there is cross-basin oscillation that causes movement perpendicular to the long axis of the ship.

Historical Information

Wilson et al. (1968) provide a thorough background on previous work performed in understanding harbor resonance in the Los Angeles and Long Beach harbors up to 1968, and some of the following is drawn from this source.

Mention of problems because of long waves in Los Angeles and Long Beach harbors appeared in correspondence to the Corps of Engineers in 1913 (McKinstry 1914). The letters described surge of 15 to 18 ft along the wharf and sway of as much as 8 to 12 ft on and off the wharf occurring every 2 min or so for a harbor configuration with only a very limited development compared with today's harbor. Science Engineering Associates (July 1968) presented a review of work concerning long waves in Los Angeles and Long Beach harbors up to 1968. A letter in the just-mentioned reference by D. E. Hughes, U.S. Army Corps of Engineers, San Pedro, CA, dated October 11, 1922, gave perhaps the earliest useful description of the long-wave phenomenon:

> Some associate surge with high tide, others with low, but long and varied observation indicates no connection between surge and tide; nor yet between surge and local storms, for only occasionally do vessels fool surge at San

> Pedro outer harbor wharves when the sea is rough just outside the breakwater.
>
> The present opinion, shared by many, is that the surge is caused by low waves or undulations of great length, which in turn are due to coalescence of short waves from far distant storms. The effective feature is the great length with resultant long period of duration, whereby a head is created and sustained which causes flow into areas which may not be in the direct path of the wave itself.

Though analysis later in the report may not entirely agree with all of the above, the association of surge and wind waves was an important observation in light of more recent studies that will be discussed in the next chapter.

The U.S. Coast and Geological Survey performed a detailed tide and current survey throughout the harbors in 1936 in which water-surface oscillations were quantified. Dependent on location, they identified the occurrence of oscillations with periods from 1 to 60 min, which could be divided into two groups of between 1 to 10 min and 30 to 60 min, with the 60-min period the predominant period for the second group. These longer period waves (30-60 min) had no effect on moored ships, while the shorter period range did.

In the early 1970s, prototype ship motion and wave data were collected in the harbors during a 1-year data acquisition program (Durham et al. 1976). Long-period wave energy was measured at 14 locations. A parameterized numerical study of wave-induced motion of berthed ships in Los Angeles East Channel indicated the 25- to 600-sec period range created the maximum response to surge.

As noted from the above, long waves in the 25- to 600-sec period range have been responsible for moored-ship motion in the harbors. Calculating wavelengths for 25- to 600-sec waves in depths of 10 to 40 m gives a range of wavelengths from 250 to over 10,000 m, indicating that waves "fit" existing basins within the harbors. With the large range of wavelengths that may interact with a large range of basin sizes, one might expect the possibility of achieving resonant wave conditions at many locations in the harbors. The existence of wave resonance can mean that amplification of offshore energy may occur within harbor basins. A preliminary remark, which will be discussed in detail later, is that typically, there is long-period wave energy in the ocean that covers the full-period range of long waves that may cause moored-ship motion. The next chapter will examine the generation and sources of these long waves.

3 Long Waves and the Local Wind Wave Climate

Introduction

Various investigators have reported an association of long-period wave energy with local short-period wave energy. A source of long-period wave phenomena discussed by Longuet-Higgins and Stewart (1964) describes it in terms of wind wave groups and the resulting setup and setdown. Under a group of high wind waves, the average sea surface is lower. Under the following lower waves, the average sea surface is higher. This is due to a "Bernoulli equation" effect, where, considering conservation of energy, under regions of high waves, the velocity field is high, so pressure or water level is low. Under low waves or low velocities, pressure or water elevation is higher. Thus, the trough and crest of a "bound" long wave are formed. The "bound long wave" refers to the connection of the long wave to the short-wave envelope as seen in Figure 6. The bound wave is released as a "free" wave when short waves break or meet some discontinuity, such as abrupt change in bathymetry or a breakwater. The free long waves that are created at the shoreline (and/or incident on the shoreline) may then be reflected out to sea. These reflected long waves can be trapped by the longshore contours (where they are refracted back into shore) or reflected back out to sea dependent on their angle of approach and their wave period. The possible origin of this wave-grouping phenomenon is explained by

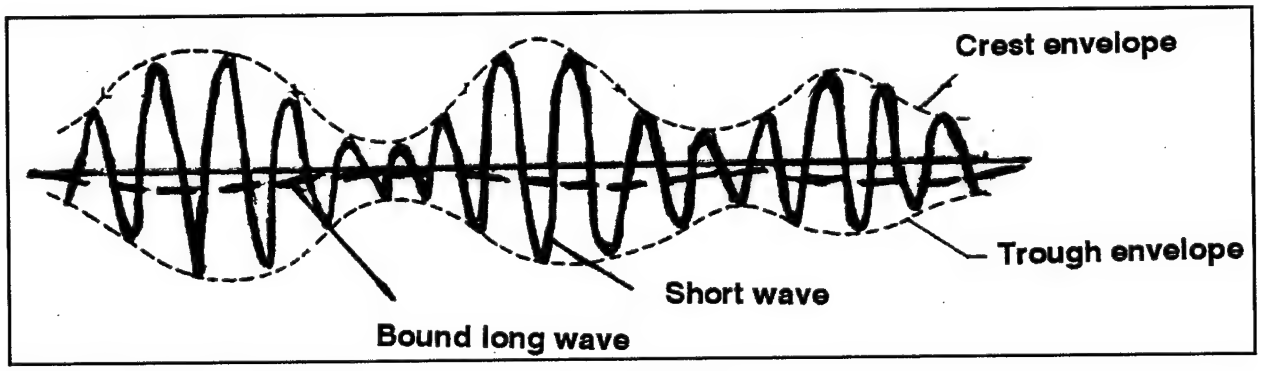

Figure 6. Relation of short-wave system and bound long wave

Benjamin and Feir (1967), who say that long-period sidebands could be generated because of wave instability, which creates an amplitude modulation of the wave train. Others have explained nonlinear couplings of short-wave spectral components that result in energy transfer from short- to long-wave frequencies (Hasselmann 1962). Okihiro, Guza, and Seymour (1993) found the energy transfer to long waves dependent on water depth and directional spread of energy. Energy transfer is stronger in shallow water and for narrow directional spread.

Because of the apparent association of long waves with short waves, a discussion of the origination of short waves approaching the southern California shoreline is presented to define the probable basic origins of long-wave energy that enters the harbors. There are other possible mechanisms for the creation of long waves (discussed later).

General Wind Wave Climate

Wind waves approaching the Los Angeles-Long Beach harbors can be generated by local winds or from distant storms. Locally generated waves are called "sea" and have steep slopes, short crests, and sharp peaks with much variation in direction, wavelength, and height. Waves from distant storms are usually called swell and, in their area of generation, were "sea"; but after they leave the generating area, they become more sinusoidal, with more uniform direction and period. Hubertz, Payne, and Farrar (1995) describe the principal sources of swell in the North Pacific as developing from the following:

a. Extratropical storms in the central North Pacific.

b. Trade winds.

c. Tropical storms, referred to as typhoons west of the international dateline, and hurricanes east of it.

d. Extratropical storms in the Southern Ocean.

Of the above, only the trade winds do not affect the southern California coast, since these winds always blow from east to west.

The North Pacific extratropical storms move from west to east and because of long fetches can create large waves. The offshore islands and the southern exposure of the harbors provide some reducing effect on swell from this source (see Figure 7). Most swell during the Northern Hemisphere winter comes from this source. Examination of "Southern California Hindcast Wave Information" (Jensen et al. 1992) Station 14, located just south of the harbors (33.67N, 118.12W), indicates that for hindcasting over a 20-year period, mean wave height is 0.9 m with mean period of 10.1 sec for waves from the west. The statistics for waves from 270 deg (which represents 90 percent of waves hindcast at sta 14) are shown in Figure 8.

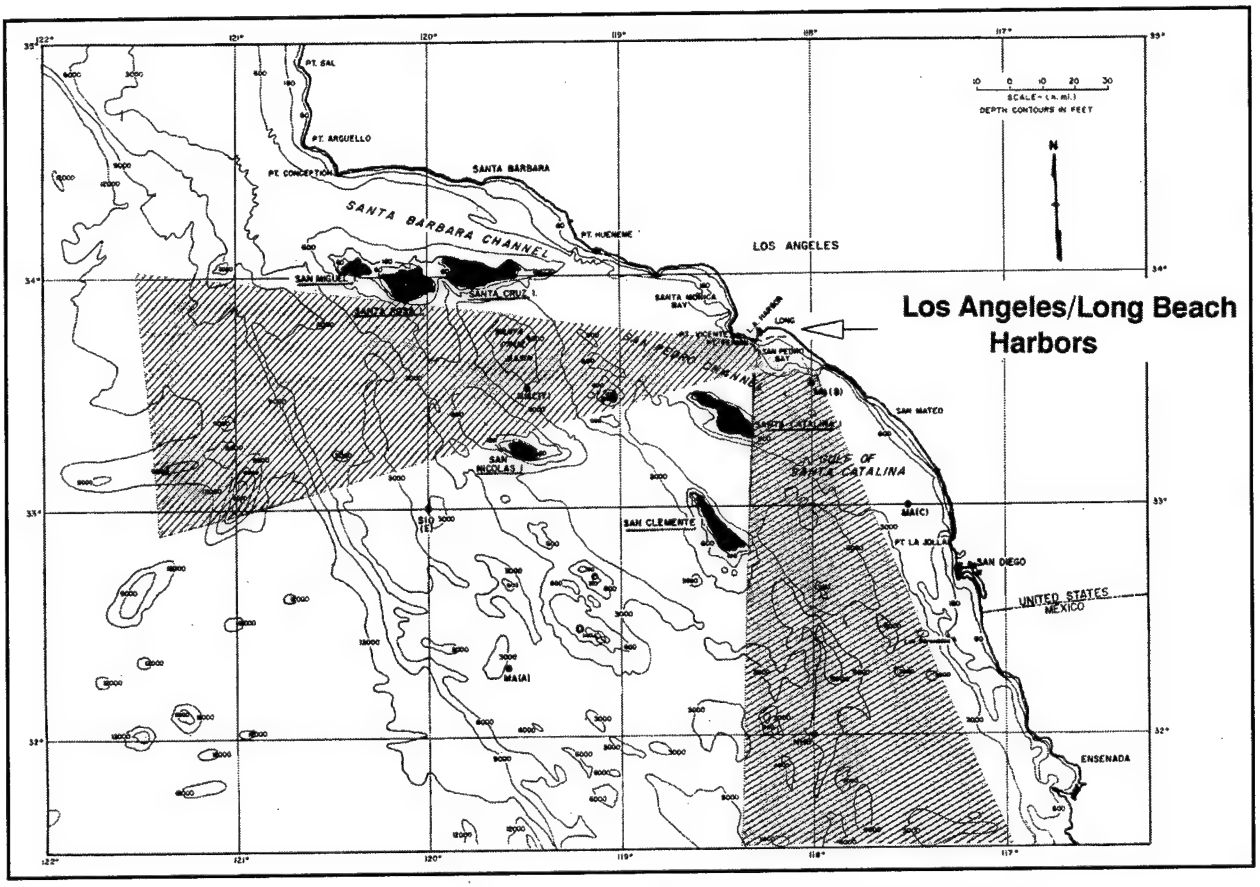

Figure 7. Offshore islands and wave windows for Los Angeles and Long Beach harbors

The Pacific tropical storms generally move from east to west off the Mexican coast, though they can turn northward, but rarely move as far as southern California. They can send strong southern swell to the vicinity of the harbors during late summer and early autumn (Tracey and Hubertz 1990) because of the strong rotation of their wind field. For 10 hurricanes that traveled north of 24 deg N latitude, for a station adjacent to the harbors, Tracey and Hubertz (1990) hindcast that average significant wave height for swell was between 0.4 and 2.4 m; maximum significant wave height was between 0.4 and 3.2 m, and wave period associated with maximum height was between 9.1 and 12.5 sec.

The Southern Ocean, which surrounds Antarctica and circles the earth there, has winds primarily from the west with frequent gale-force magnitude. Because of long fetches in conjunction with the travel of waves along great circle paths, waves propagating to the northeast from south of Australia and New Zealand can reach the North Pacific and, in particular, the southern California coastline (Hubertz, Payne, and Farrar 1995). The strongest systems occur during the Southern Hemisphere winter, which is the Northern Hemisphere's summer. Measured southern swell for 1988-89 at National Oceanic and Atmospheric Administration Buoy 46042 (36.8N, 122.4W) varied from 0.1 to 1.1 m significant wave height, and wave period varied from 12.5 to 22.5 sec. Directions at the buoy because of the

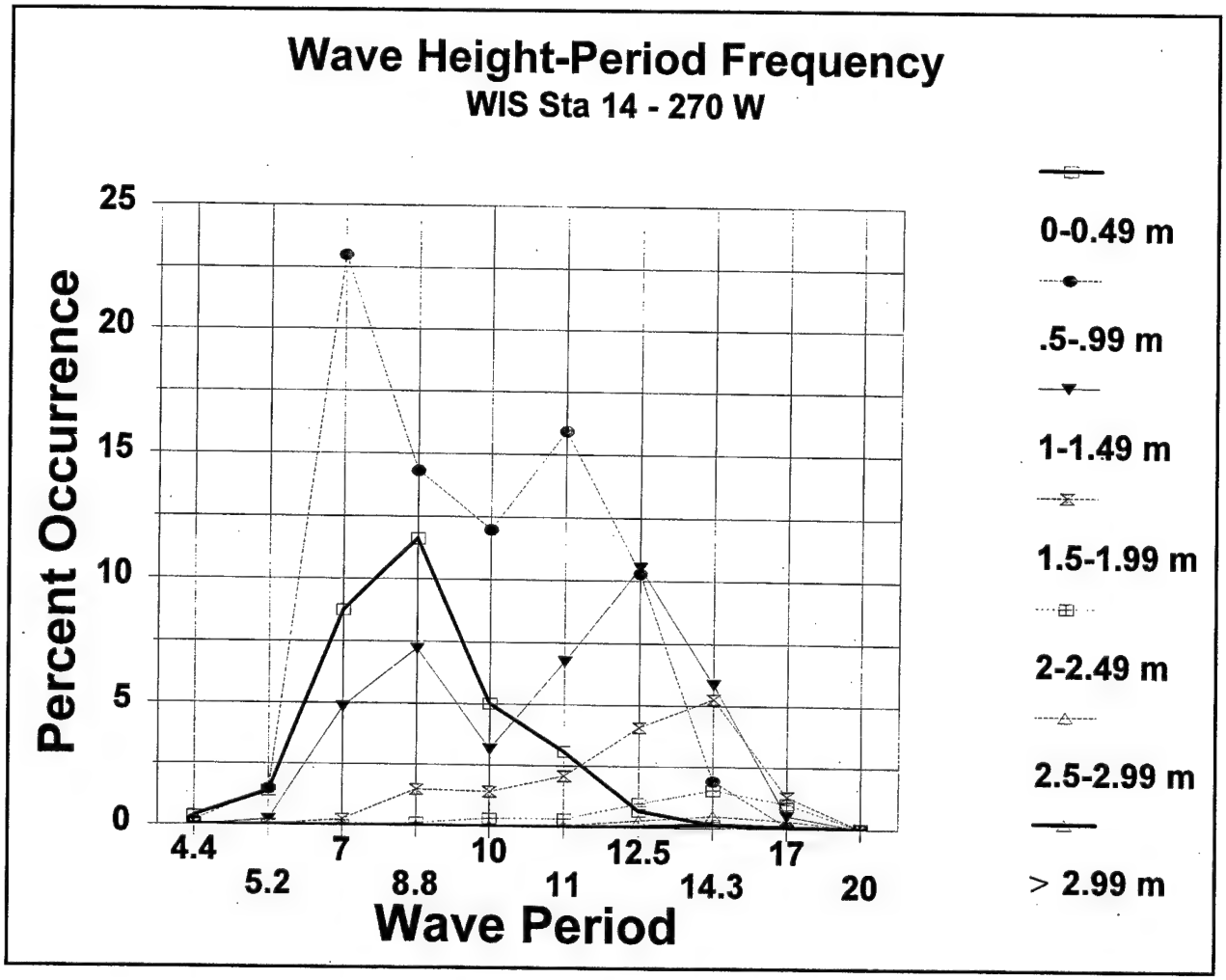

Figure 8. Wave height-period frequency for waves from 270 deg west, WIS sta 14

Southern Hemisphere swell were from 150-220 deg centered at 180 deg (Hubertz, Payne, and Farrar 1995).

A directional wave gauge was installed on Chevron Oil Platform Edith in 1984 (see Figure 9 for location; water depth was about 50 m; gauge depth was 10 m). Summary direction and height information are shown on wave roses for April-September and October-March time periods over 6 years (Figure 10). The dominance of waves from the west window in the fall-winter and waves from the south window in the spring-summer are noted.

In summary, the harbors' local wave climate is affected by swell from both tropical hurricanes and the Southern Hemisphere in the June-September period. These waves approach the harbors from the southern window. Winter storms in the Northern Pacific generally approach through the western window.

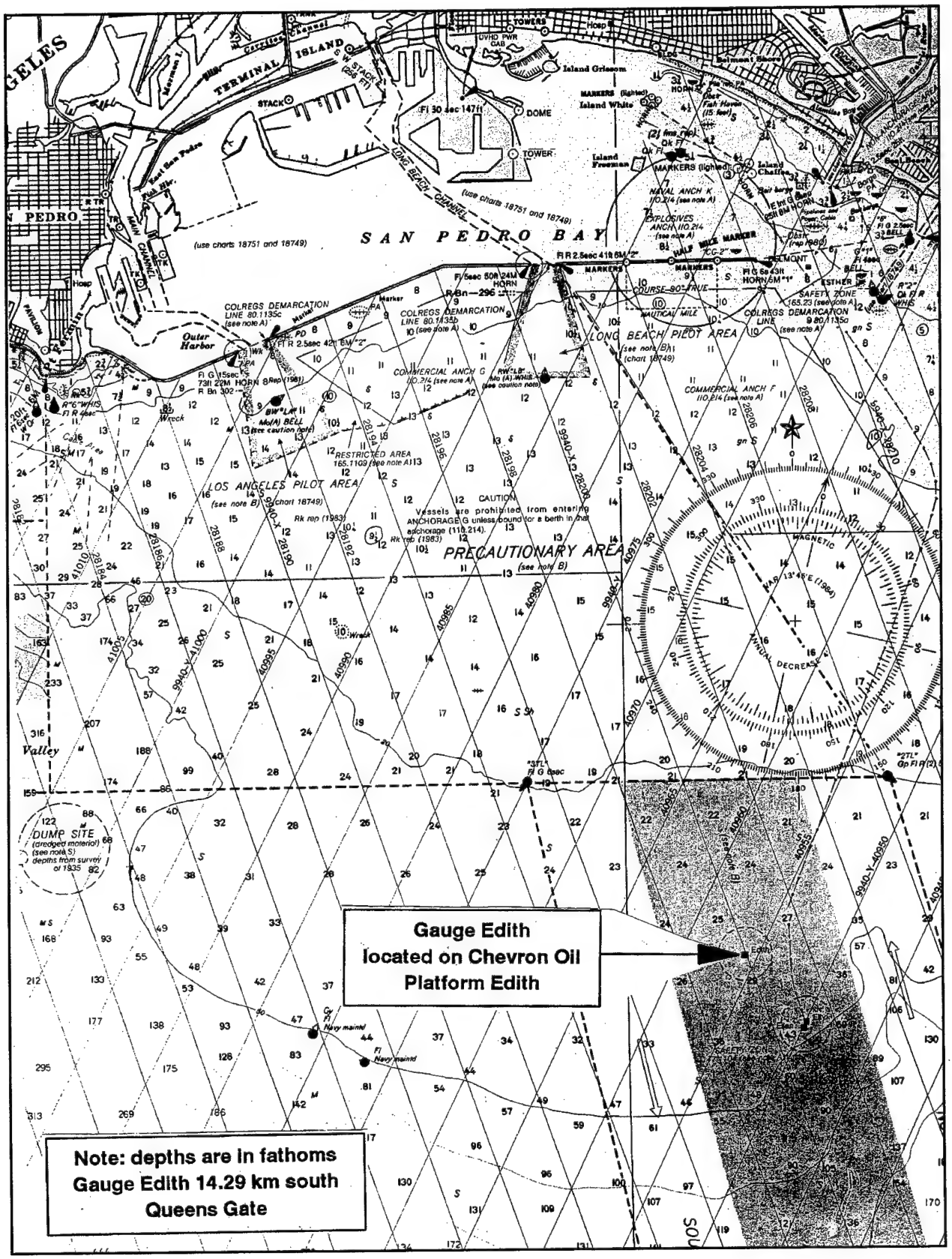

Figure 9. Location of offshore wave gauge on Chevron Oil Company Platform Edith

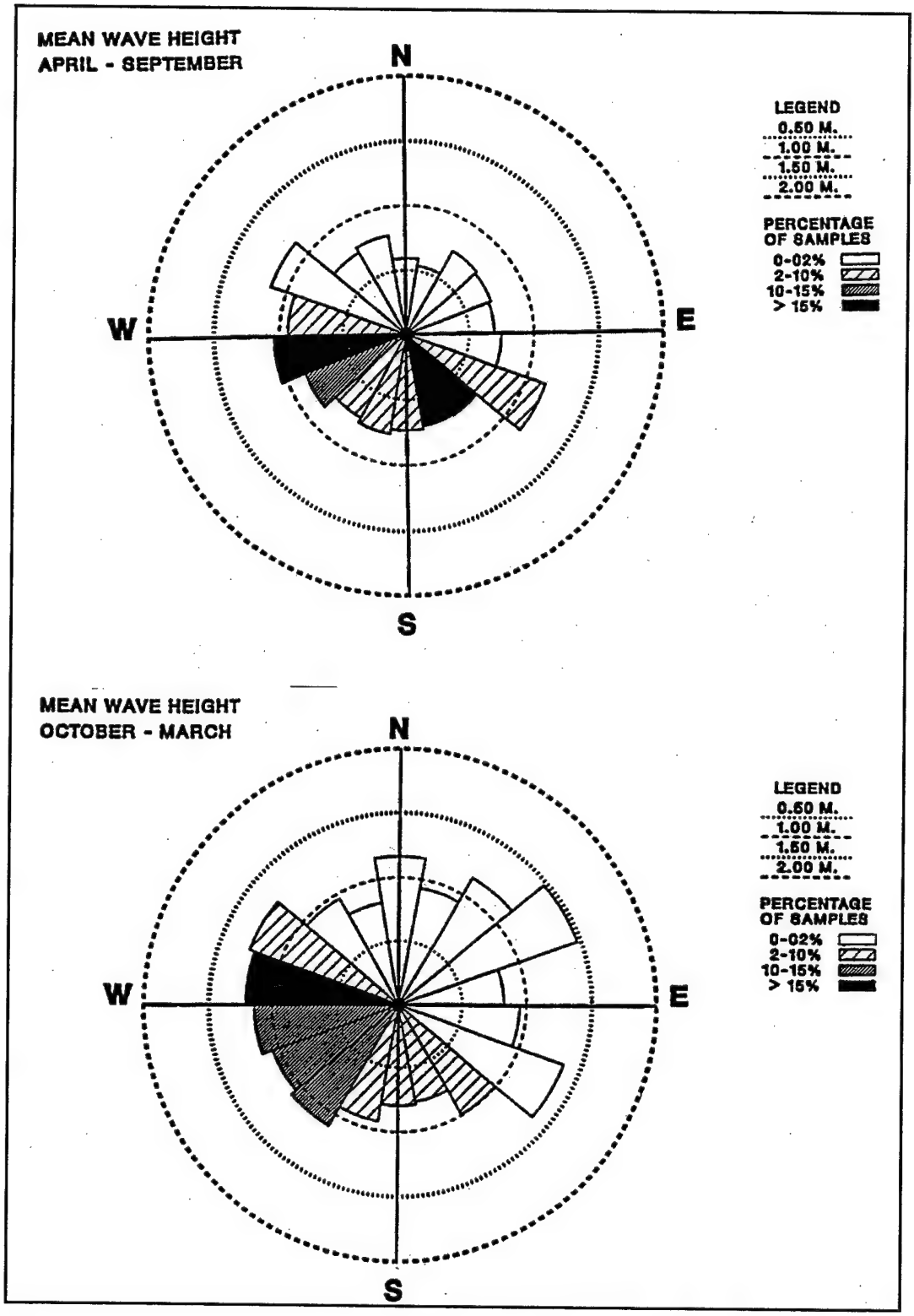

Figure 10. Wind wave information at Platform Edith (ocean gauge) from 1985-1991 (Rosati, McKinney, and Puckette 1998)

Simple Correlation of Long Waves to Short-Wave Energy Sources

As noted above, hurricanes, tropical storms, and Southern Hemisphere swell send wind waves into the harbors. Examination of the 1985 hurricane and tropical storms season for the eastern Pacific and the occurrence of Southern Hemisphere swell also explained increases in long-wave energy measured at Platform Edith. Storms off Mexico that exhibited strong, possible, and no correlation with long-wave energy collected at a gauge Edith 8 miles south of the harbors (see Figure 9) are shown in Figure 11. The locations when wind was a maximum are shown. The strongest response was from storms in the range of 110-125 deg longitude and above 15 deg latitude. The general movement of these storms ranged from west to northwest. The response at gauge Edith for the June-July 1985 period is shown in Figure 12. The effects of the Southern Hemisphere swell and Hurricane Delores are clearly seen on long-wave energy. Figure 13 shows short- and long-period wave energy at gauge Edith during the winter season (January-February 1986) when most of the energy is associated with waves approaching from the west. Once again, long-period energy responds in direct proportion to short-wave energy at the ocean gauge.

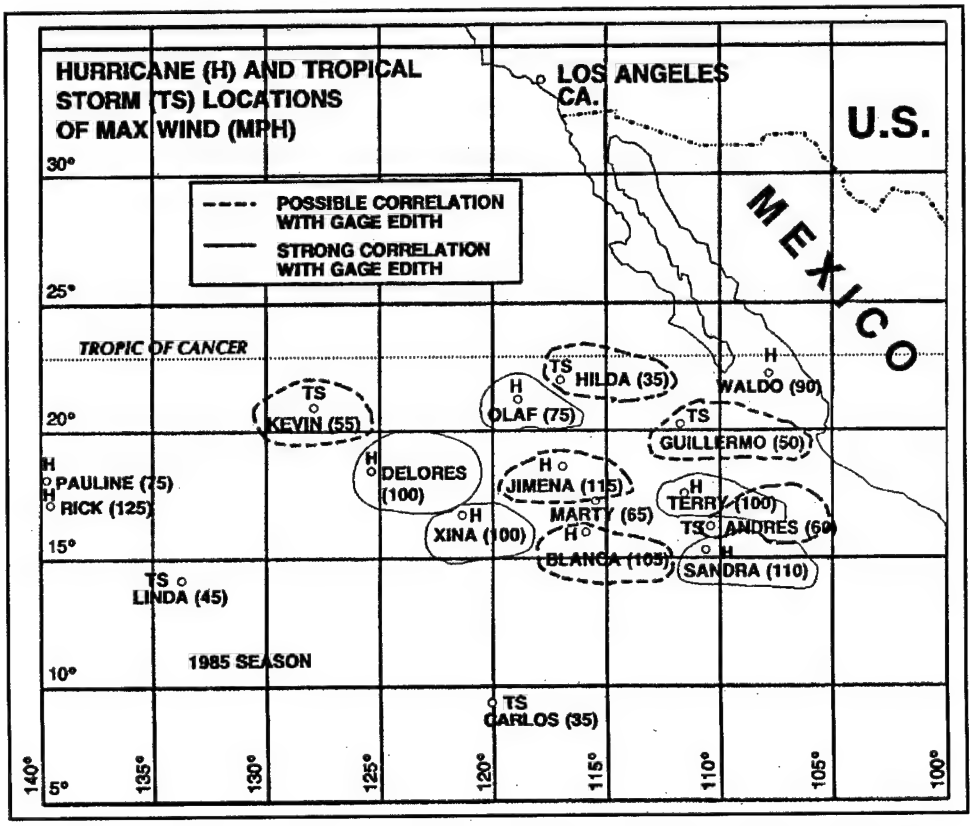

Figure 11. Correlation of 1985 Eastern Pacific hurricanes and tropical storms to long waves at Platform Edith

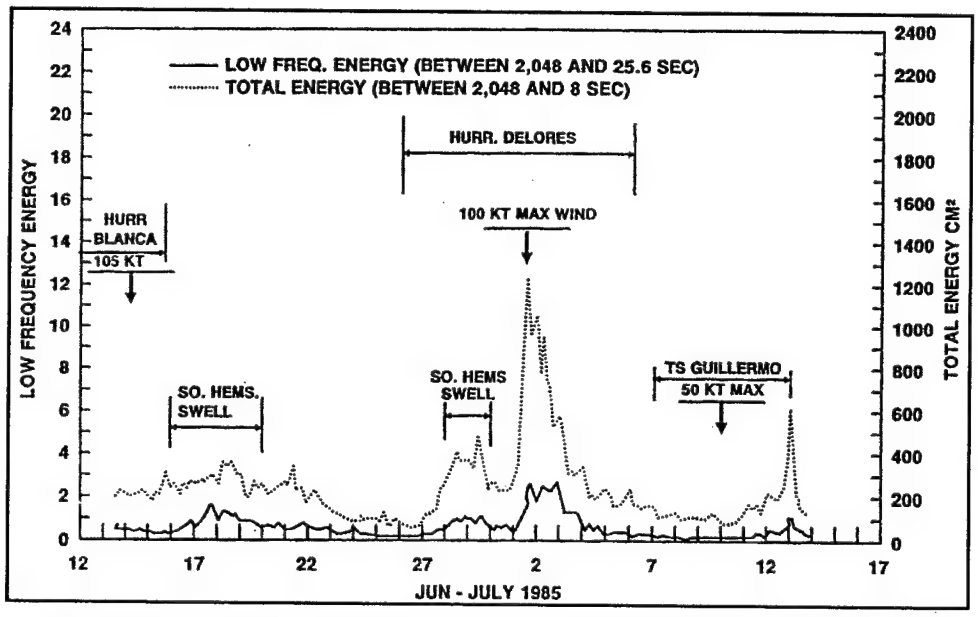

Figure 12. Correspondence of long-wave energy and total wave energy at Platform Edith to hurricanes, tropical storms, and Southern Hemisphere swell, June-July 1985

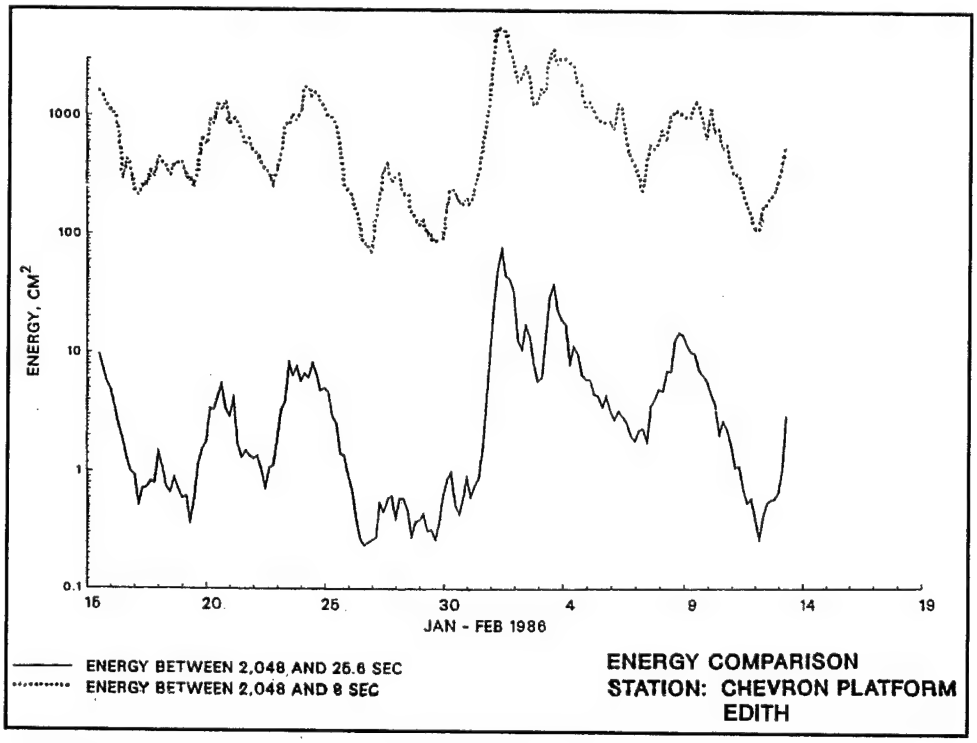

Figure 13. Correspondence of long-wave energy and total energy at Platform Edith to winter storms, January-February 1986

4 Prototype Data and Harbor Resonance

Location of Data-Collection Gauges

Eight self-recording pressure gauge instruments (seven in the harbors and one on Platform Edith outside the harbors) were initially used to acquire long-period wave data (Figure 14). Later they were replaced by an automated measurement system. The automated system used upgraded versions of the eight pressure gauges and telemetered data via remote transmitting units (RTUs) to a central computer in the Port of Long Beach Headquarters. This computer was connected via a data link to data acquisition

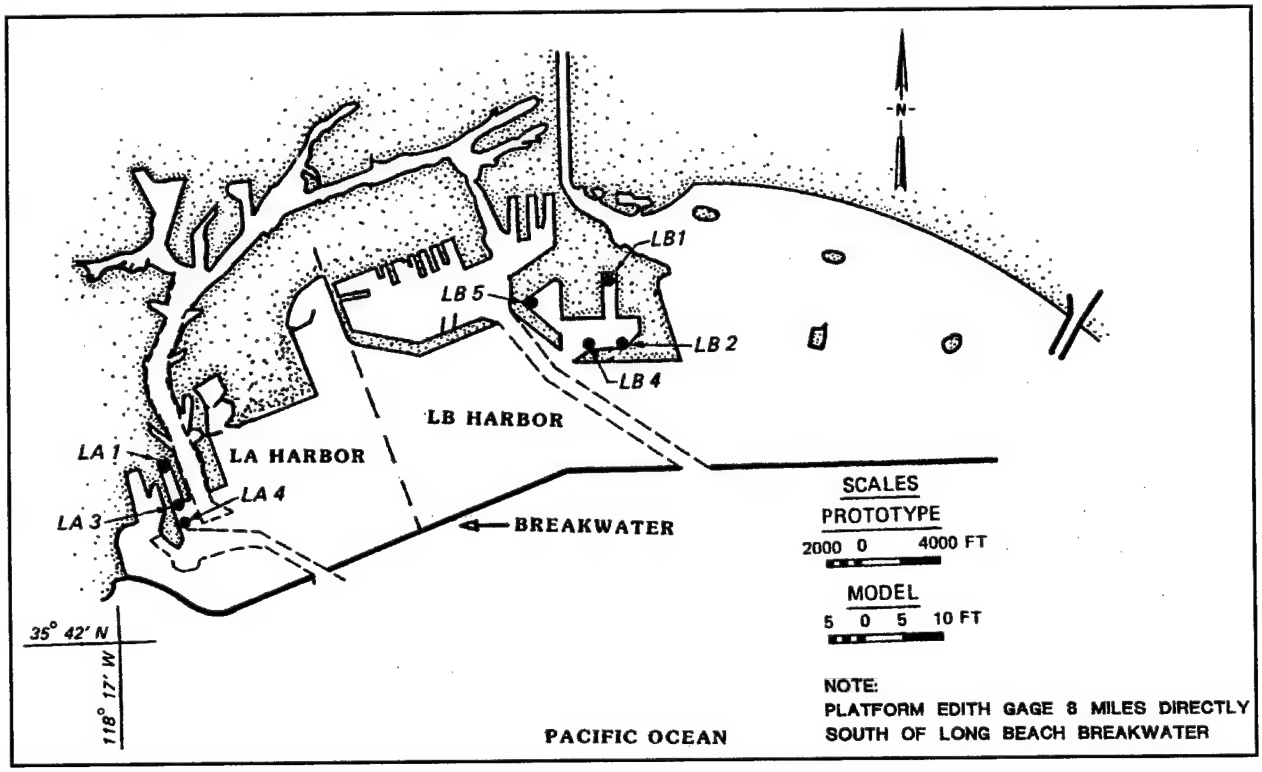

Figure 14. Initial wave gauge locations in harbors (1984)

and analysis computers at ERDC. Wave data were successfully collected at all sites during the HME study and provided input to other tasks. At the initiation of this work, about 2 years of long-period wave data had been collected at gauge Edith and at the seven harbor gauges. More data became available as the study progressed. Initially, data were collected in the harbor using Sea Data Model 635-11 wave gauges at a frequency of 1 Hz for 2,048 sec at 2-hr intervals. Data at the offshore gauge were collected at 4-hr intervals with a Sea Data 635-12 directional gauge to measure short-period directional spectra as well as long-period spectra. The long-wave raw data are edited, filtered, and spectrally analyzed, then presented in tabular form for 20 spectral bands covering periods 25.6 through 2,048 sec. Data at Platform Edith are analyzed in a separate program. Rosati and Puckette (1993) provide information on the data-collection instrumentation, analysis parameters, and additional gauge locations deployed. It should be noted that the Sea Data Corporation gauges contained a Paroscientific quartz pressure sensor that provides very accurate water-level information. Resolution of wave height was 0.045 cm and accuracy was 0.4 cm, so that even small long waves were detected.

Summary Analysis of Long-Wave Information

Introduction

The analysis discussed in the previous paragraph determines how much energy is distributed in different wave periods (or frequencies, the inverse of period). Typically, this continuum of periods is broken up into increments or "bands." Table 1 shows these bands and the period range each band represents. Discussion that follows will focus on period bands ranging from 32 to 512 sec since this is the range believed most important to the response of moored ships.

Table 1
Prototype Period Band Resolved for Prototype Data

Period Band	Band Range
25.6	25.0 - 26.2
26.9	26.2 - 27.6
28.4	27.6 - 29.2
30.1	29.2 - 31
32	31 - 33
34	33 - 35
36	35 - 38
39	38 - 40
42	40 - 44
46	44 - 48
51	48 - 53
56	53 - 60
64	60 - 68
73	68 - 78
85	78 - 93
102	93 - 113
128	113 - 146
170	146 - 204
256	204 - 341
512	341 - 1022

Average energy distributions

Using approximately 3 years of data (1984-87), an interim collation of long-wave information was prepared for each gauge location and each energy band at that location to help understand the response of the harbor to long waves. Figures 15 and 16 show examples of average energy at Platform Edith and gauge LB2, respectively. The average energy across the Edith gauge energy bands is fairly uniform. Gauge LB2 increases in wave energy at certain period bands because of harbor resonance at these

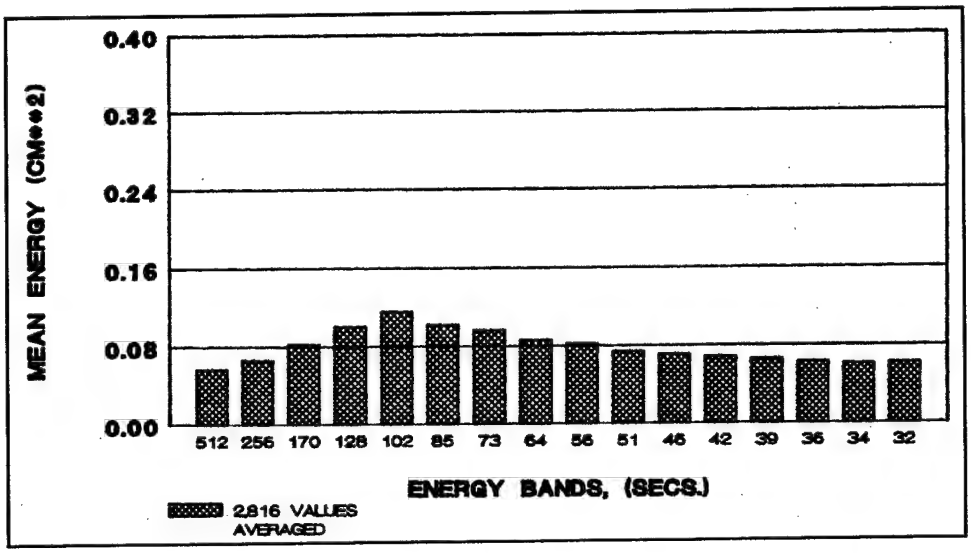

Figure 15. Average wave energy at ocean gauge Edith for 32- to 512-sec period range, February 1985 to April 1987

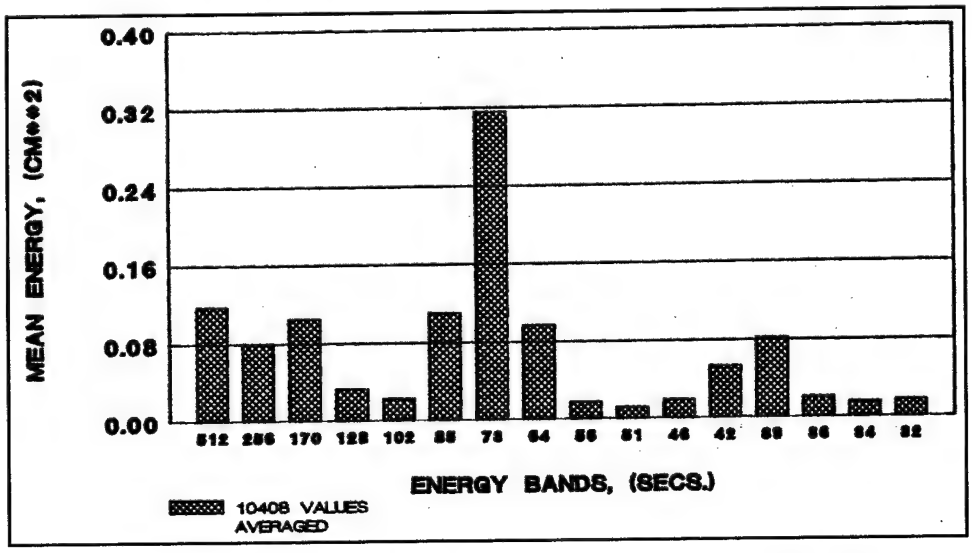

Figure 16. Average wave energy at Long Beach Harbor gauge LB2 for 32- to 512-sec period range, February 1984 to August 1987

energy band periods. Figure 16 indicates this is especially true at 73 sec (compare with ocean energy at Platform Edith). This variation in energy with wave-period band is characteristic for that specific site and is similar in shape whether the ocean energy is small or large. This characteristic shape will remain the same for a particular location until a change is made to the basin. For example, deepening or filling in parts of the basin can cause changes to the resonant periods, and shifts to new resonant wave periods may occur. Figure 17 shows the average energy in various period bands for both locations for a 1-month duration, which was an energetic month with significant storms. The same variation in energy with period band exists for this month as for the entire data set. Only the energy level is different for this stormy month. It is interesting to compare the energy

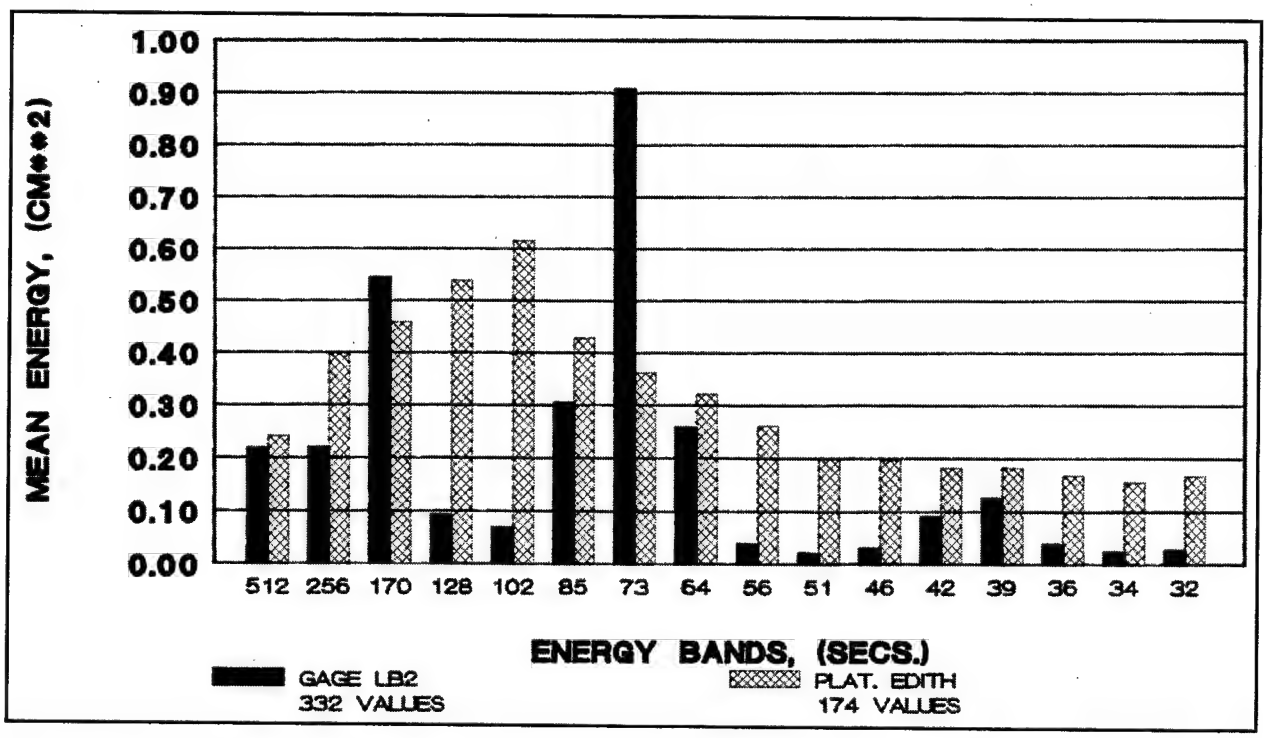

Figure 17. Average wave energy at gauges LB2 and Edith for 32- to 512-sec period for 15 January 1986 to 13 February 1986

levels at Edith with LB2 and see that the 73-sec period band at gauge LB2 stands out as significantly greater than the offshore energy at Edith because of harbor resonance in the basin in the period range covered by this band of energy. The 170-sec period band has slightly higher average energy than the ocean. All other period bands in the basin have less energy than the ocean. Similar data for the other gauges are included in Plates 1-8. Plate 9 shows average total long-wave period wave energy measured for this data set. Gauge LA1 has the greatest total long-wave energy level, and it is interesting to note that it is an inactive berthing location because of mooring difficulties experienced in the past at that location. It should be noted that fairly coarse period resolution data are presented for these early data sets. Recent changes in data acquisition methods permit the collection of longer data records, which translates into data analysis being performed at finer period (or frequency) resolution at the same level of statistical confidence.

High-low monthly energy

Another summary plot generated for the long-period wave data contains the monthly high-low-mean total long-period energy. Figure 18 shows two examples of this. Level of energy at gauge LA1 in East Channel of Los Angeles Harbor is considerably greater than that at gauge LB5 in Long Beach Harbor's Basin 6 of the Southeast Basin complex. Also interesting to note is the maximum energy was 360 cm^2, which is equivalent to a significant wave height of 0.76 m, a very large magnitude for long-period

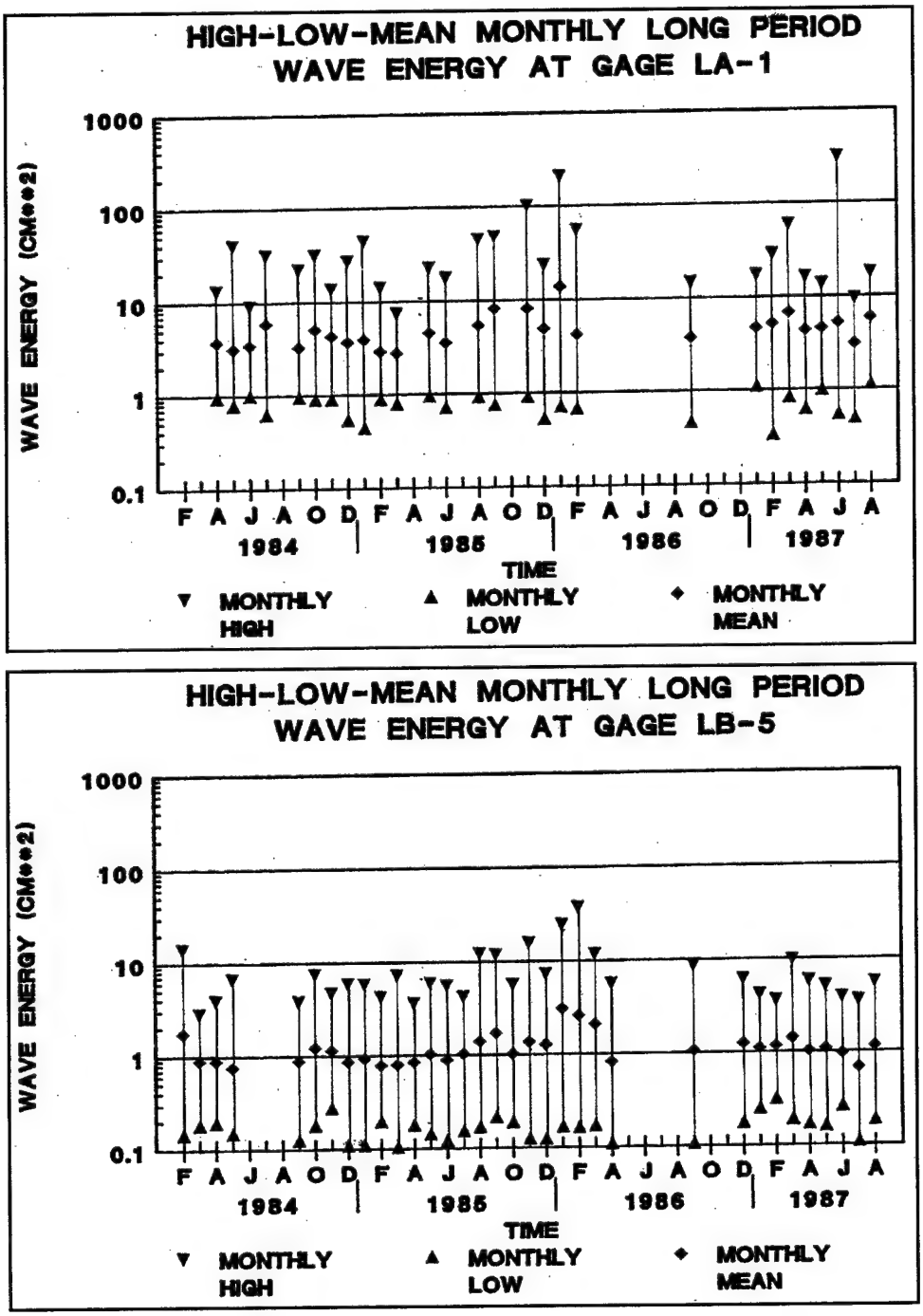

Figure 18. High-low-mean monthly wave energy at Los Angeles Harbor gauge LA1 and Long Beach Harbor gauge LB5, April 1984 to August 1987

waves. High-low plots for all gauges are in Plates 10-17. Common to all is the logarithmic variation from the monthly low to the monthly mean to the monthly high. Thus, the difference between the lowest energy level to the highest is about one hundred times. Wave heights are proportional to the square root of the energy so maximum to minimum wave height ratios are about 10.

Seasonal trends

Plates 18-20 show total long-wave energy for the 3-year data set used for summary analysis. Trends seen indicate high energy in the winter followed by declining energy in the spring with slight increases in the summer. Also of interest is the increase of total long energy in the harbors relative to that measured at the ocean gauge on Platform Edith during lower energy periods. This can be related to a variety of factors, some of which are discussed below, including effect of wave direction, energy losses in the harbors for higher energy levels, and perhaps a type of efficiency factor for wave type, with the southerly swell of summer containing relatively more long-period energy when compared with that contained in waves accompanying a more local storm system.

Energy occurrence

The long-wave energy in each period band for each gauge was sorted from smallest to largest value and plotted against the time a certain value could be exceeded. Figure 19 shows an example of this for gauges Edith and LB2 for the 73-sec energy band. The curve is normalized to a 1-year period, so values read off the vertical energy axis represent a certain number of hours per year that energy will be above that level, as read off the horizontal axis. Of interest to note is the decrease in ratio between the two energy occurrence curves as energy levels increase. The ratio is over a

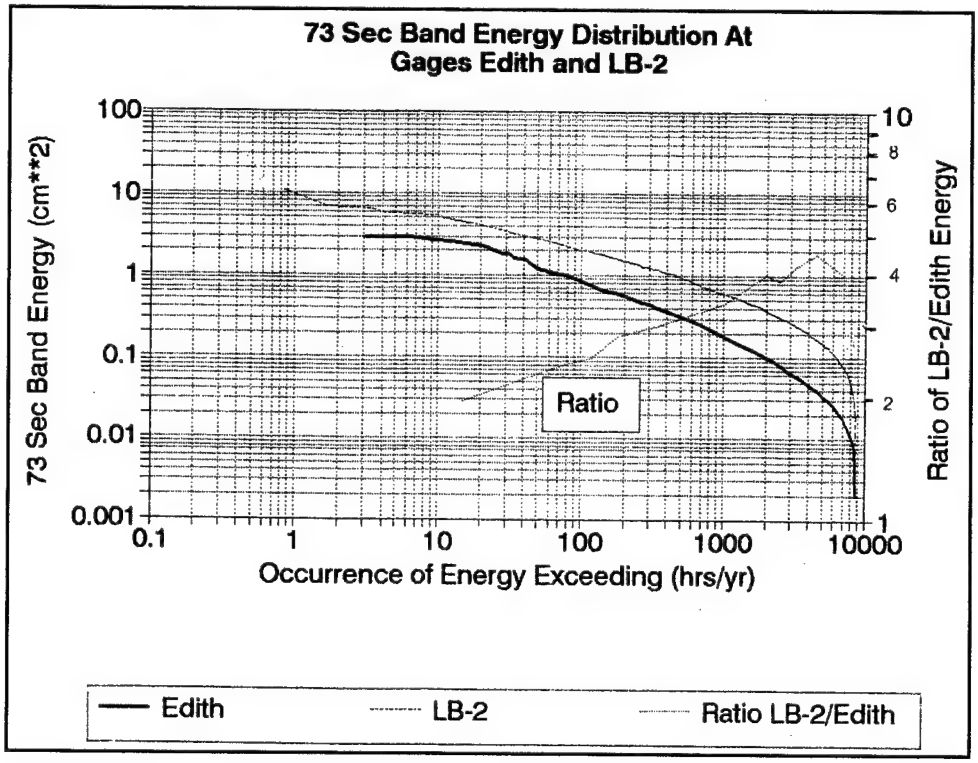

Figure 19. Exceedance curves for 73-sec energy band at ocean gauge Edith and harbor gauge LB2

value of four at low-energy levels and decreases to about two near the 10-hr value on the occurrence exceedance axis. This most likely represents the effect of wave direction. The higher energy levels typically represent energy from the west, which can be reduced at the harbor relative to the gauge at Edith, 8 miles south of the harbors. Also, energy losses in the harbors' basins may increase during high-energy conditions, which would reduce the ratio. Another possibility might be an increase in reflected long-period energy during high-energy conditions that is reflected from the shoreline and added to the incident energy associated with the incoming waves. The adjacent shorelines do not lend themselves to this effect for the larger waves approaching from the west. Figure 20 shows monthly long-period wave-energy averages for gauges Edith and LB2; the high-energy winter season with waves from the west shows Edith with greater total long-wave energy, while for most of the summer season, LB2 is greater except for August. This trend was seen for all gauges at all wave-period bands. Plots for all period bands for gauges Edith, LA1, and LB2 are included in Plates 28-36. The other gauges' data are on file at the Coastal Engineering Research Center.

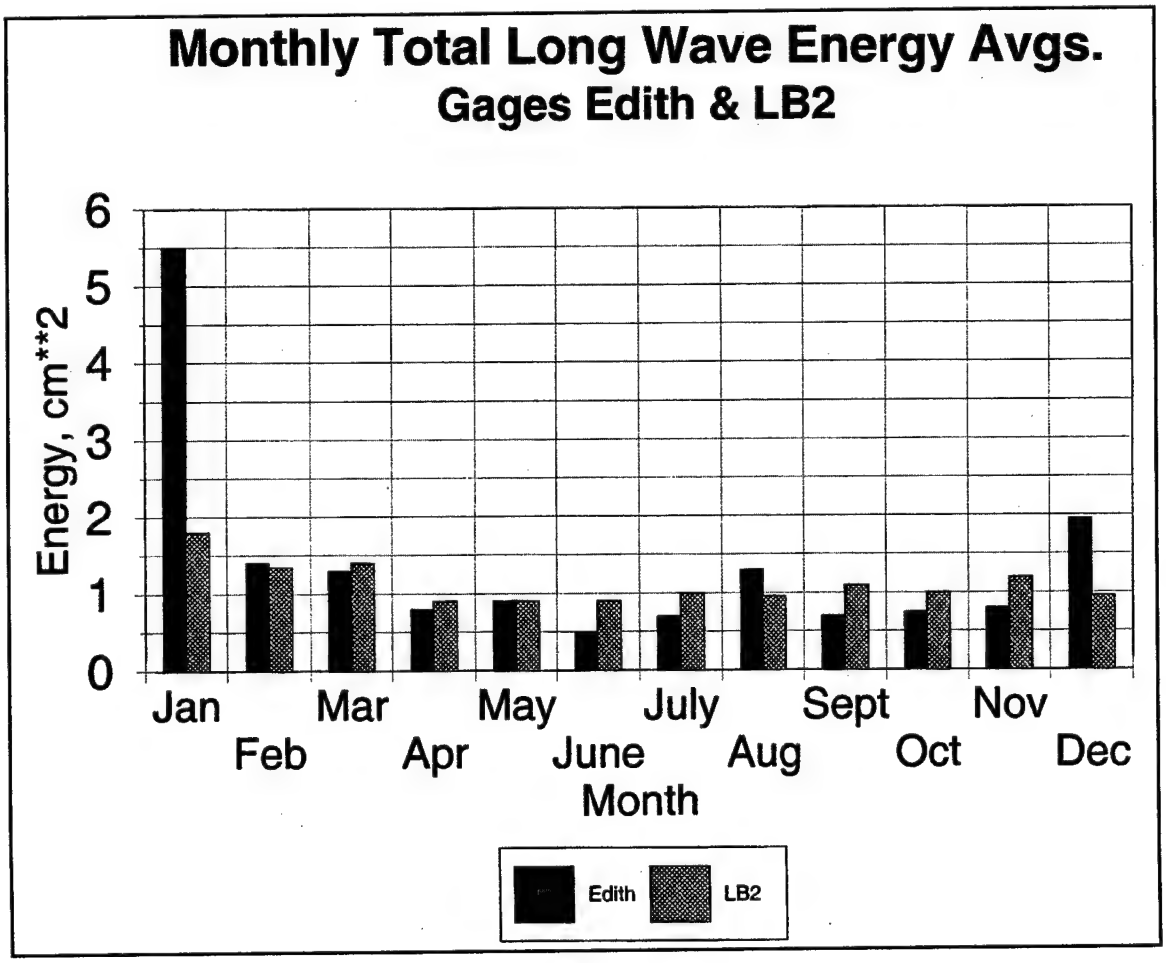

Figure 20. Monthly total (for years of 1985-1987) long-period wave-energy averages at ocean gauge Edith and harbor gauge LB2

Harbor resonance relative to gauge Edith

Using the energy occurrence information discussed in the previous paragraph, a type of statistical set of wave-height amplification factors for each harbor gauge was determined. Figure 21 shows the wave-height amplification factors for the 4,000- and 10-hr/year levels of occurrence. As noted above, amplification factors are reduced at high-energy conditions. The bar plot indicates the level of energy at the high-energy 10-hr/year level. Plates 37-43 are similar plots for all gauges. It should be noted that all wave-height amplifications are relative to gauge Edith; these amplifications cover a fairly wide period band; and wave-height amplifications can be higher for certain smaller portions of the band, as the value is an average one for the range of periods it covers.

Summary

The long-wave data collected over the 32- to 512-sec period bands at each harbor site show a characteristic wave-energy response dependent on gauge location. The response may vary in magnitude because of offshore wave conditions; but the change is relative, and the characteristic response shape is maintained (see Figure 21 bar graph). Different harbor gauge locations have different energy levels for the same incident ocean-energy conditions because of various degrees of wave amplification at each location. Further discussion of the relationship of long waves approaching the harbors with respect to the short waves follows.

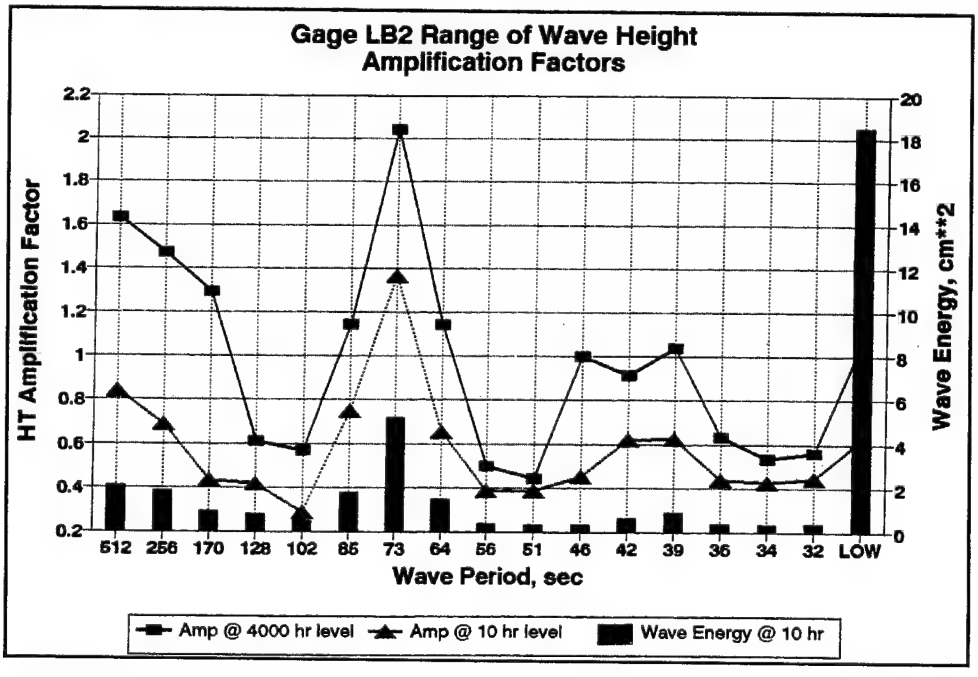

Figure 21. Wave-height amplification factors for long-wave energy bands at gauge LB2 at the 4,000- and 10-hr/year exceedance levels and wave energy at 10-hr/year exceedance level

5 Analysis of Long Waves

Short-Period Wave—Long-Period Wave Correlation

As noted in Chapter 3, the rise in the short wind wave energy is accompanied by an increase in long-wave energy no matter what the originating source, i.e., hurricanes, Southern Hemisphere swell from storms between Antarctica and Australia, or the closer weather systems in the Northern Pacific. In recent years, more work has been done to correlate the short-period wave to the associated long-period wave. Primarily, this work focused on the relationship of short-wave to long-wave amplitude. Bowers (1980) was one of the first to quantitatively associate wind waves and long waves in intermediate water depths. Okihiro, Guza, and Seymour (1993) and Herbers et al. (1992) also have analyzed field data to examine short- and long-period wave correlations.

Total ocean short-period to total ocean long-wave period energy correlation

The total long-wave energy at the ocean gauge on Platform Edith correlates well with the short-wave energy measured there. Figure 22 shows this correlation using average monthly values. Figures 23a and 23b show correlations for two specific data sets for individual values recorded every 4 hr. Both the winter and summer seasons show the same level of correlation, with the June and December data sets having correlation coefficients, R^2, with values of 0.77 and 0.74, respectively. This indicates good correlation, with a value of 1.0 meaning perfect correlation.

Total ocean short-period to ocean long-wave period energy bands correlation

A month-long data set for June-July 1985 showed strong correlation of gauge Edith total short-period energy to individual long-period energy bands at Edith. Figure 24 shows correlations for all the month-long data and for a 4-day event, i.e., more energetic conditions.

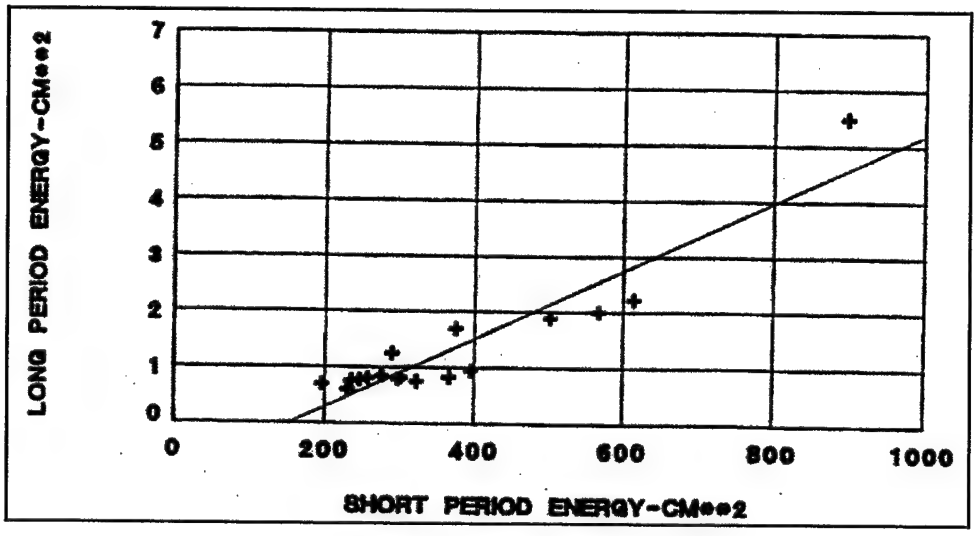

Figure 22. Long (25-1,024 sec) versus short (8-25 sec) monthly average wave energy at ocean gauge Edith

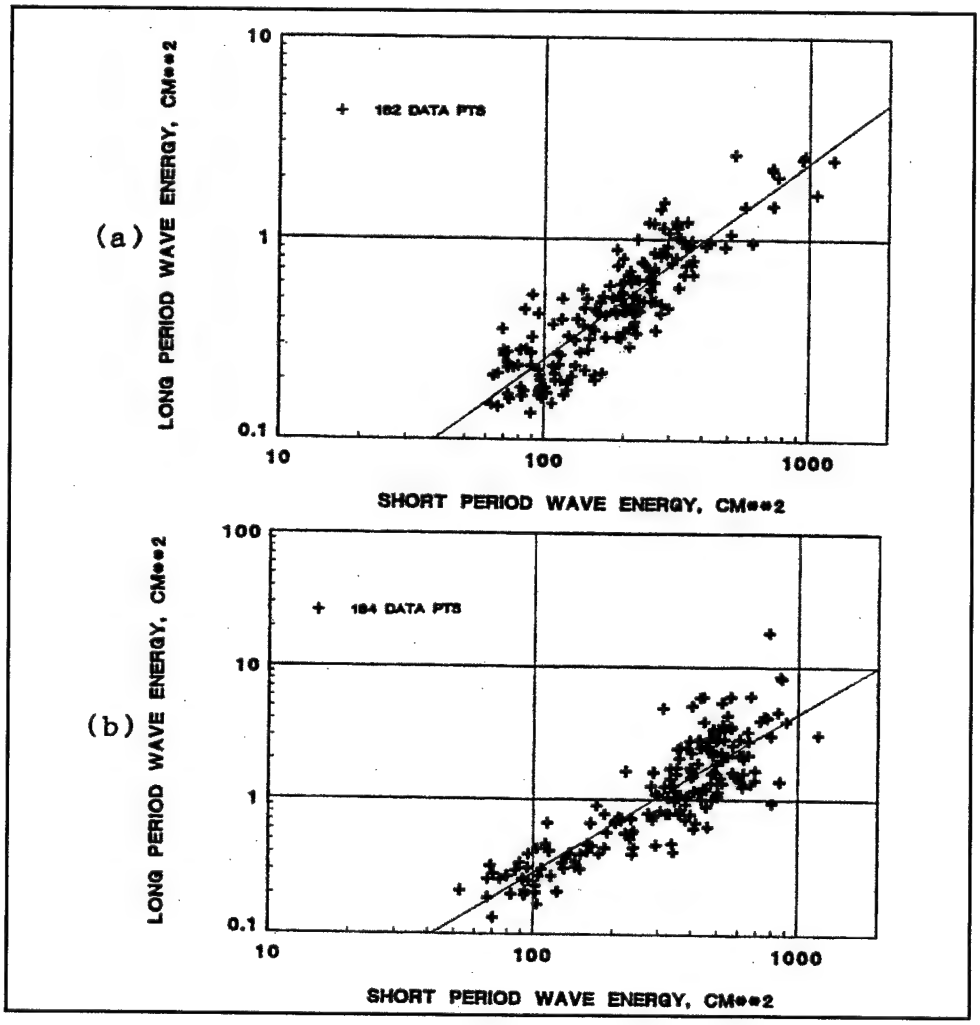

Figure 23. Long (25-1,024 sec) versus short (8-25 sec) wave-energy individual events at ocean gauge Edith for (a) June 1985 and (b) December 1985

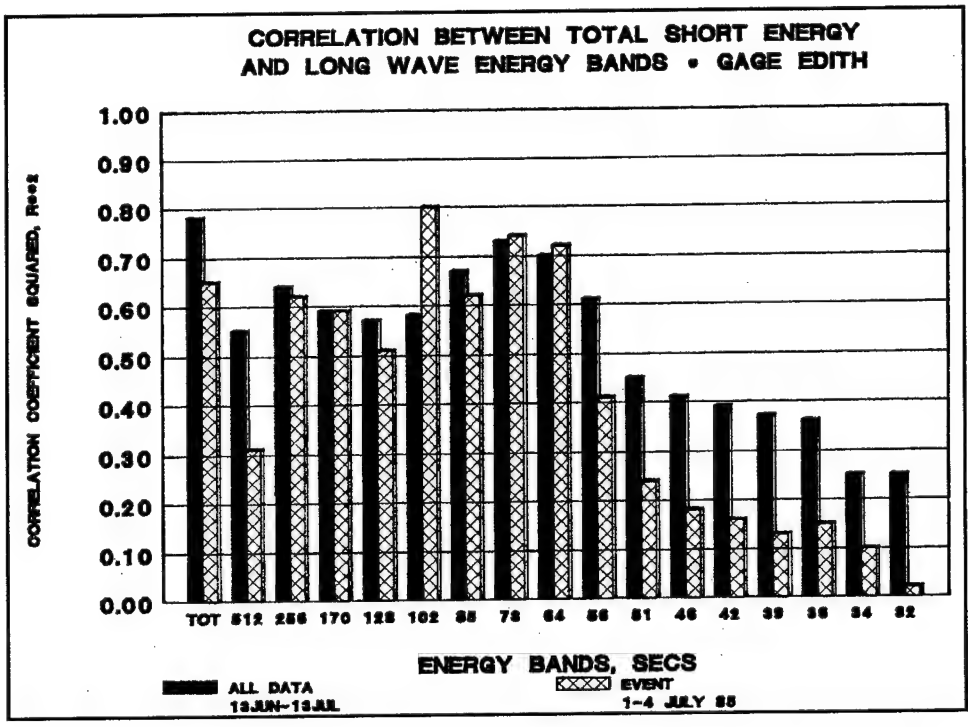

Figure 24. Correlation of gauge Edith short-period wave energy and long-wave energy bands (32-512 sec) and total long-wave energy for 13 June - 13 July 1985

Correlations were strongest for 256- to 64-sec bands. The falloff of correlations in the 51- to 32-sec range is interesting in regard to an examination of short- and long-wave period correlation discussed later. The event was a "swell" event with most of the energy in a 10- to 14-sec wave period and not much in lower periods. Later analysis indicates that lower short-wave periods correlate to smaller long-wave periods, so the event has a falloff in correlation at smaller long periods. Also 4- to 8-sec energy is not present in this data set because of the cutoff frequency for raw data analysis being 8 sec; this fact probably explains some falloff in correlation for the entire month-long data at long periods below 56 sec.

Total ocean short-period to total harbor long-period energy correlation

In Figure 25, a 1-month record of total short energy at the ocean gauge Platform Edith is plotted versus the 25- to 512-sec energy for the harbor gauge LA3 (see Figure 14 for gauge location). As the ocean short-wave energy increases and decreases, so does the harbor long-wave energy. There is considerable spread in these data because certain resonant long-wave periods may not be as strongly activated for one short-wave train as for another. A better correlation might be achieved by correlating to individual frequency bands of harbor long waves. This is discussed next.

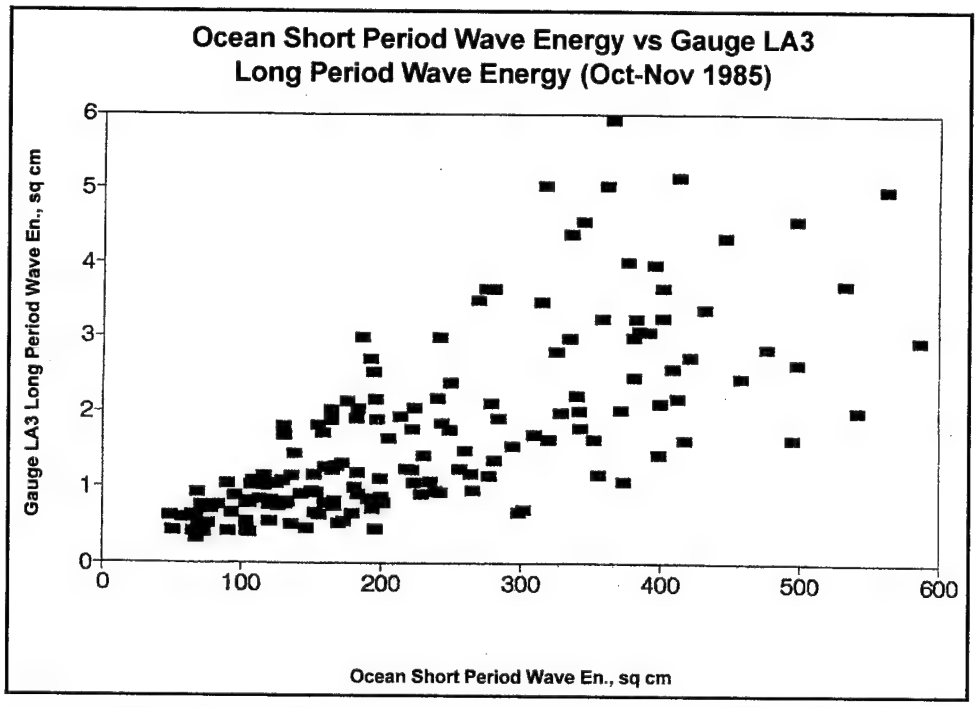

Figure 25. Ocean gauge Edith short-period wave energy versus harbor gauge LA3 long-wave energy, October-November 1985

Total ocean short-period to harbor long-period wave bands correlation

The correlation of the short-period energy measured at ocean gauge Edith and the long-period energy bands measured in the harbor at gauge LB2 also produced reasonable correlation (Figure 26). Once again, the fall-off at shorter long periods was probably attributable to reasons discussed above. Interesting to note is the lack of any correlation to energy in the 512-sec band, indicating this period response may not be related to wind wave energy, but possibly be a harmonic of a local shelf oscillation perhaps forced by wind or tide. Correlations with some long-period bands in the harbor can be expected to be small if there is not very much energy at that band, but an examination of the average energy at gauge LB2 in Figure 16 shows that the 102-sec band, which has much lower energy relative to the 512 band, has a good correlation to short-period wave energy in the ocean.

Another data set, for the winter season, was examined, and results are shown in Figure 27. Correlation coefficients are slightly lower than for the summer season results, but increase when only the high-energy condition is considered. Once again, the 73-sec period has the highest correlation because it has the greatest amount of energy among the wave-period energy bands because of its high resonant response.

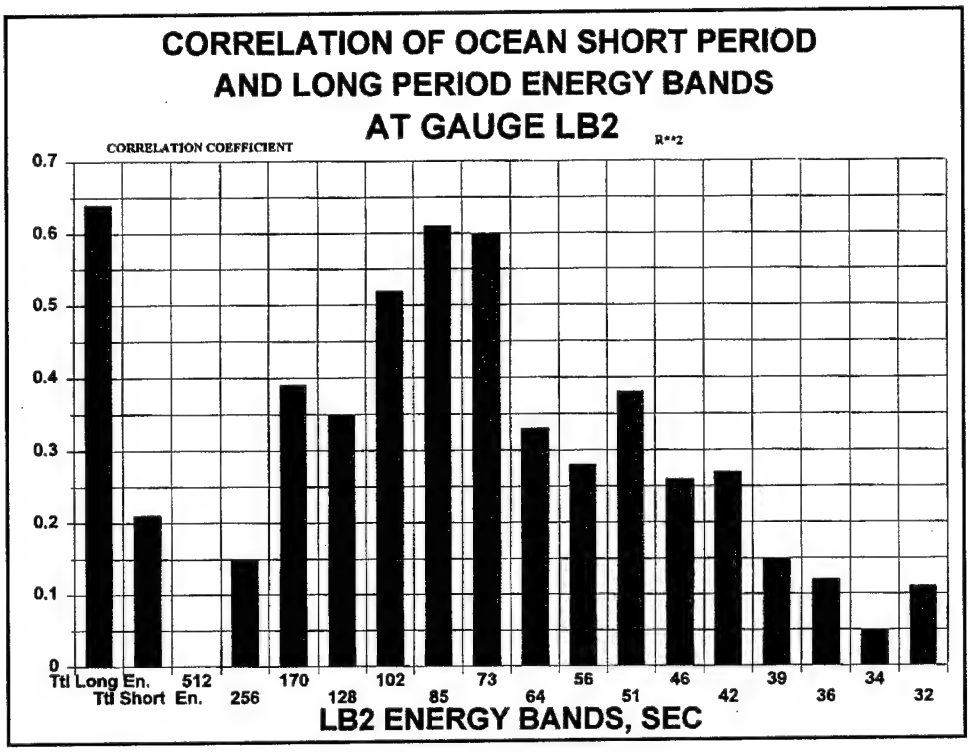

Figure 26. Correlation of short-period wave energy at ocean gauge Edith and long-wave energy bands at harbor gauge LB2, June 1985

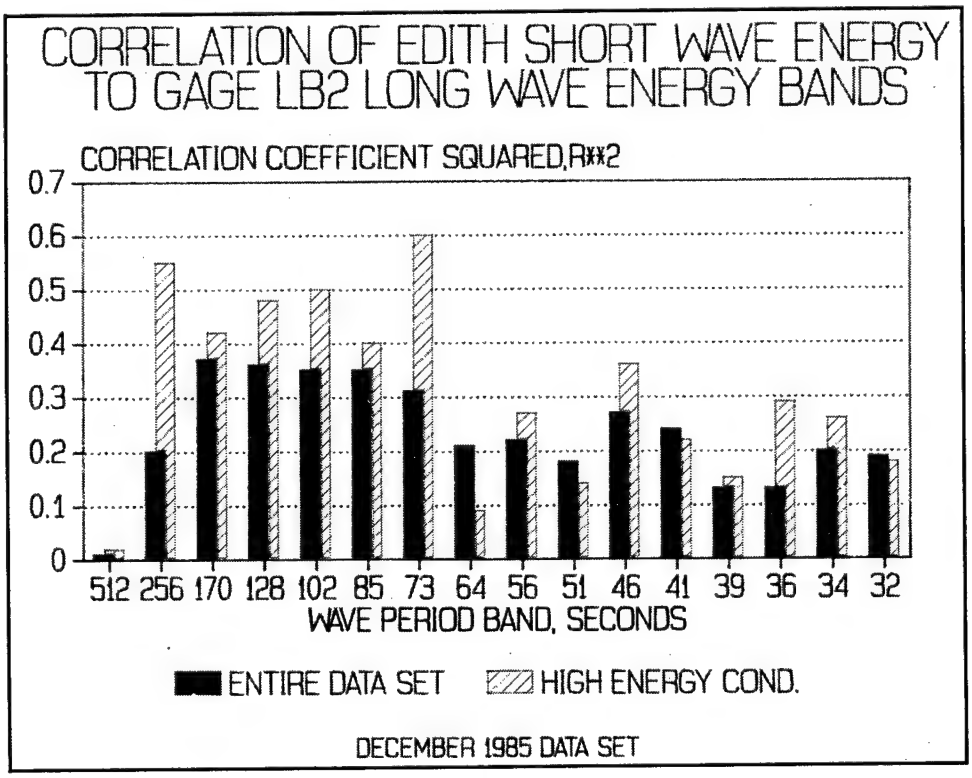

Figure 27. Correlation of short-period wave energy at ocean gauge Edith and long-wave energy bands at harbor gauge LB2, December 1985

Correlation of individual ocean and harbor wave-energy period bands

The results of correlating all the energy bands at gauge Edith to gauge LB2 for 187 cases in June 1985 are presented in a contour plot of correlation coefficient R. The top part of Figure 28 is the lower left corner of the bottom figure. Correlation is best where energy is highest at the 73- and

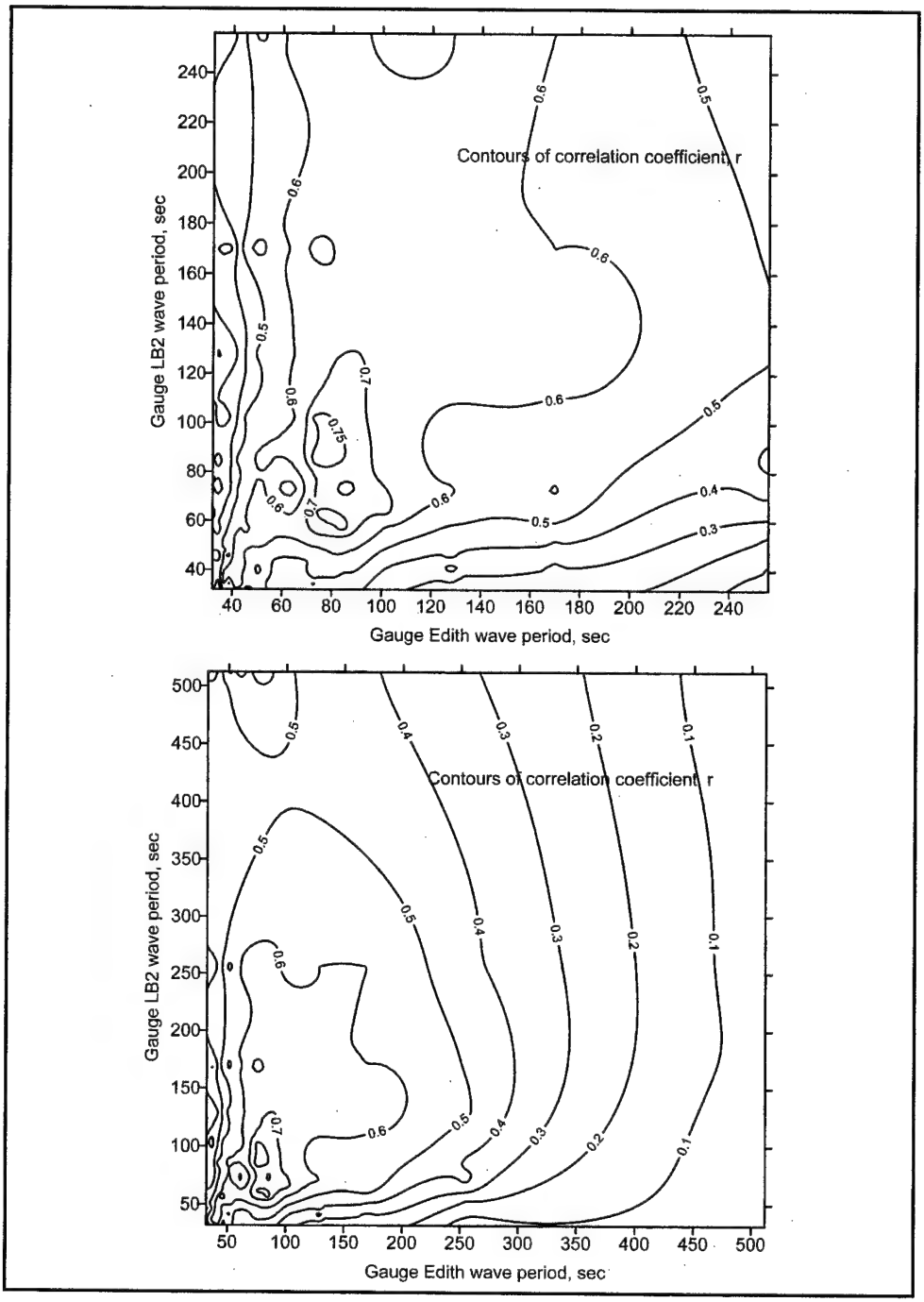

Figure 28. Correlation of individual wave-period energy bands between ocean gauge Edith and harbor gauge LB2, June 1985 (182 cases)

85-sec energy bands, which are the resonant periods for the basin. Correlations of this nature are weaker because absolute energy levels are usually low for individual bands and there is a time lag between ocean and harbor on the order of 15 min for wave travel. These wave records were typically gathered on the hour for a 34-min duration so that one was seeing the same waves for analysis about half the time, though one makes assumptions of stationarity for the analysis. The 512-sec energy band at Edith does not correlate with the basin gauge. A bubble plot (Figure 29) where individual points have diameters proportional to the average energy at gauge LB2 indicates there was significant energy in the 512-sec energy band, yet the correlation coefficient is close to zero.

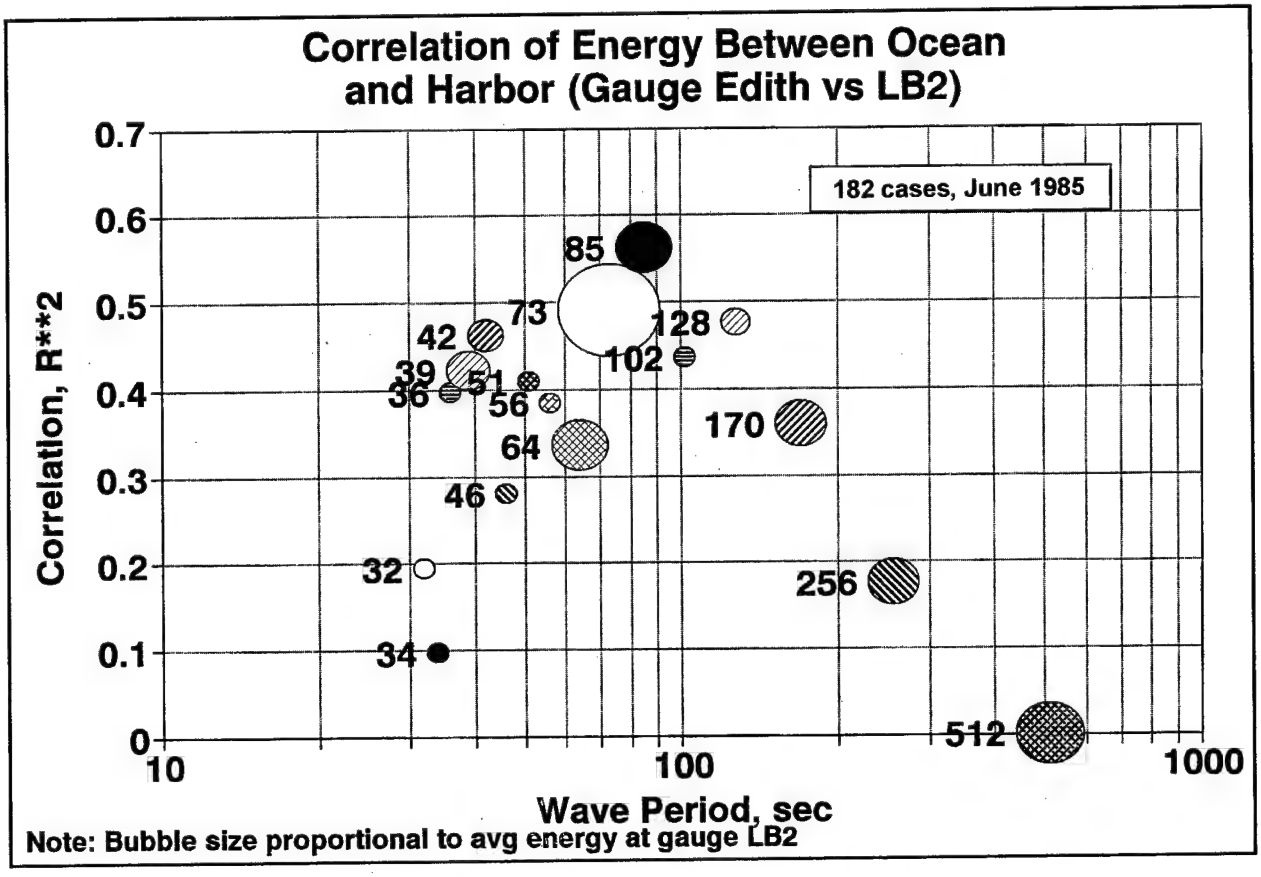

Figure 29. Correlation of individual wave-period energy bands between ocean gauge Edith and harbor gauge LB2 with regard to energy at gauge LB2, June 1985

Summary

The above sets of correlation information explain that the long-wave energy that affects the harbors is strongly tied to the short-wave energy approaching the harbors and the long energy transforms uniformly into the harbor probably because of the relatively large depths associated with these harbors. Also, the periods in the 512-sec energy band in the harbors do not correlate with the ocean long-period energy, indicating another source, other than short-period waves, forces this period range.

Detailed Analysis of a 1-Month Data Set

A 1-month data set at Gauge Edith from the January-February 1986 time period was examined in detail. Long- and short-wave spectra for 174 continuous (every 4 hr) data records were analyzed with $\Delta f = 0.00195$ Hz for the entire range of long and short frequencies. An examination of the long-short wave correlation is shown in Figure 30. The log-linear

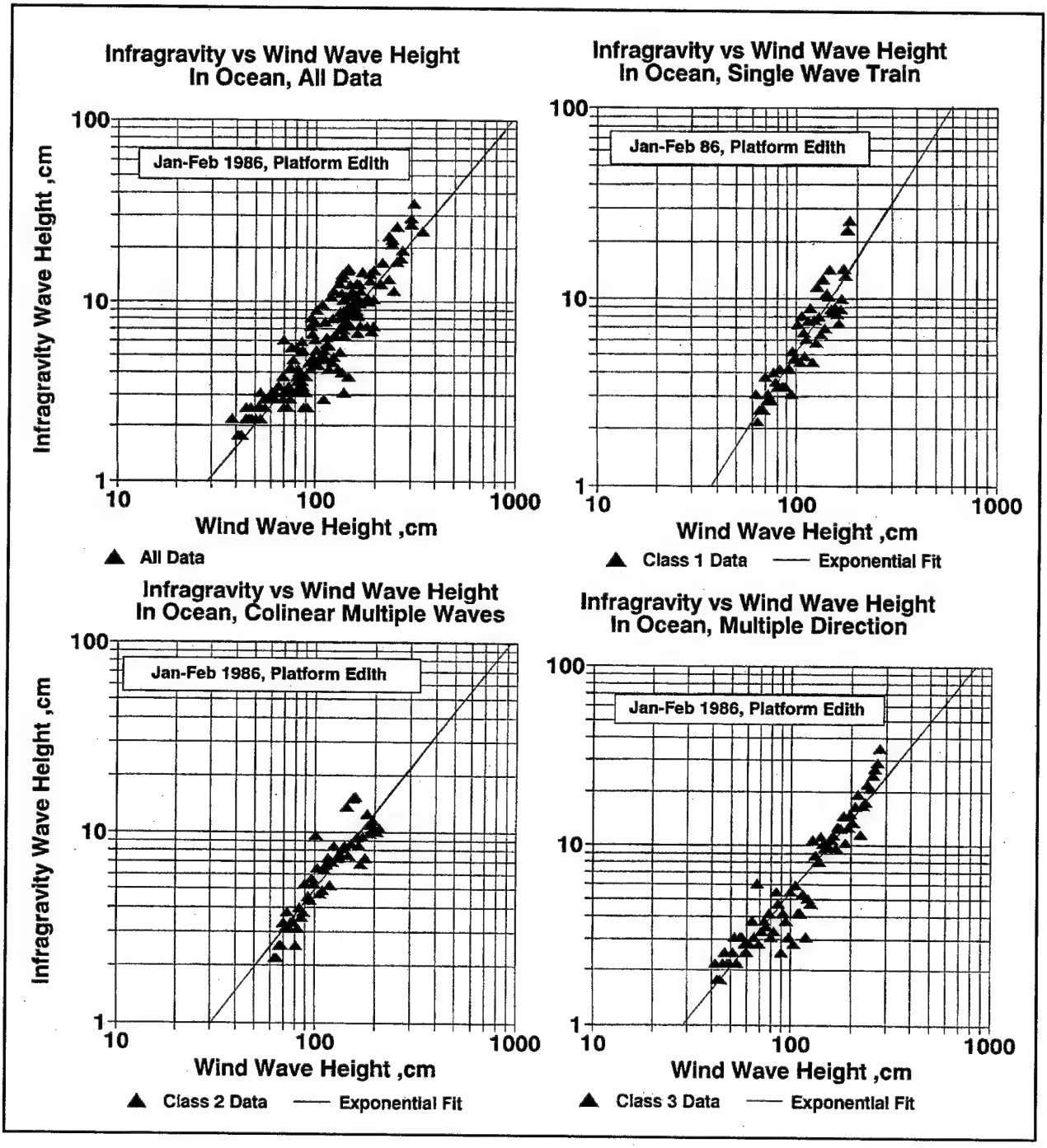

Figure 30. Relation of long-period wave height to short-period wave height at ocean gauge Edith

relationship between long or infragravity wave height and the associated wind wave height can be noted. When these data were separated into three classes, based on whether there was one primary wave (Class 1), a unidirectional multiple wave (Class 2), or a multiple directional wave (Class 3), it was anticipated that long-wave energy relative to short-wave energy would decrease for multiple-direction wave spectra (discussed by Bowers (1992)), as well as for multiple-wave collinear spectra. However, the best exponential fit equations were found, and their associated correlation coefficients, R^2, were determined; most likely, the error band for the coefficients would not permit such a conclusion. At a water depth of the Edith gauge (52 m), directional effects on the level of long-period energy with respect to short-period wave energy was minimal.

$$\textit{Alldata: } H_L = 0.0169\, H^{1.287} \quad (R^2 = 0.89,\ 174\ \textit{cases})$$

$$\textit{OneWaveTrain: } H_L = 0.0181\, H^{1.273} \quad (R^2 = 0.84,\ 54\ \textit{cases})$$

$$\textit{ColinearWaves: } H_L = 0.0159\, H^{1.29} \quad (R^2 = 0.85,\ 52\ \textit{cases})$$

$$\textit{MultipleDirection: } H_L = 0.0167\, H^{1.298} \quad (R^2 = 0.93,\ 68\ \textit{cases})$$

Surprising was the fact that the strongest correlation of long to short energy was for waves of multiple direction, though this data set had an average energy level higher than the other two data sets, a condition for improving correlation.

Also of interest was the close correlation of spectral shape of the short and long spectrum and the relationship of peak periods. Figure 31 shows three such spectra representing the three classes discussed above. This similarity in shape led to correlating peak periods of the long and short spectra to one another, indicating trends for shorter wind wave periods to correlate to shorter long waves and longer wind wave periods relating to longer long-wave periods. Figure 32 shows this correlation for the data set. The prototype data analysis provided data up to the 512-sec period band, with the next lowest band being 256 sec. As was noted in correlations between the long-wave energy band at the ocean gauge and the short-wave energy there, the 256-sec band showed strong correlation with short-period wave energy, but the 512-sec band showed no correlation to short-period wave energy. The plot of Figure 32 seems to indicate this also, with the 512-sec period band having no occasions of peak period occurrence. The general trend for this curve will be discussed further in the next section.

Relationship to Theory

Long-wave height

Theoretical development of bound long-wave theory has led to some easily applied formulas for calculation of the long-wave height. Bowers (1992) presents the equation

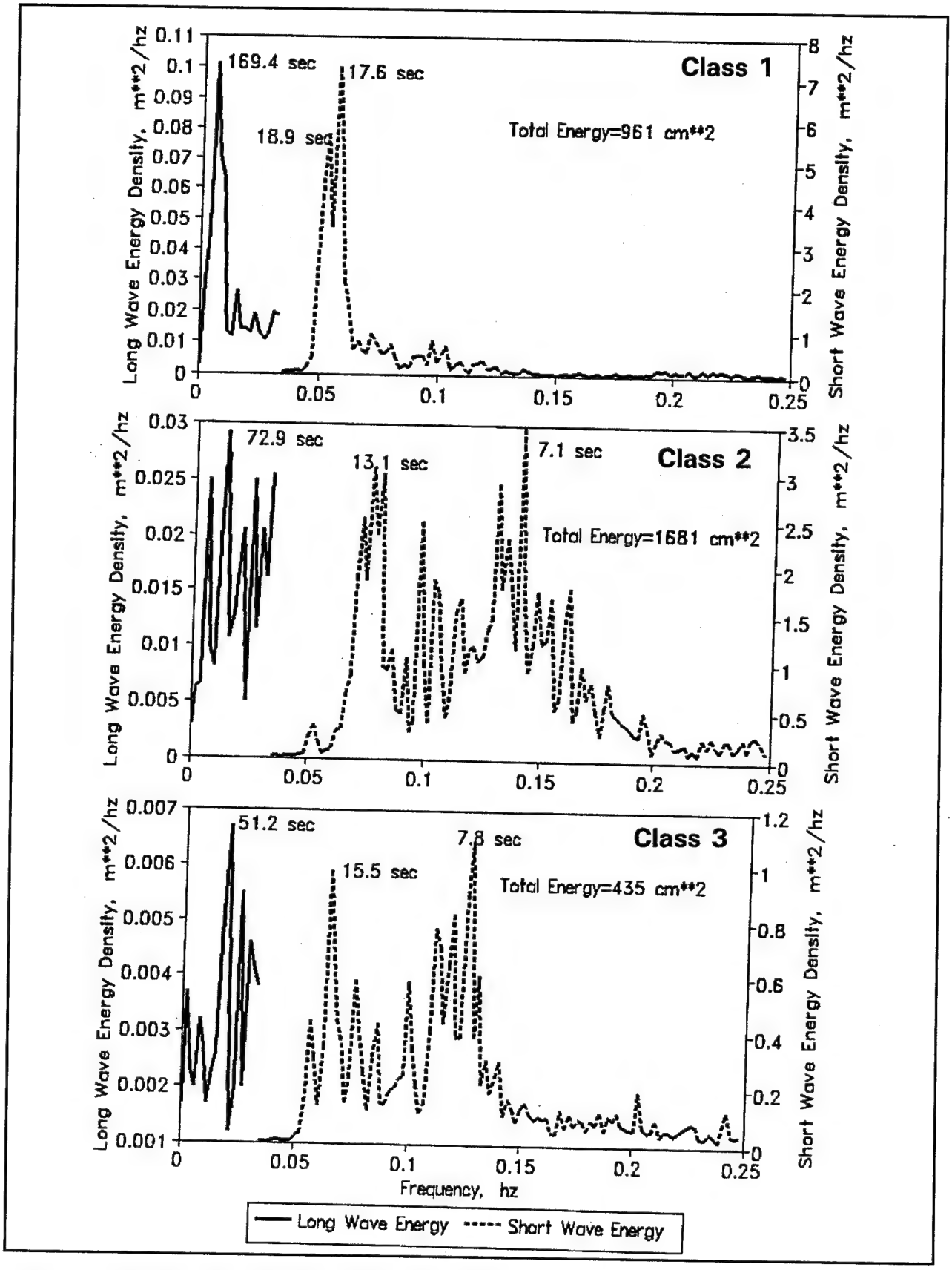

Figure 31. Similarity of long- and short-period wave spectra

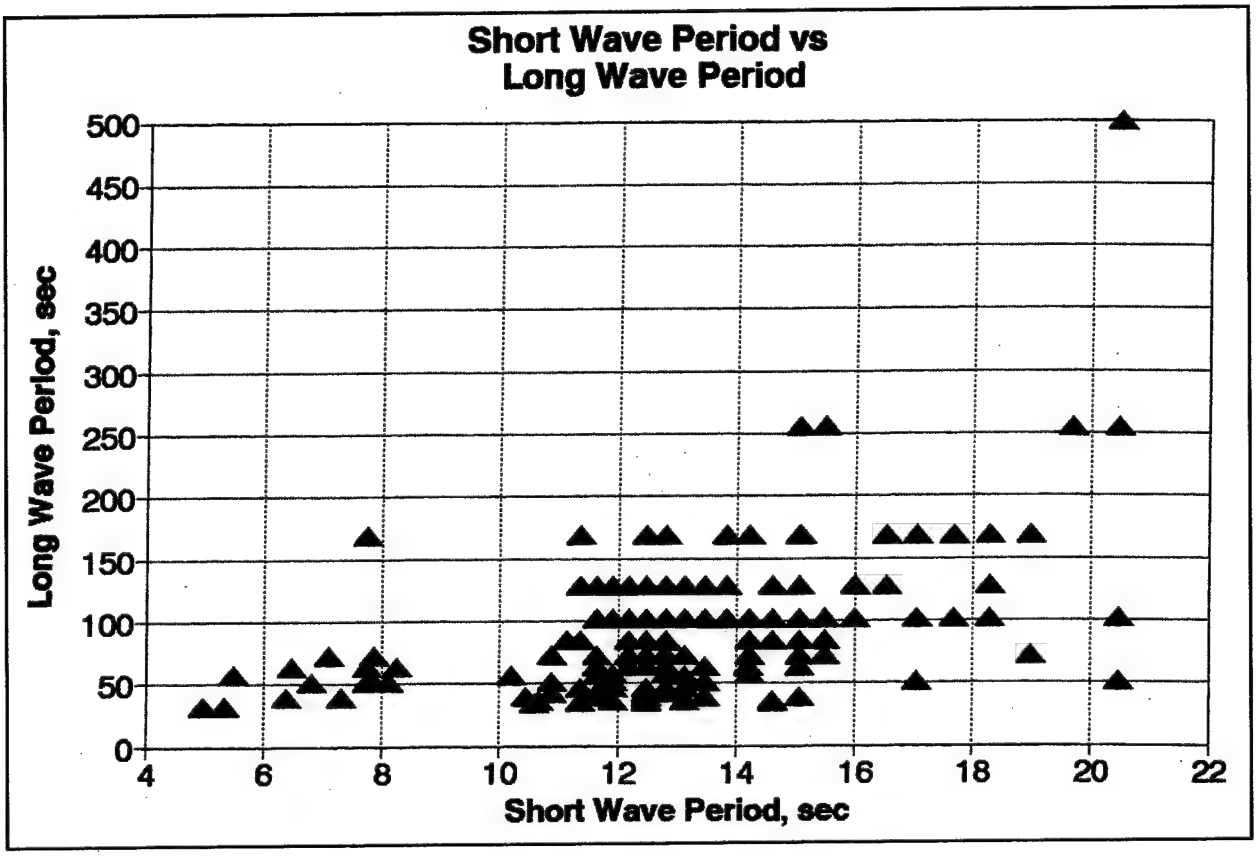

Figure 32. Long-wave period versus short-wave period, January-February 1986

$$H_L = 0.074 \frac{H^2 T^2}{h^2} \tag{2}$$

with

H_L = long-wave height, m

H = short-period significant wave height, m

T = short-wave period, sec

h = water depth, m

Using this equation, a detailed data set from January-February 1986 was examined. The calculated bound long wave was compared with the actual measurements at Platform Edith. Figure 33 shows the results that indicate that the calculated bound energy is only a fraction of the measured long energy. Others have observed this same result (Okihiro, Guza, and Seymour 1993; Bowers 1980).[1] Typically, the difference in energy is called free energy and is postulated to originate from the effect of breaking wave

[1] Personal Communication, 1995, F. E. Sargent, U.S. Army Engineer Waterways Experiment Station, Vicksburg, MS.

groups at the shoreline, where the bound wave is freed and reflected seaward where it may become a "trapped" wave that is "caught" along the shoreline by being refracted shoreward where it is again reflected seaward and so on, or it is completely reflected seaward. Also, the movement of the breaker zone has been found to generate free long waves. The location of Platform Edith (see Figure 9, then Figure 7) does not lend itself to receiving this free energy from the adjacent shoreline because of its distance from the shoreline and especially for waves from the west, which would be reflected south, away from the gauge. Because of the strong correlation between the measured short-period wave height and long-period wave height in relatively deep water, it would appear that there must be free waves associated with the bound wave in the original wave train moving shoreward. Figure 34 shows a comparison between Platform Edith and a gauge at Angels Gate, oceanward of the entrance to Los Angeles Harbor (20-m depth), that was installed in 1991. Of interest is the close correspondence of long-energy level over the 12.9-km distance between Edith and Angels Gate, while short waves at Angels Gate have reduced significantly because of refraction. The waves during this time period were from the west, so little reflected energy would be expected at gauge Edith. This then is indicative that the incoming long-wave energy was fairly uniform over the distance from Edith to the harbors; that most of the energy at Angels Gate and Edith was free wave energy; and that this free energy was associated with the incoming short waves in deeper water, west of the gauges.

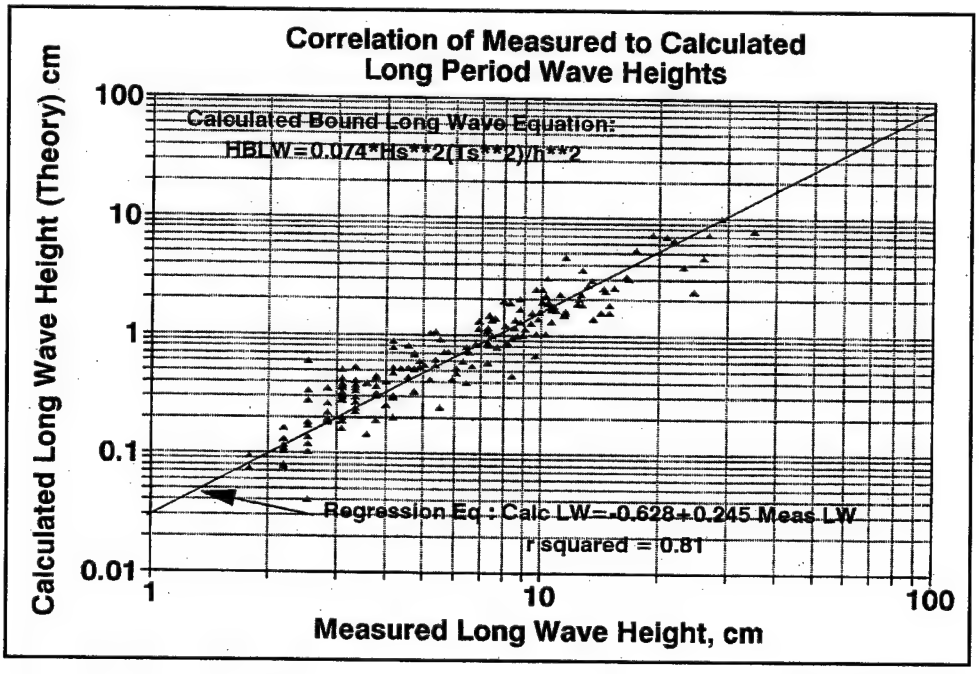

Figure 33. Correlation of measured to calculated long-period wave height

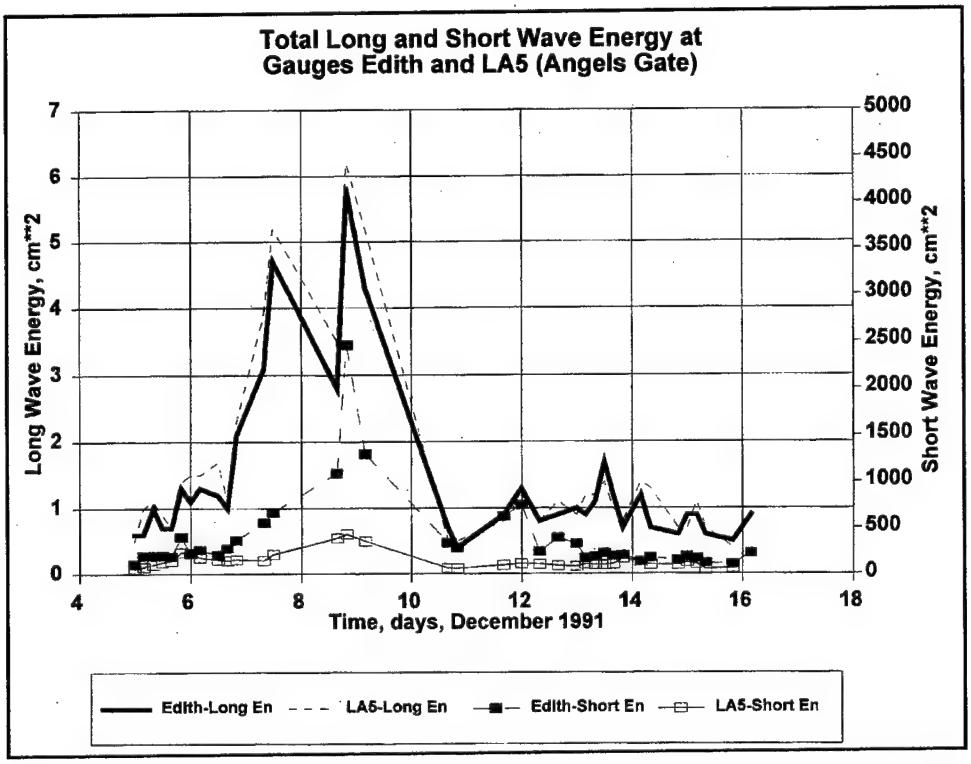

Figure 34. Total long- and short-wave period energy at ocean gauges Edith and LA5 (Angels Gate), December 1991

Correlation of short-wave period and long-wave period

As discussed earlier for the analyzed January-February 1986 data set, there appears to be some correlation of period between long- and short-wave period. Figure 35 shows that generally as the primary short-wave period rises, so does the long-wave period. Bound long-wave theory is developed based on summing frequency differences of all the short component waves of the spectrum. It has been shown that wave interaction near the short-wave spectrum peak forces long waves (Elgar and Guza 1985). Therefore, it would be reasonable to expect frequency differences at the peak short period to be the dominating long-wave periods. For example, period differences (inverse of frequency) for a 16-sec wave of 1 sec result in a long period of

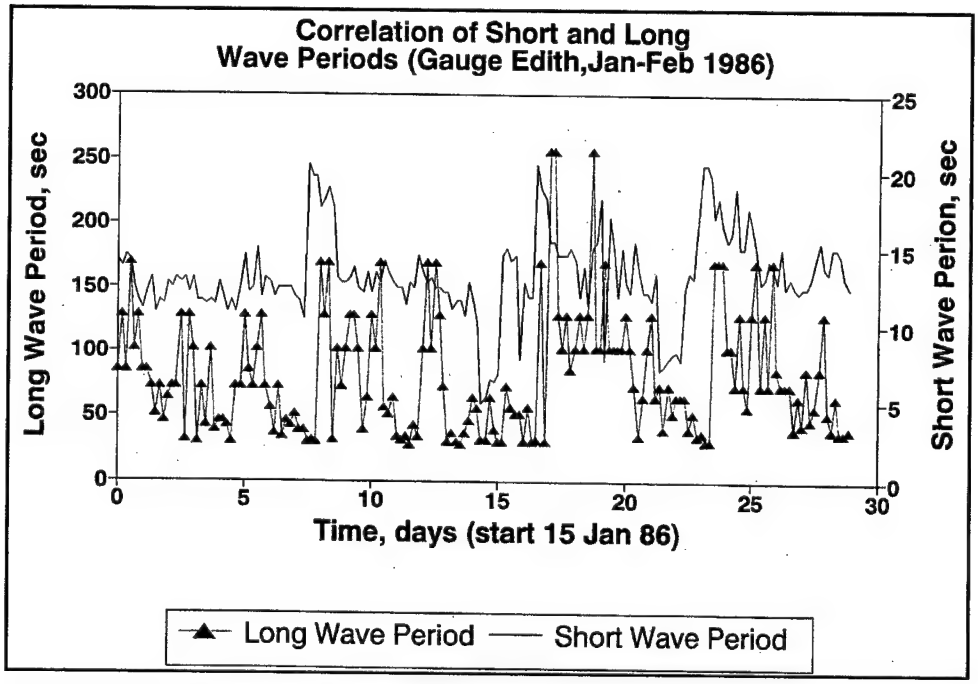

Figure 35. Long- and short-wave period, January-February 1986

$$\Delta f_{s_1} = \frac{1}{16} - \frac{1}{17} = 0.00367\ Hz \quad and \quad \Delta f_{s_2} = \frac{1}{15} - \frac{1}{16} = 0.00416\ Hz$$

$$\therefore T_{L_1} = \frac{1}{f_{l_1}} = 272\ sec \quad and \quad T_{L_2} = \frac{1}{f_{L_2}} = 240\ sec$$

Following this logic, a curve can be made for the range of short-wave periods as seen in Figure 36. This can then serve as a model to relate long- and short-wave periods. Comparing the trend of Figure 36 to the data of Figure 32, the trend shown seems to be a reasonable model. The curve of Figure 36 appears to be somewhat of an upper-bound for the prototype data of Figure 32. This would be a likely result because the simple model assumes two pure sine waves with a frequency difference of 1 sec, while there are many frequencies existing in the real data. For example, if frequency differences are 2 or 3 sec, the curve drops as seen in Figure 37. Of interest to note is that for usual short-wave period range up to 22 sec, the correlating long wave extends to just under 500 sec. This is in agreement with the previous result where it was seen that the 512-sec energy band does not correlate well with short-period wave energy.

Identification of the response of various long-period wave-energy bands with respect to the period of the approaching short waves is illustrated in Figure 38. A plot of short-period wave energy approaching the harbor with time as measured at Platform Edith is presented. Also plotted is the

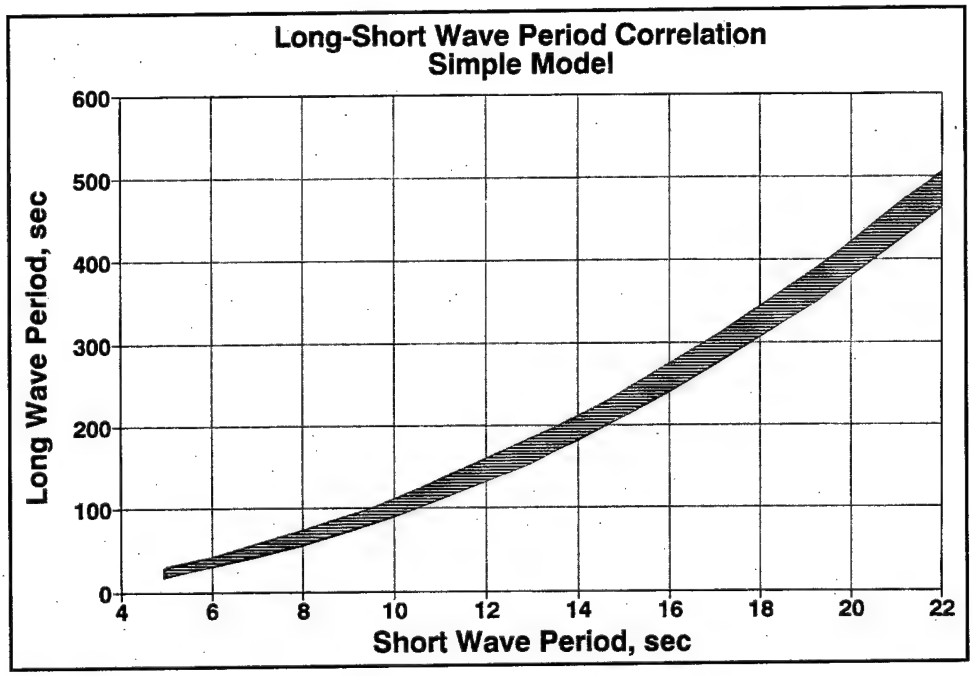

Figure 36. Long- and short-wave period correlation, sample model

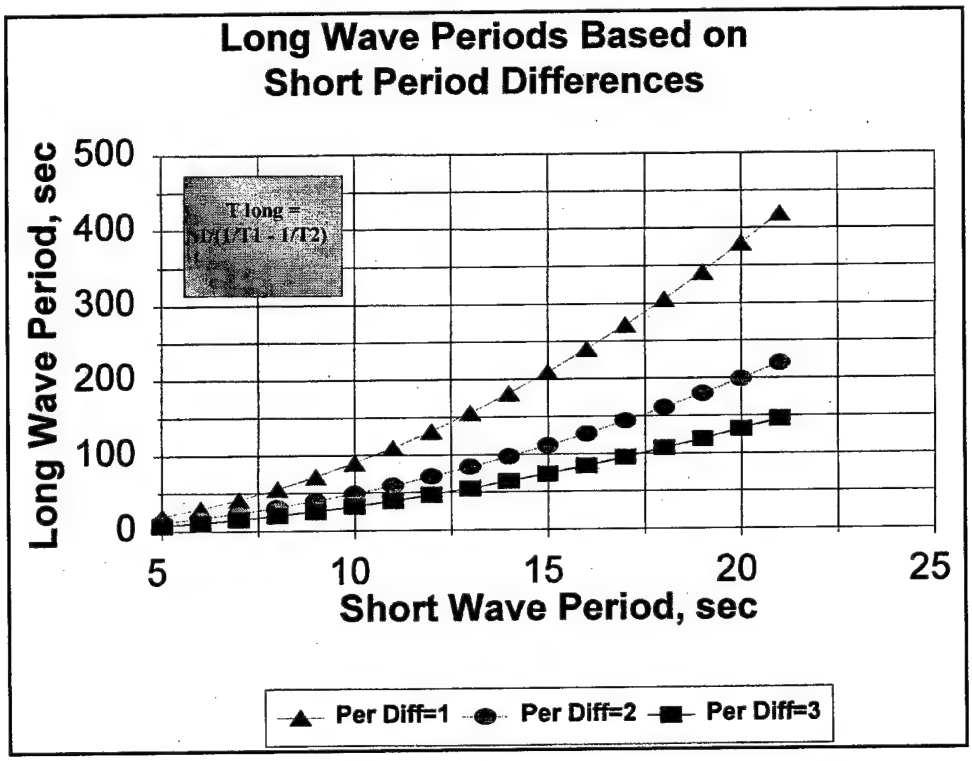

Figure 37. Long-wave period based on short-wave period differences of 1, 2, and 3 sec

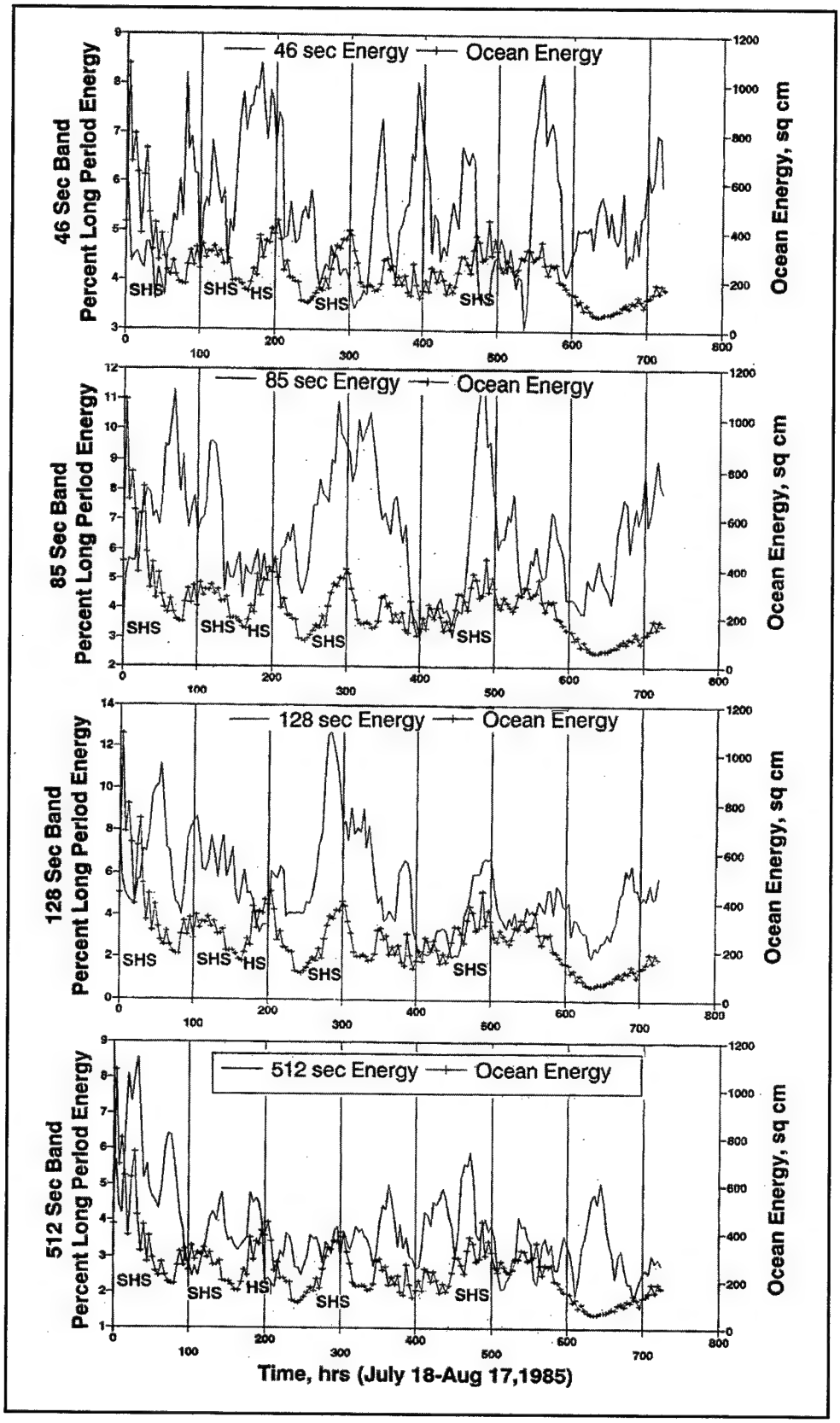

Figure 38. Correlation of long- and short-wave period based on increases in percent of total long energy in long-energy bands

variation of percent of total long-wave energy for a given frequency band at Platform Edith. The sources are noted on the figure. SHS indicates Southern Hemisphere swell, with periods greater than 16 sec, and HS is hurricane swell with periods in the range of 9-12 sec. The actual periods during peak energy are located just above the bottom axis of the plots in the figure. Note that longer period peak wind waves (SHS) are associated with increases of percent of total long-wave energy of the longer long-wave periods. In particular, the 85- and 128-sec period bands respond well to the SHS, while the 46-sec band tends to decrease as a percentage of total long-period energy (hour 300 shows this trend especially well). In the time period proceeding 200 hr, during the arrival of hurricane swell, the percent of energy in the 46-sec band rises, while 85- and 128-sec bands decrease as a percentage of long-period energy. Finally, the 512-sec energy band tends to show little or no correlation to these swell events and seems to peak about every 2 days.

Plots similar to Figure 38 are included in Plates 44 to 59 for the January-February 1986 data set. Plate 60 shows how a short wind wave period varied during that time period, showing the primary wave period where peak short-period energy occurs, secondary period, the period of second highest energy and also whether there was a single-wave train, multiple-wave trains moving in the same direction (collinear), or multiple-wave trains moving in different directions. An examination of these plots confirms the cursory look described in the previous paragraph. A way to look at these data is to note the deviation from the average percentage of long-wave period energy for a given band. When this is done, one sees the following:

a. When an "event" occurs (i.e., there is a rapid rise in the ocean energy curve, e.g., at hours 120, 200, 400-500, and 600), the percent energy in the 32- to 46-sec range of bands (Plates 44 to 49) declines. These events for this data set typically have wave periods greater than 12 sec, so a strong response at these periods is not expected using the simple model of Figure 36.

b. The 51- to 64-sec bands (Plates 50 to 52) tend to show increases over their average energy level for waves in the 8- to 13-sec range of short-wave periods. They increase in percent level for events in this period range.

c. The 73- and 85-sec bands show increases in response for periods in the range of 12 to 16 sec (Plates 53 and 54).

d. The 102- and 128-sec period energy bands have the greatest percentage of energy responses for the very energetic event from 400 to 500 hr (Plates 55 and 56). The greatest effect occurs for wave periods in a 12- to 15-sec range.

e. The 170- and 256-sec period energy bands respond strongly to the events when short-wave periods are longest, especially for 20-sec wave periods (Plates 57 and 58).

f. The 512-sec period energy band fluctuations with respect to ocean energy appear to be more random, with the greatest increase at a low ocean energy level (Plate 59).

Summary

Long-wave periods appear to correlate well with associated short-wave periods. Using a 10-year data set for frequency of occurrence of short-wave period from a gauge at Sunset Beach (located at the eastern end of the harbors), the most frequently occurring periods are in the 13- to 17-sec range (Figure 39). From the analysis above, this would indicate that the most frequent and possibly energetic long-wave periods are 73- to 128-sec bands. In fact, the long-wave energy distribution measured at Edith (Plate 1) indicates that the 102-sec band has the highest average energy peak with 128-, 85-, and 73-sec bands near the peak. Figure 40 also shows average monthly distribution at gauge Edith for a 3-year period. Peak long-period ocean energy usually occurs at 73-, 85- or 102-sec bands. Important with regard to this is that moored ships are affected by this range of periods. Wavelengths for this range of periods in 13- to 20-m depths of water vary between 600 and 1,500 m, so that the opportunity for wave amplification is present in many harbor locations.

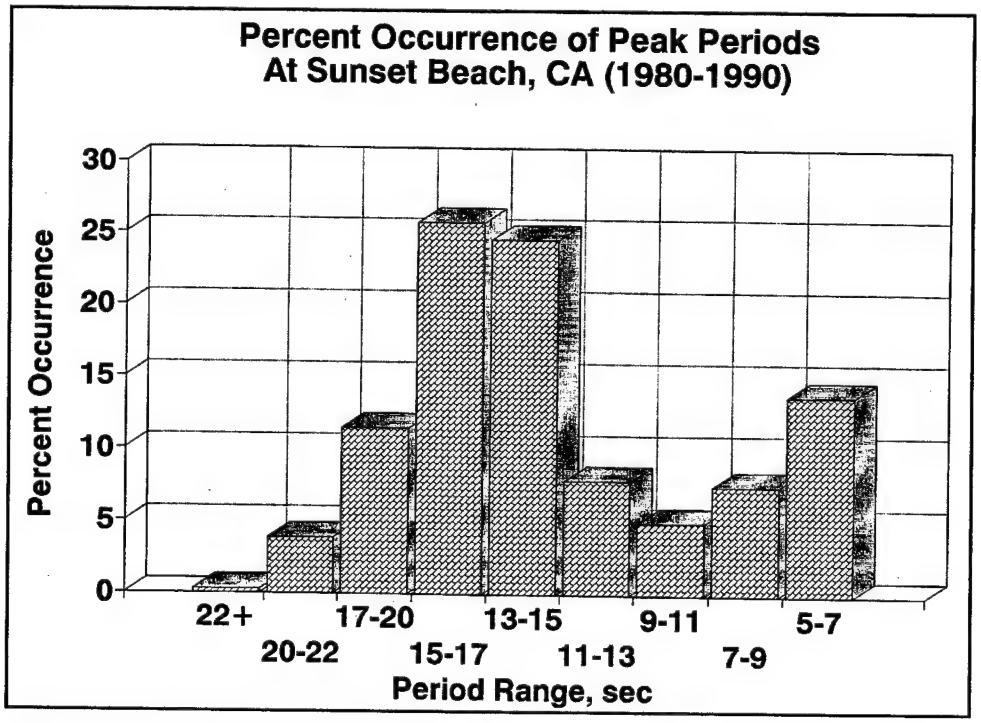

Figure 39. Percent occurrence of peak short-wave periods at Sunset Beach, CA, 1980-1990

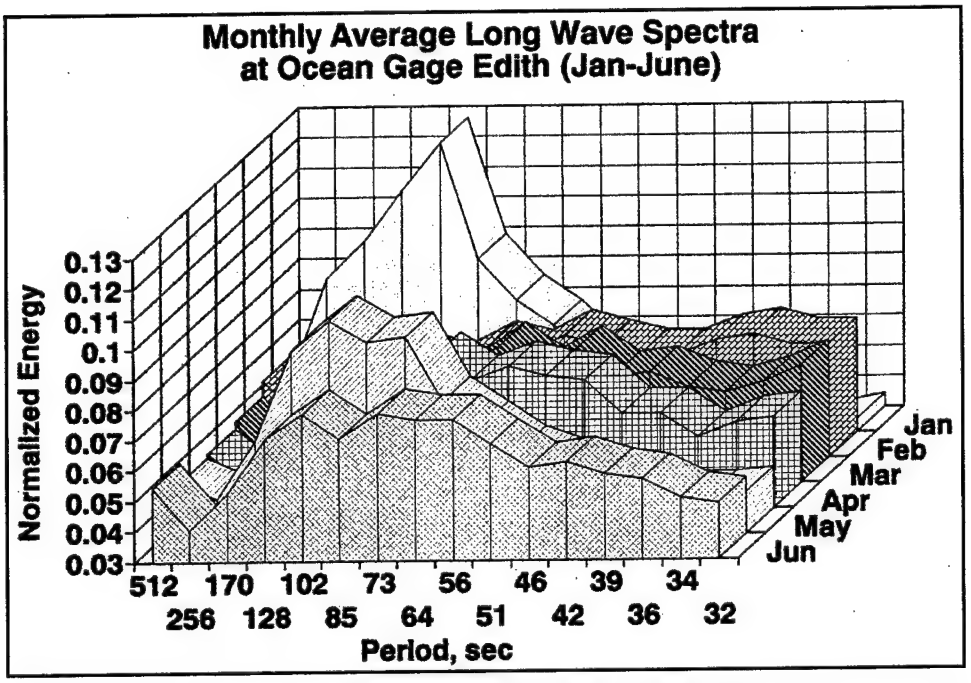

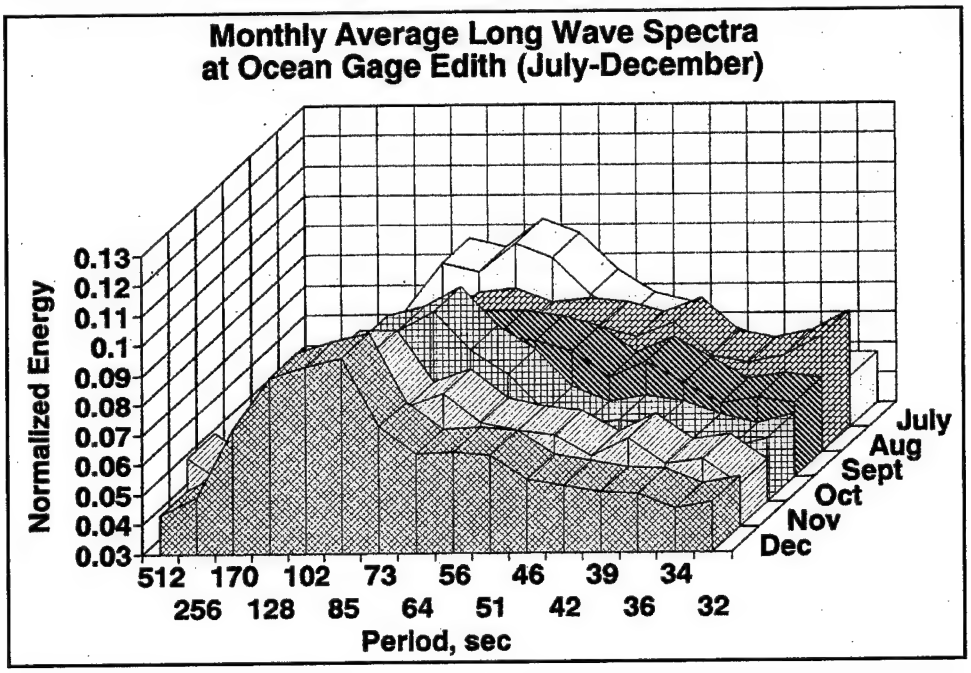

Figure 40. Monthly average long-wave spectra at ocean gauge Edith

6 Long Waves and Moored Ships

Correlation of Moored-Ship Motion to Long Waves

Long-wave periods (30 sec and higher) may be in the same range as the natural frequency of a moored-ship system. Thus, the ship may respond with strong movement, causing difficult loading/unloading conditions or even damage to the facilities. Further compounding difficulties, the long-period waves may occur at resonant frequencies of the basins in which ships are moored. A complex harbor configuration, such as the Los Angeles-Long Beach harbors, creates the possibility of many different resonant frequencies occurring in the different berths. An examination of prototype moored-ship movement and associated wave conditions follows.

Ship-motion observations

The Ports of Long Beach and Los Angeles have been making observations at certain locations in their harbors and noting when ship motion is greater than usual. A somewhat subjective light, medium, or heavy motion scale has been used, and a form (Plate 61) is filled out by personnel working at the berth describing the mooring condition and mode of movement. Totaling a 5-year group of observations at Berth 245, Port of Long Beach, near gauge LB2 (see Figure 14), cargo-handling difficulties were distributed as seen in Figure 41. An analysis by Burke (1987)[1] of the monthly level of motion where "light" motion has a numerical value of 1, "medium" a value of 2, and "heavy" a value of 3 is seen in Figure 42. There is a definite bimodal trend for maximum average level of motion curve of Figure 42. With peaks at February and July, it appears Southern Hemisphere swell and hurricane swell may produce as much troublesome mooring conditions as the high-energy winter storms from the west at this berth location.

[1] Unpublished Memorandum, 1987, Michael Burke, Port of Long Beach, CA.

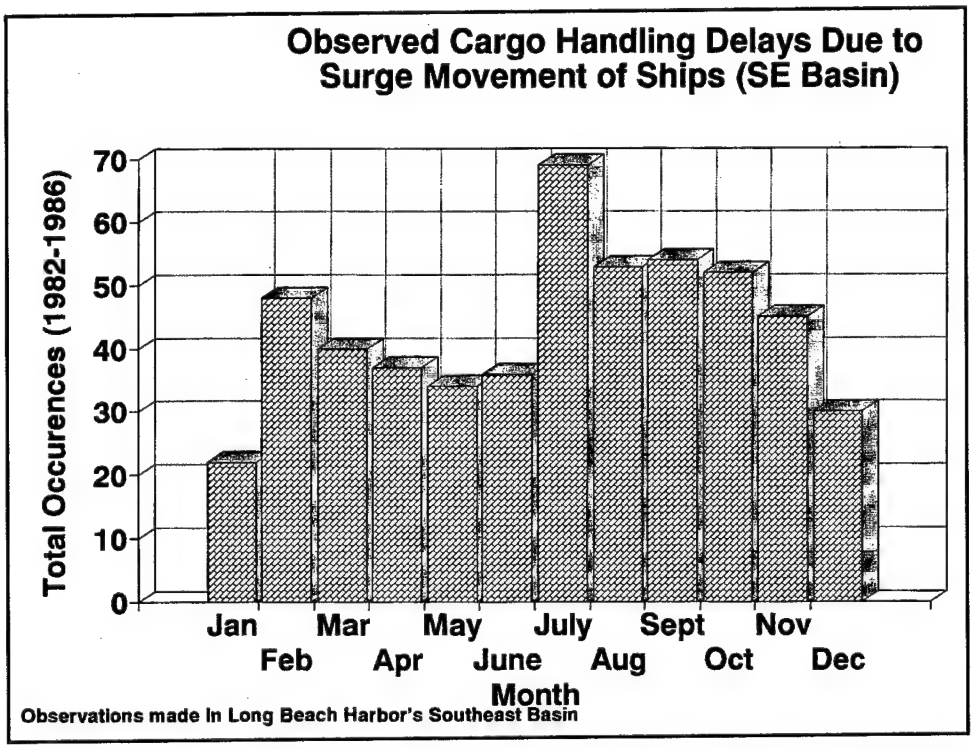

Figure 41. Observed cargo-handling delays because of surge movement of ships in Long Beach's Southeast Basin

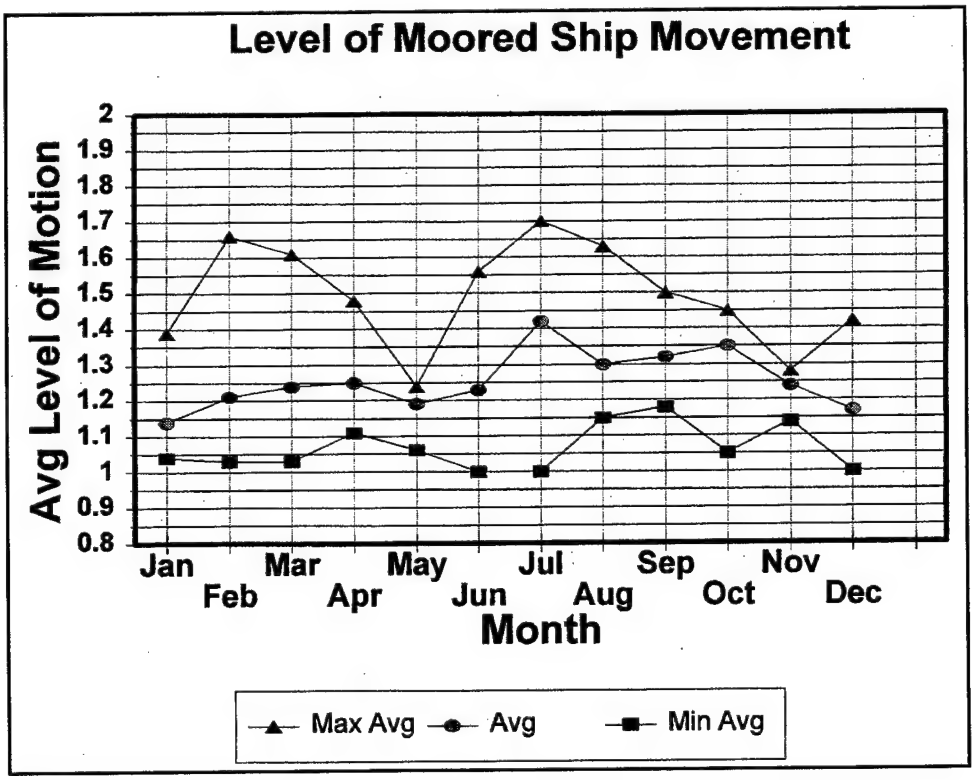

Figure 42. Maximum, minimum, and average level of motion by month in Long Beach's Southeast Basin (Unpublished Memorandum, 1987, Michael Burke, Port of Long Beach, CA)

Information on long-period waves that were occurring during the ship-movement observations was identified. Figure 43 shows the energy at the various wave-period bands for the three classifications of movement, along with the average energy observed (noted in insert box) at gauge LB2, which was located at the berth being monitored. Energy during light-motion observations is less than the usual average level at all but the 73-sec energy band, indicating this period range is likely to be important for the container-ship movement at this berth location. Energies in other bands also are higher than average for the medium- and heavy-motion categories. The comparison of total energies for light, medium, and heavy motion (see insert box of Figure 7) to the total long-period energy distribution at gauge LB2 (Plate 62) reveals that these are not extremely high energies on the occurrence curve. However, no downtime was recorded for any of the limited data tabulated, but loading/unloading difficulties were evidently encountered.

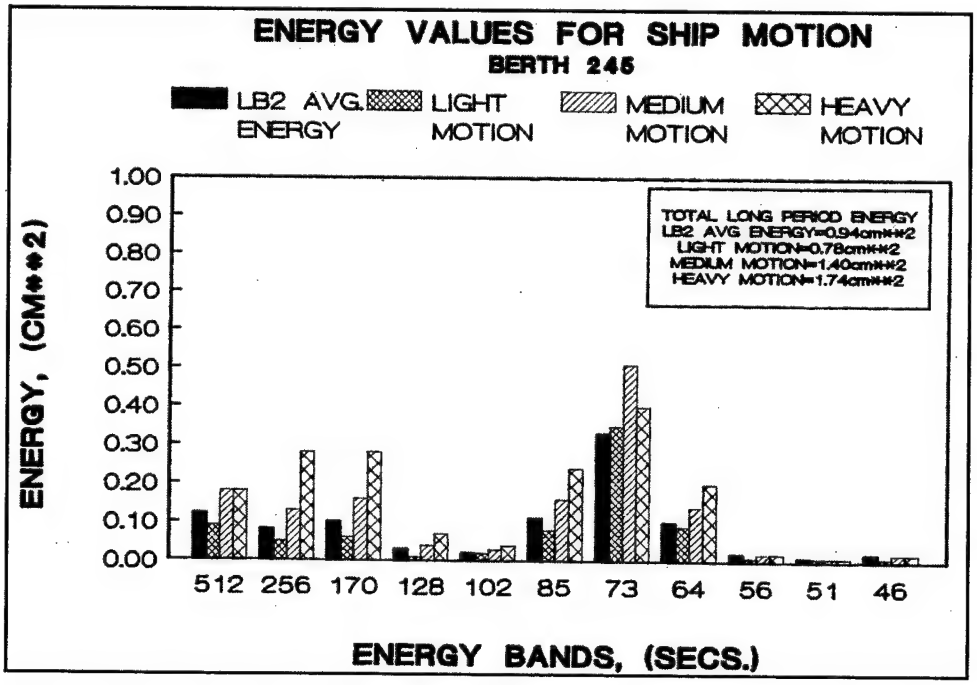

Figure 43. Energy values for moored-ship-motion events at Long Beach Berth 245

Since some criteria for ship movement are based on wave height, the energy bands at gauge LB2 covering 41-205 sec, thought most important for moored-ship movement, were summed together and a wave height determined using Equation 1. Scatter plots of long-period wave height (41-205 sec) versus total energy measured at LB2 (covering wave periods from 8-1,024 sec) separated into light, medium, and heavy motion are seen in Figure 44 for 1982-84 data and indicate wave heights ranging between 2 and 17 cm for notable ship movement. Plates 63 and 64 are plots that contain similar information for 1984-86 and 1987-88, respectively. Average wave heights for these two groups were 3.65 and 2.82 cm, covering all levels of movement.

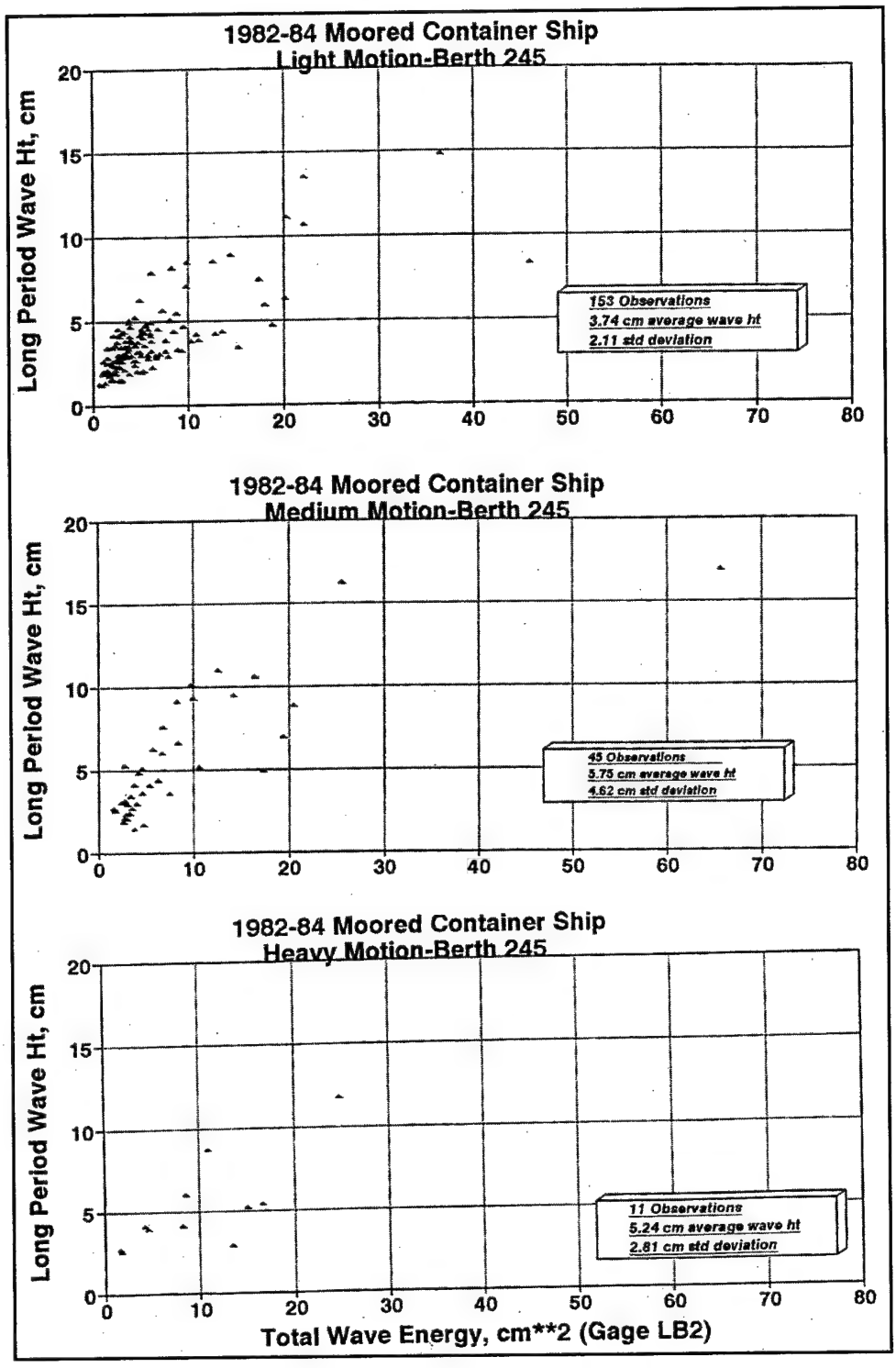

Figure 44. 1982-1984 long-wave height at Long Beach Berth 245 during light, medium, and heavy moored-ship-motion events

A plot of the maximum energy at gauge Edith for each individual period band that occurred when data were available during the movement observations in the 1984-87 period appears in Plate 65. The energy value at one wave energy is not necessarily occurring simultaneously as that at another band. The average energy level for each band is also shown. The greatest value of ocean energy during moored-ship-movement events occurs at the 171-sec energy band and decreases somewhat smoothly toward the smaller periods.

Moored-Ship Wave-Height Criteria

Based on field studies, Wilson (1967) determined a relationship between long-wave period and wave height that indicates the level at which problems for berthed ships might occur. Examining Wilson's relationship in Figure 45, one sees that as the long-wave period increases, a greater wave height is required to cause damage. Another reference suggests that for 100-percent cargo handling efficiency rate, the significant wave height for long waves should be less than 5-10 cm if man-made fiber lines are used and should be less than 10-15 cm if steel wires are used for mooring.[1] Comparing this to Wilson's curve, one sees that the two criteria are in reasonable agreement. Also, the wave heights collected at Berth 245 (gauge LB2) fall in the vicinity of Wilson's value of about 9 cm for a

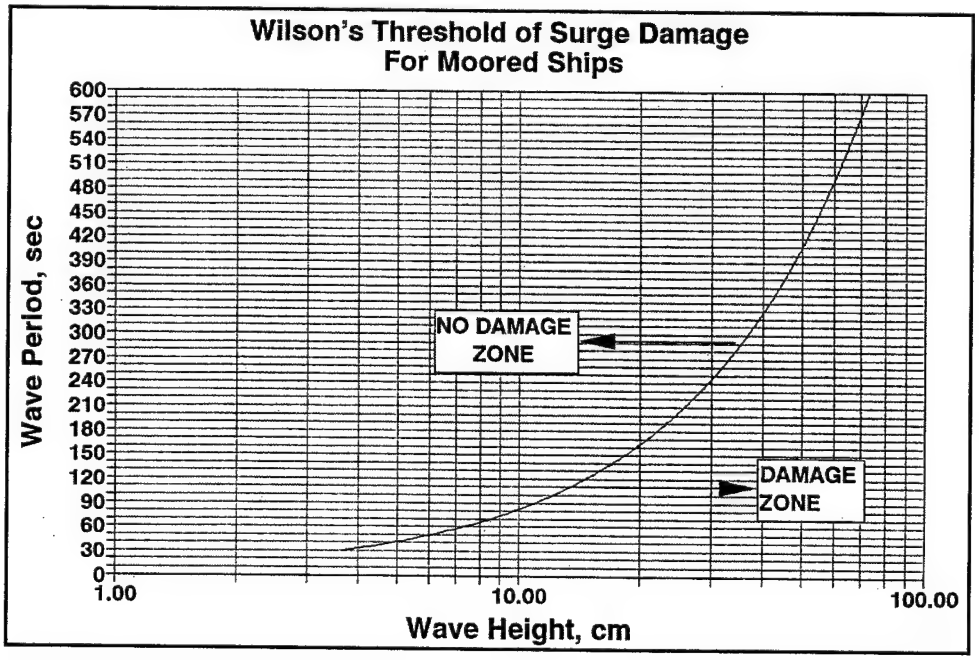

Figure 45. Wilson's threshold wave height for surge damage of moored ships

[1] Personal communication, 13 October 1993, Drs. Kimo Walker and Paul Szwetlot, Pier 400 Design Consultants, Los Angeles, CA.

70-sec wave, the dominant period at that berth, though most values are less and no instances of damage were reported over the period studied.

Long-Wave Energy Occurrence/Downtime

In order to relate the ocean wave activity to downtime for unloading/loading, first response curves for a given harbor location relative to some location in the ocean are determined by physical and/or numerical models of long-wave oscillations in the harbor. Using energy or wave-height exceedance curves (as discussed in Chapter 4) at the ocean gauge, each gauge and each energy band at that gauge can be related to the ocean gauge, and energy (or wave height) exceedance curves for the harbor gauge site can be developed. Using the results of a numerical ship-motion model (e.g., Sargent, in preparation), which will indicate the level of energy that would cause loading/unloading problems, and the energy exceedance curves, downtime can be determined.

7 Summary and Conclusions

A major activity of the Los Angeles-Long Beach Harbors Model Enhancement Program was Task A.3, Harbors Resonance Analysis. The work involved in this activity focused on understanding the long waves, which can cause harbor resonance in the range of wave period that can contribute to difficult mooring conditions for large vessels such as container ships. This was done by examining prototype long-wave data collected at one ocean gauge and seven harbor gauges. Conclusions reached from this analysis were as follows:

a. Long waves have caused surge and associated mooring problems in the Ports since the turn of the century.

b. Long waves (periods ranging from 30 to 500 sec) can be associated with the wind waves that approach the Los Angeles and Long Beach harbors. In particular, increases in short-period wave energy (5- to 25-sec wave periods) are accompanied by increases in long-wave energy, no matter where the source of incoming energy is from (e.g., Southern Hemisphere swell, hurricane swell, or winter storms from the west).

c. Ocean long-wave energy (from 32 to 512 sec) is on the average fairly uniformly distributed, with the peak occurring at a 102-sec energy band (covering periods of 93-113 sec).

d. The long-wave data collected at each harbor site show a characteristic wave energy response dependent on gauge location over period bands from 32 to 512 sec. The response may vary in magnitude because of offshore wave conditions, but the change is relative and the characteristic response shape is maintained.

e. Different harbor gauge locations have different energy levels for the same incident ocean energy conditions because of various degrees of wave amplification at each location.

f. Correlation information explains that the long-wave energy that affects the harbors is strongly tied to the short-wave energy approaching the harbors and the long energy transforms uniformly

into the harbor probably because of the relatively large depths (15-30 m) associated with these harbors.

g. Periods in the 512-sec energy band in the harbors do not correlate with the ocean short-period energy, indicating another source, other than short-period waves, forces this period range.

h. Close correlation of spectral shape of the short and long spectra and short- and long-peak periods was seen.

i. Correlating peak periods of the long and short spectra to one another indicated trends for shorter wind wave periods to correlate to shorter long waves and longer wind wave periods relating to longer long-wave periods.

j. The most frequently occurring short-wave periods are in the 13- to 17-sec range, and the most frequent and energetic ocean long-wave periods are 73- to 128-sec period bands.

k. Calculated bound long-wave heights when compared with measured long-wave heights at ocean gauge Edith are a small percentage (5 percent) for low-energy conditions and increase to about 25 percent for high-energy conditions.

l. Measured long-wave energy at ocean gauge Edith and at an ocean gauge at Los Angeles Harbors Angels Gate indicates similar long-period energy and wave height at both locations (gauges 14.3 km apart), while short-wave heights are significantly different. Apparently, long-wave energy associated with incoming short waves is uniformly distributed in the local offshore region adjacent to the harbors.

m. Moored ships are affected by the range of long-wave periods mentioned in conclusion *j*. Wavelengths for this range of periods in 13- to 20-m depths of water vary between 600 and 1,500 m, so that the opportunity for wave amplification is present in many harbor locations.

n. Moored-ship movements have two peak periods of activity, with limited data indicating February and July as months of maximum activity for the Los Angeles and Long Beach harbors. These periods are associated with peak times of short- and long-wave activity in the winter and summer season.

o. Observations of significant moored-ship movement indicate long-wave heights of 2 to 17 cm occurred in conjunction with the events. These wave heights were based on the energy measured in the harbor berth in the 41- to 205-sec period range. Long-wave energy in the ocean was at a lower level.

References

Benjamin, T. B., and Feir, J. E. (1967). "The disintegration of wave trains on deep waters; Part 1, Theory," *Journal of Fluid Mechanics* 27(3), 417-430.

Bowers, E. C. (1980). "Long period disturbances due to wave groups." *Proceedings of the Seventeenth Coastal Engineering Conference, Volume 1.* ASCE, New York, 610-23.

_____. (1992). "Low frequency waves in intermediate depths." *Proceedings of the Twenty-third Coastal Engineering Conference, Volume 1.* ASCE, New York, 832-45.

Durham, D. L., Thompson, J. K., Outlaw, D. G., and Crosby, L. G. (1976). "Los Angeles and Long Beach harbors model study; Report 3, Analyses of wave and ship motion," Technical Report H-75-4, U.S. Army Engineer Waterways Experiment Station, Vicksburg, MS.

Elgar, S., Guza, R. T. (1985). "Observations of bispectra of shoaling surface gravity waves," *Journal of Fluid Mechanics* (161), 425-448.

Hasselmann, K. (1962). "On the non-linear energy transfer in a gravity wave spectrum, 1. General theory," *Journal of Fluid Mechanics* (12), 481-500.

Herbers, T. H. C., Elgar, S. Guza, R. T., and O'Reilly, W. C. (1992). *Proceedings of the Twenty-third Coastal Engineering Conference, Volume 1.* ASCE, New York, 846-59.

Hubertz, J. M., Payne, J. B., and Farrar, P. D. (1995). "Hindcasting swell from the Southern Ocean along the U.S. Pacific coast," WIS Report 32, U.S. Army Engineer Waterways Experiment Station, Vicksburg, MS.

Jensen, R. E., Hubertz, J. M., Thompson, E. F., Reinhard, R. D., Borup, B. J., Brandon, W. A., Payne, J. B. Brooks, R. M., and McAneny, D. S. (1992). "Southern California hindcast wave information," WIS Report 20, U.S. Army Engineer Waterways Experiment Station, Vicksburg, MS.

Longuet-Higgins, M. S., and Stewart, R. W. (1964). "Radiation stresses in water waves: A physical discussion with applications," *Deep Sea Research* 11, 529.

McGehee, D. D. (1991). "Los Angeles and Long Beach Harbors Model Enhancement Program, measured response of moored ships to long-period waves," TR CERC-91-12, U.S. Army Engineer Waterways Experiment Station, Vicksburg, MS.

McKinstry, C. H. (1914). Los Angeles and Long Beach Harbors, California; Report of the Corps of Engineers, Document No. 896, House of Representatives, 63rd Congress, 2nd Session, Washington, DC, April 14, 1914.

Okihiro, M., Guza, R. T., and Seymour, R. J. (1993). "Excitation of seiche observed in a small harbor," *Journal of Geophysical Research* 98(C10), 18201-18211.

Rosati, J., and Puckette, P. T. (1993). "Measurement and analysis of wave data in Los Angeles and Long Beach harbors." *Proceedings, WAVES 93, The Second Symposium on Ocean Wave Measurement and Analysis.*

Rosati, J., McKinney, J. P., and Puckette, P. T. (1998). "Los Angeles and Long Beach Harbors Model Enhancement Program: Prototype wave data summary," Technical Report CHL-98-21, U.S. Army Engineer Waterways Experiment Station, Vicksburg, MS.

Sargent, F. E. "Los Angeles and Long Beach Harbors Model Enhancement Program, calibration and verification of MSMAP using LA-LB prototype data," Report in preparation, U.S. Army Engineer Waterways Experiment Station, Vicksburg, MS.

Seabergh, W. C. (1985). "Los Angeles and Long Beach Harbors Model Study, deep-draft dry bulk export terminal, Alternative No. 6: Resonant response and tidal circulation studies," Miscellaneous Paper CERC-85-8, U.S. Army Engineer Waterways Experiment Station, Vicksburg, MS.

Seabergh, W. C., and Thomas L. J. (1993). "Los Angeles and Long Beach Harbors Model Enhancement Program, improved physical model harbor resonance methodology," Technical Report CERC-93-17, U.S. Army Engineer Waterways Experiment Station, Vicksburg, MS.

Tracey, B. A., and Hubertz, J. M. (1990). "Hindcast hurricane swell for the coast of Southern California," WIS Report 21, U.S. Army Engineer Waterways Experiment Station, Vicksburg, MS.

Wilson, B. W. (1967). "The threshold of surge damage for moored ships." *Institute of Civil Engineers, Volume 38*. London, 107-132.

Wilson, B. W. (1972). "Seiches." *Advances in hydroscience*. Ven Te Chow, ed., Vol 8-1972, Academic Press, New York, 1-94.

Wilson, B. W., Jen, Y., Hendrickson, J. A., and Soot, H. (1968). "Final report, wave and surge-action study for Los Angeles-Long Beach harbors," Volume 1, Prepared for U.S. Army Engineer District Los Angeles, Science Engineering Associates, San Marino CA.

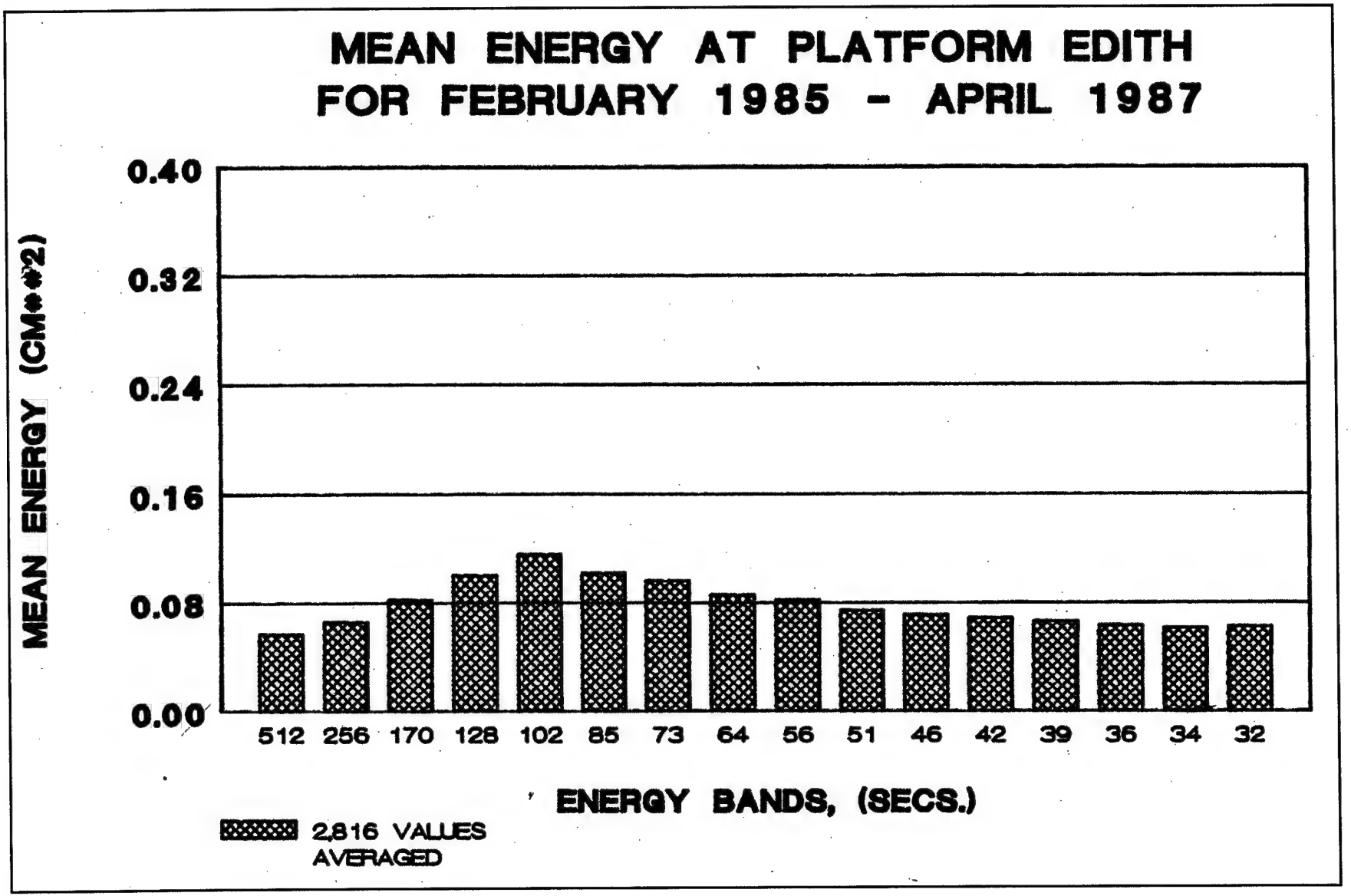
MEAN ENERGY AT PLATFORM EDITH
FOR FEBRUARY 1985 - APRIL 1987
MEAN ENERGY (CM**2)
0.40
0.32
0.24
0.16
0.08
0.00
512 256 170 128 102 85 73 64 56 51 46 42 39 36 34 32
ENERGY BANDS, (SECS.)
2,816 VALUES AVERAGED

Plate 1

Plate 2

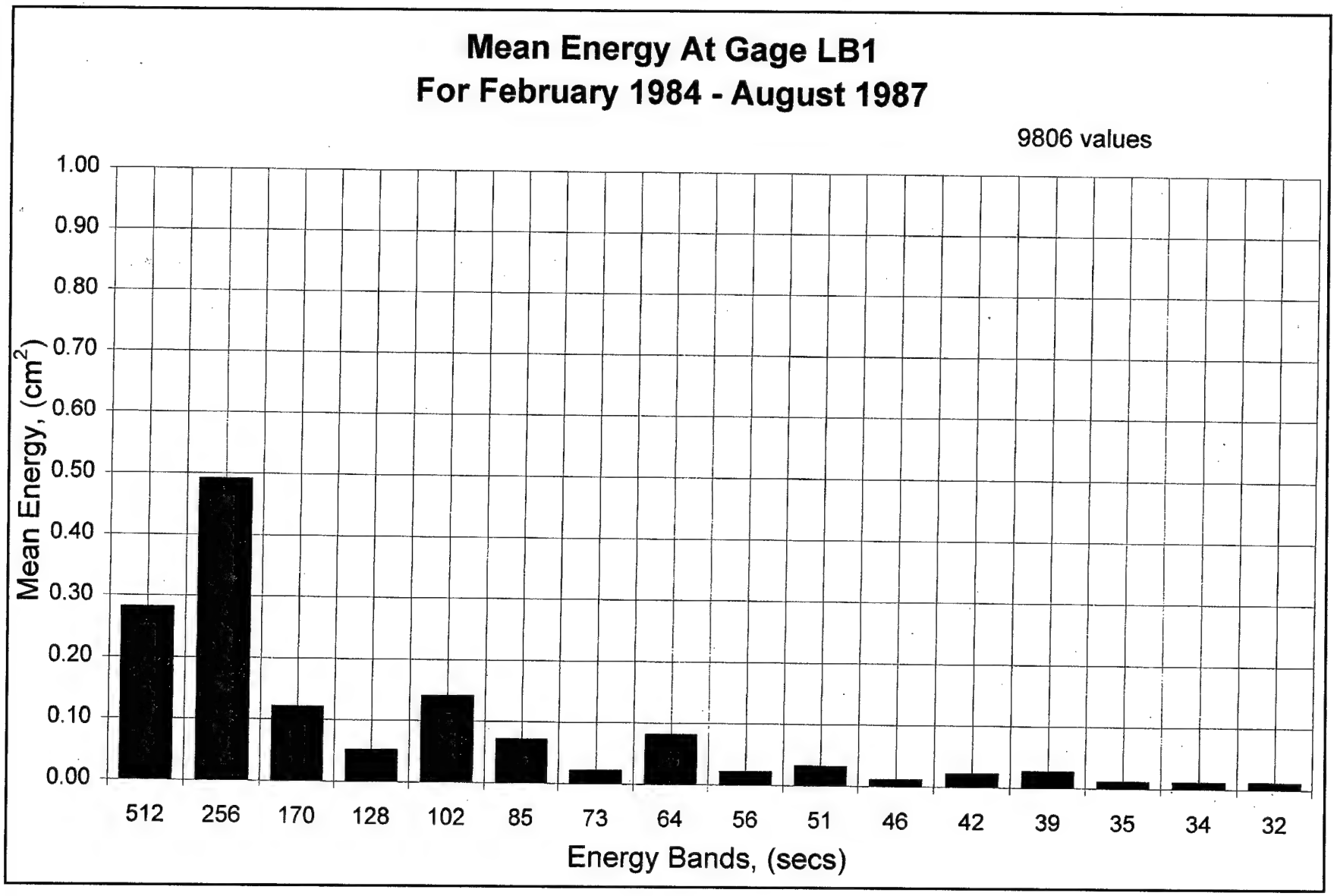
Mean Energy At Gage LB1
For February 1984 - August 1987
9806 values
Mean Energy, (cm2)
1.00
0.90
0.80
0.70
0.60
0.50
0.40
0.30
0.20
0.10
0.00
512
256
170
128
102
85
73
64
56
51
46
42
39
35
34
32
Energy Bands, (secs)

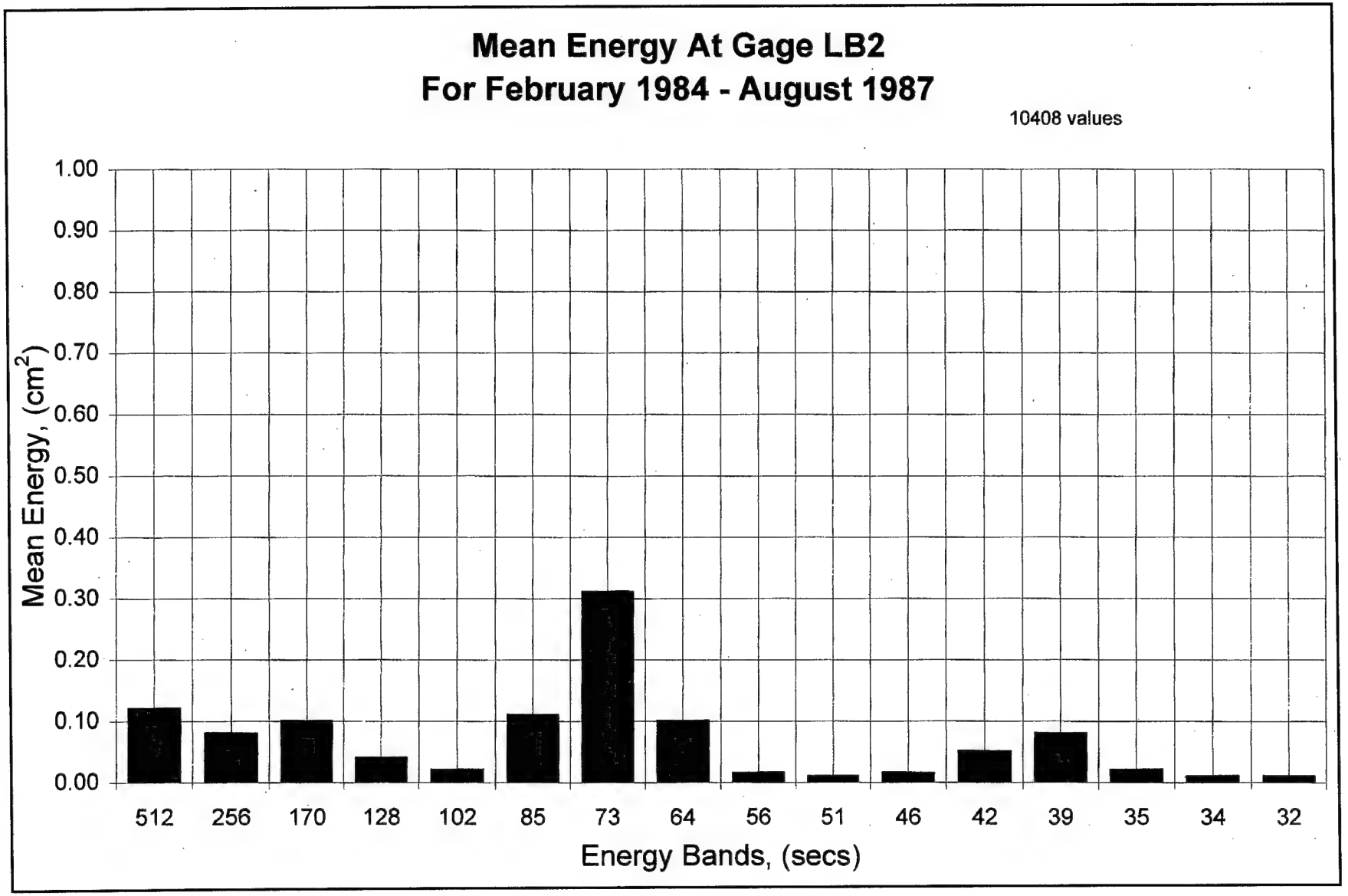
Mean Energy At Gage LB2
For February 1984 - August 1987
10408 values
Mean Energy, (cm2)
1.00
0.90
0.80
0.70
0.60
0.50
0.40
0.30
0.20
0.10
0.00
512
256
170
128
102
85
73
64
56
51
46
42
39
35
34
32
Energy Bands, (secs)

Plate 3

Plate 4

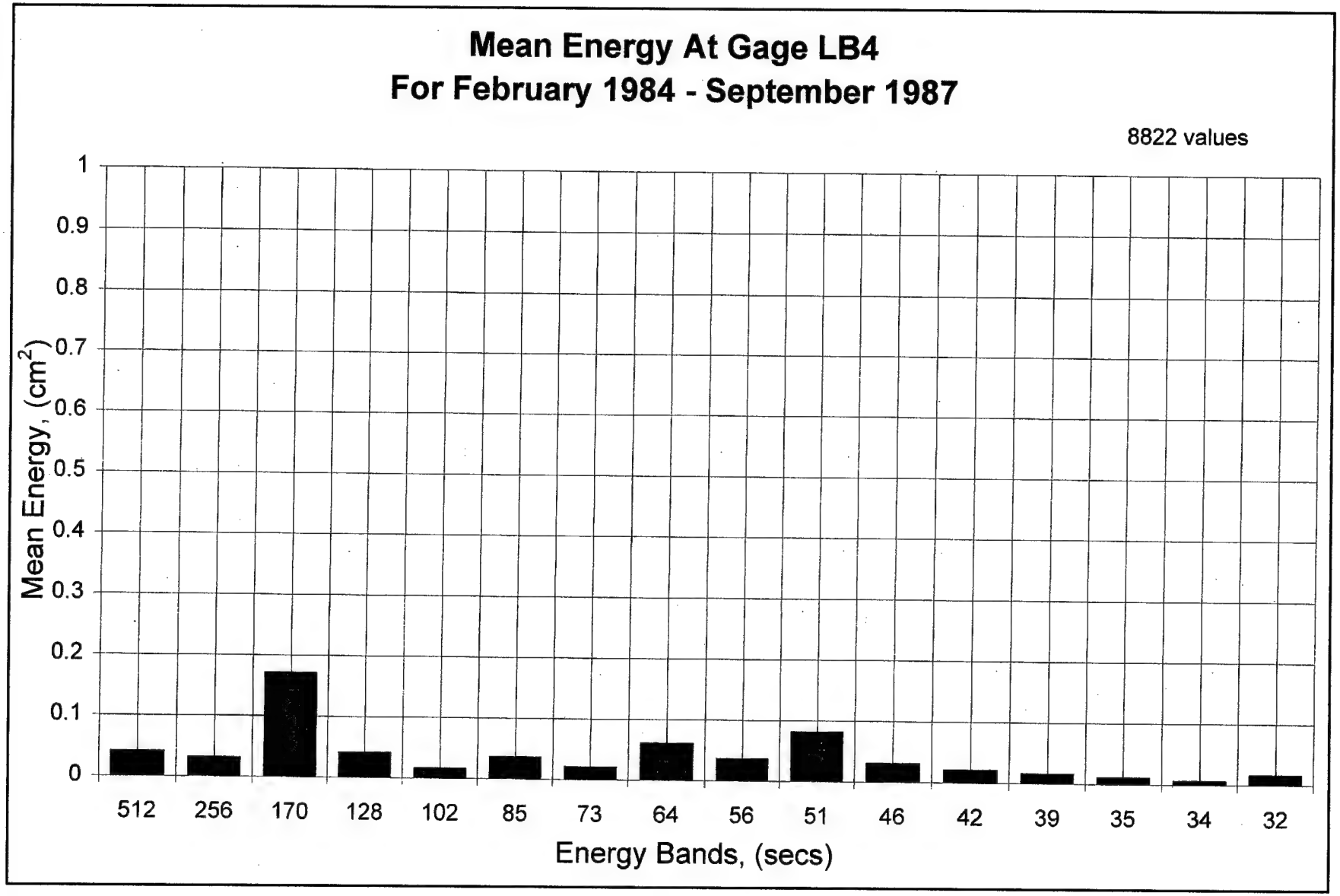
Mean Energy At Gage LB4
For February 1984 - September 1987
8822 values
Mean Energy, (cm2)
1
0.9
0.8
0.7
0.6
0.5
0.4
0.3
0.2
0.1
0
512
256
170
128
102
85
73
64
56
51
46
42
39
35
34
32
Energy Bands, (secs)

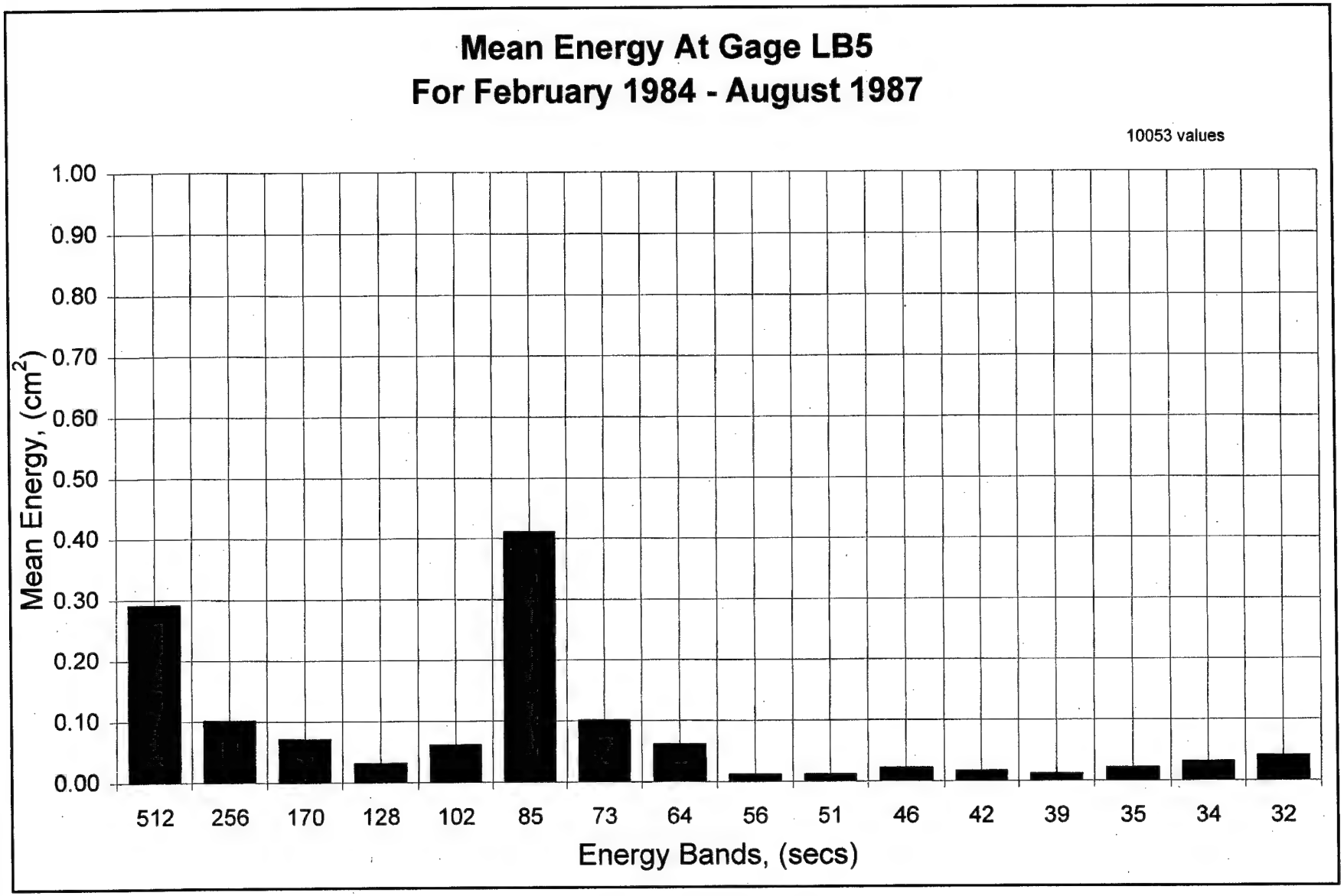
Mean Energy At Gage LB5
For February 1984 - August 1987
10053 values
1.00
0.90
0.80
0.70
0.60
0.50
0.40
0.30
0.20
0.10
0.00
Mean Energy, (cm2)
512
256
170
128
102
85
73
64
56
51
46
42
39
35
34
32
Energy Bands, (secs)

Plate 5

Plate 6

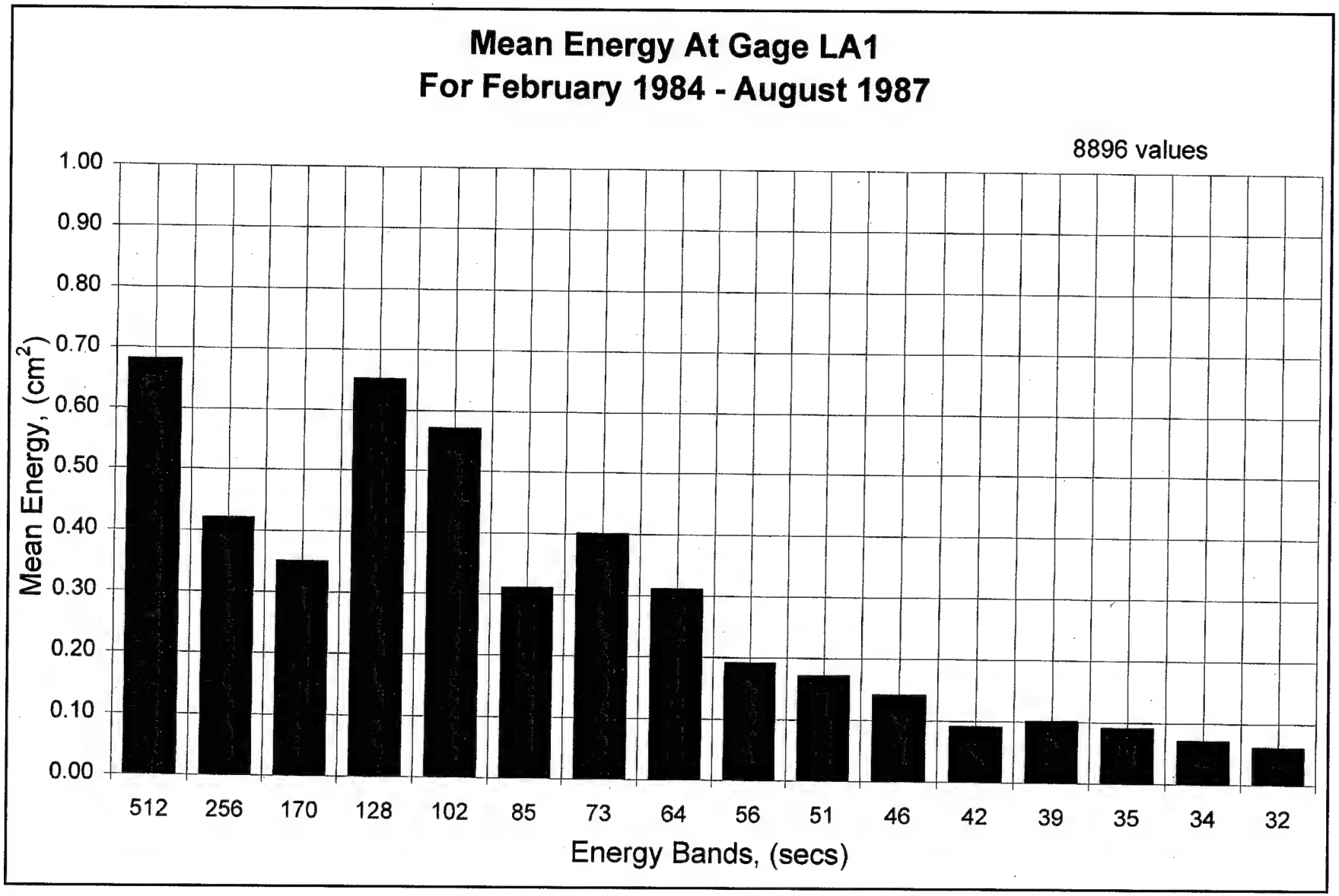
Mean Energy At Gage LA1
For February 1984 - August 1987
8896 values
1.00
0.90
0.80
0.70
0.60
0.50
0.40
0.30
0.20
0.10
0.00
Mean Energy, (cm2)
512
256
170
128
102
85
73
64
56
51
46
42
39
35
34
32
Energy Bands, (secs)

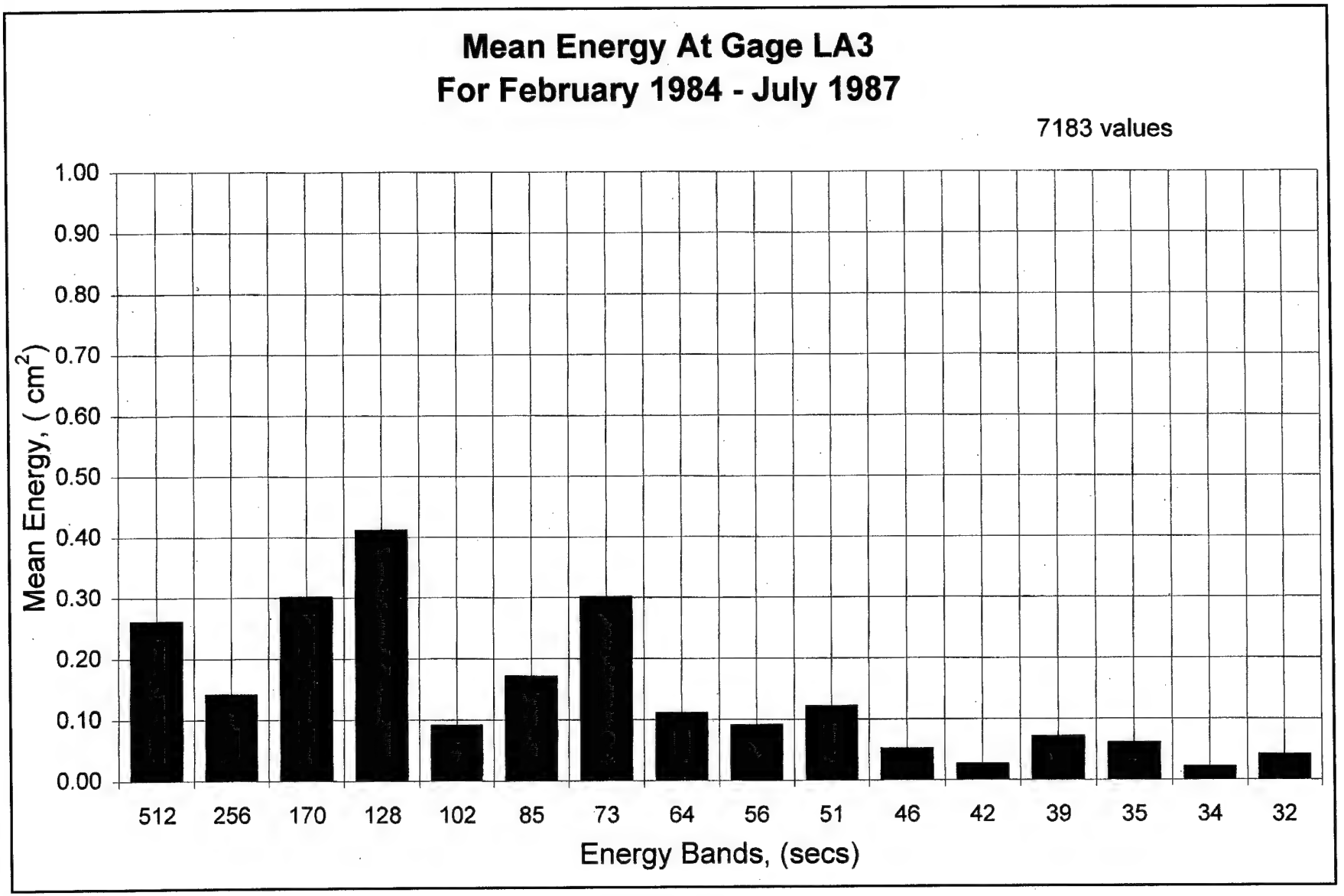
Mean Energy At Gage LA3
For February 1984 - July 1987
7183 values
1.00
0.90
0.80
0.70
0.60
0.50
0.40
0.30
0.20
0.10
0.00
Mean Energy, (cm2)
512
256
170
128
102
85
73
64
56
51
46
42
39
35
34
32
Energy Bands, (secs)

Plate 7

Plate 8

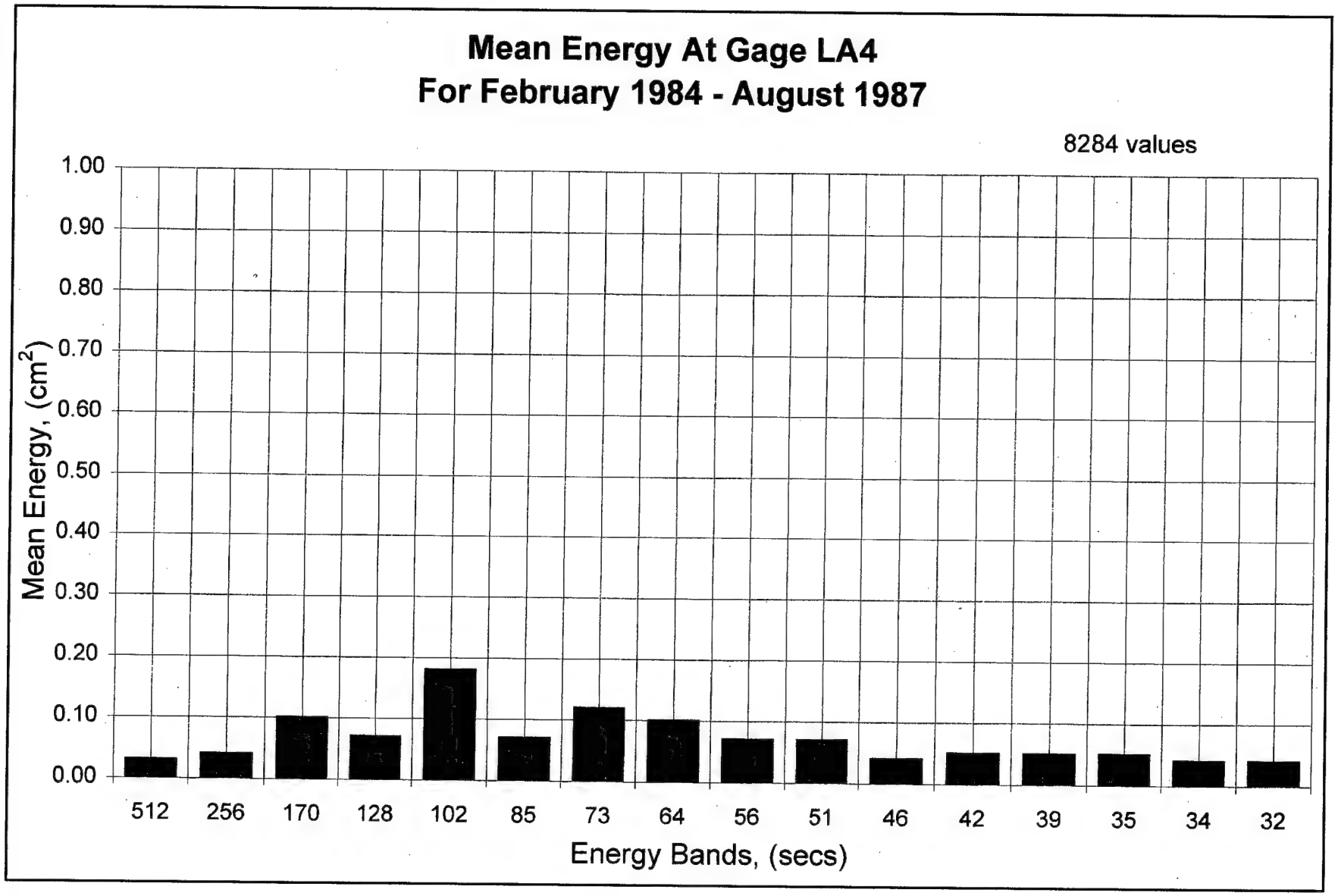
Mean Energy At Gage LA4
For February 1984 - August 1987
8284 values
Mean Energy, (cm2)
1.00
0.90
0.80
0.70
0.60
0.50
0.40
0.30
0.20
0.10
0.00
512
256
170
128
102
85
73
64
56
51
46
42
39
35
34
32
Energy Bands, (secs)

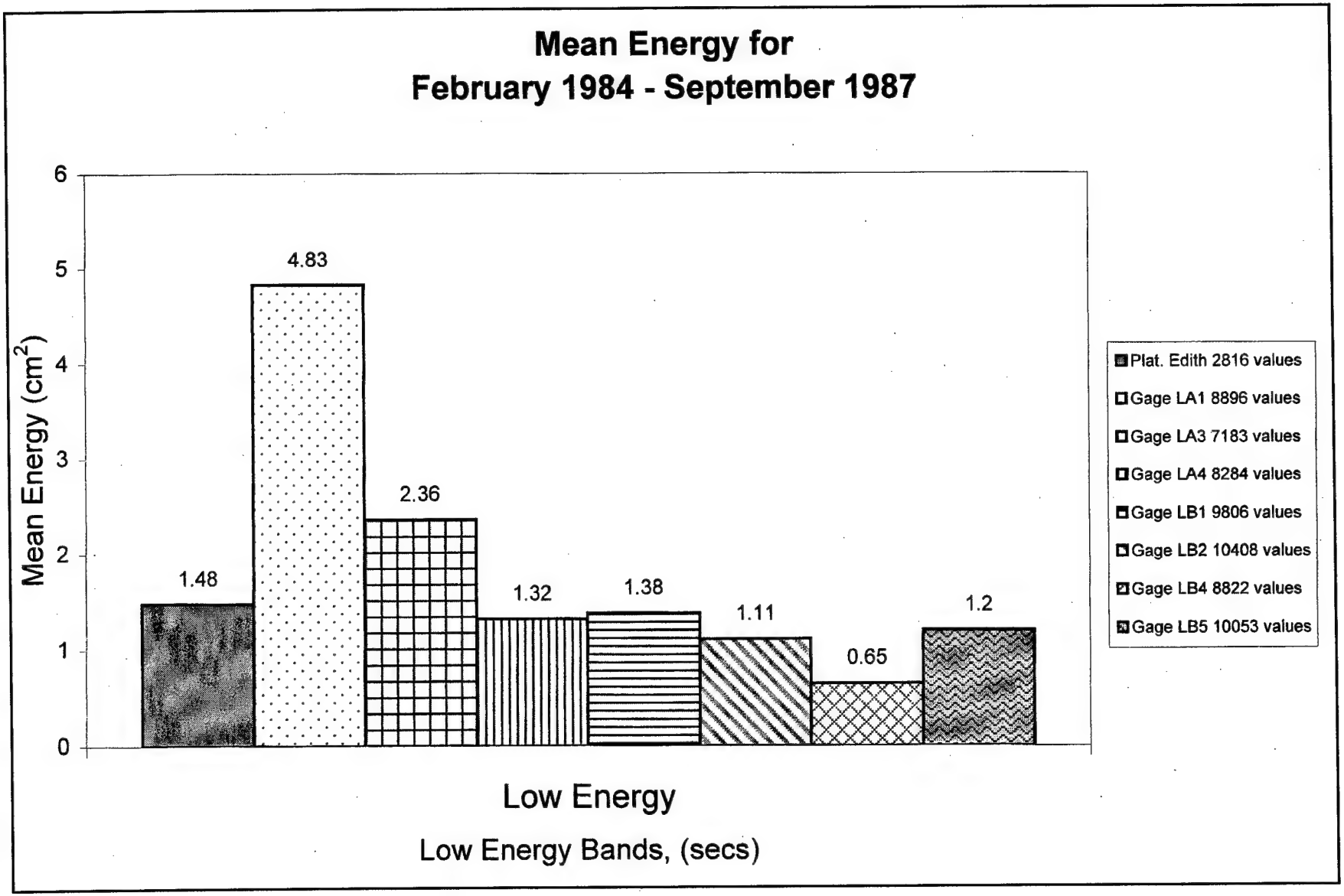
Mean Energy for
February 1984 - September 1987
Mean Energy (cm2)
6
5
4
3
2
1
0
4.83
2.36
1.48
1.32
1.38
1.11
0.65
1.2
Plat. Edith 2816 values
Gage LA1 8896 values
Gage LA3 7183 values
Gage LA4 8284 values
Gage LB1 9806 values
Gage LB2 10408 values
Gage LB4 8822 values
Gage LB5 10053 values
Low Energy
Low Energy Bands, (secs)

Plate 9

Plate 10

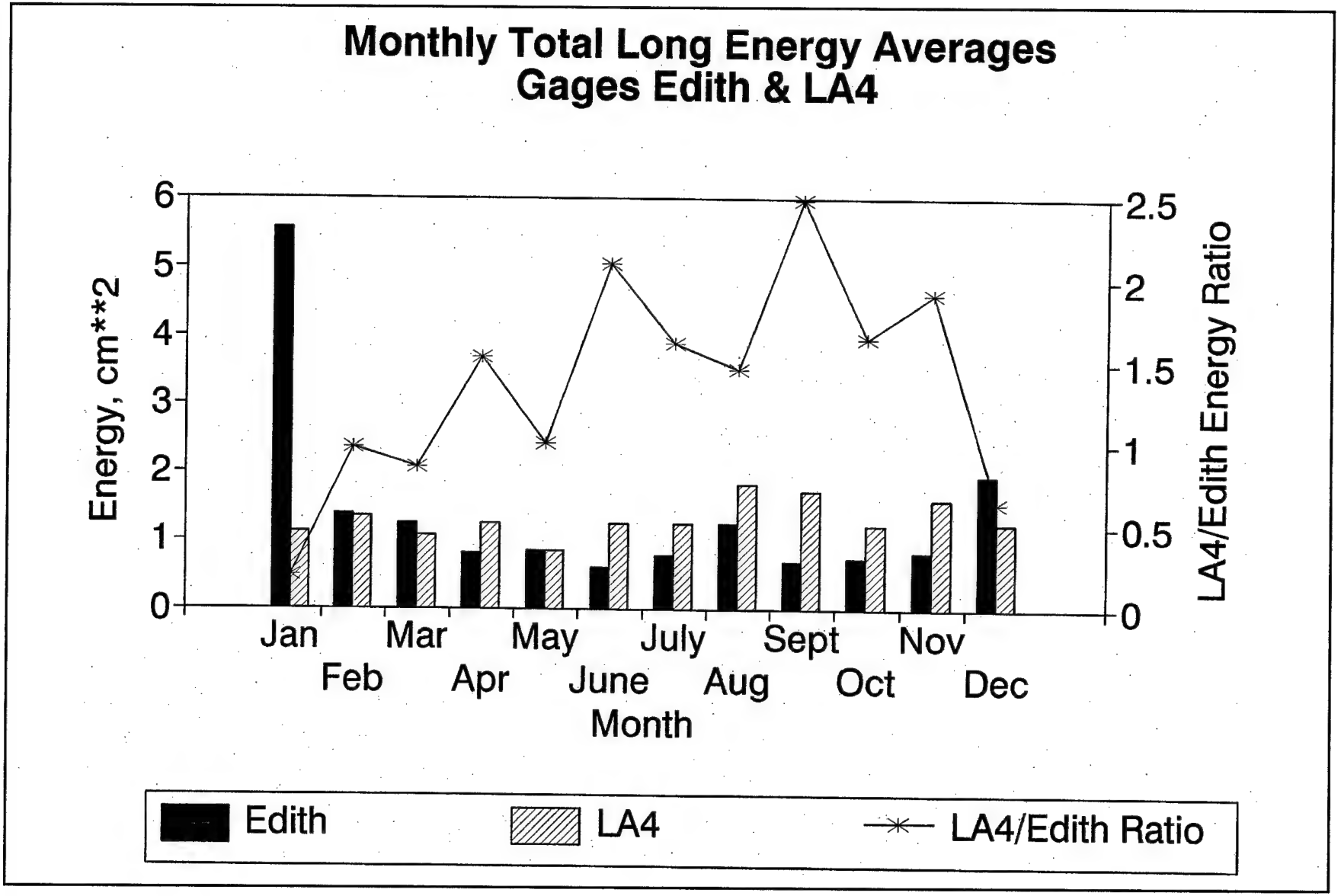
Monthly Total Long Energy Averages
Gages Edith & LA4
Energy, cm**2
LA4/Edith Energy Ratio
0
1
2
3
4
5
6
0
0.5
1
1.5
2
2.5
Jan
Feb
Mar
Apr
May
June
July
Aug
Sept
Oct
Nov
Dec
Month
Edith
LA4
LA4/Edith Ratio

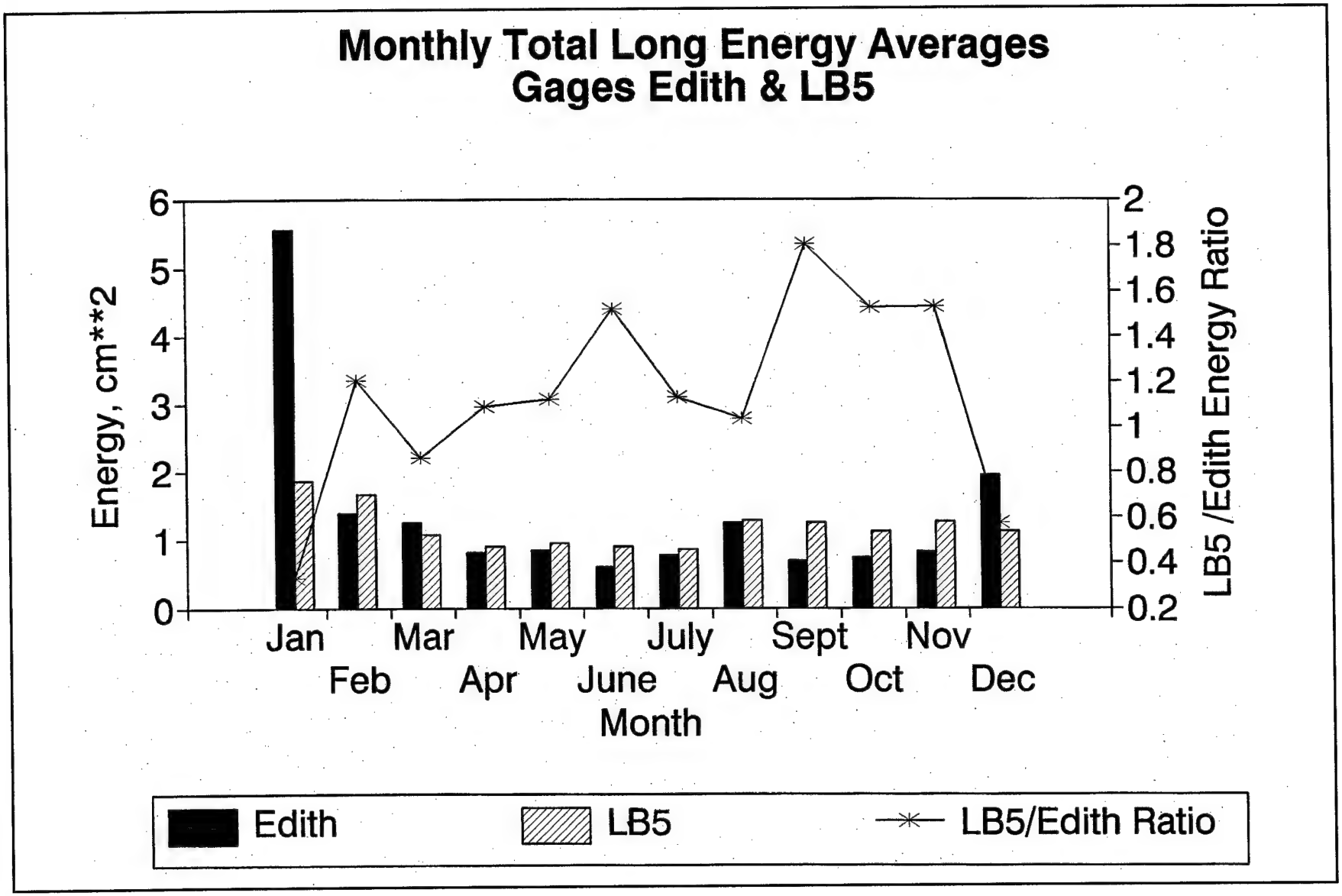
Monthly Total Long Energy Averages
Gages Edith & LB5
Energy, cm**2
0
1
2
3
4
5
6
LB5 /Edith Energy Ratio
0.2
0.4
0.6
0.8
1
1.2
1.4
1.6
1.8
2
Jan
Feb
Mar
Apr
May
June
July
Aug
Sept
Oct
Nov
Dec
Month
Edith
LB5
LB5/Edith Ratio

Plate 11

Plate 12

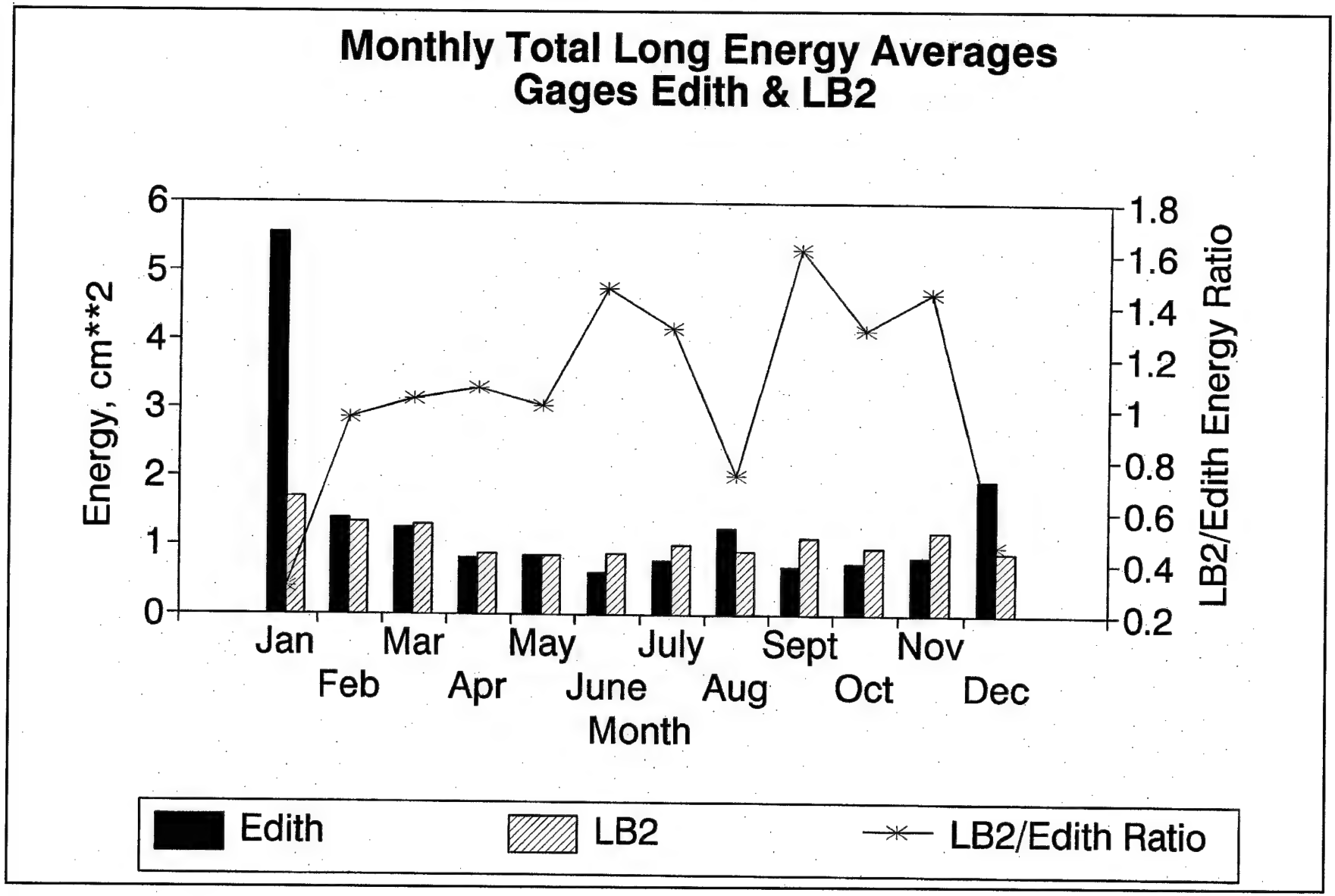
Monthly Total Long Energy Averages
Gages Edith & LB2
Energy, cm**2
0
1
2
3
4
5
6
LB2/Edith Energy Ratio
0.2
0.4
0.6
0.8
1
1.2
1.4
1.6
1.8
Jan
Feb
Mar
Apr
May
June
July
Aug
Sept
Oct
Nov
Dec
Month
Edith
LB2
LB2/Edith Ratio

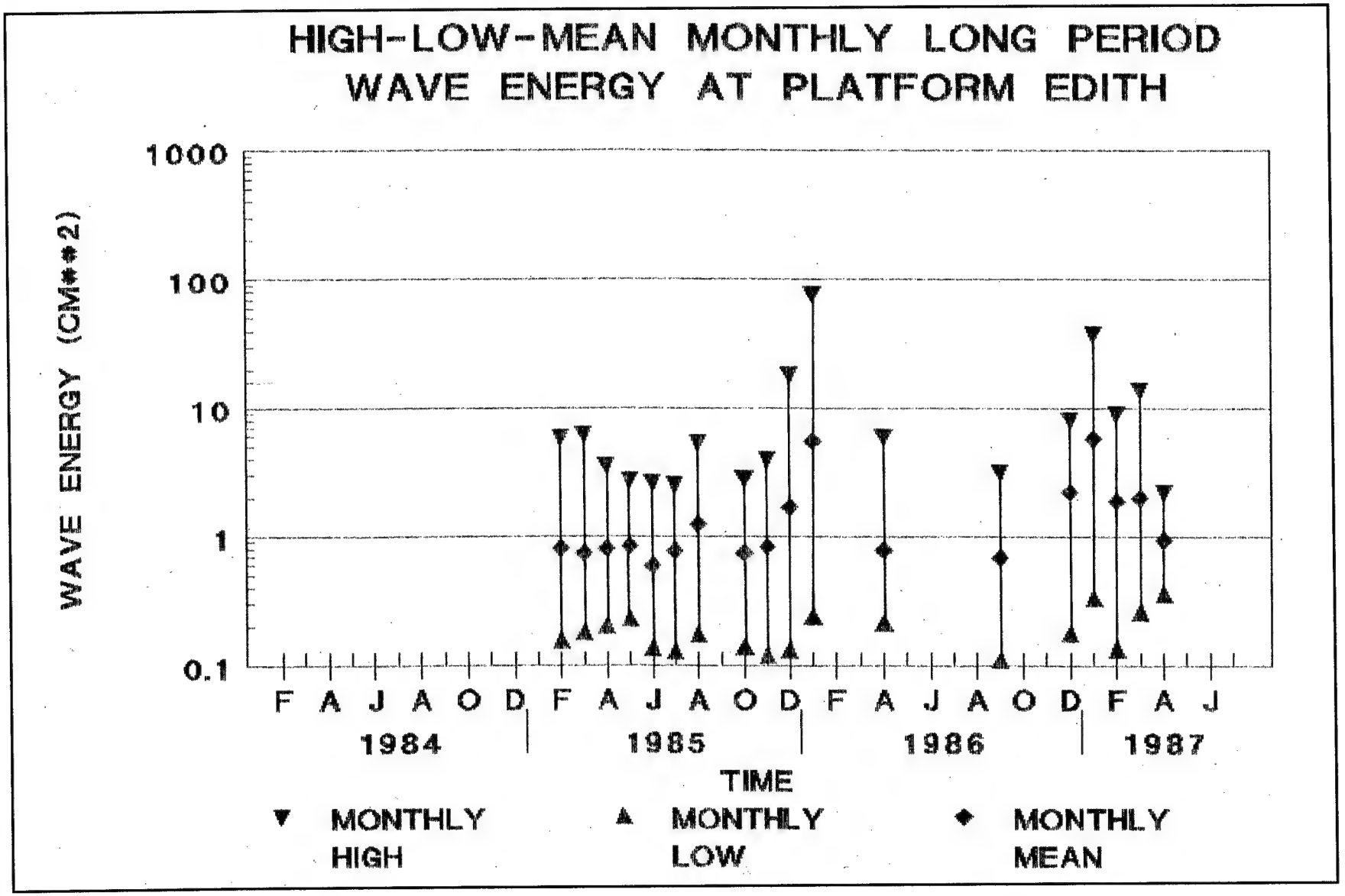
HIGH-LOW-MEAN MONTHLY LONG PERIOD
WAVE ENERGY AT PLATFORM EDITH
WAVE ENERGY (CM**2)
1000
100
10
1
0.1
F A J A O D F A J A O D F A J A O D F A J
1984
1985
1986
1987
TIME
MONTHLY HIGH
MONTHLY LOW
MONTHLY MEAN

Plate 13

Plate 14

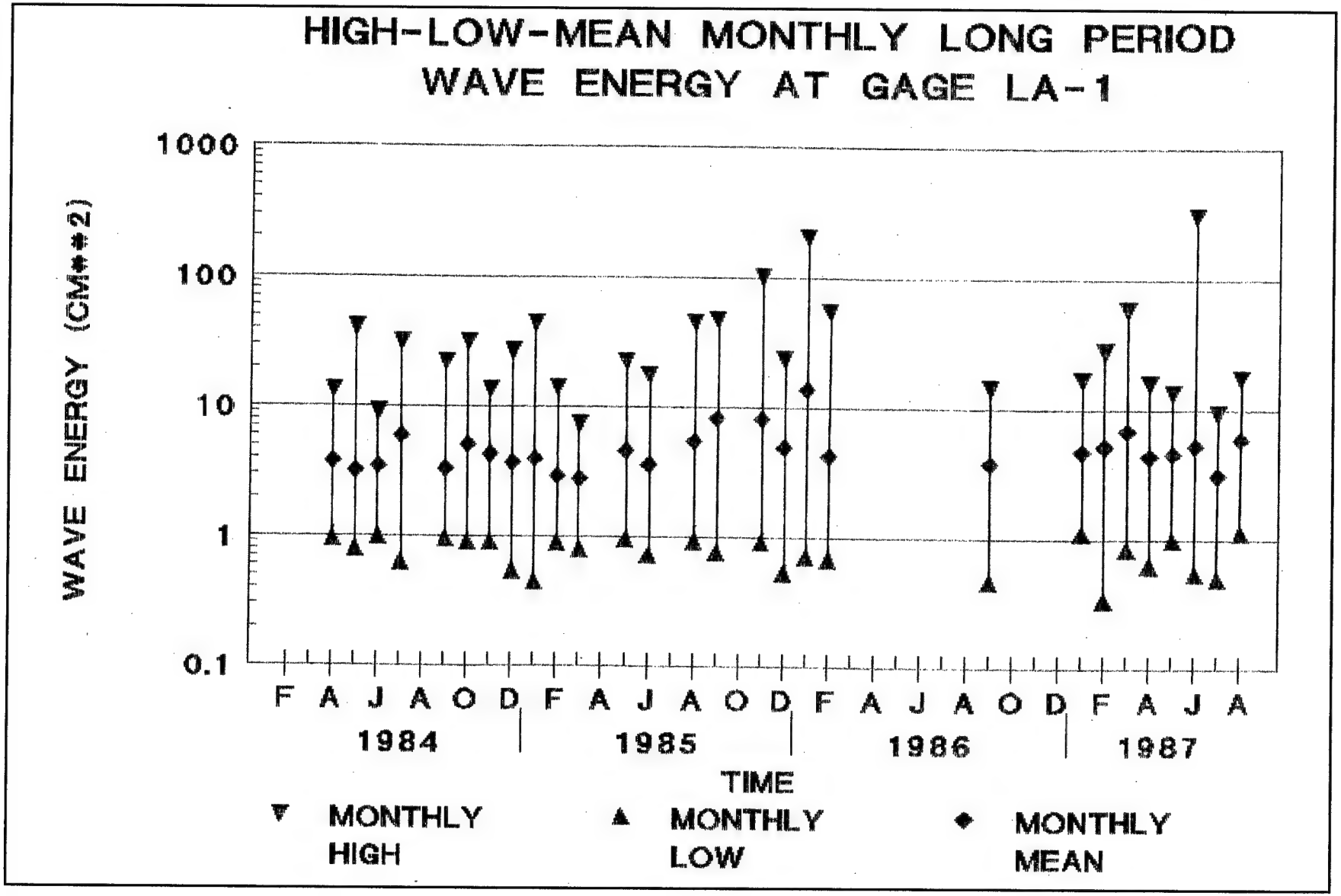
HIGH-LOW-MEAN MONTHLY LONG PERIOD
WAVE ENERGY AT GAGE LA-1
WAVE ENERGY (CM**2)
1000
100
10
1
0.1
F A J A O D F A J A O D F A J A O D F A J A
1984
1985
1986
1987
TIME
MONTHLY HIGH
MONTHLY LOW
MONTHLY MEAN

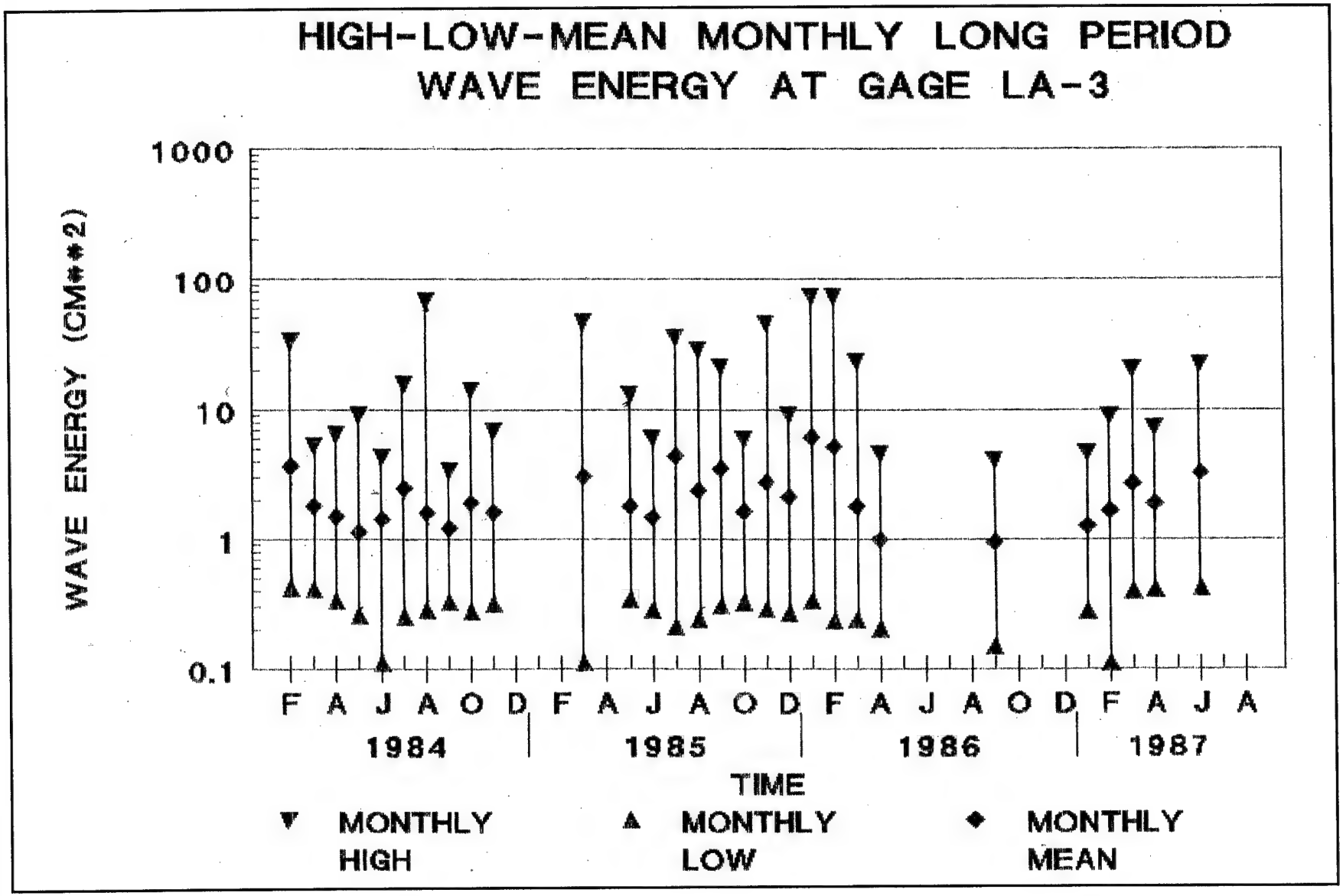
HIGH-LOW-MEAN MONTHLY LONG PERIOD
WAVE ENERGY AT GAGE LA-3
WAVE ENERGY (CM**2)
1000
100
10
1
0.1
F A J A O D F A J A O D F A J A O D F A J A
1984
1985
1986
1987
TIME
MONTHLY HIGH
MONTHLY LOW
MONTHLY MEAN

Plate 15

Plate 16

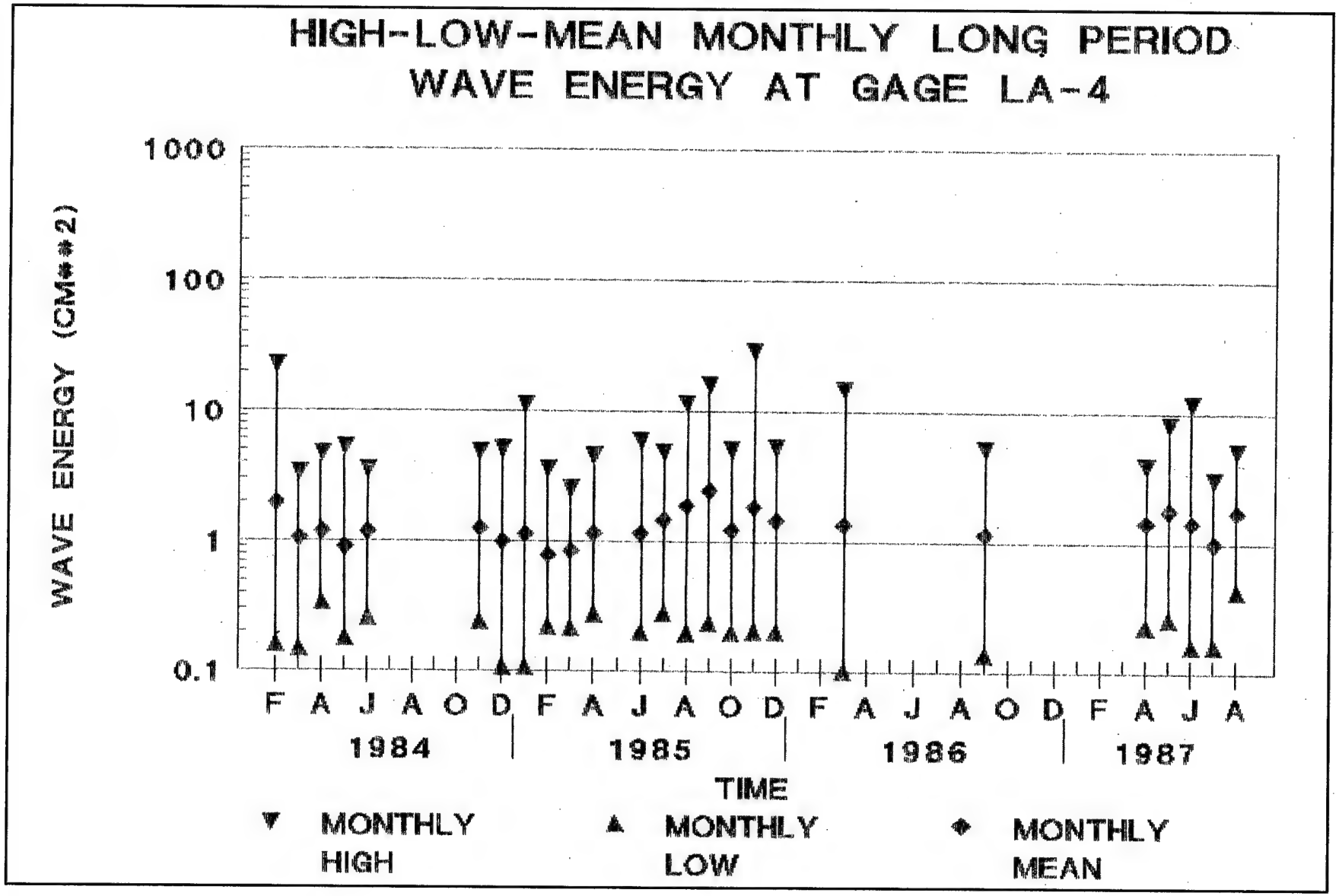
HIGH-LOW-MEAN MONTHLY LONG PERIOD
WAVE ENERGY AT GAGE LA-4
WAVE ENERGY (CM**2)
1000
100
10
1
0.1
F A J A O D F A J A O D F A J A O D F A J A
1984
1985
1986
1987
TIME
MONTHLY HIGH
MONTHLY LOW
MONTHLY MEAN

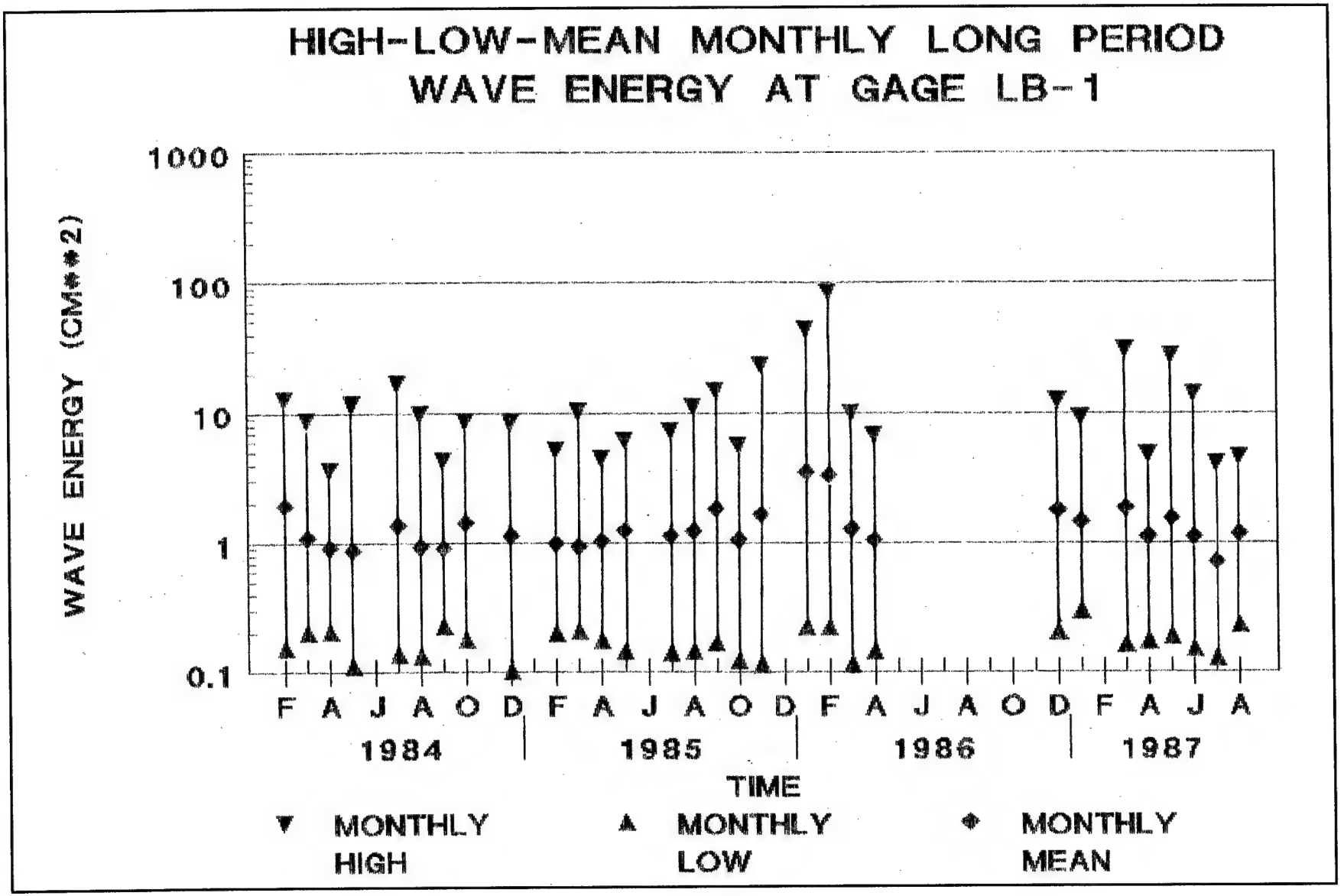
HIGH-LOW-MEAN MONTHLY LONG PERIOD
WAVE ENERGY AT GAGE LB-1
WAVE ENERGY (CM**2)
1000
100
10
1
0.1
F A J A O D F A J A O D F A J A O D F A J A
1984
1985
1986
1987
TIME
MONTHLY HIGH
MONTHLY LOW
MONTHLY MEAN

Plate 17

Plate 18

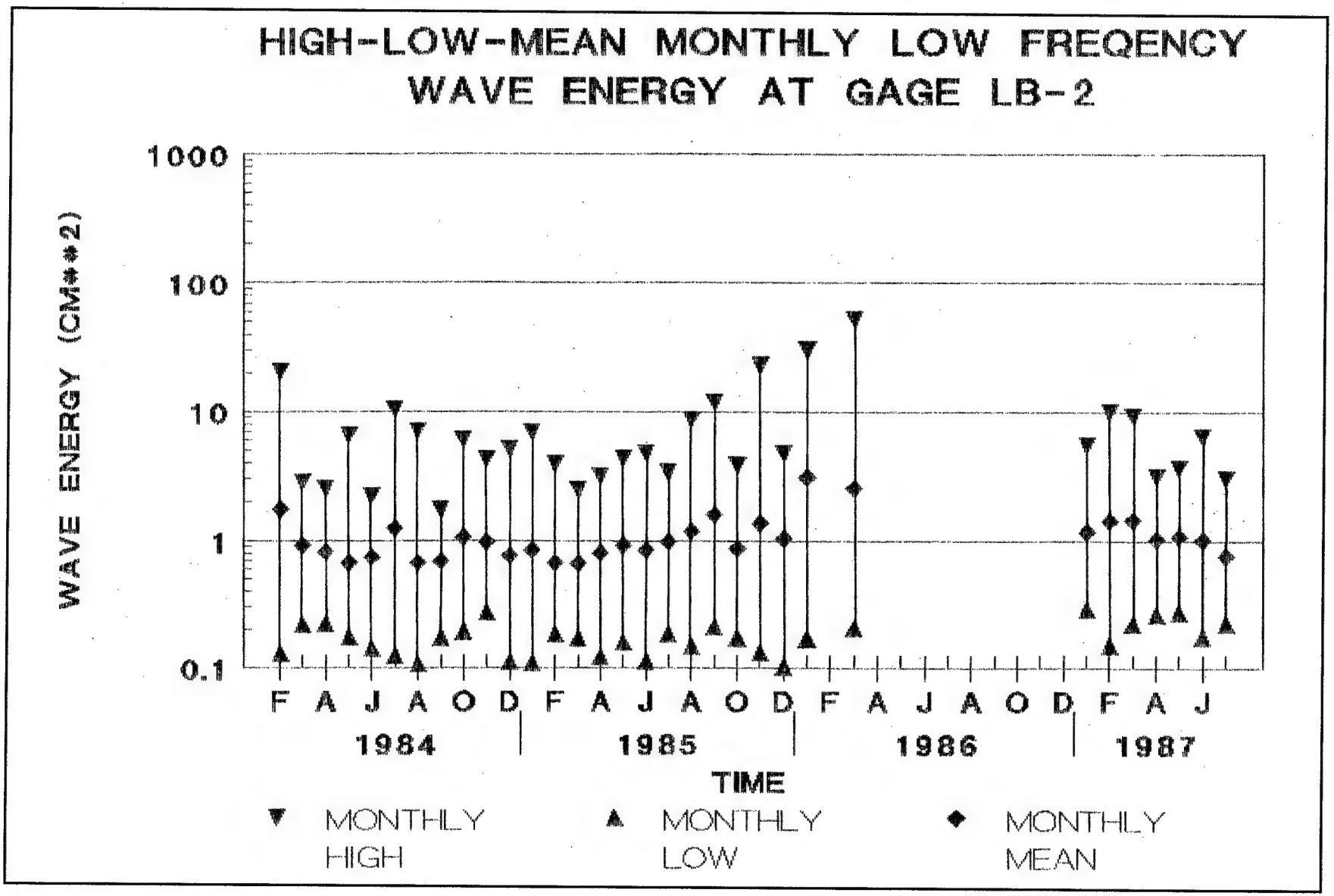
HIGH-LOW-MEAN MONTHLY LOW FREQENCY
WAVE ENERGY AT GAGE LB-2
WAVE ENERGY (CM**2)
1000
100
10
1
0.1
F A J A O D F A J A O D F A J A O D F A J
1984
1985
1986
1987
TIME
MONTHLY HIGH
MONTHLY LOW
MONTHLY MEAN

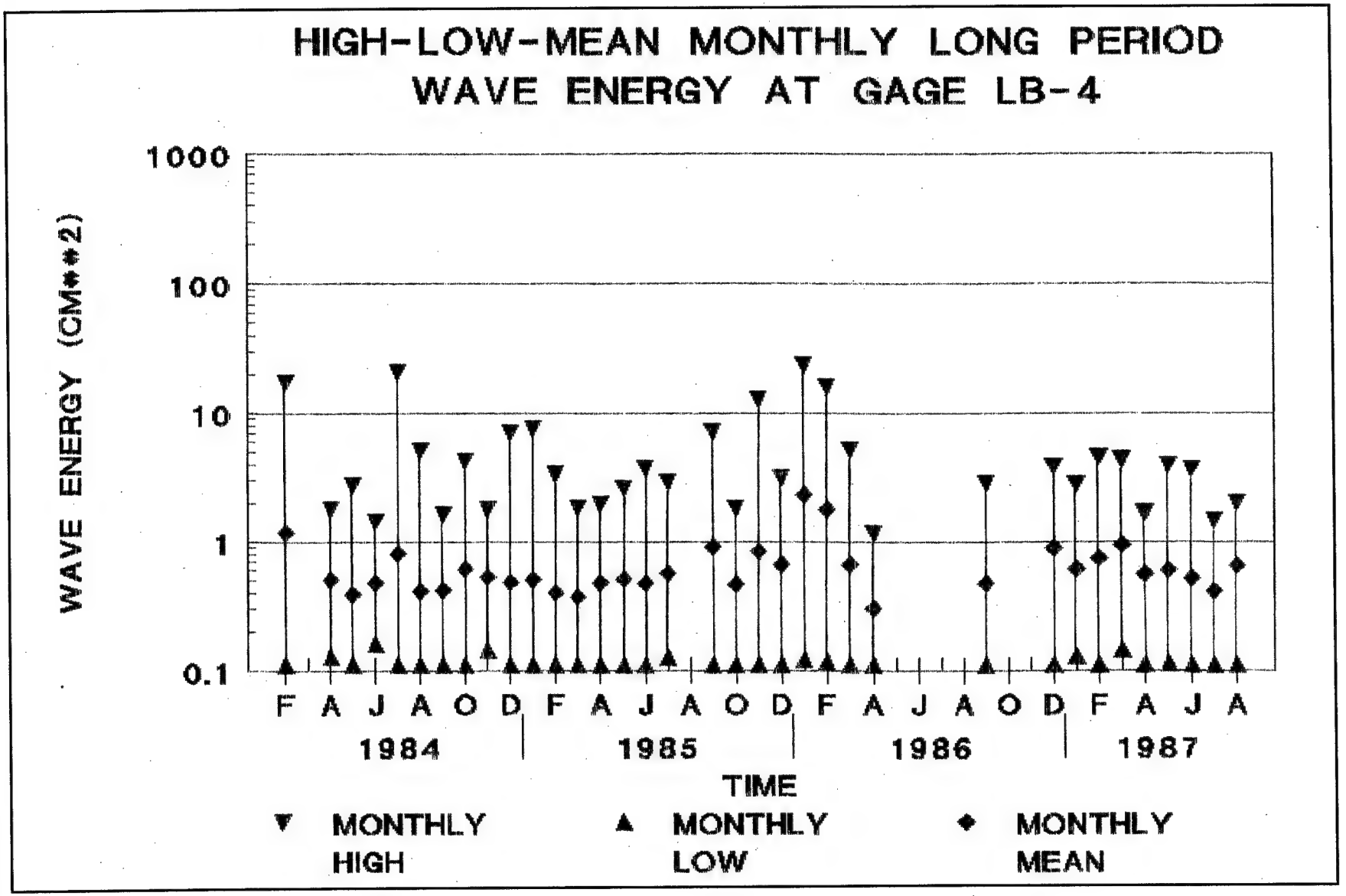
HIGH-LOW-MEAN MONTHLY LONG PERIOD
WAVE ENERGY AT GAGE LB-4
WAVE ENERGY (CM**2)
1000
100
10
1
0.1
F A J A O D F A J A O D F A J A O D F A J A
1984
1985
1986
1987
TIME
MONTHLY HIGH
MONTHLY LOW
MONTHLY MEAN

Plate 19

Plate 20

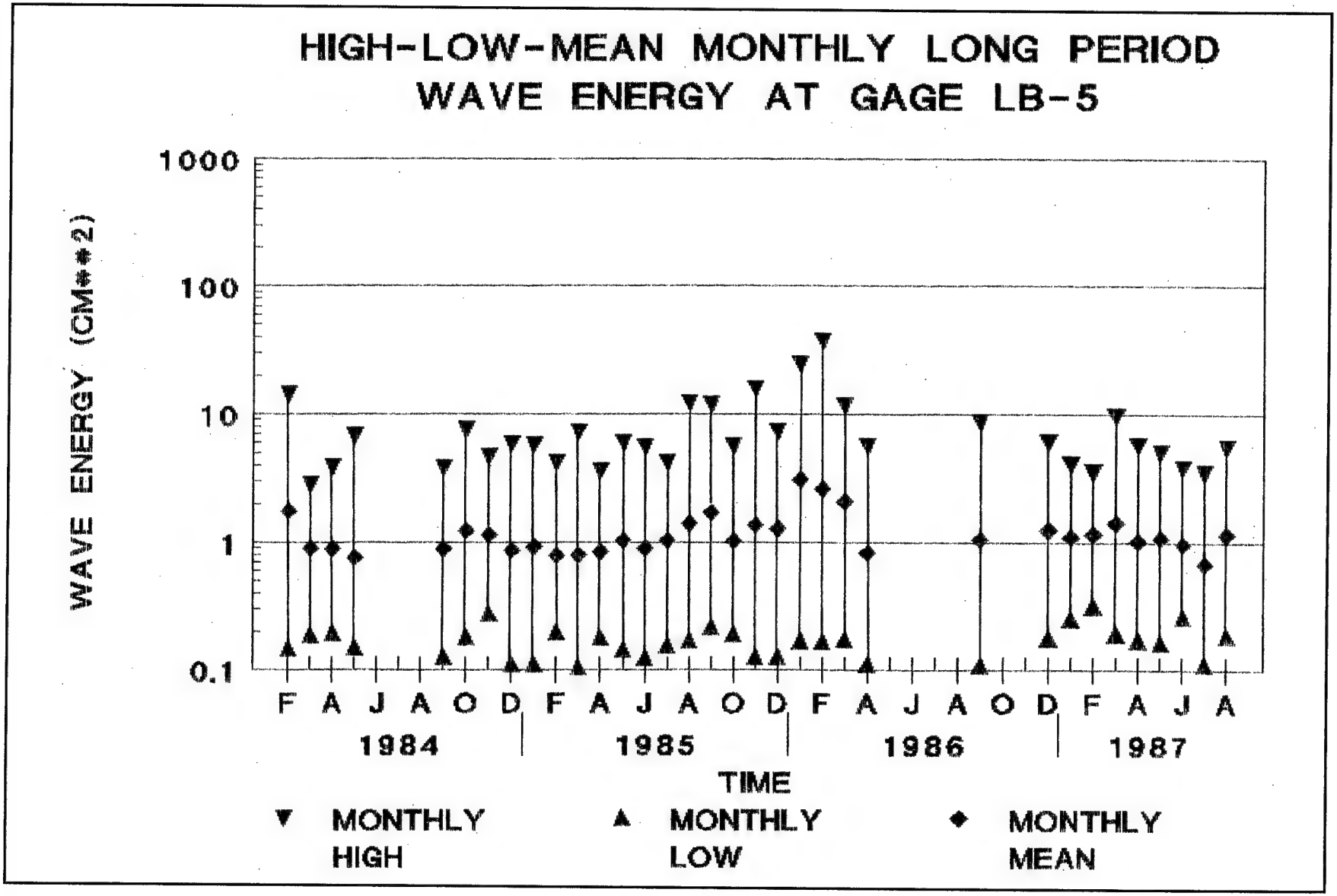
HIGH-LOW-MEAN MONTHLY LONG PERIOD
WAVE ENERGY AT GAGE LB-5
WAVE ENERGY (CM**2)
1000
100
10
1
0.1
F A J A O D F A J A O D F A J A O D F A J A
1984
1985
1986
1987
TIME
MONTHLY HIGH
MONTHLY LOW
MONTHLY MEAN

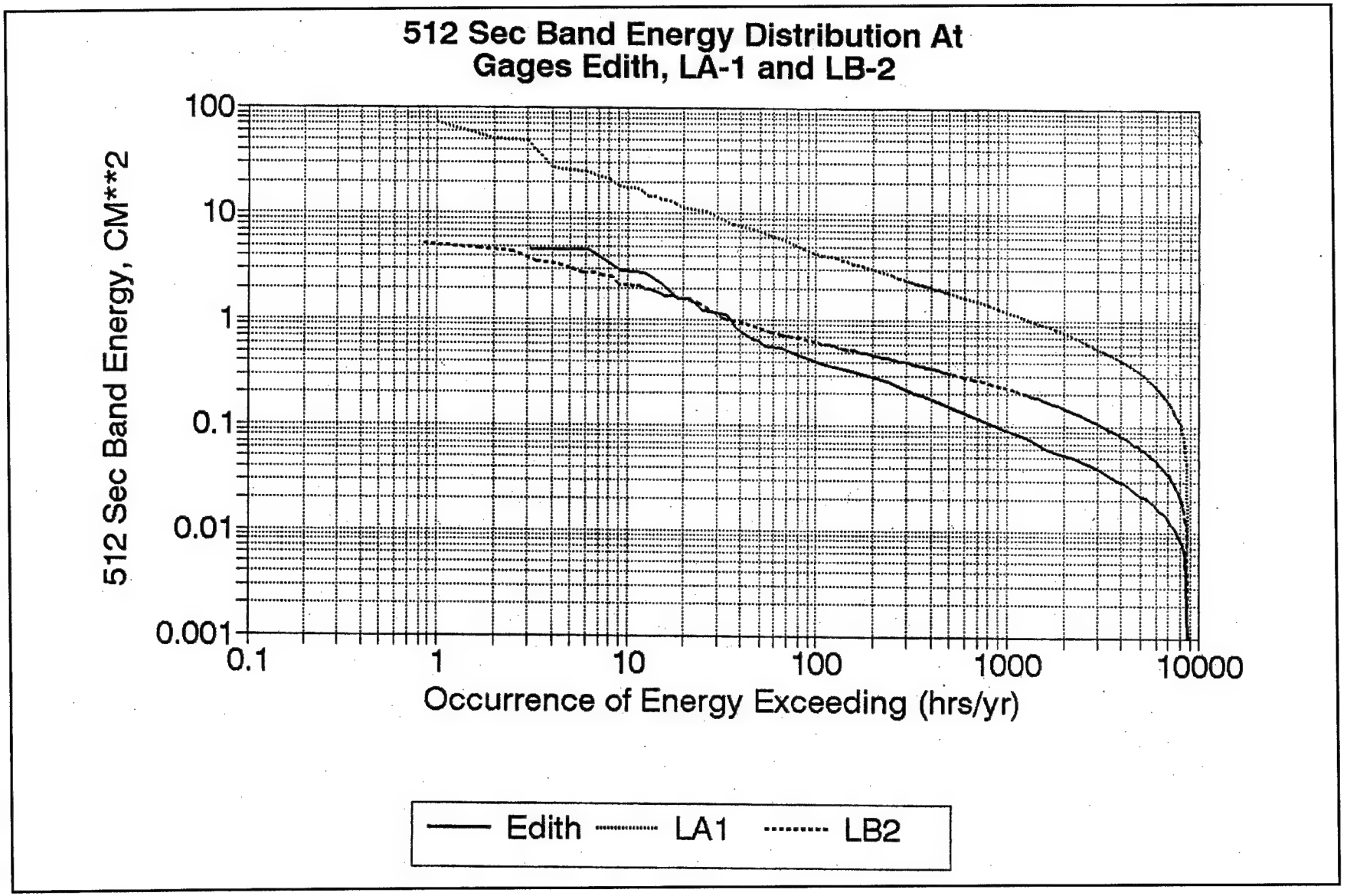
512 Sec Band Energy Distribution At
Gages Edith, LA-1 and LB-2
512 Sec Band Energy, CM**2
100
10
1
0.1
0.01
0.001
0.1
1
10
100
1000
10000
Occurrence of Energy Exceeding (hrs/yr)
Edith
LA1
LB2

Plate 21

Plate 22

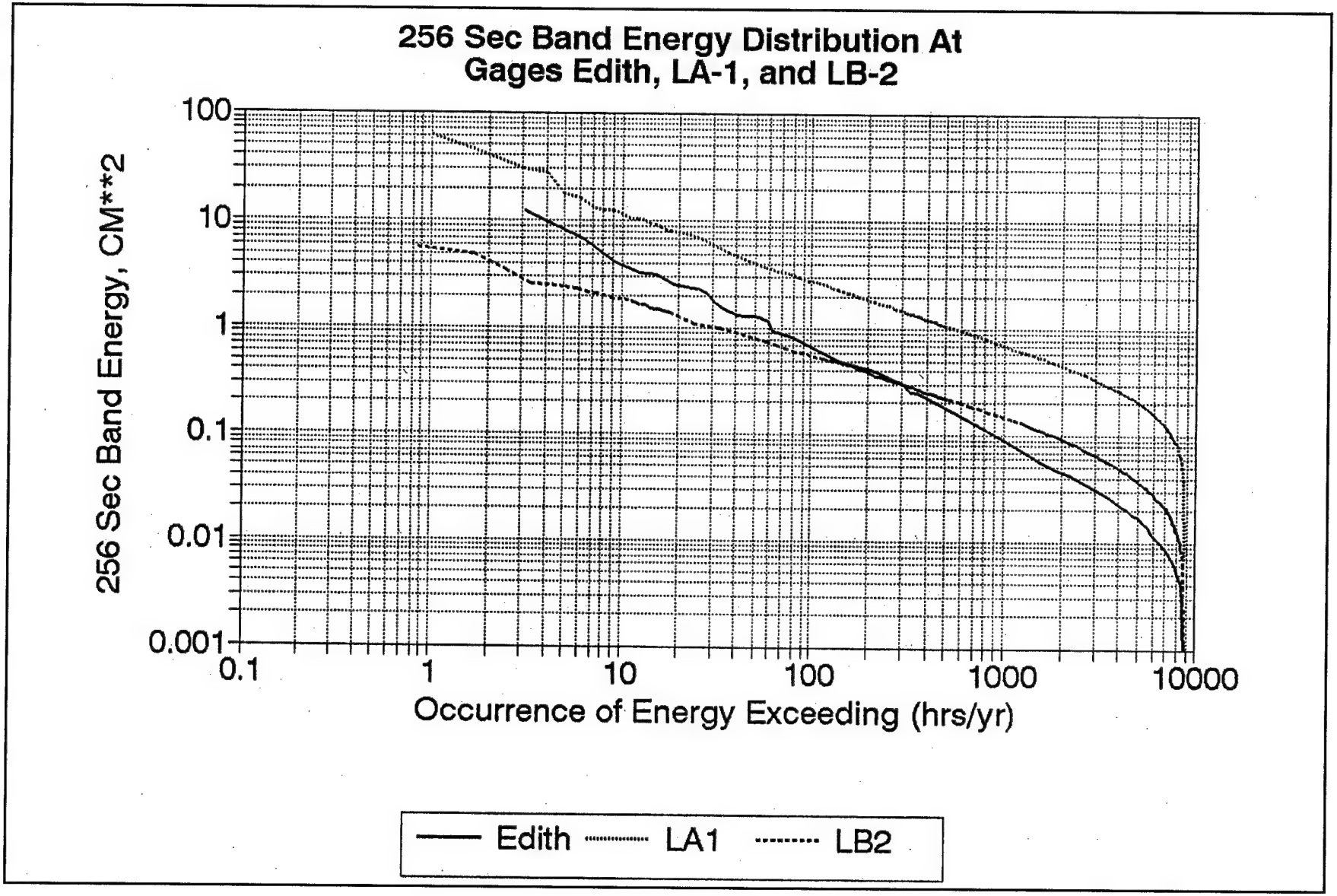
256 Sec Band Energy Distribution At
Gages Edith, LA-1, and LB-2
256 Sec Band Energy, CM**2
100
10
1
0.1
0.01
0.001
0.1
1
10
100
1000
10000
Occurrence of Energy Exceeding (hrs/yr)
Edith
LA1
LB2

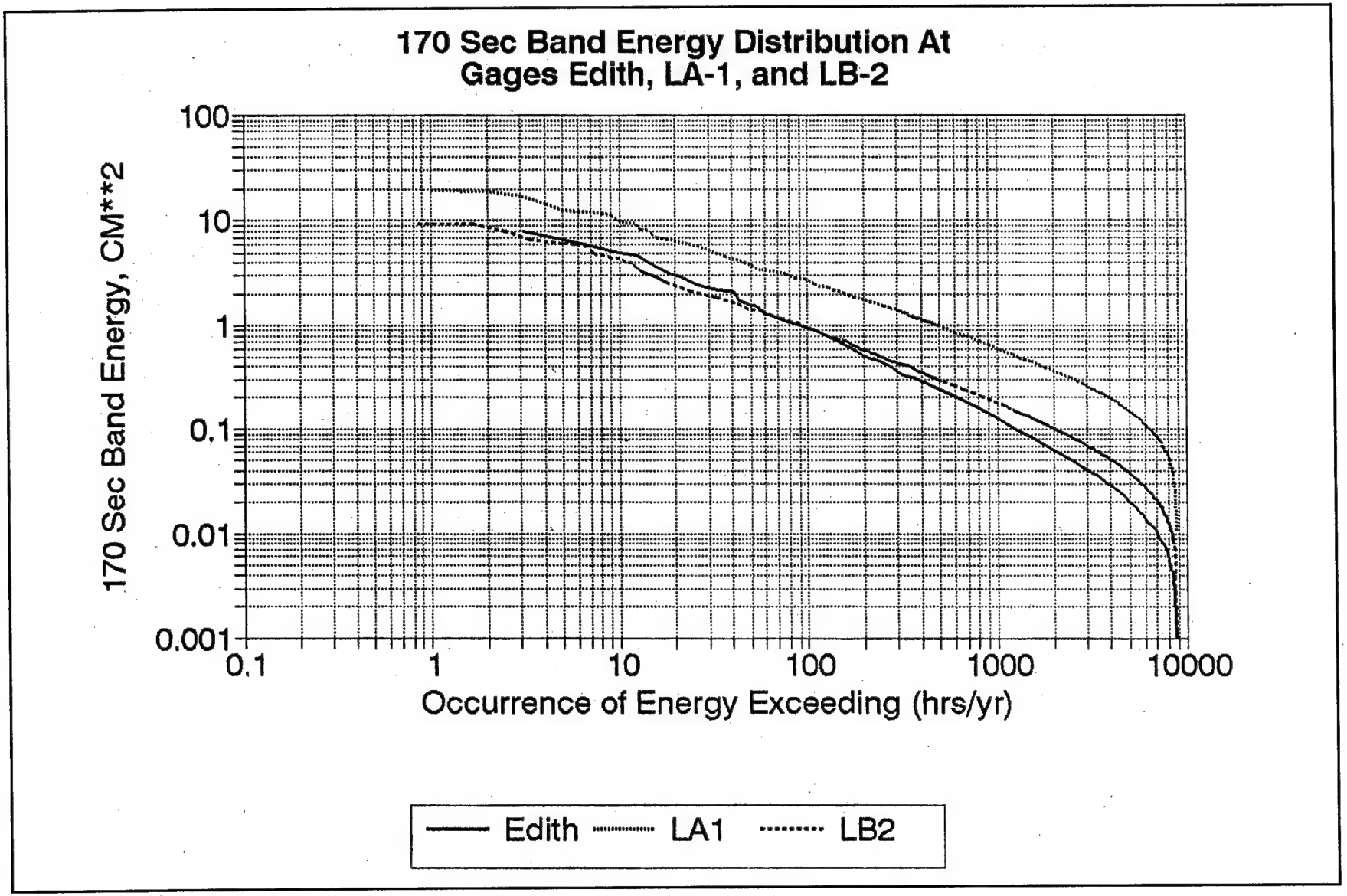
170 Sec Band Energy Distribution At
Gages Edith, LA-1, and LB-2
170 Sec Band Energy, CM**2
100
10
1
0.1
0.01
0.001
0.1
1
10
100
1000
10000
Occurrence of Energy Exceeding (hrs/yr)
Edith
LA1
LB2

Plate 23

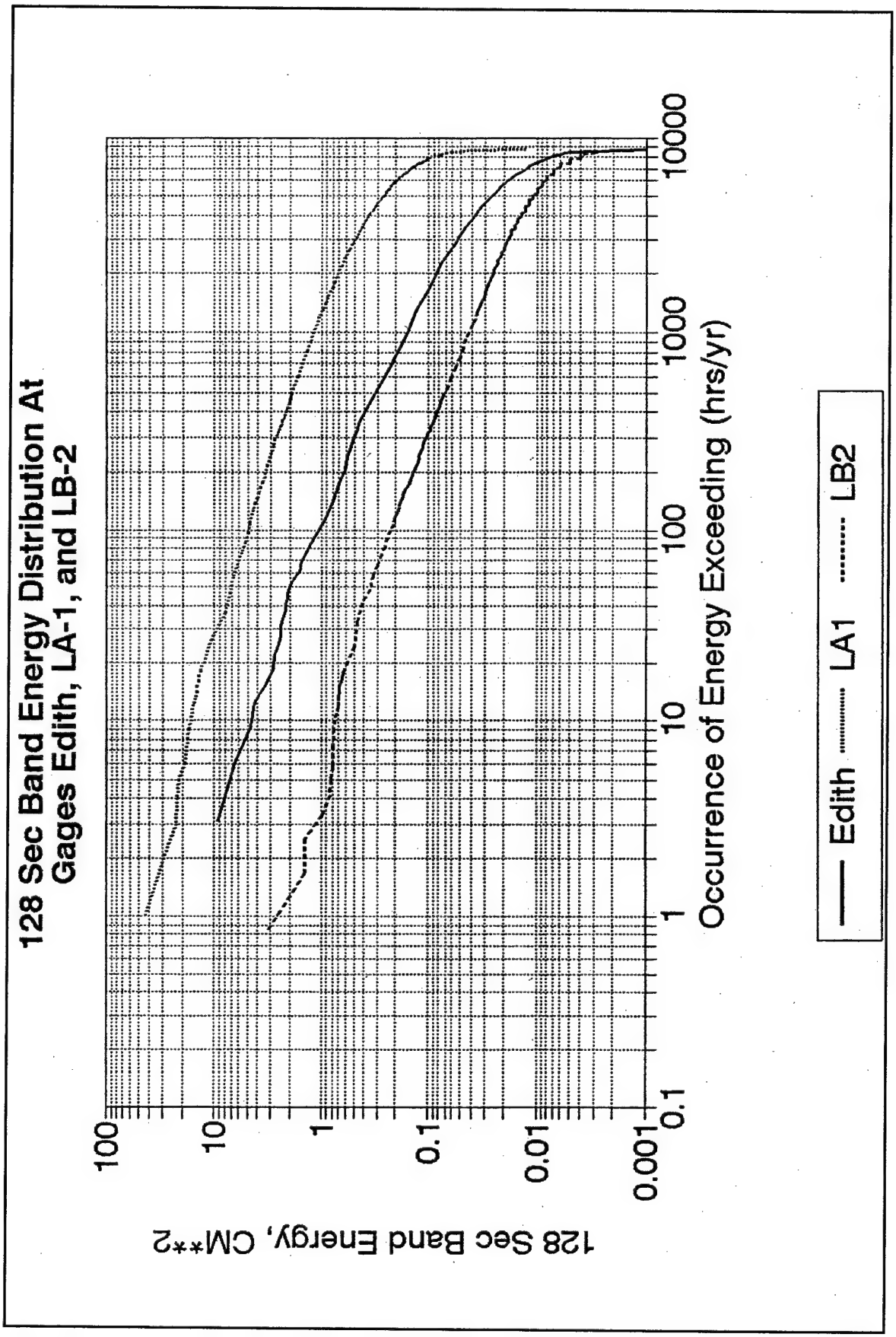
128 Sec Band Energy Distribution At
Gages Edith, LA-1, and LB-2
128 Sec Band Energy, CM**2
100
10
1
0.1
0.01
0.001
0.1
1
10
100
1000
10000
Occurrence of Energy Exceeding (hrs/yr)
Edith
LA1
LB2

Plate 24

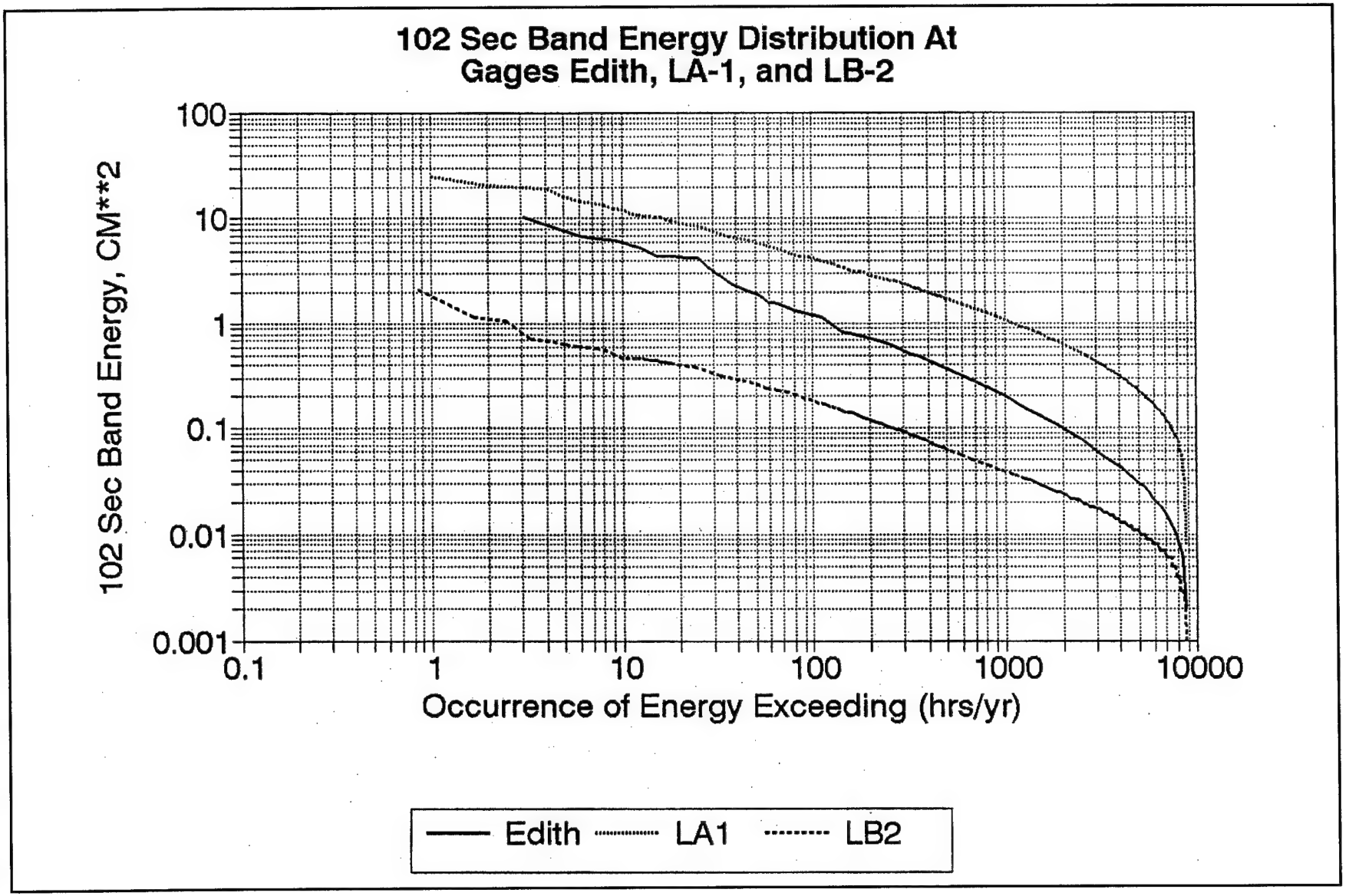
102 Sec Band Energy Distribution At
Gages Edith, LA-1, and LB-2
102 Sec Band Energy, CM**2
100
10
1
0.1
0.01
0.001
0.1
1
10
100
1000
10000
Occurrence of Energy Exceeding (hrs/yr)
Edith
LA1
LB2

Plate 25

Plate 26

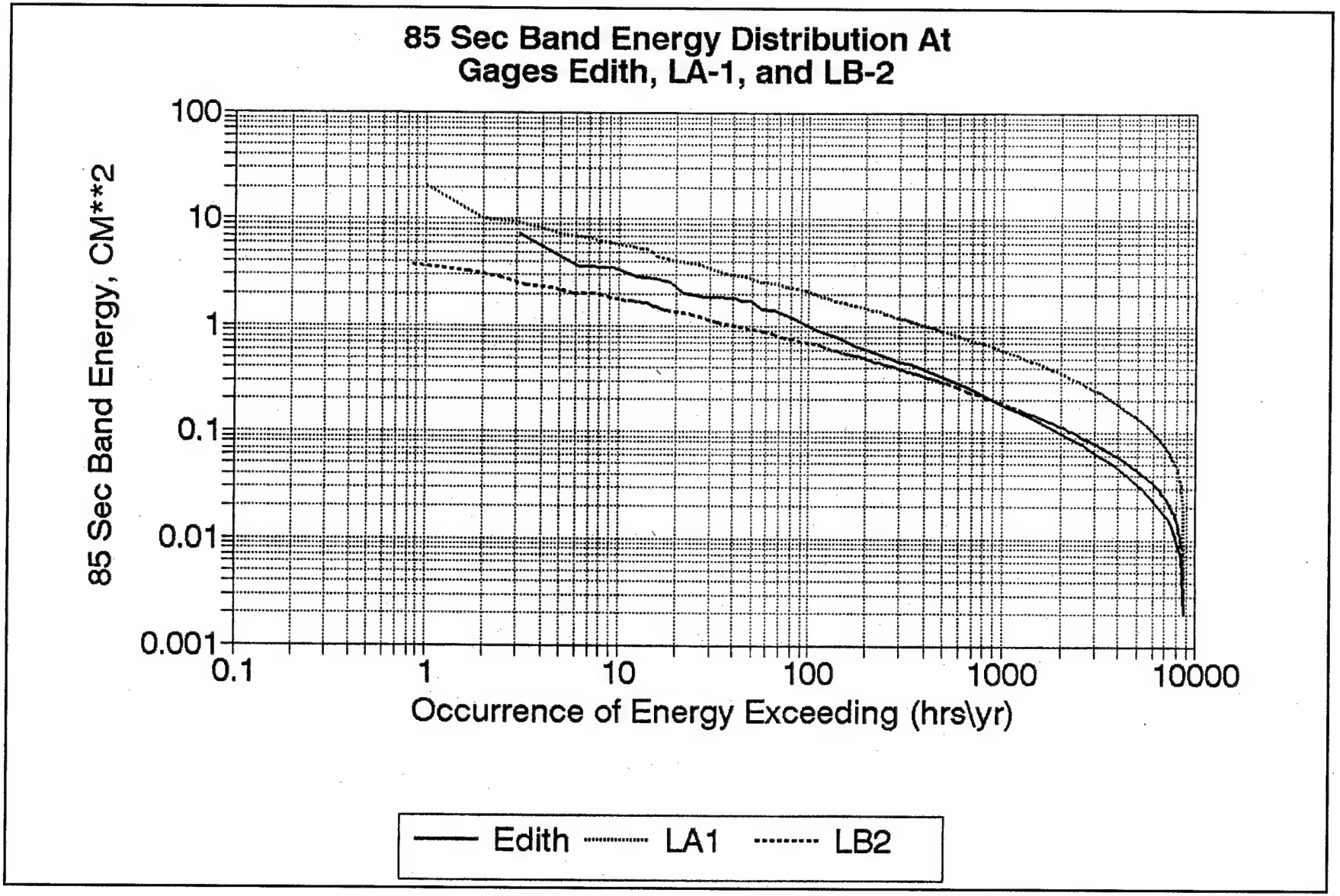
85 Sec Band Energy Distribution At
Gages Edith, LA-1, and LB-2
85 Sec Band Energy, CM**2
100
10
1
0.1
0.01
0.001
0.1
1
10
100
1000
10000
Occurrence of Energy Exceeding (hrs\yr)
Edith
LA1
LB2

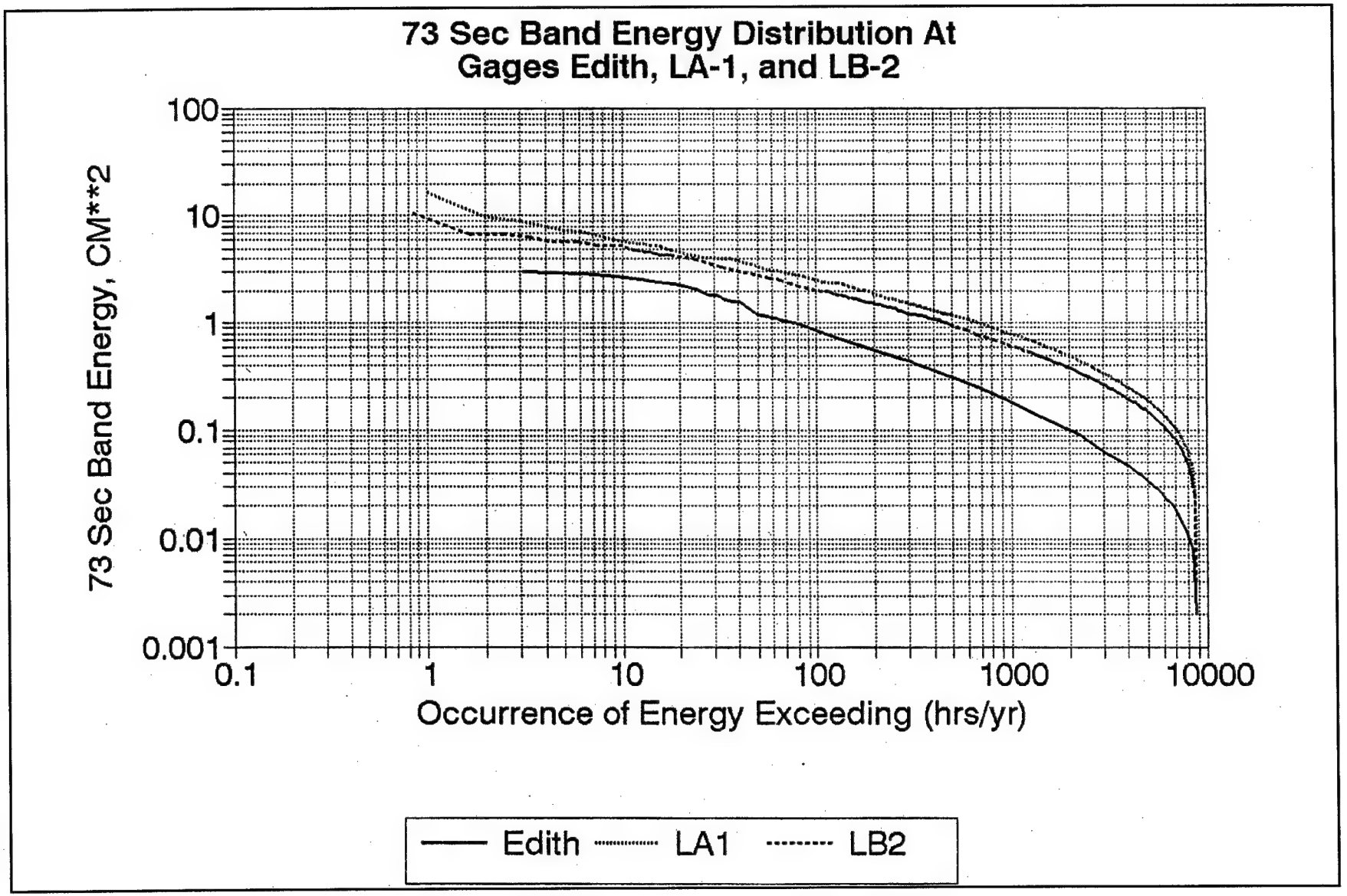
73 Sec Band Energy Distribution At
Gages Edith, LA-1, and LB-2
73 Sec Band Energy, CM**2
100
10
1
0.1
0.01
0.001
0.1
1
10
100
1000
10000
Occurrence of Energy Exceeding (hrs/yr)
Edith
LA1
LB2

Plate 27

Plate 28

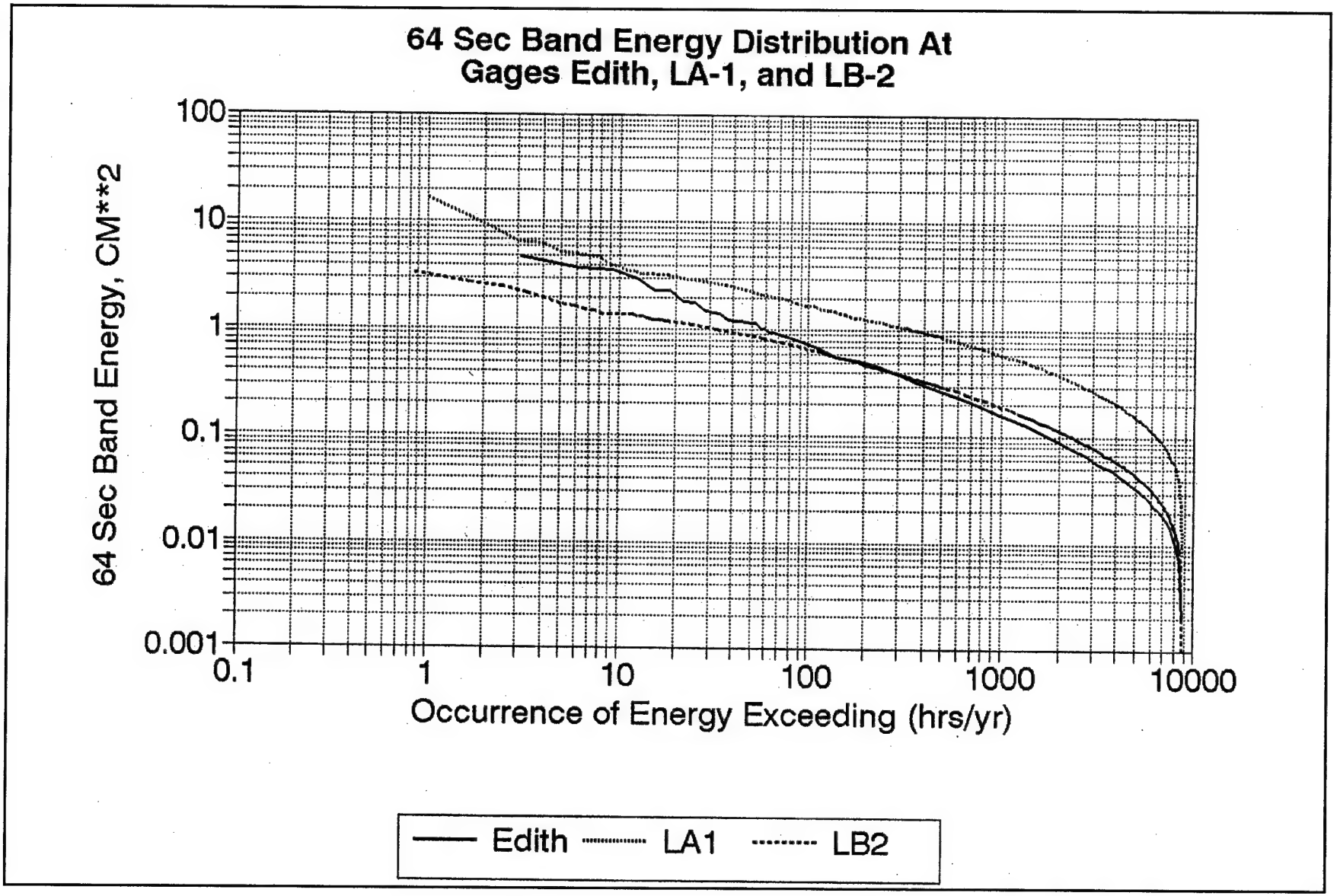
64 Sec Band Energy Distribution At
Gages Edith, LA-1, and LB-2
64 Sec Band Energy, CM**2
100
10
1
0.1
0.01
0.001
0.1
1
10
100
1000
10000
Occurrence of Energy Exceeding (hrs/yr)
Edith
LA1
LB2

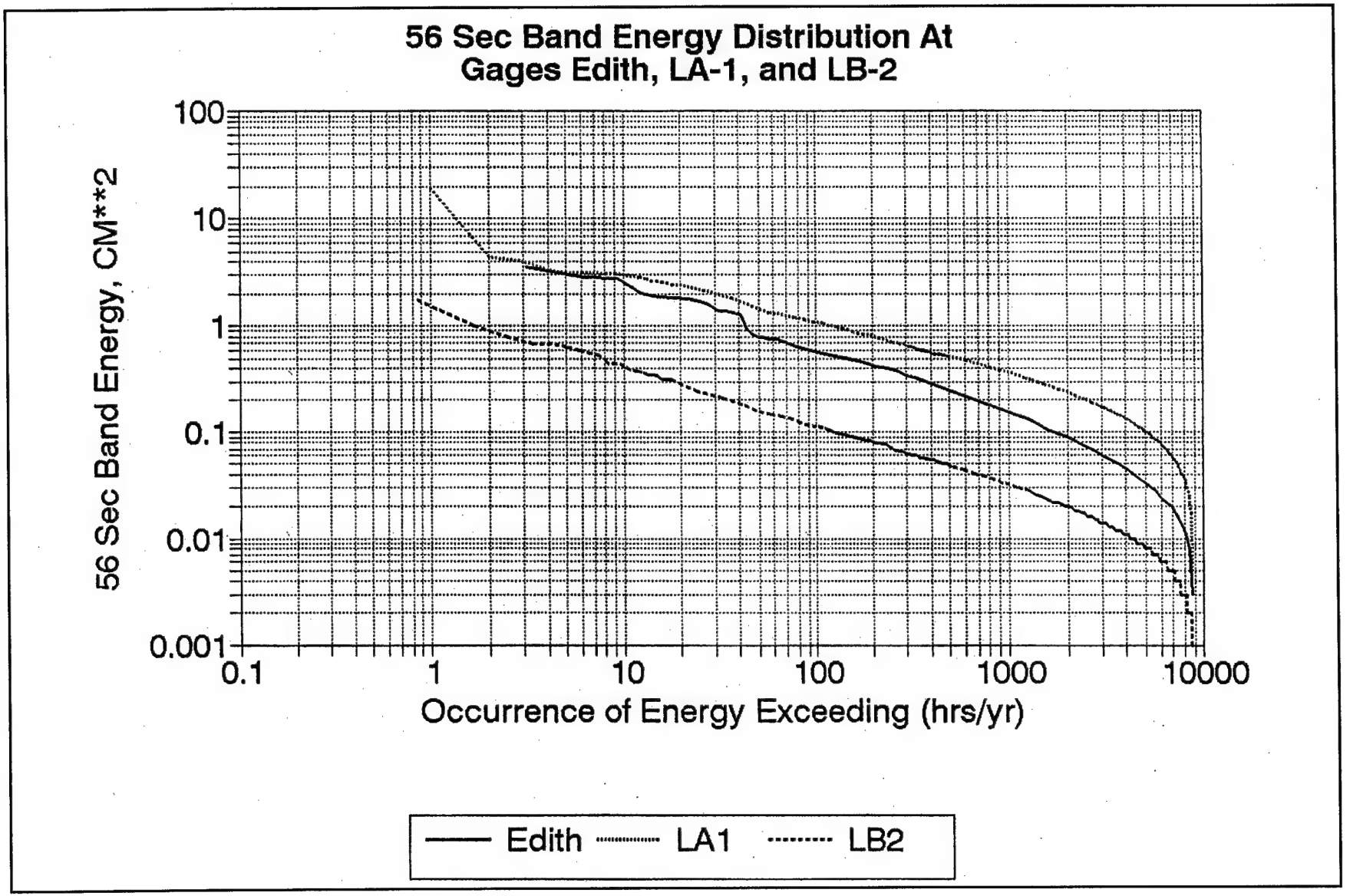
56 Sec Band Energy Distribution At
Gages Edith, LA-1, and LB-2
56 Sec Band Energy, CM**2
100
10
1
0.1
0.01
0.001
0.1
1
10
100
1000
10000
Occurrence of Energy Exceeding (hrs/yr)
Edith
LA1
LB2

Plate 29

Plate 30

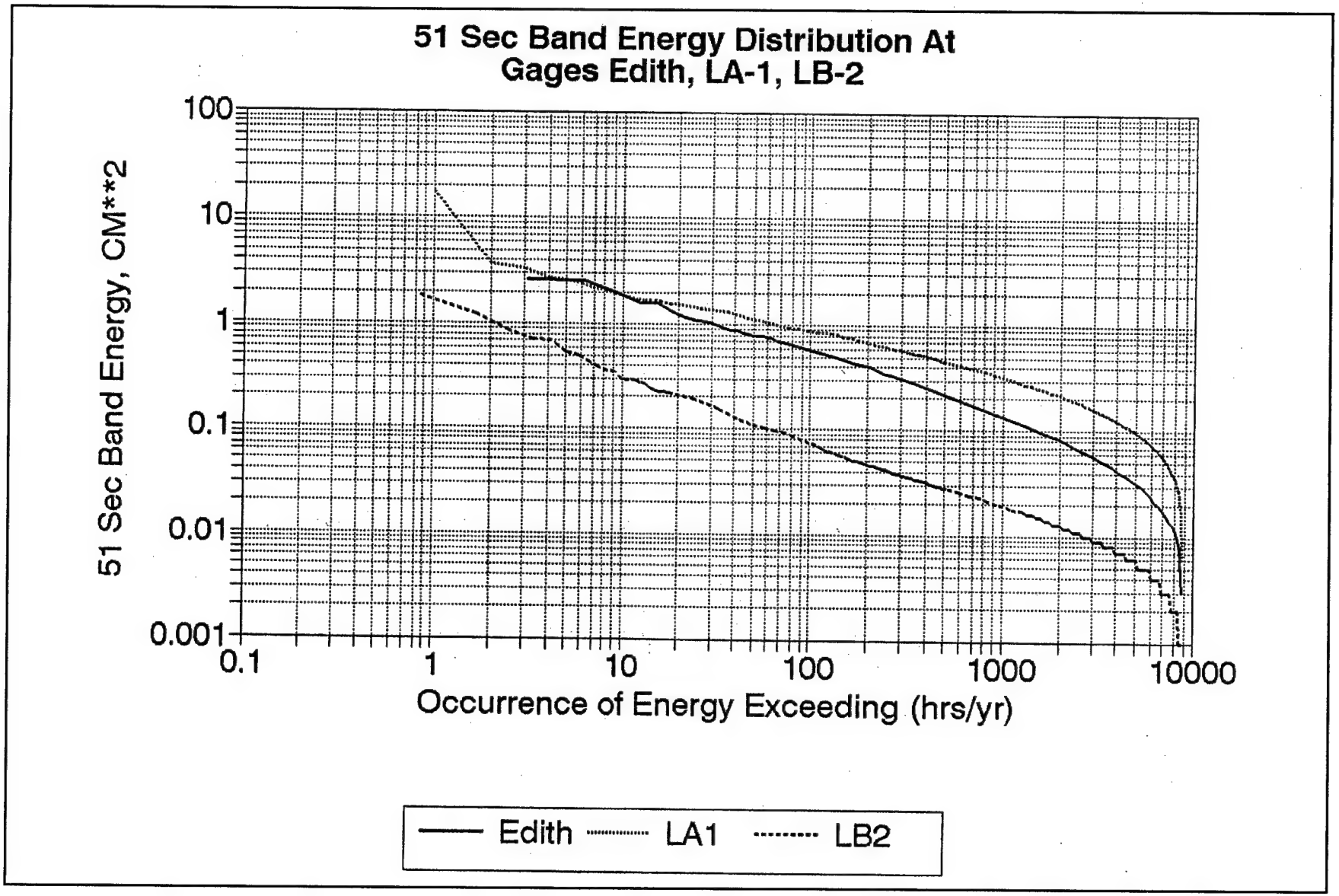
51 Sec Band Energy Distribution At
Gages Edith, LA-1, LB-2
51 Sec Band Energy, CM**2
100
10
1
0.1
0.01
0.001
0.1
1
10
100
1000
10000
Occurrence of Energy Exceeding (hrs/yr)
Edith
LA1
LB2

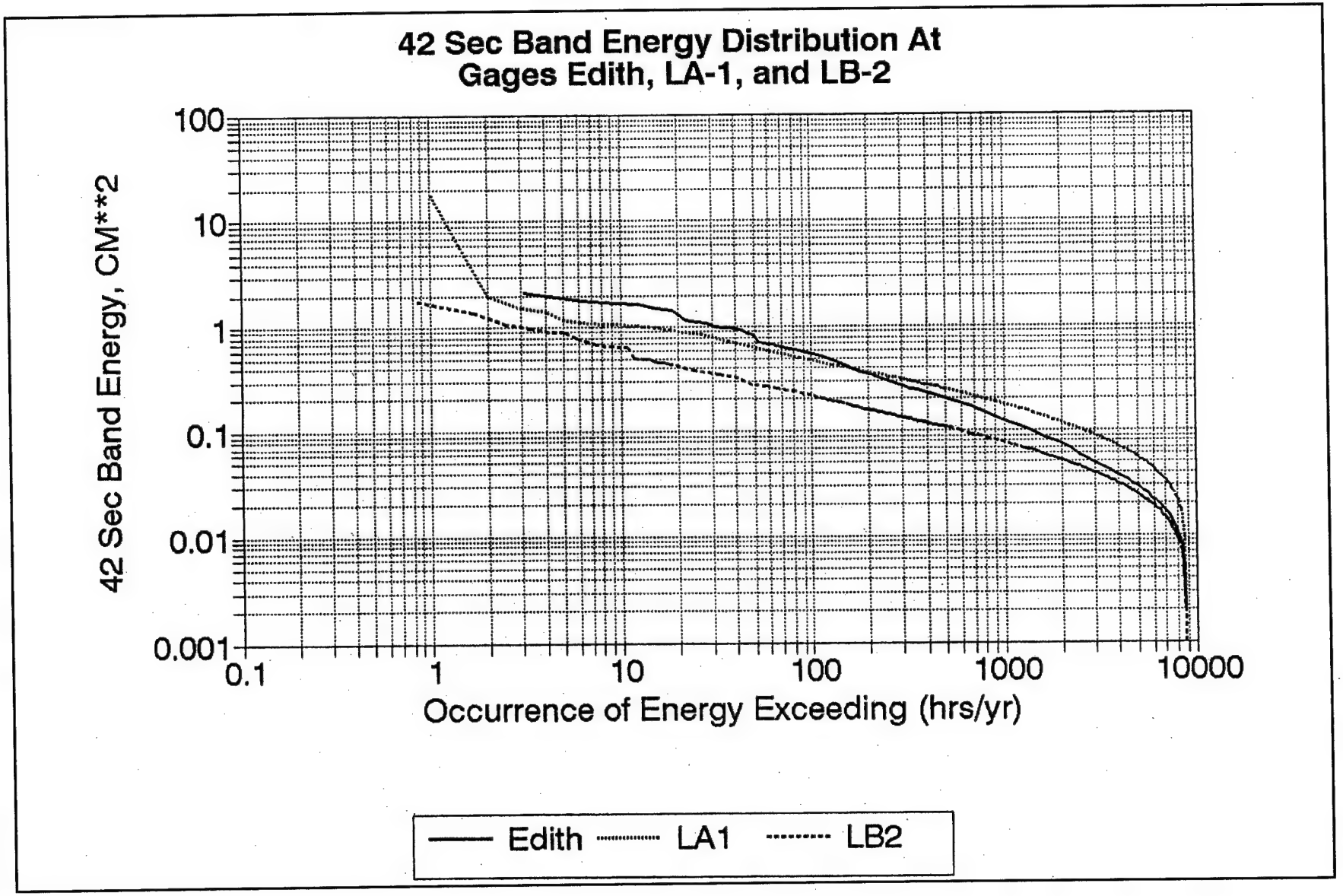
42 Sec Band Energy Distribution At
Gages Edith, LA-1, and LB-2
42 Sec Band Energy, CM**2
100
10
1
0.1
0.01
0.001
0.1
1
10
100
1000
10000
Occurrence of Energy Exceeding (hrs/yr)
Edith
LA1
LB2

Plate 31

Plate 32

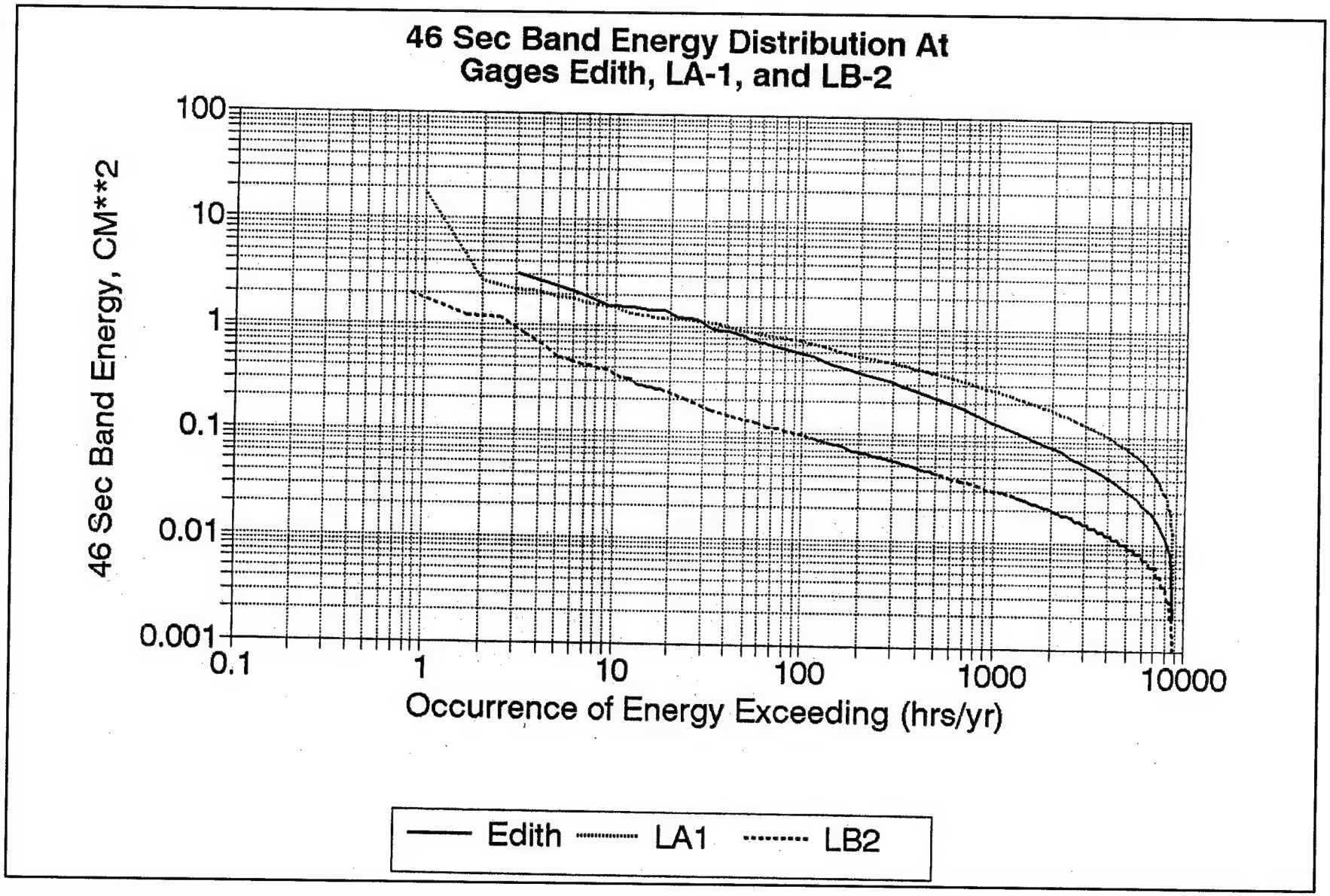
46 Sec Band Energy Distribution At
Gages Edith, LA-1, and LB-2
46 Sec Band Energy, CM**2
100
10
1
0.1
0.01
0.001
0.1
1
10
100
1000
10000
Occurrence of Energy Exceeding (hrs/yr)
Edith
LA1
LB2

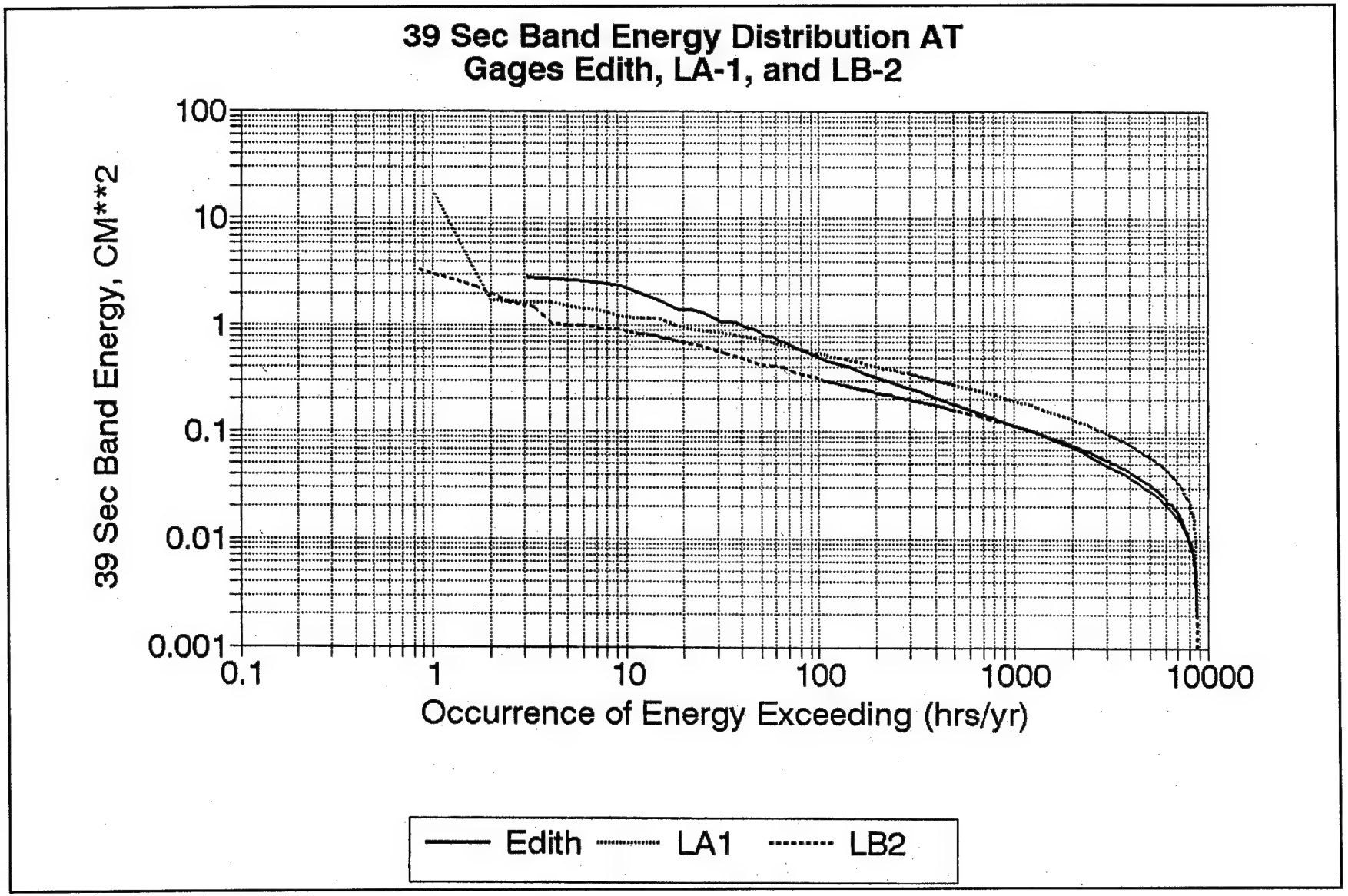
39 Sec Band Energy Distribution AT
Gages Edith, LA-1, and LB-2
39 Sec Band Energy, CM**2
100
10
1
0.1
0.01
0.001
0.1
1
10
100
1000
10000
Occurrence of Energy Exceeding (hrs/yr)
Edith
LA1
LB2

Plate 33

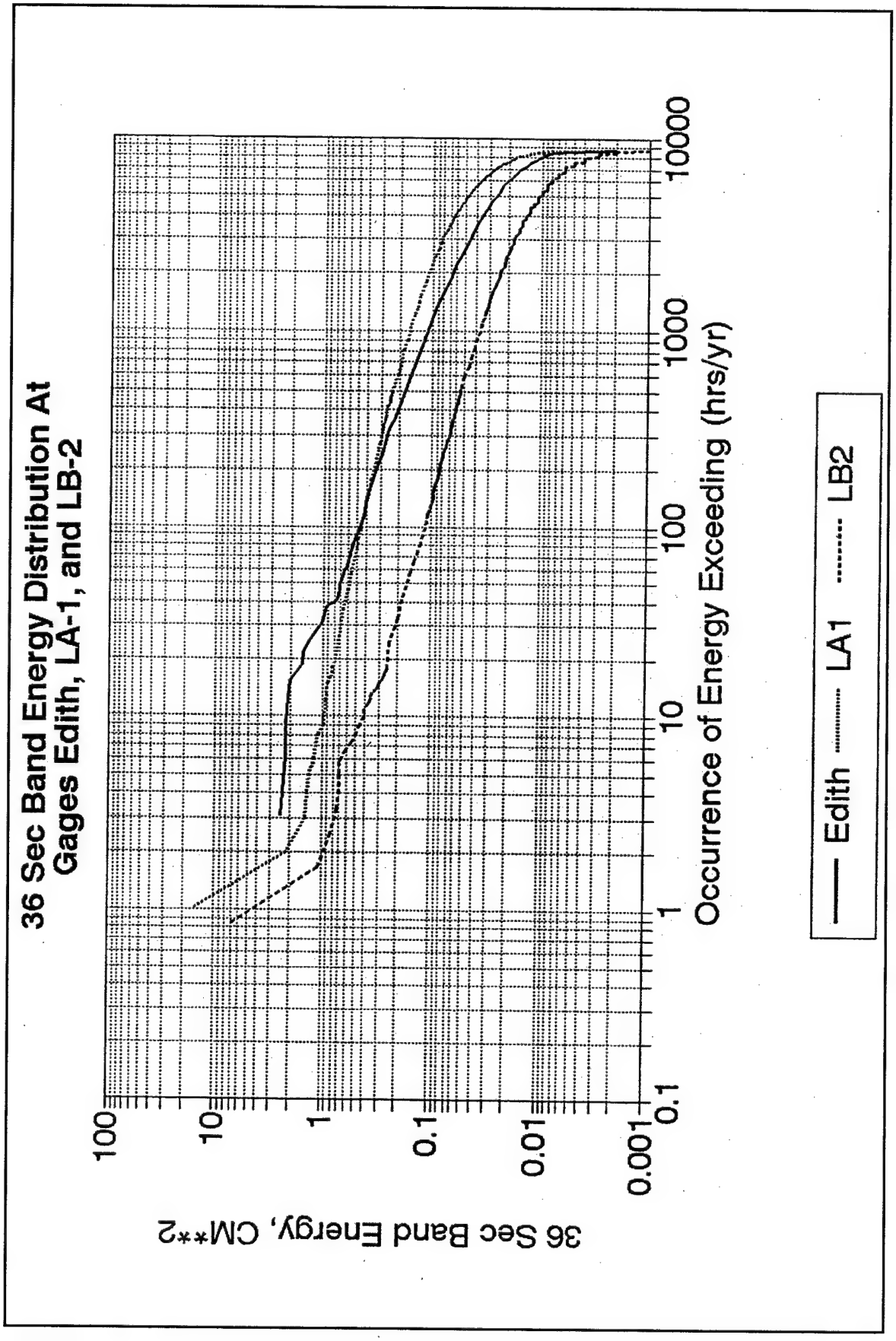
36 Sec Band Energy Distribution At
Gages Edith, LA-1, and LB-2
36 Sec Band Energy, CM**2
100
10
1
0.1
0.01
0.001
0.1
1
10
100
1000
10000
Occurrence of Energy Exceeding (hrs/yr)
Edith
LA1
LB2

Plate 34

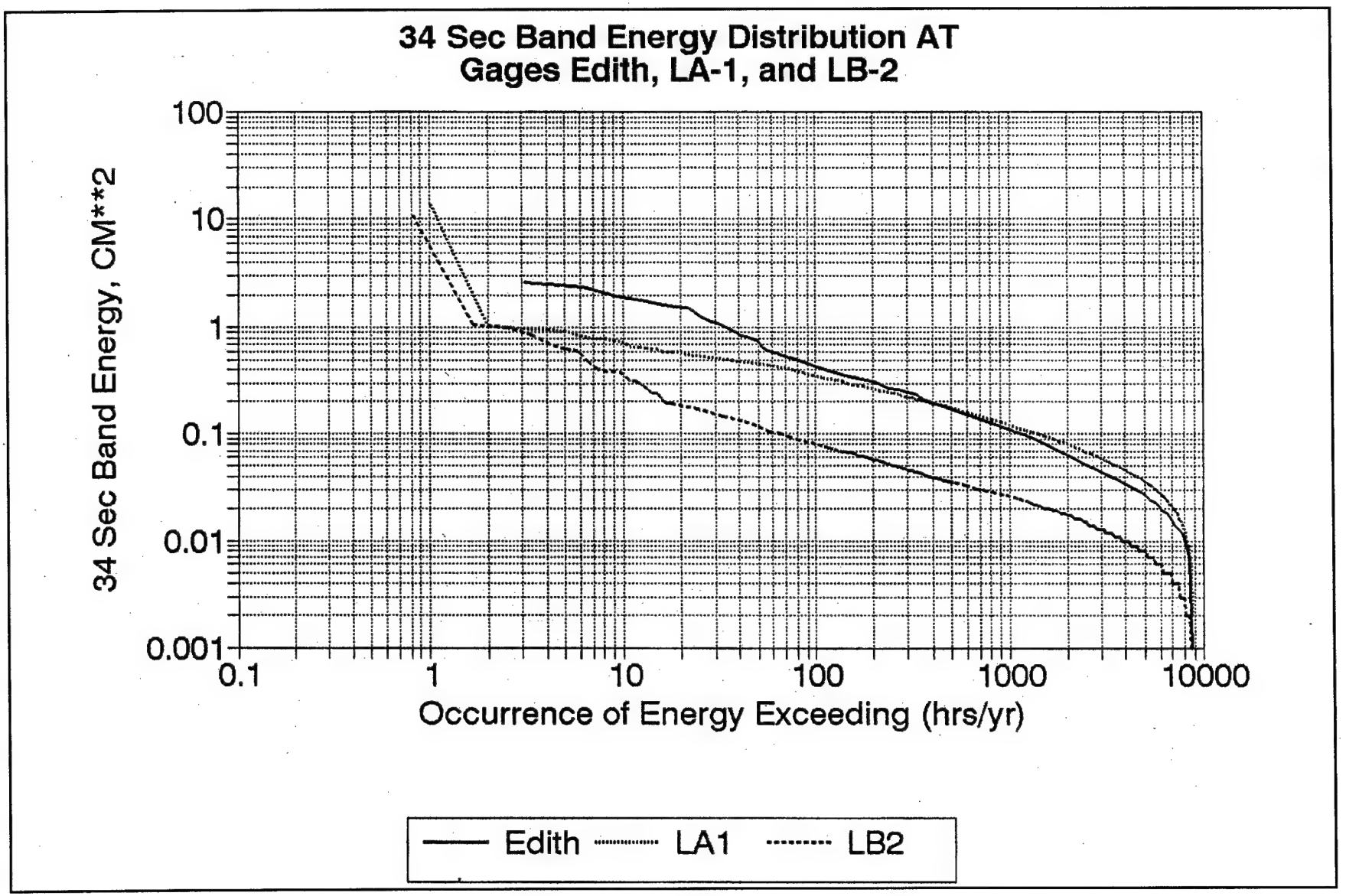
34 Sec Band Energy Distribution AT
Gages Edith, LA-1, and LB-2
34 Sec Band Energy, CM**2
100
10
1
0.1
0.01
0.001
0.1
1
10
100
1000
10000
Occurrence of Energy Exceeding (hrs/yr)
Edith
LA1
LB2

Plate 35

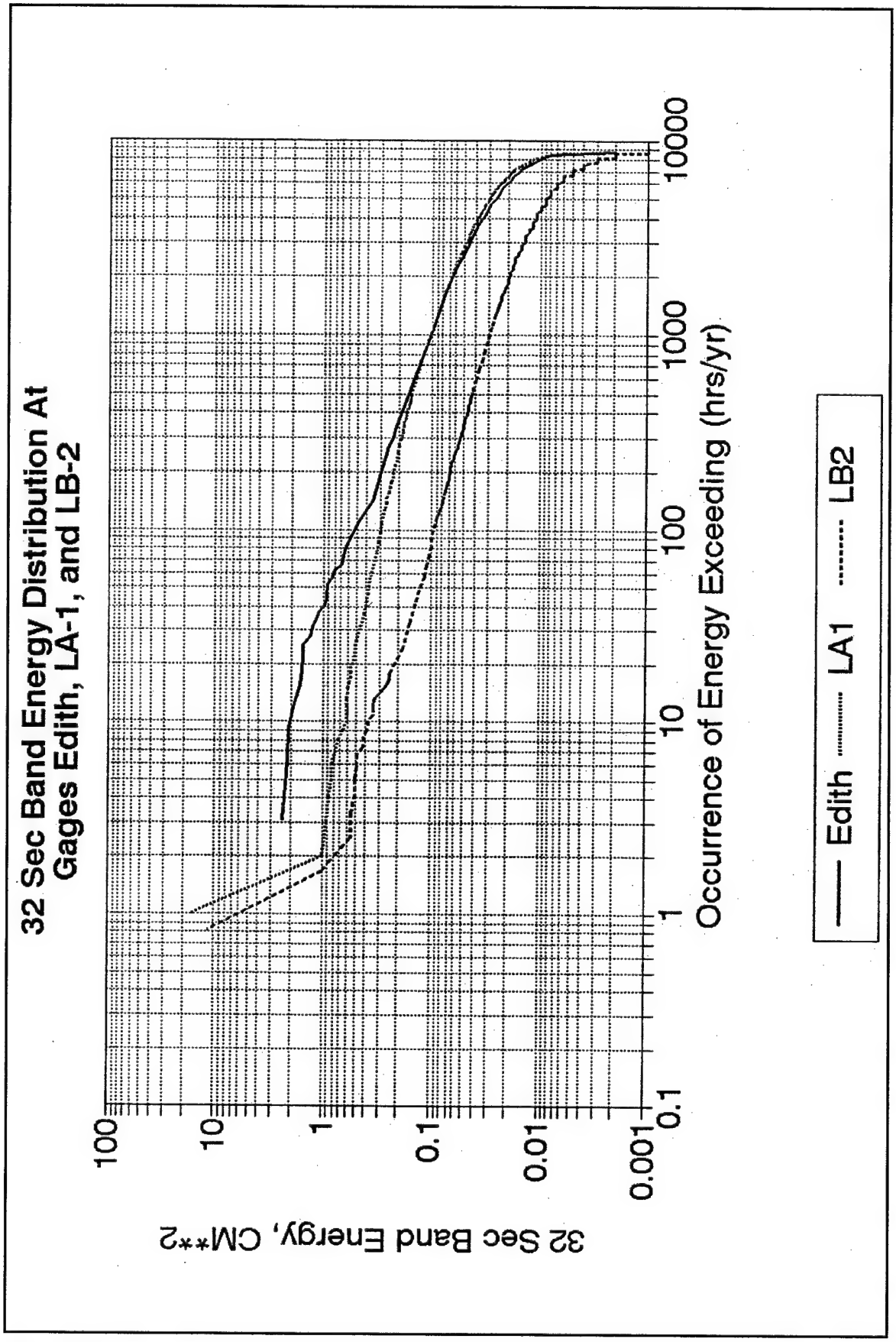
32 Sec Band Energy Distribution At
Gages Edith, LA-1, and LB-2
32 Sec Band Energy, CM**2
100
10
1
0.1
0.01
0.001
0.1
1
10
100
1000
10000
Occurrence of Energy Exceeding (hrs/yr)
Edith
LA1
LB2

Plate 36

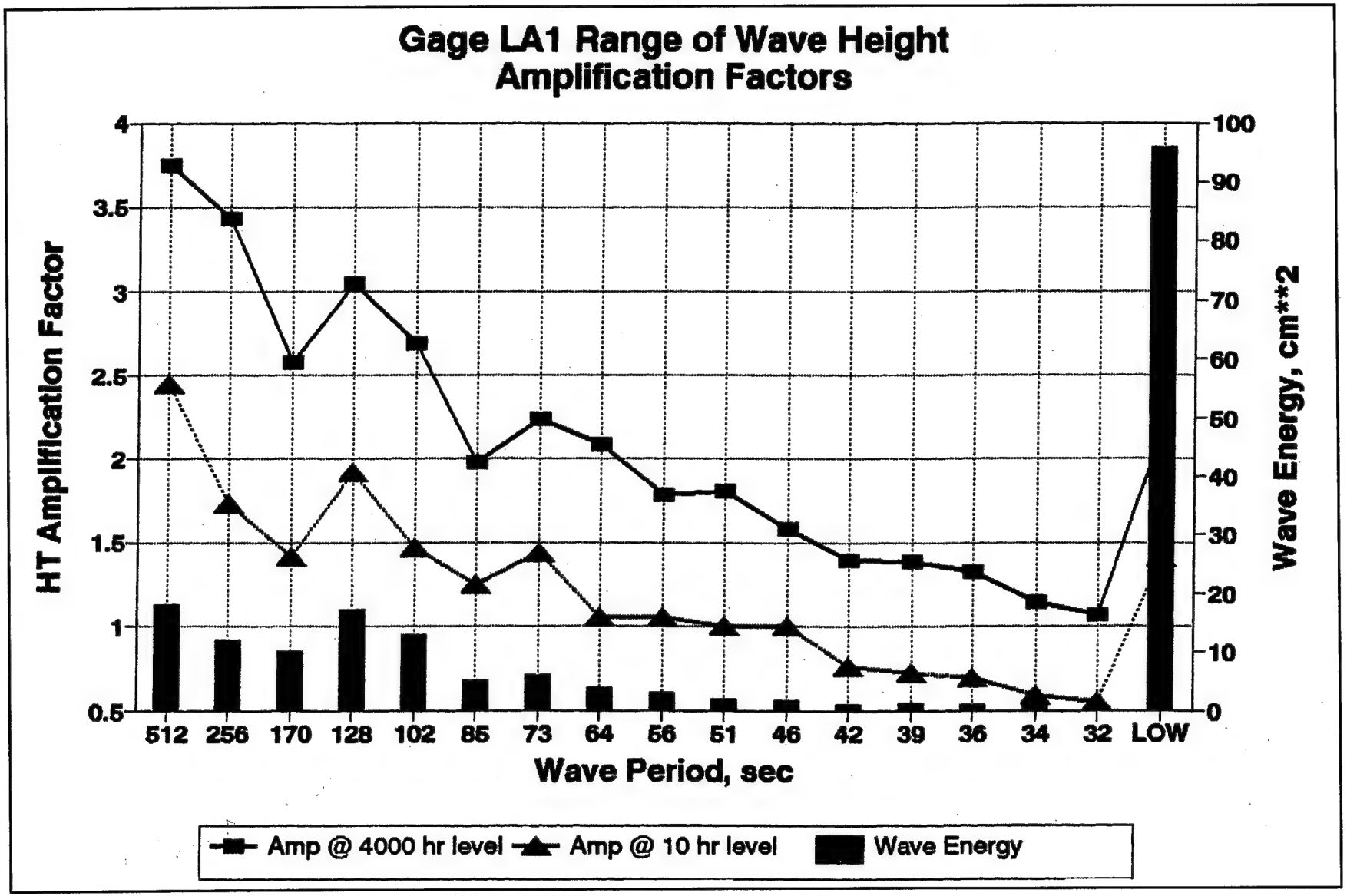
Gage LA1 Range of Wave Height
Amplification Factors
HT Amplification Factor
Wave Energy, cm**2
Wave Period, sec
4
3.5
3
2.5
2
1.5
1
0.5
100
90
80
70
60
50
40
30
20
10
0
512
256
170
128
102
85
73
64
56
51
46
42
39
36
34
32
LOW
Amp @ 4000 hr level
Amp @ 10 hr level
Wave Energy

Plate 37

Plate 38

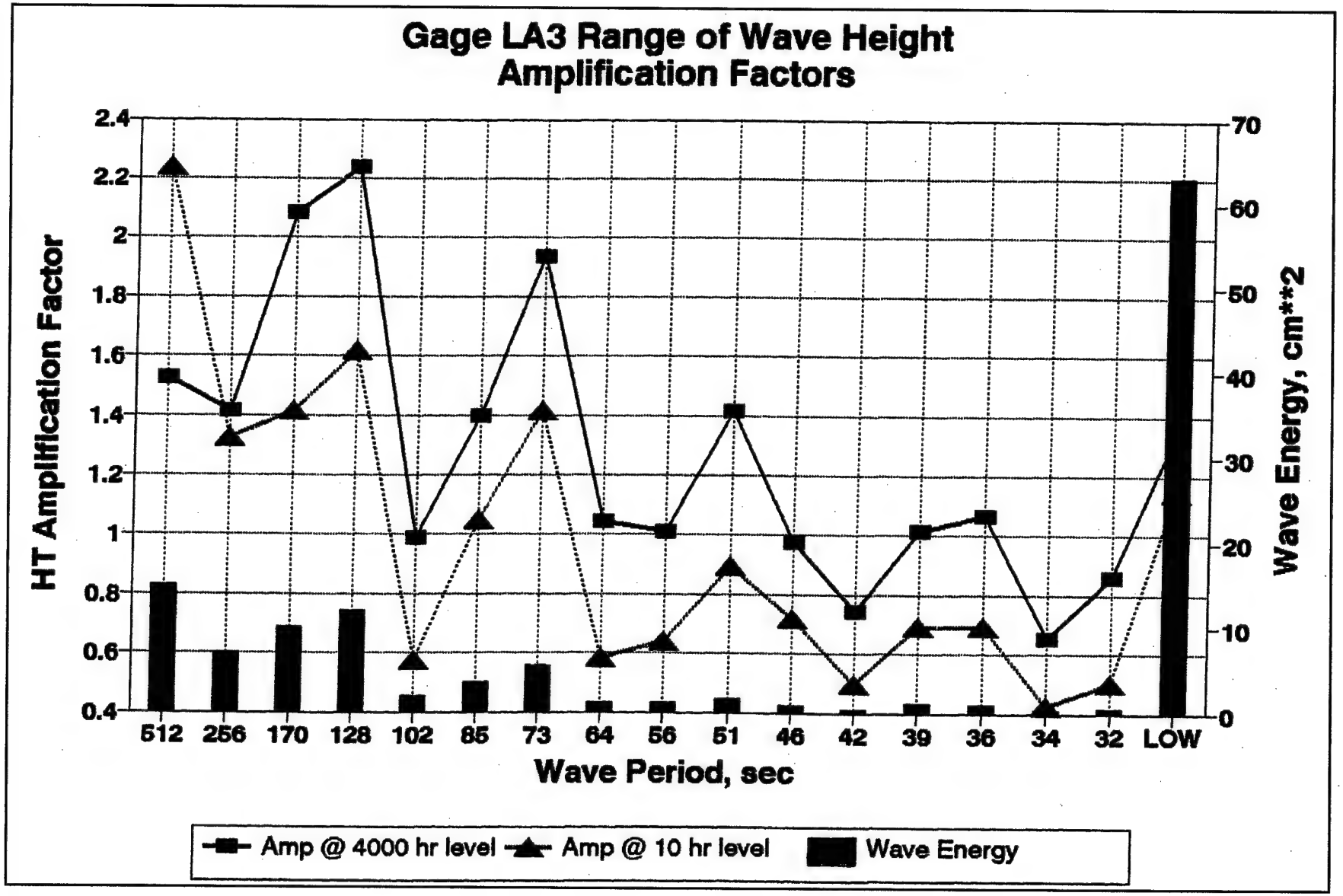
Gage LA3 Range of Wave Height
Amplification Factors
HT Amplification Factor
2.4
2.2
2
1.8
1.6
1.4
1.2
1
0.8
0.6
0.4
Wave Energy, cm**2
70
60
50
40
30
20
10
0
512
256
170
128
102
85
73
64
56
51
46
42
39
36
34
32
LOW
Wave Period, sec
Amp @ 4000 hr level
Amp @ 10 hr level
Wave Energy

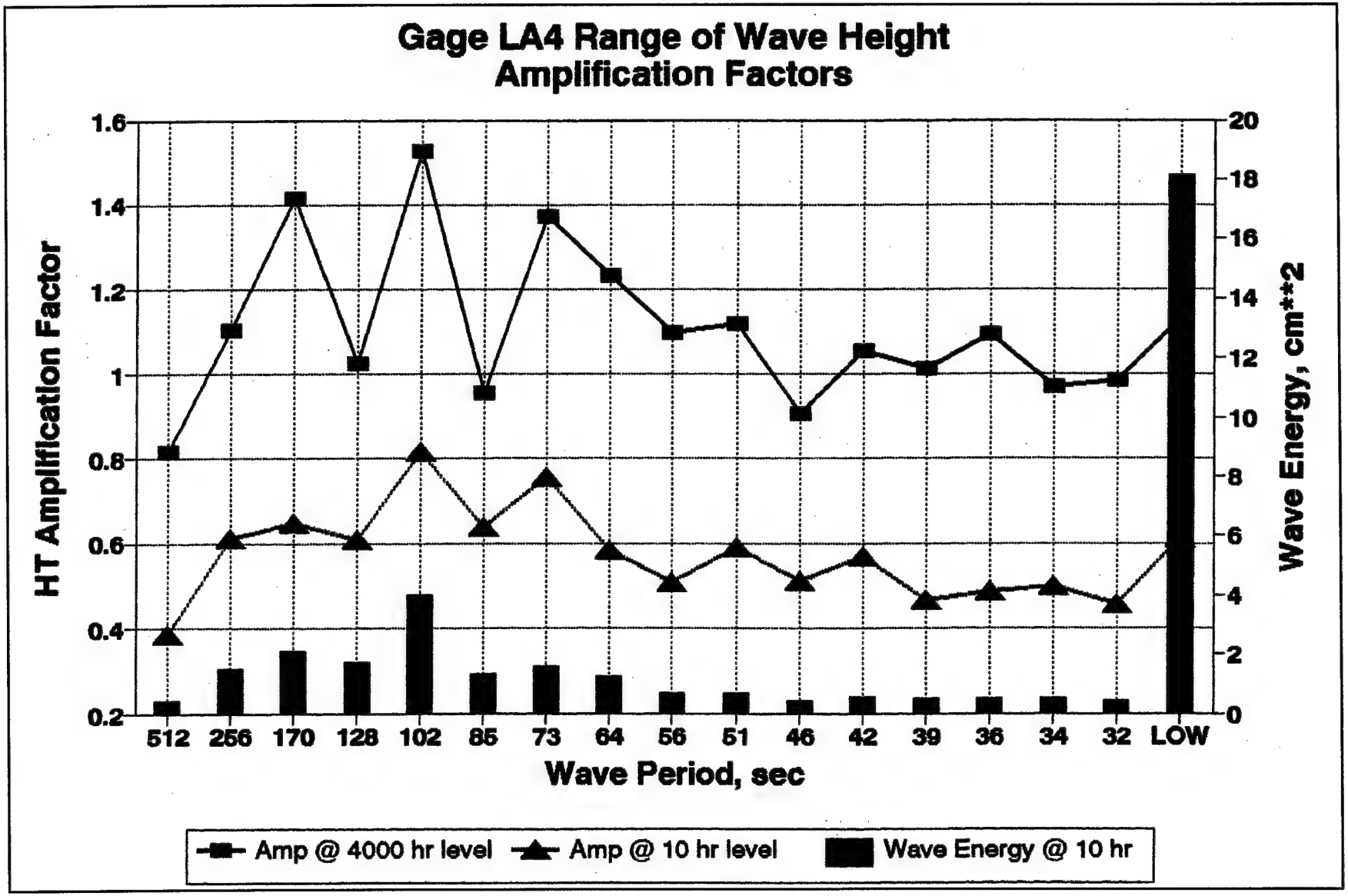
Gage LA4 Range of Wave Height
Amplification Factors
HT Amplification Factor
1.6
1.4
1.2
1
0.8
0.6
0.4
0.2
Wave Energy, cm**2
20
18
16
14
12
10
8
6
4
2
0
512 256 170 128 102 85 73 64 56 51 46 42 39 36 34 32 LOW
Wave Period, sec
Amp @ 4000 hr level
Amp @ 10 hr level
Wave Energy @ 10 hr

Plate 39

Plate 40

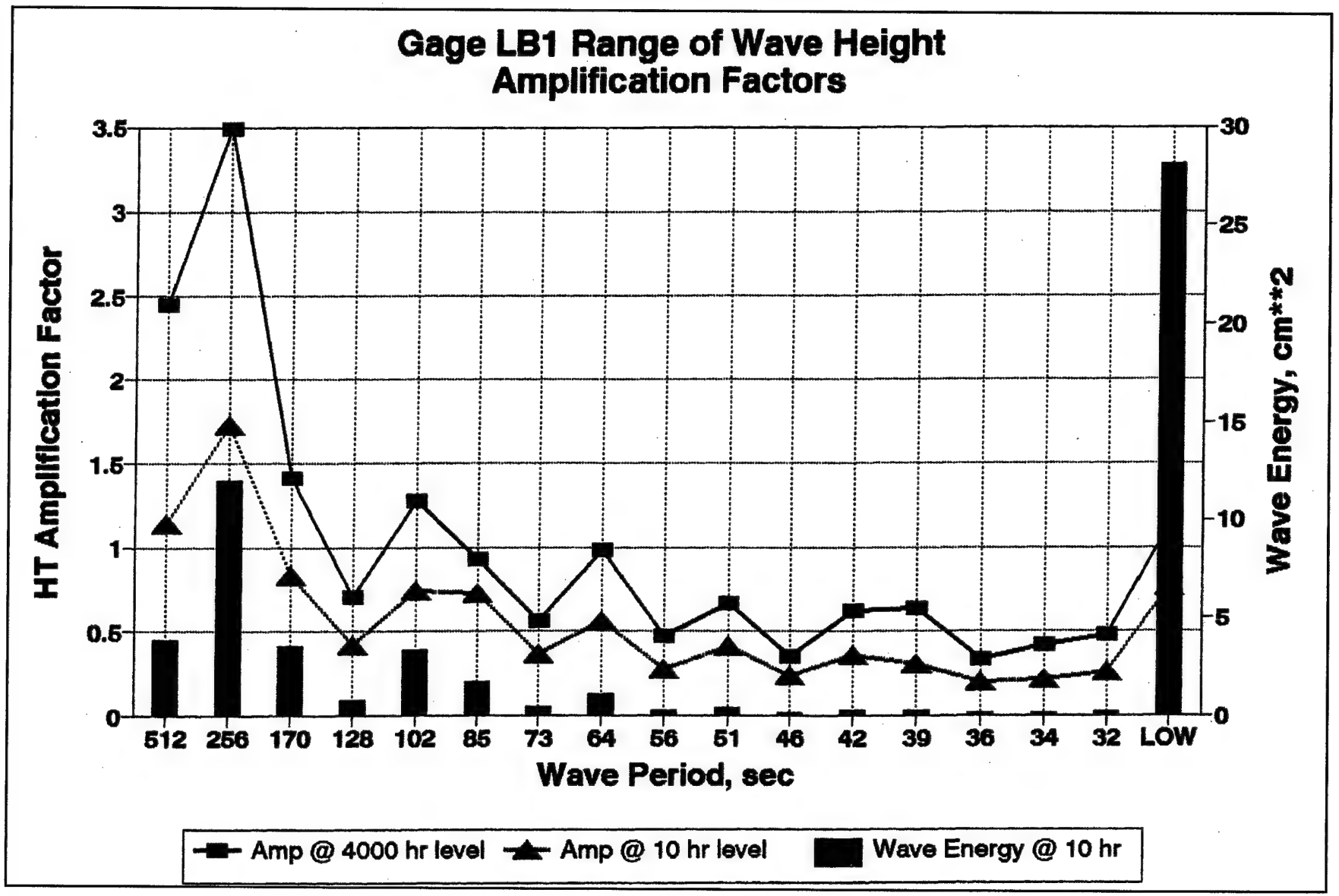
Gage LB1 Range of Wave Height
Amplification Factors
HT Amplification Factor
Wave Energy, cm**2
Wave Period, sec
3.5
3
2.5
2
1.5
1
0.5
0
30
25
20
15
10
5
0
512 256 170 128 102 85 73 64 56 51 46 42 39 36 34 32 LOW
Amp @ 4000 hr level
Amp @ 10 hr level
Wave Energy @ 10 hr

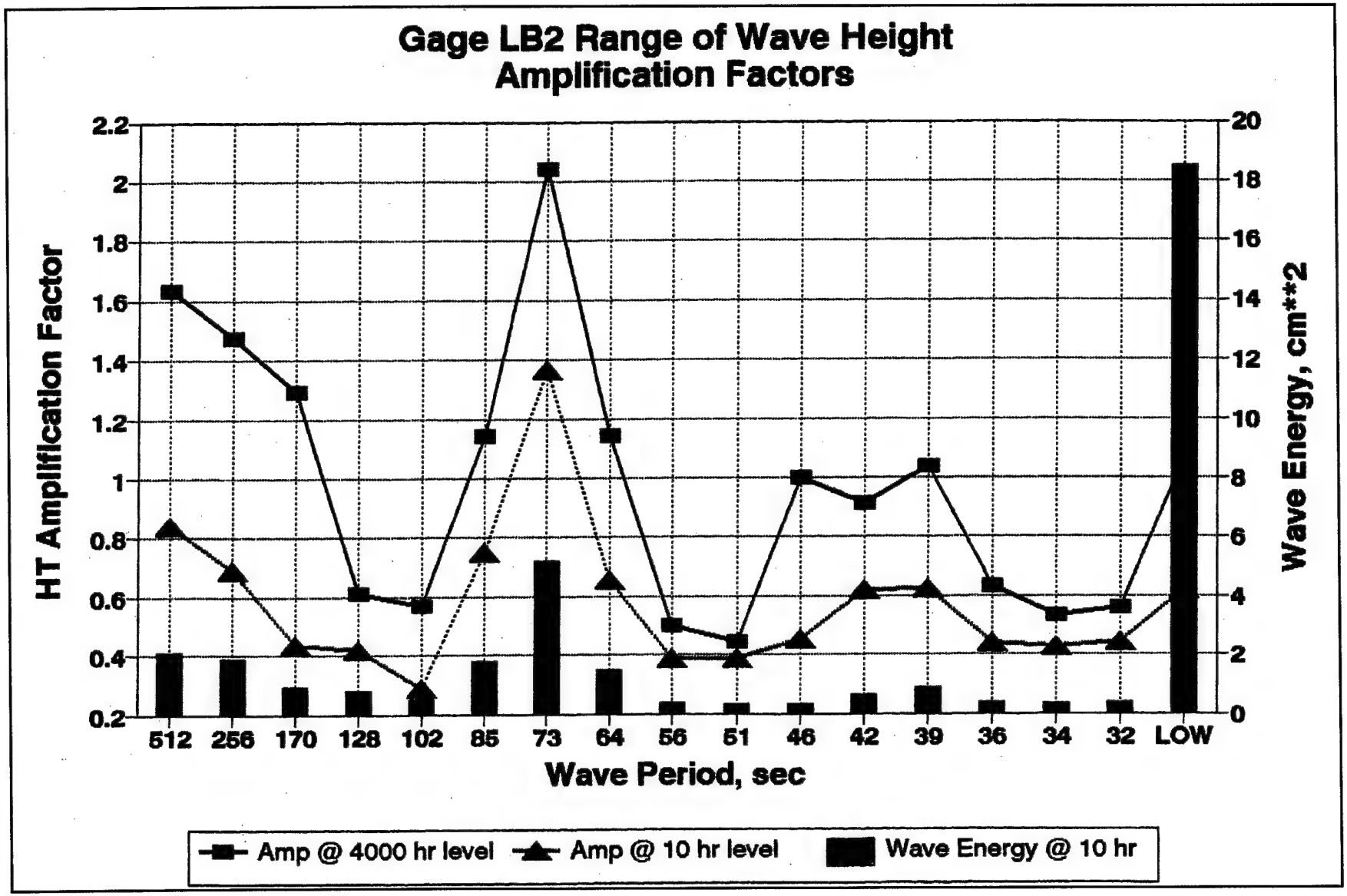
Gage LB2 Range of Wave Height
Amplification Factors
HT Amplification Factor
2.2
2
1.8
1.6
1.4
1.2
1
0.8
0.6
0.4
0.2
Wave Energy, cm**2
20
18
16
14
12
10
8
6
4
2
0
512 256 170 128 102 85 73 64 56 51 46 42 39 36 34 32 LOW
Wave Period, sec
Amp @ 4000 hr level
Amp @ 10 hr level
Wave Energy @ 10 hr

Plate 41

Plate 42

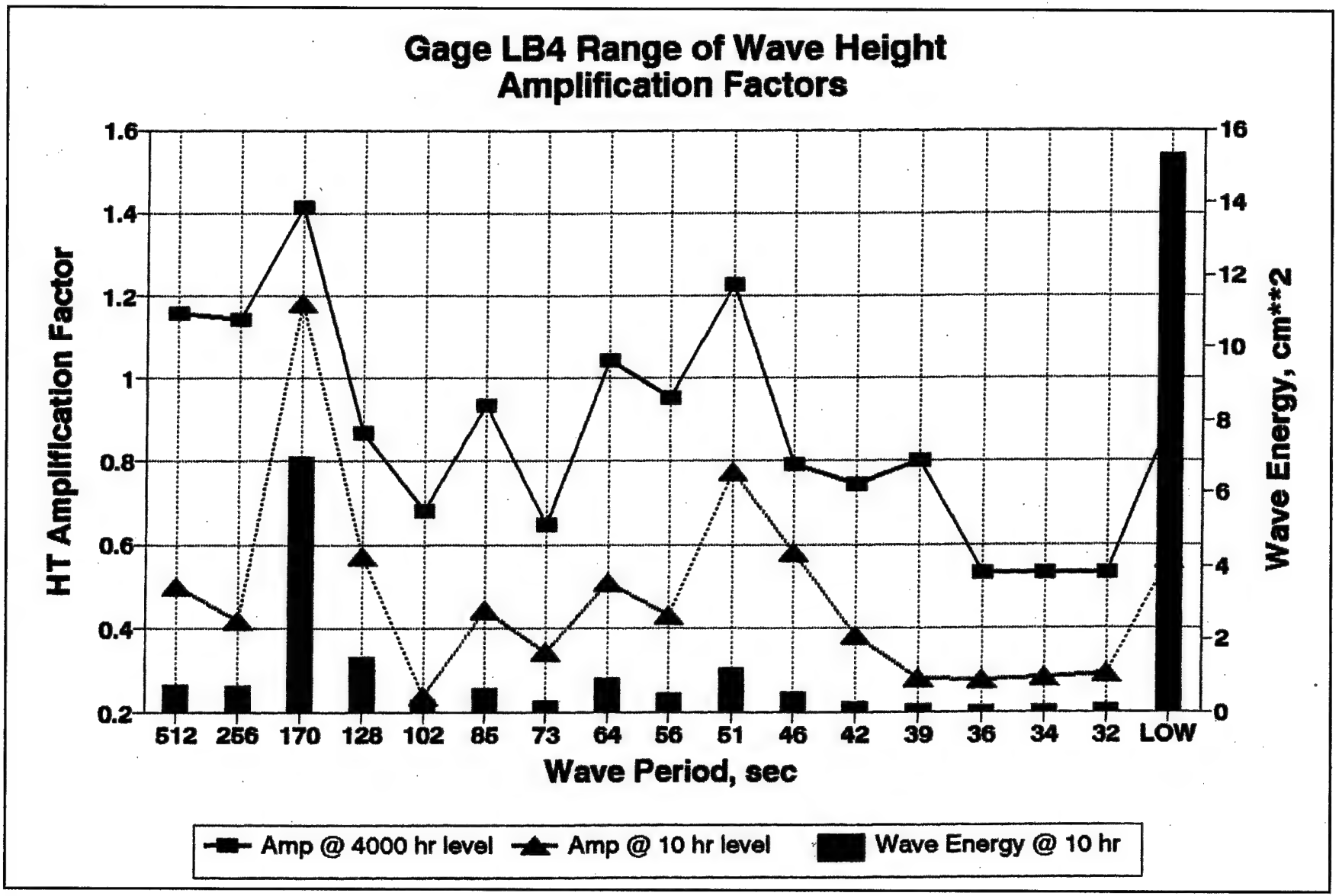
Gage LB4 Range of Wave Height
Amplification Factors
HT Amplification Factor
1.6
1.4
1.2
1
0.8
0.6
0.4
0.2
Wave Energy, cm**2
16
14
12
10
8
6
4
2
0
512 256 170 128 102 85 73 64 56 51 46 42 39 36 34 32 LOW
Wave Period, sec
Amp @ 4000 hr level
Amp @ 10 hr level
Wave Energy @ 10 hr

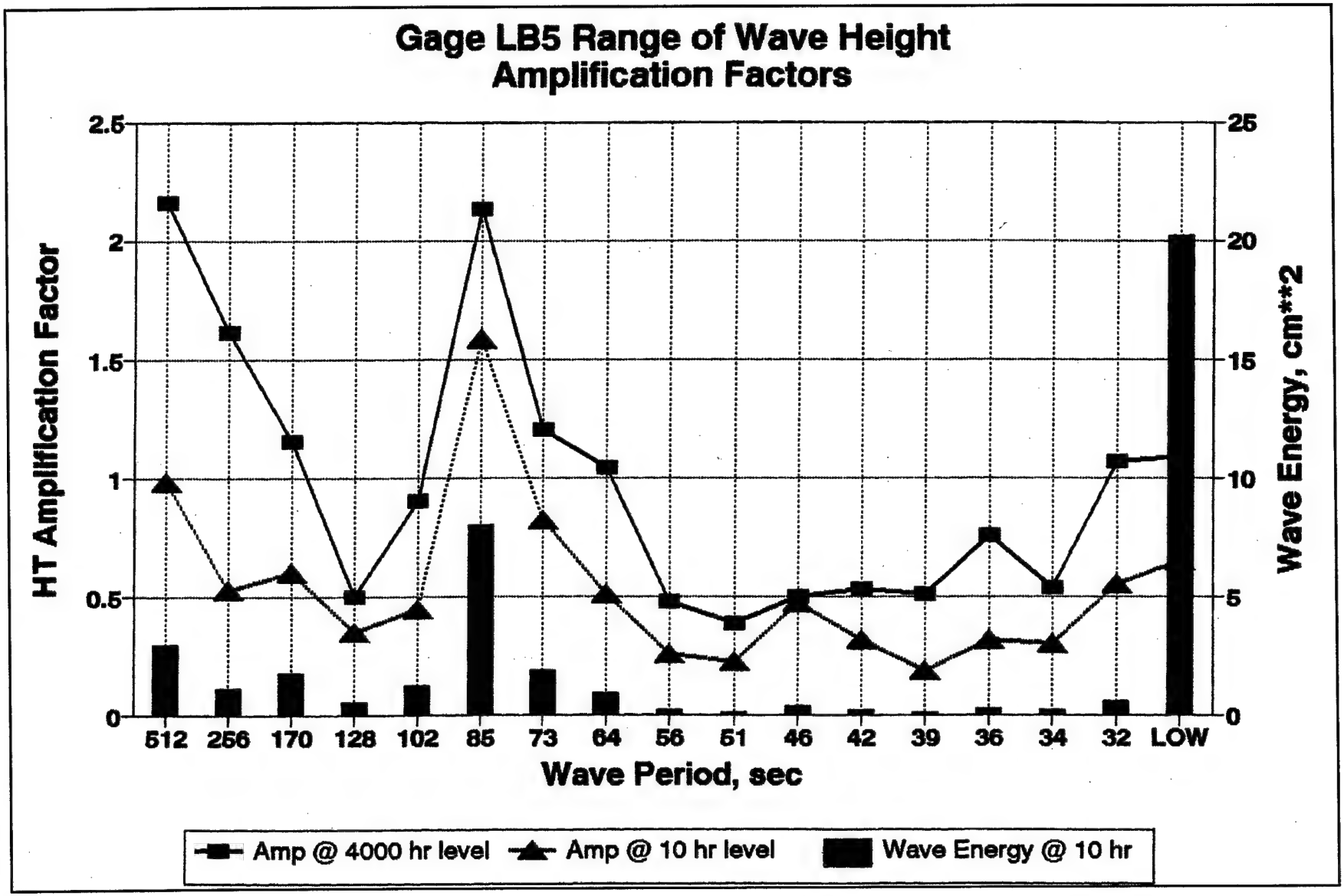
Gage LB5 Range of Wave Height
Amplification Factors
HT Amplification Factor
Wave Energy, cm**2
Wave Period, sec
2.5
2
1.5
1
0.5
0
25
20
15
10
5
0
512
256
170
128
102
85
73
64
56
51
46
42
39
36
34
32
LOW
Amp @ 4000 hr level
Amp @ 10 hr level
Wave Energy @ 10 hr

Plate 43

Plate 44

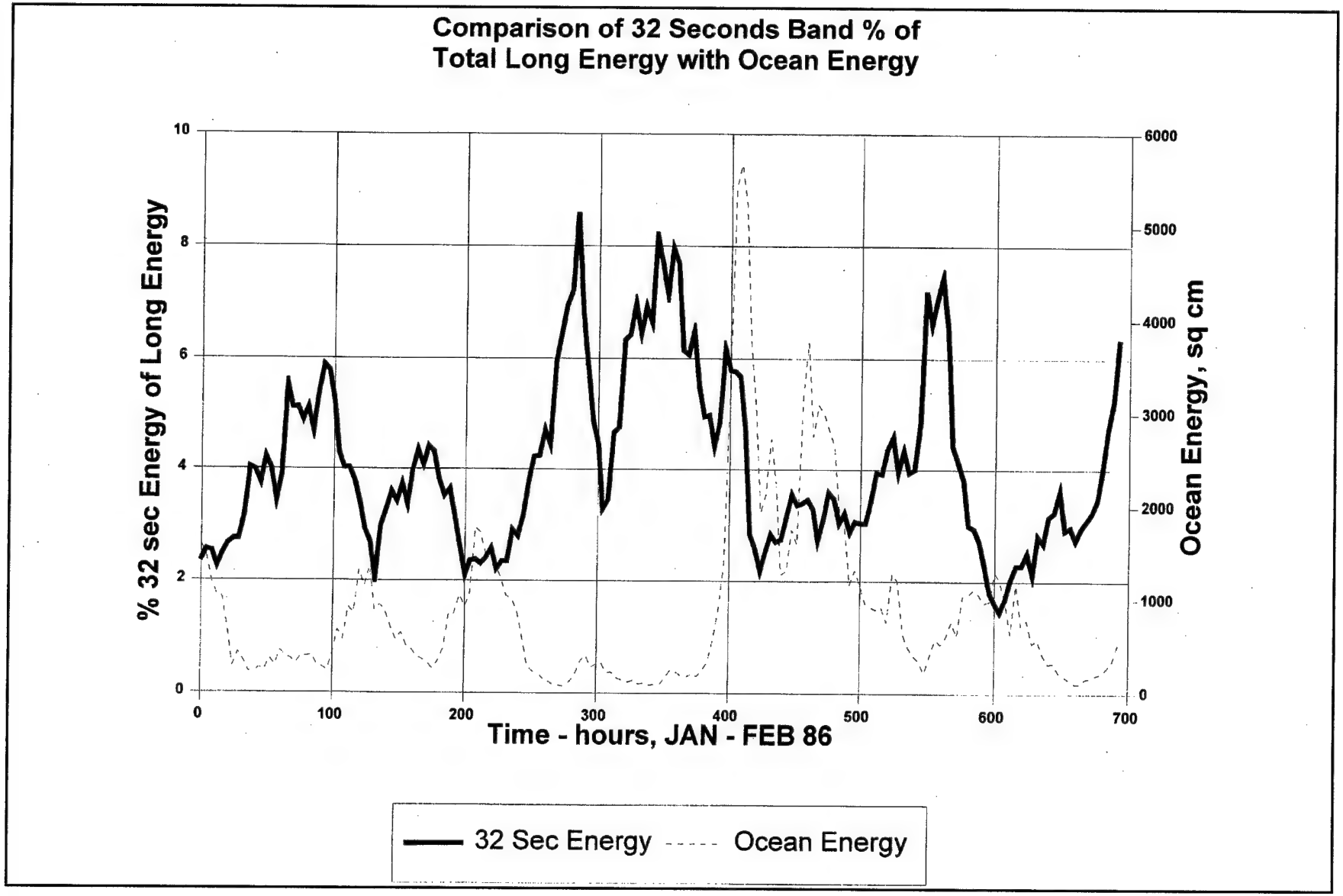
Comparison of 32 Seconds Band % of
Total Long Energy with Ocean Energy
% 32 sec Energy of Long Energy
Ocean Energy, sq cm
Time - hours, JAN - FEB 86
0
2
4
6
8
10
0
1000
2000
3000
4000
5000
6000
0
100
200
300
400
500
600
700
32 Sec Energy
Ocean Energy

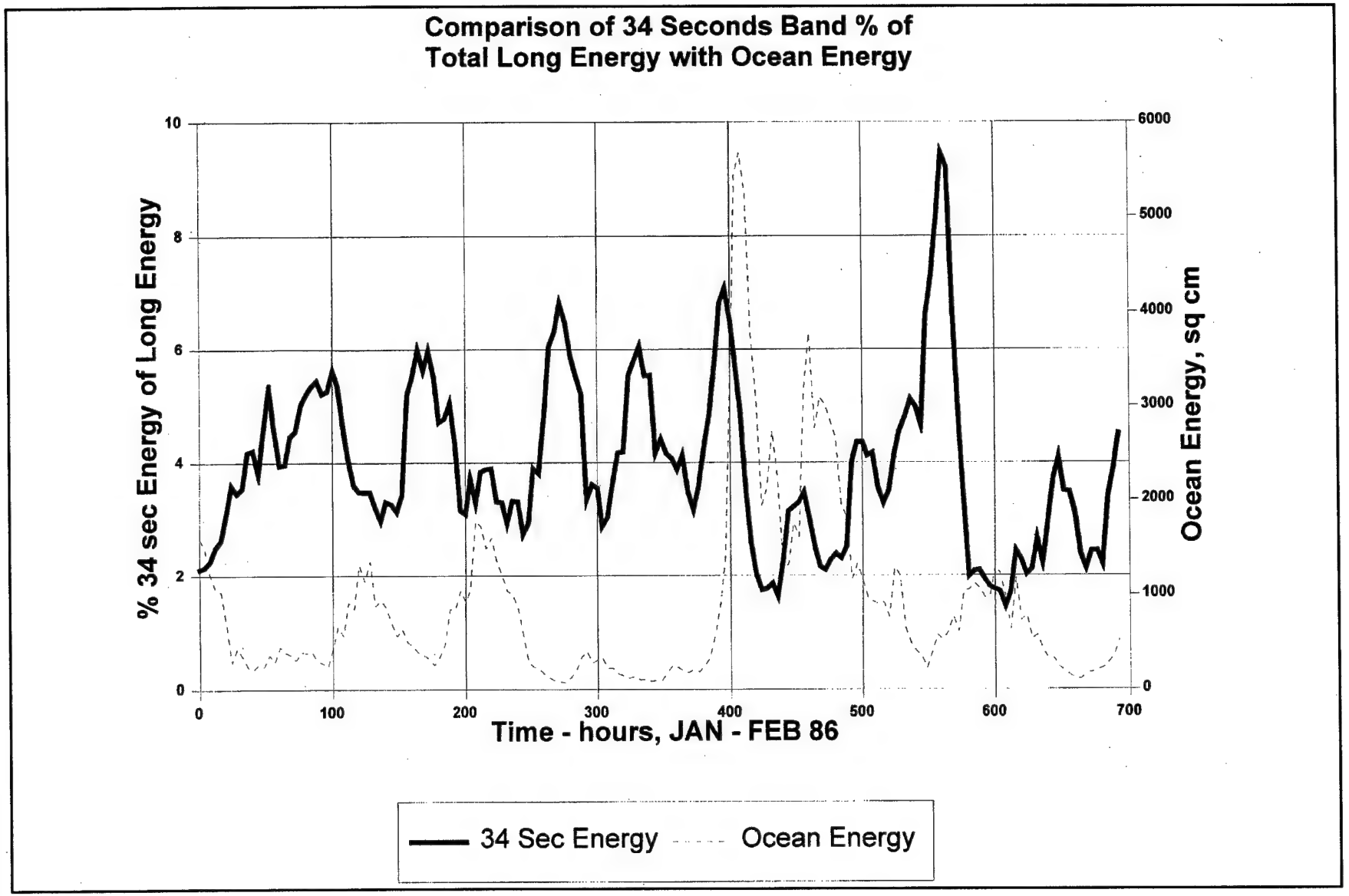
Comparison of 34 Seconds Band % of
Total Long Energy with Ocean Energy
% 34 sec Energy of Long Energy
Ocean Energy, sq cm
Time - hours, JAN - FEB 86
0
2
4
6
8
10
0
1000
2000
3000
4000
5000
6000
0
100
200
300
400
500
600
700
34 Sec Energy
Ocean Energy

Plate 45

Plate 46

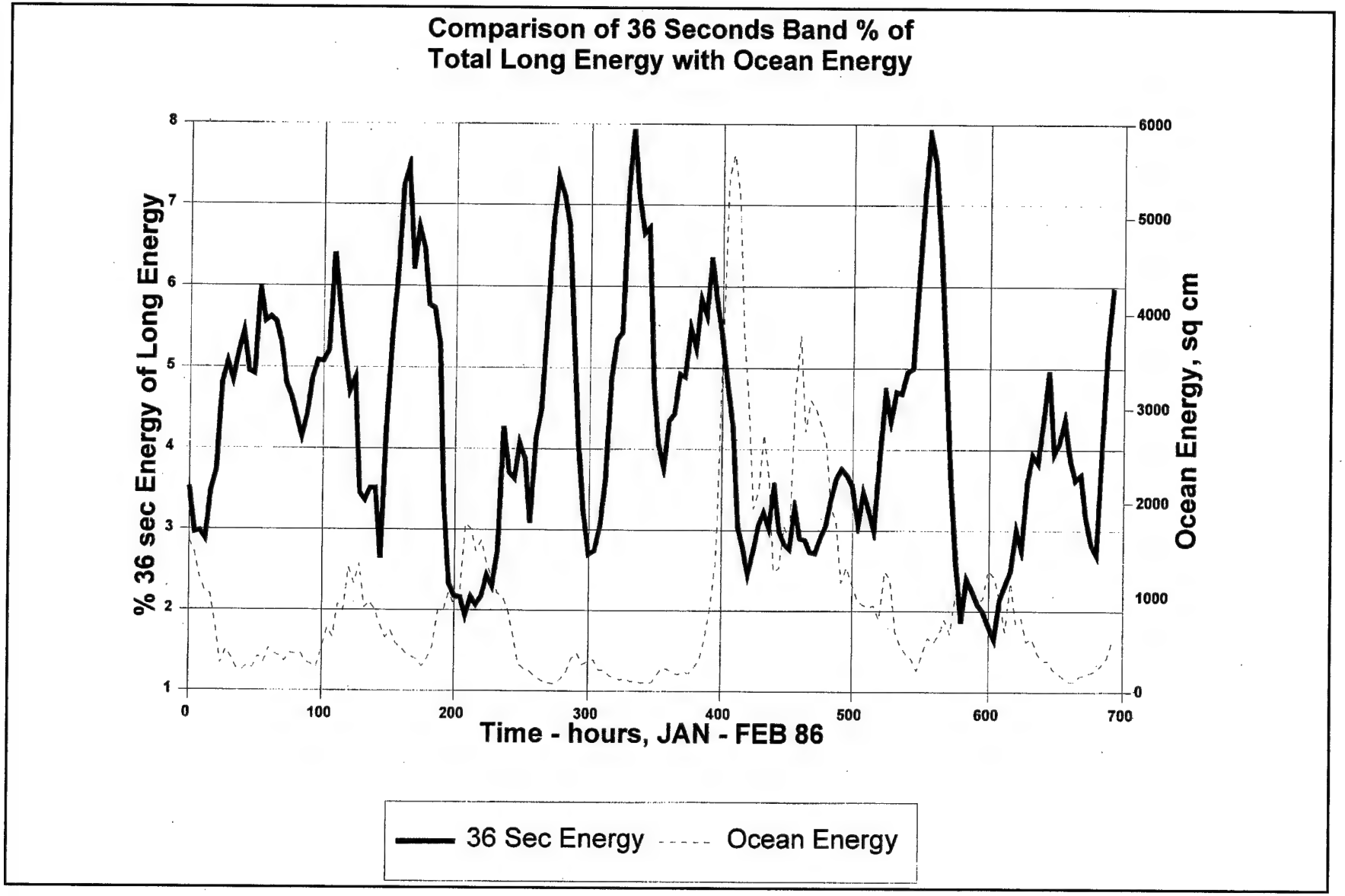
Comparison of 36 Seconds Band % of
Total Long Energy with Ocean Energy
% 36 sec Energy of Long Energy
Ocean Energy, sq cm
Time - hours, JAN - FEB 86
36 Sec Energy
Ocean Energy

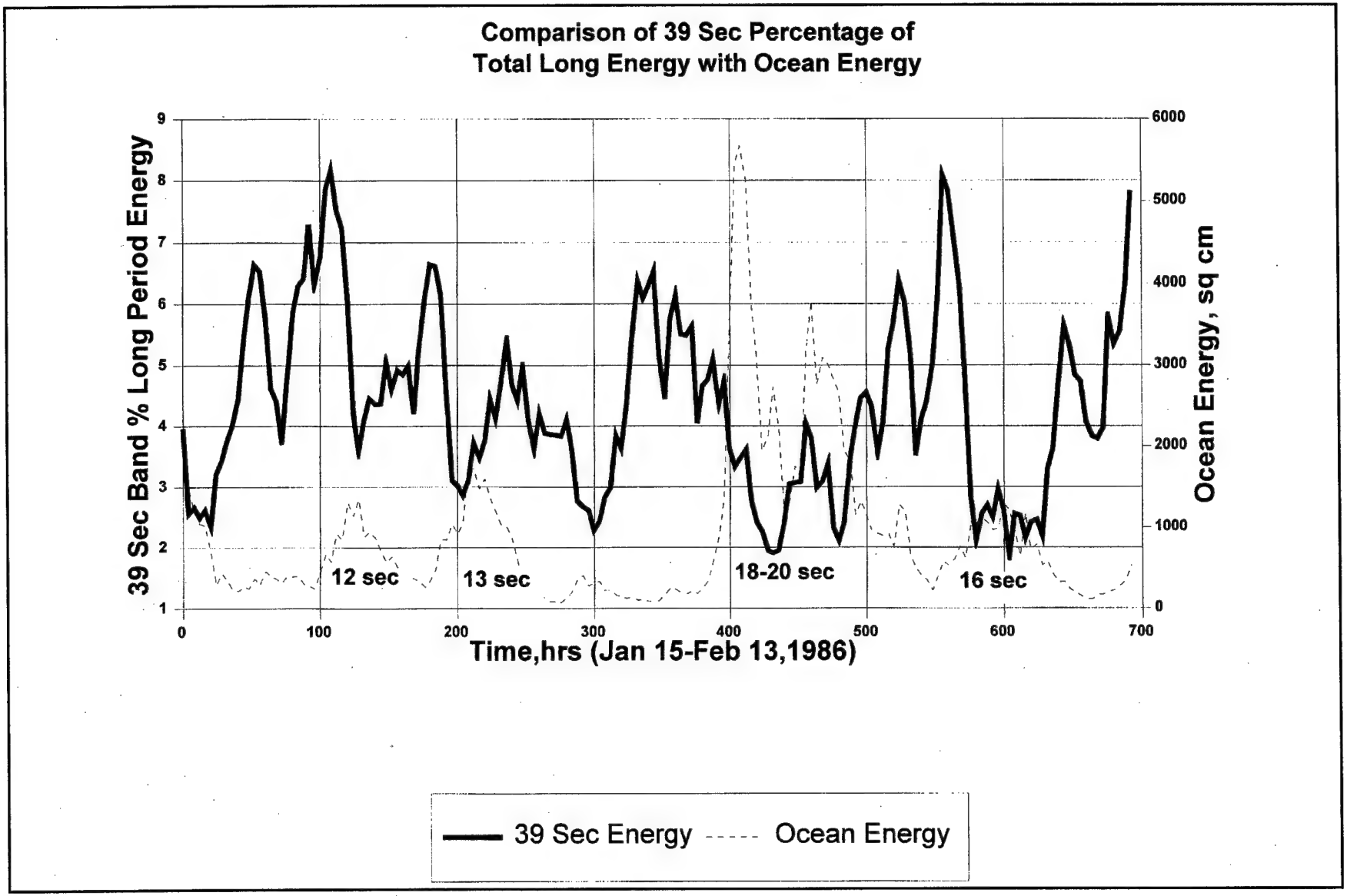
Comparison of 39 Sec Percentage of
Total Long Energy with Ocean Energy
39 Sec Band % Long Period Energy
Ocean Energy, sq cm
Time,hrs (Jan 15-Feb 13,1986)
12 sec
13 sec
18-20 sec
16 sec
39 Sec Energy
Ocean Energy

Plate 47

Plate 48

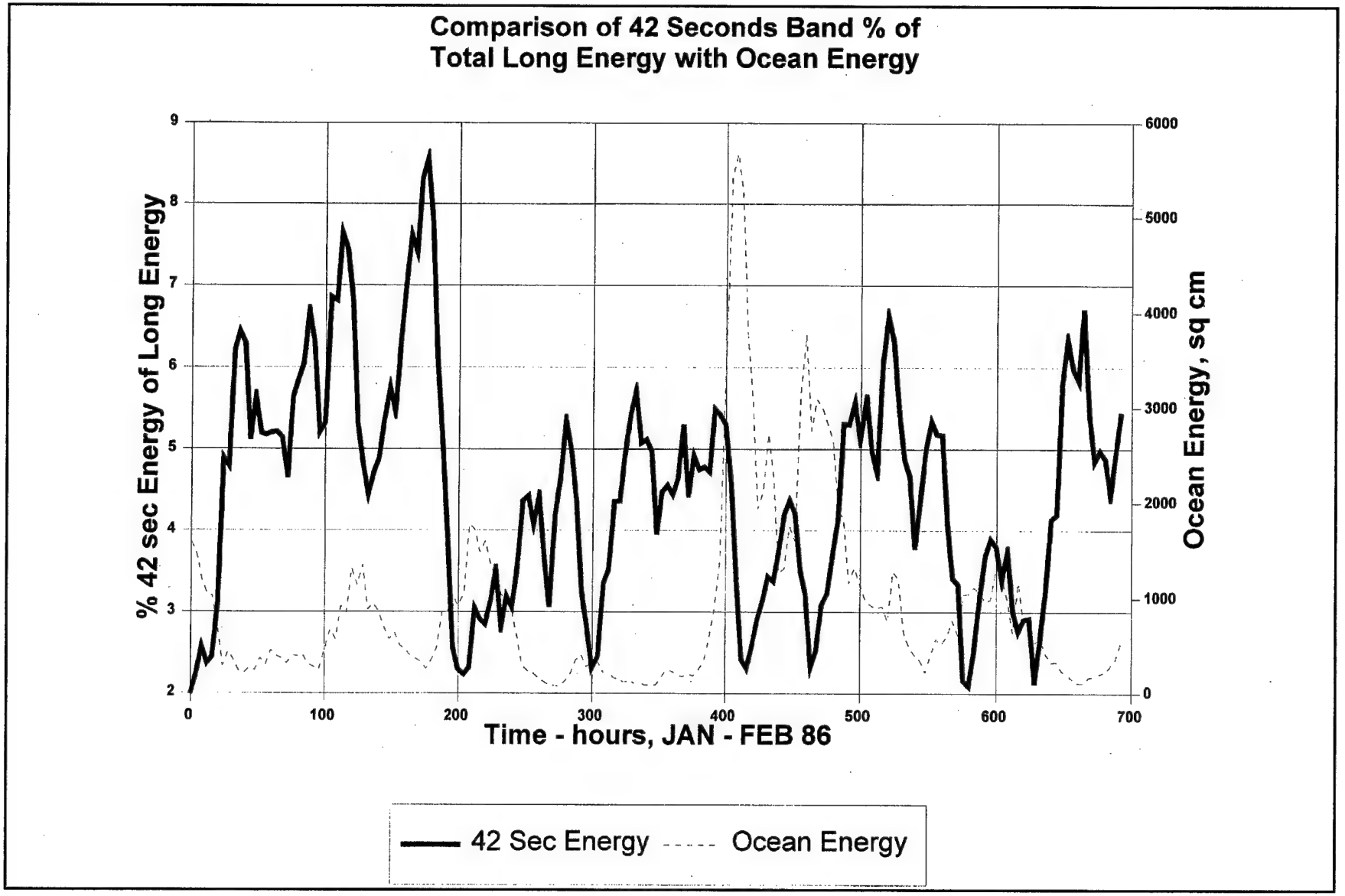
Comparison of 42 Seconds Band % of
Total Long Energy with Ocean Energy
% 42 sec Energy of Long Energy
Ocean Energy, sq cm
Time - hours, JAN - FEB 86
9
8
7
6
5
4
3
2
6000
5000
4000
3000
2000
1000
0
0
100
200
300
400
500
600
700
42 Sec Energy
Ocean Energy

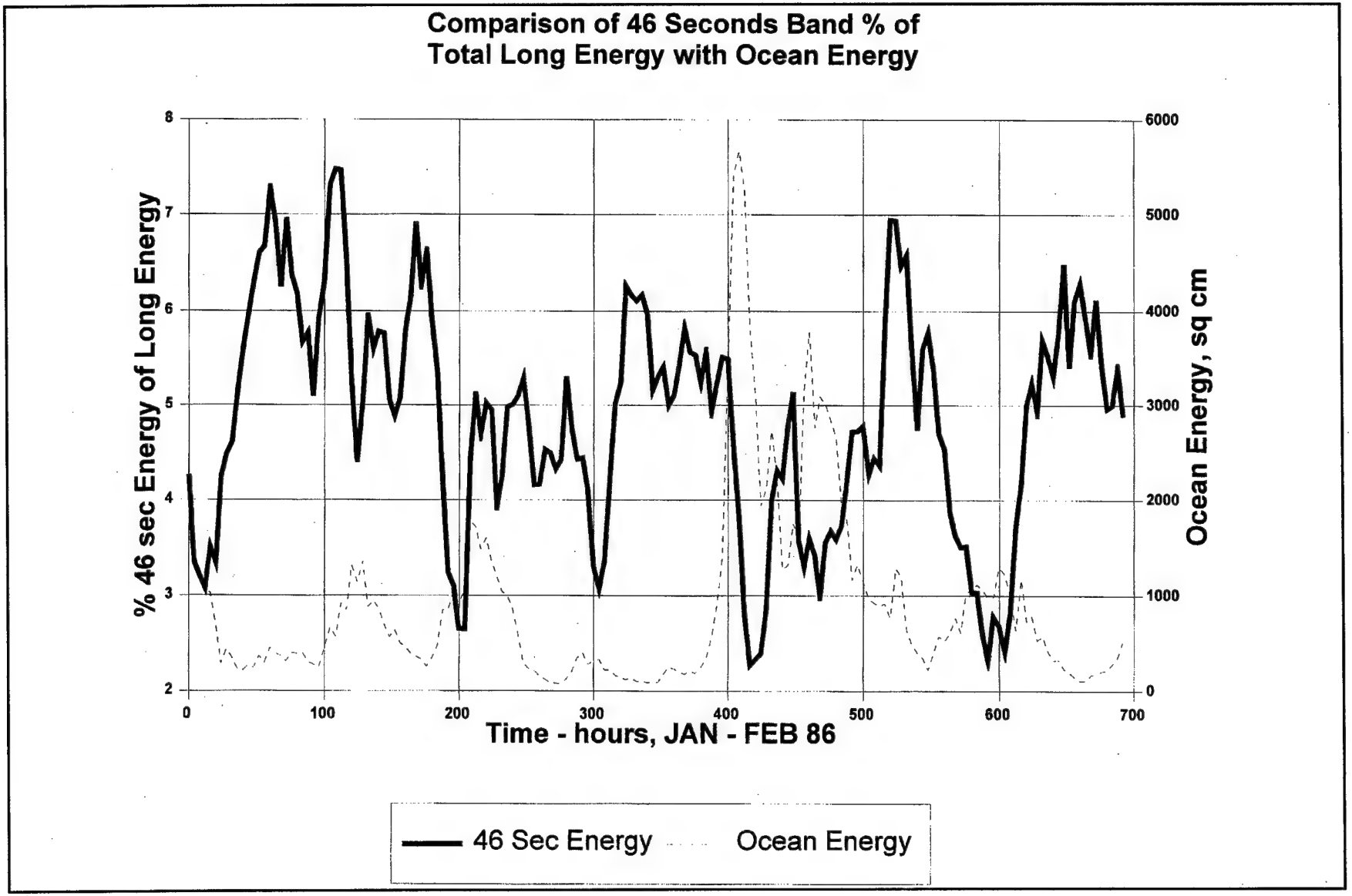
Comparison of 46 Seconds Band % of
Total Long Energy with Ocean Energy
% 46 sec Energy of Long Energy
Ocean Energy, sq cm
Time - hours, JAN - FEB 86
8
7
6
5
4
3
2
6000
5000
4000
3000
2000
1000
0
0
100
200
300
400
500
600
700
46 Sec Energy
Ocean Energy

Plate 49

Plate 50

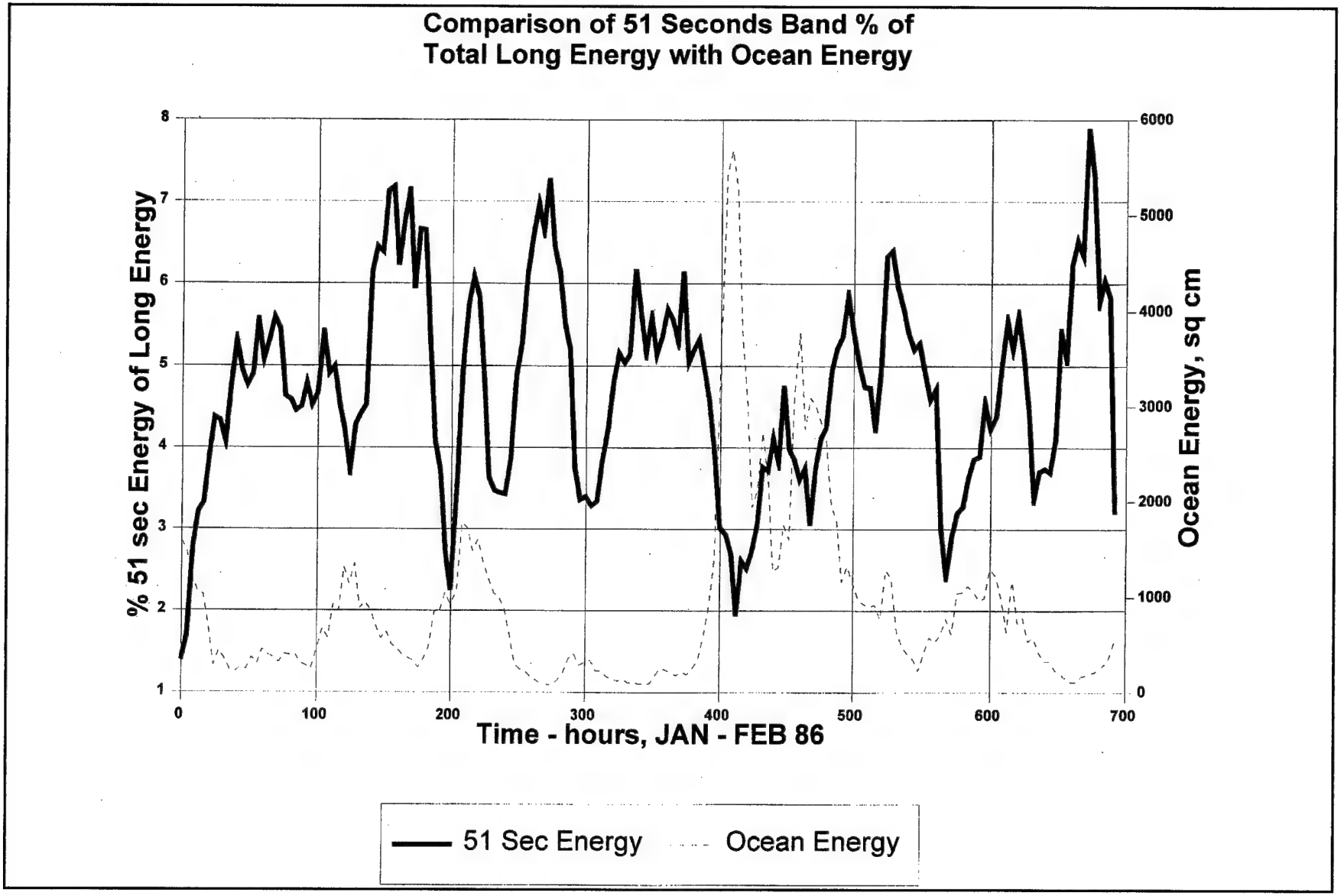
Comparison of 51 Seconds Band % of
Total Long Energy with Ocean Energy
% 51 sec Energy of Long Energy
Ocean Energy, sq cm
Time - hours, JAN - FEB 86
51 Sec Energy
Ocean Energy
1
2
3
4
5
6
7
8
0
1000
2000
3000
4000
5000
6000
0
100
200
300
400
500
600
700

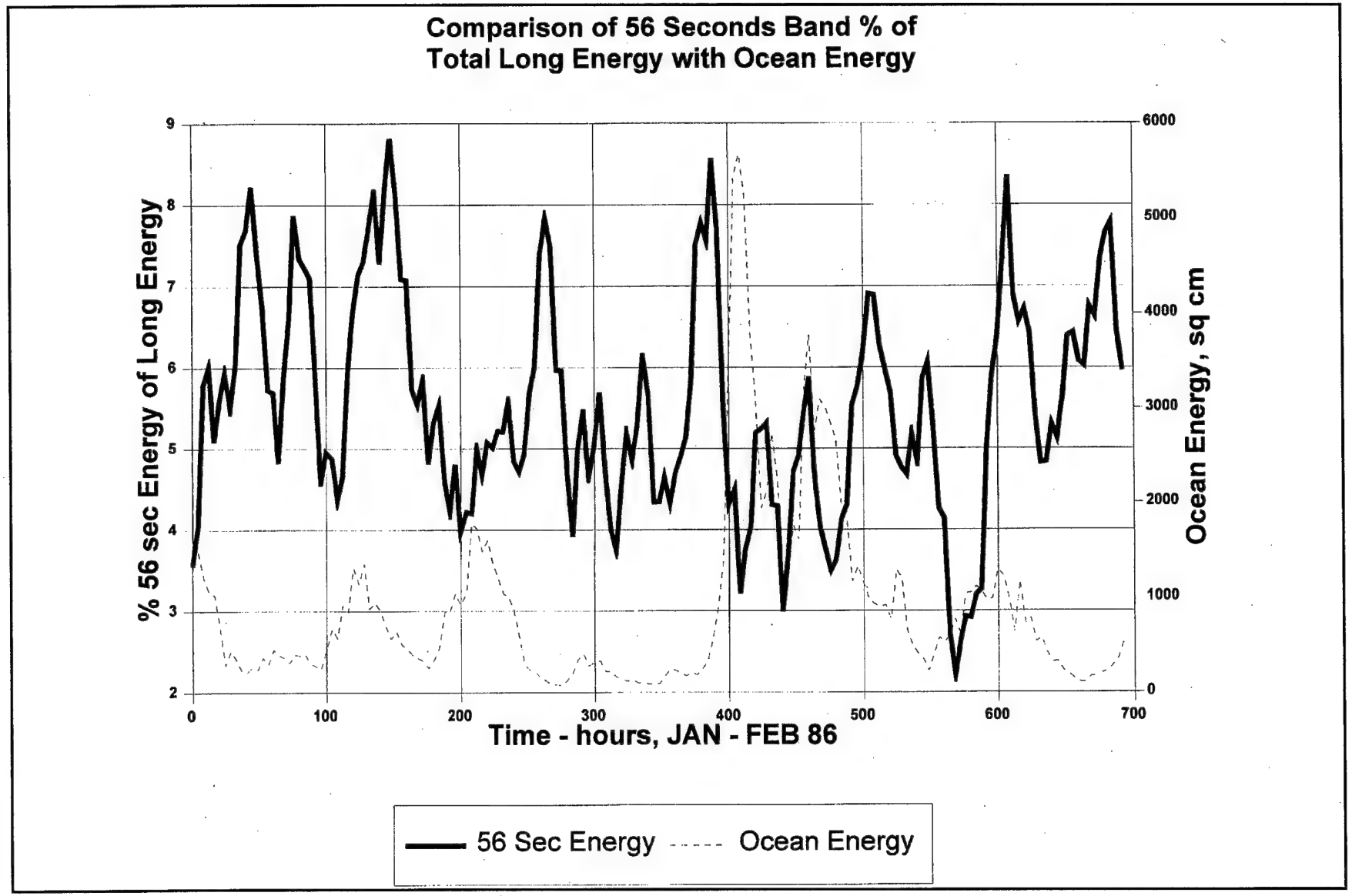
Comparison of 56 Seconds Band % of
Total Long Energy with Ocean Energy
% 56 sec Energy of Long Energy
Ocean Energy, sq cm
Time - hours, JAN - FEB 86
9
8
7
6
5
4
3
2
6000
5000
4000
3000
2000
1000
0
0
100
200
300
400
500
600
700
56 Sec Energy
Ocean Energy

Plate 51

Plate 52

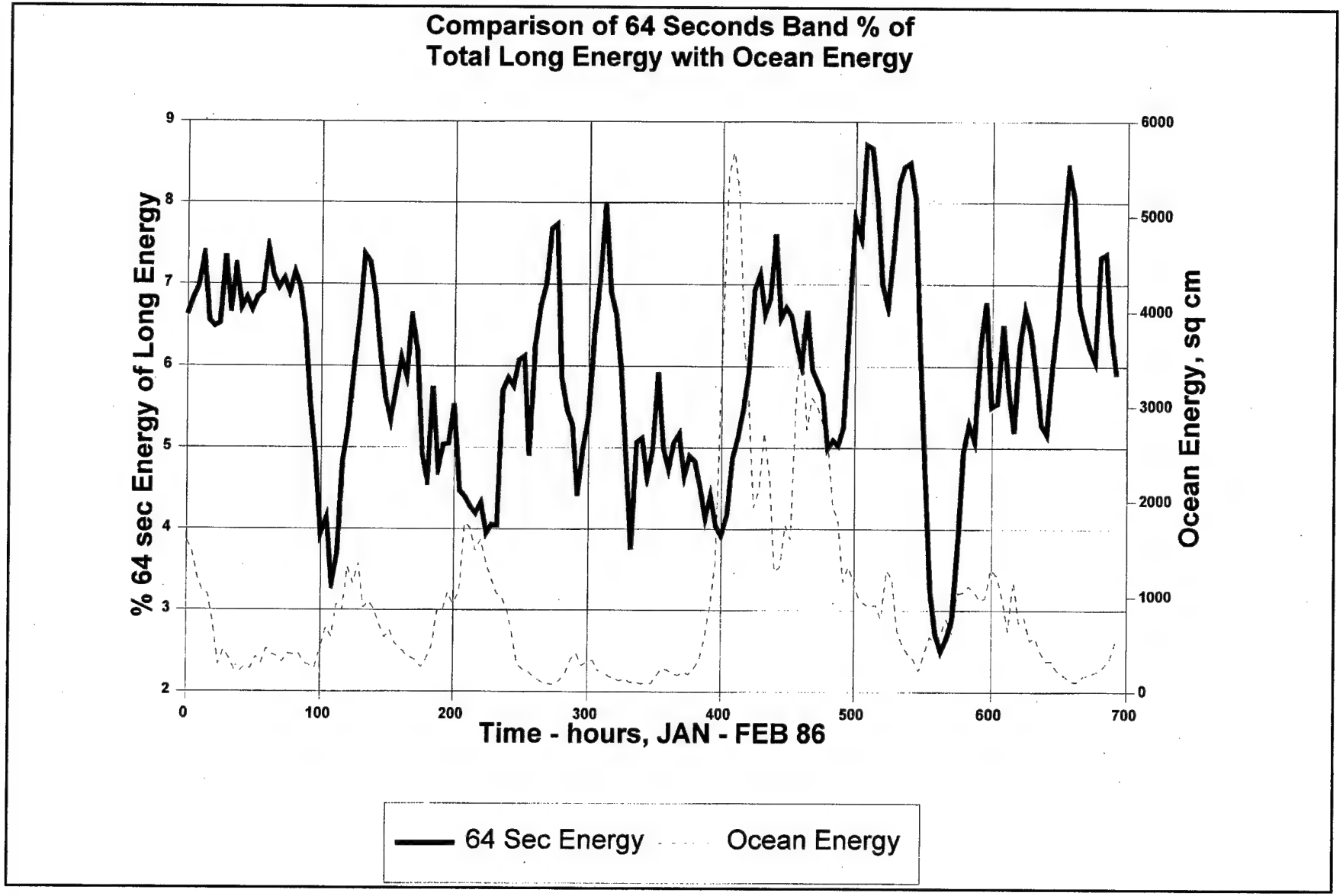
Comparison of 64 Seconds Band % of
Total Long Energy with Ocean Energy
% 64 sec Energy of Long Energy
Ocean Energy, sq cm
Time - hours, JAN - FEB 86
9
8
7
6
5
4
3
2
6000
5000
4000
3000
2000
1000
0
0
100
200
300
400
500
600
700
64 Sec Energy
Ocean Energy

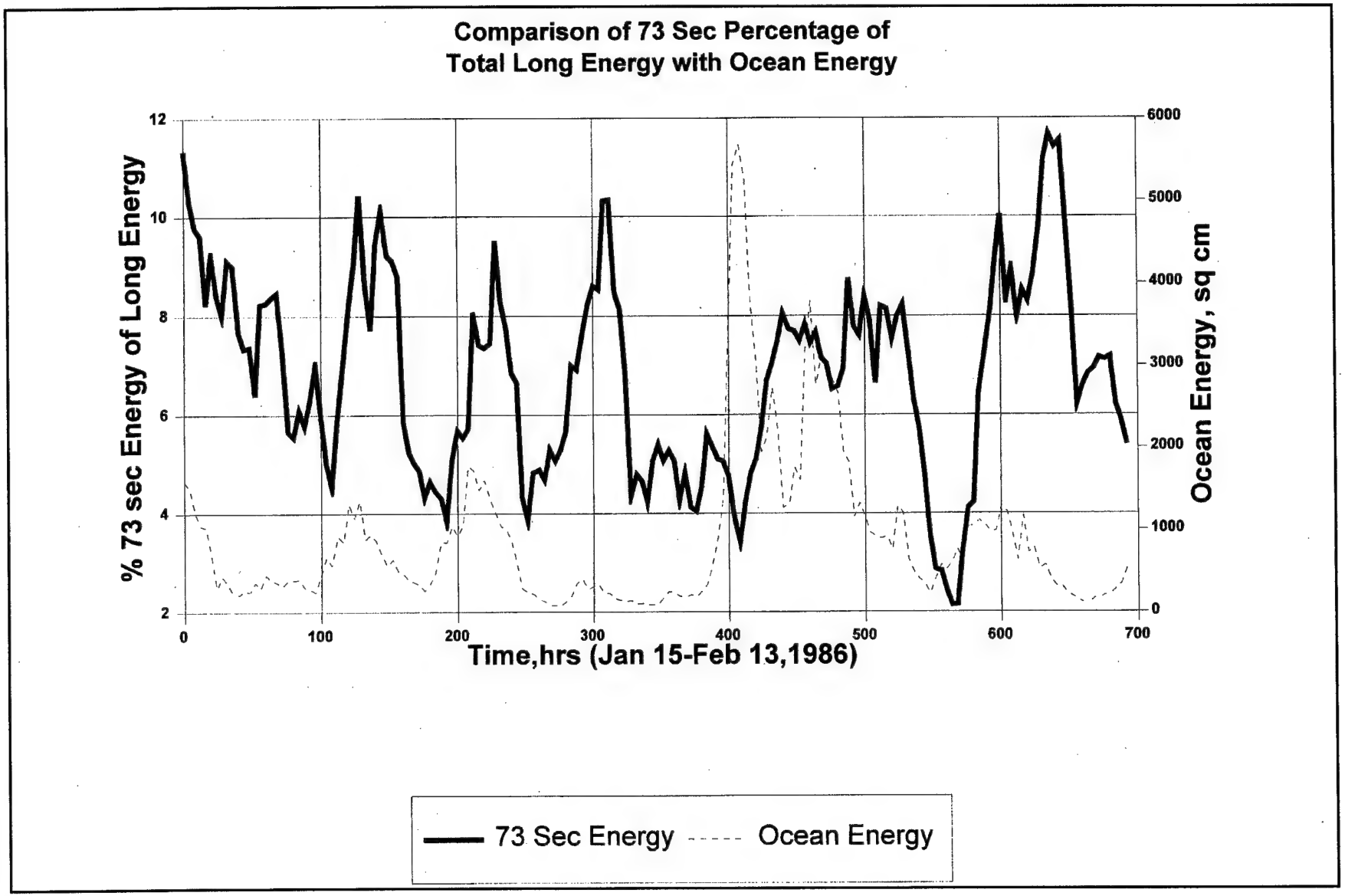
Comparison of 73 Sec Percentage of
Total Long Energy with Ocean Energy
% 73 sec Energy of Long Energy
Ocean Energy, sq cm
Time,hrs (Jan 15-Feb 13,1986)
12
10
8
6
4
2
6000
5000
4000
3000
2000
1000
0
0
100
200
300
400
500
600
700
73 Sec Energy
Ocean Energy

Plate 53

Plate 54

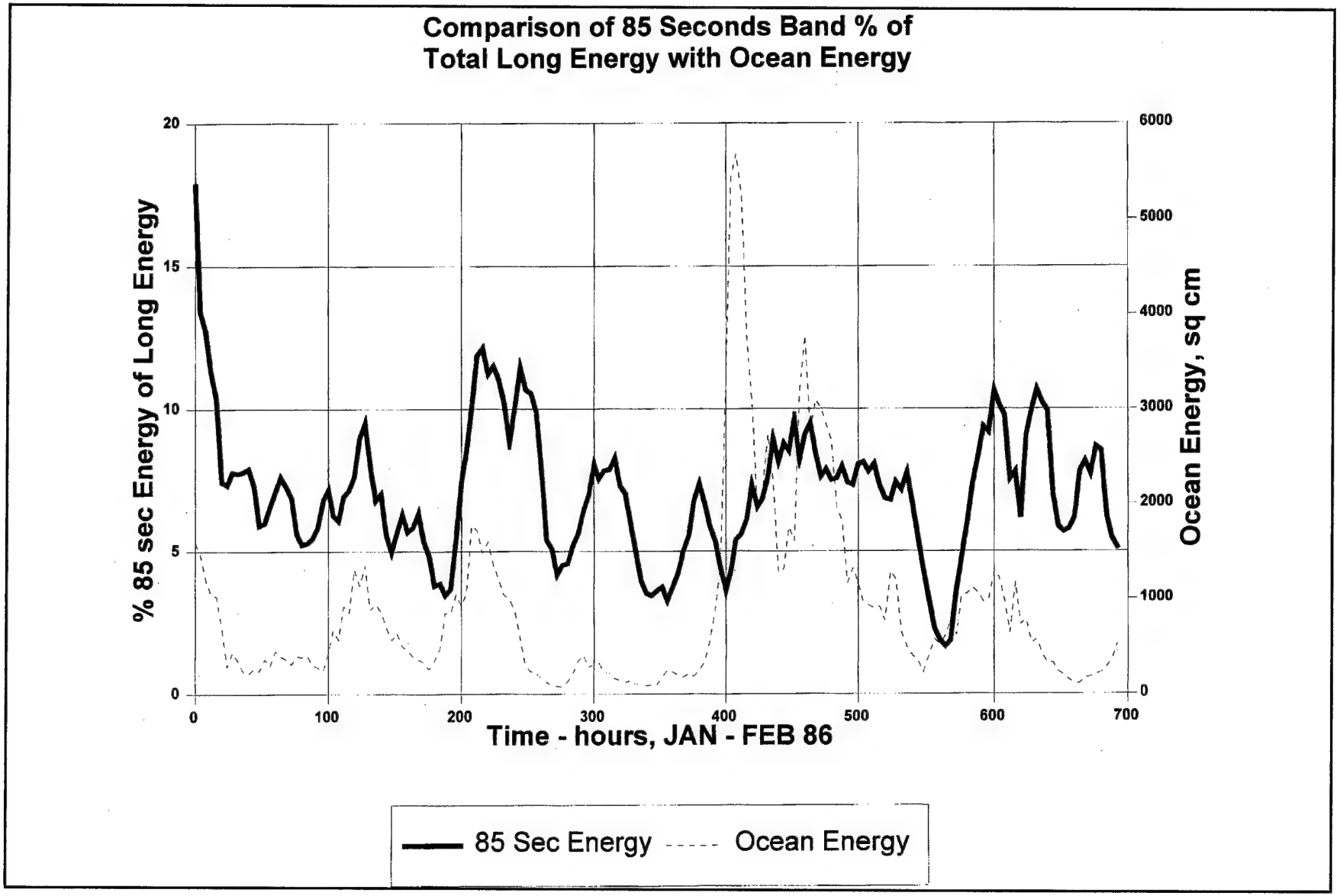
Comparison of 85 Seconds Band % of
Total Long Energy with Ocean Energy
% 85 sec Energy of Long Energy
Ocean Energy, sq cm
Time - hours, JAN - FEB 86
0
5
10
15
20
0
1000
2000
3000
4000
5000
6000
0
100
200
300
400
500
600
700
85 Sec Energy
Ocean Energy

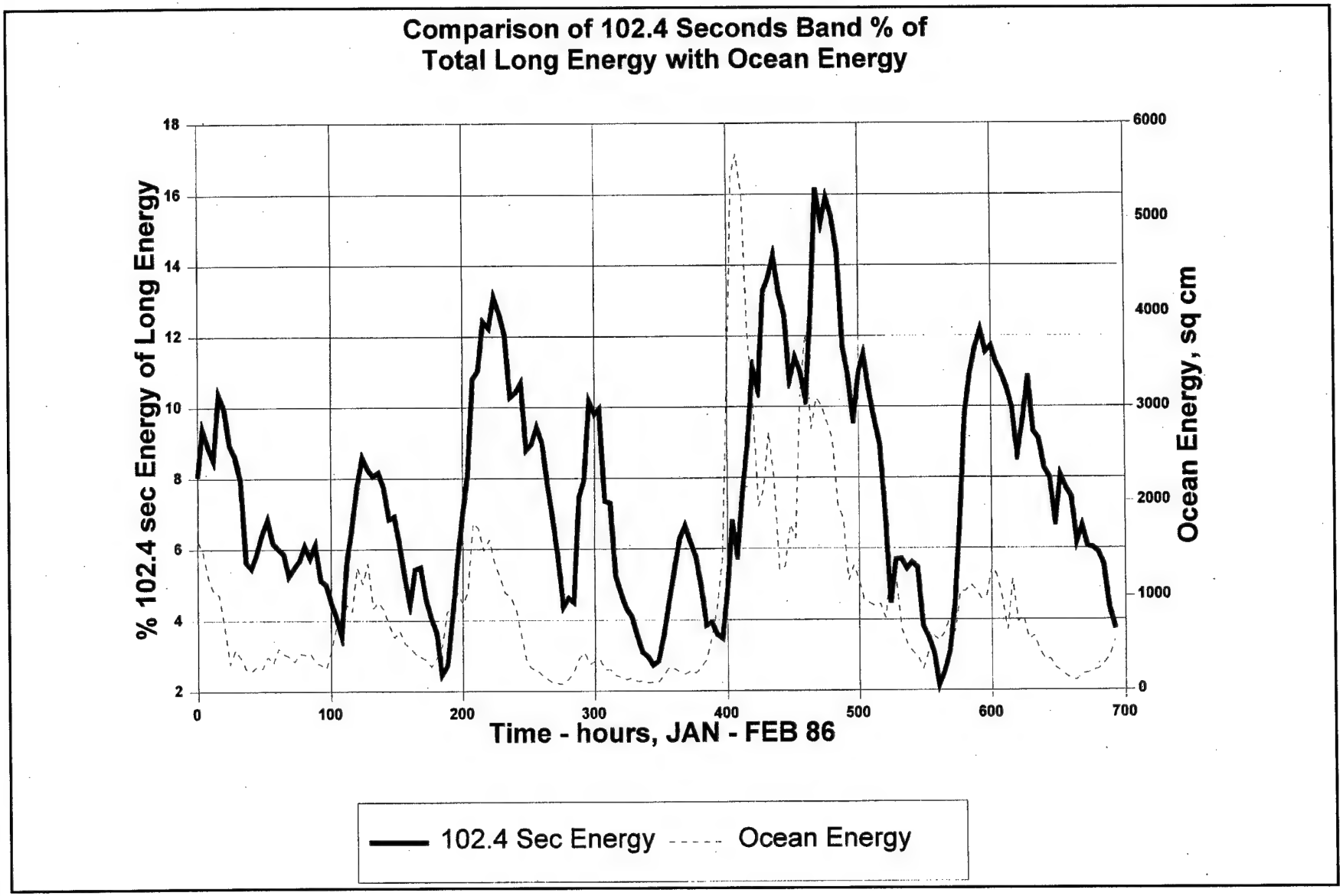
Comparison of 102.4 Seconds Band % of
Total Long Energy with Ocean Energy
% 102.4 sec Energy of Long Energy
Ocean Energy, sq cm
Time - hours, JAN - FEB 86
18
16
14
12
10
8
6
4
2
6000
5000
4000
3000
2000
1000
0
0
100
200
300
400
500
600
700
102.4 Sec Energy
Ocean Energy

Plate 55

Plate 56

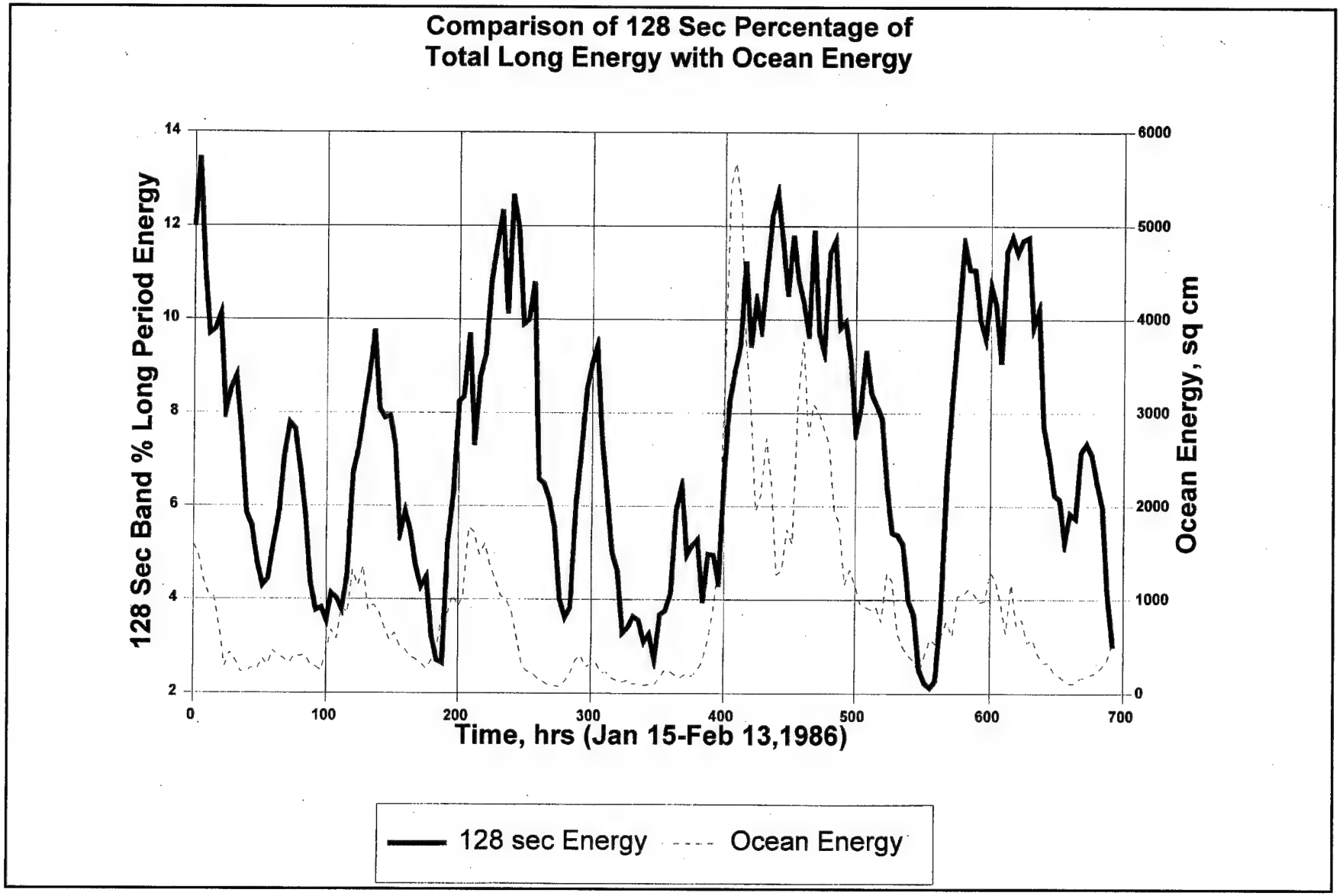
Comparison of 128 Sec Percentage of
Total Long Energy with Ocean Energy
128 Sec Band % Long Period Energy
Ocean Energy, sq cm
Time, hrs (Jan 15-Feb 13,1986)
0
100
200
300
400
500
600
700
2
4
6
8
10
12
14
0
1000
2000
3000
4000
5000
6000
128 sec Energy
Ocean Energy

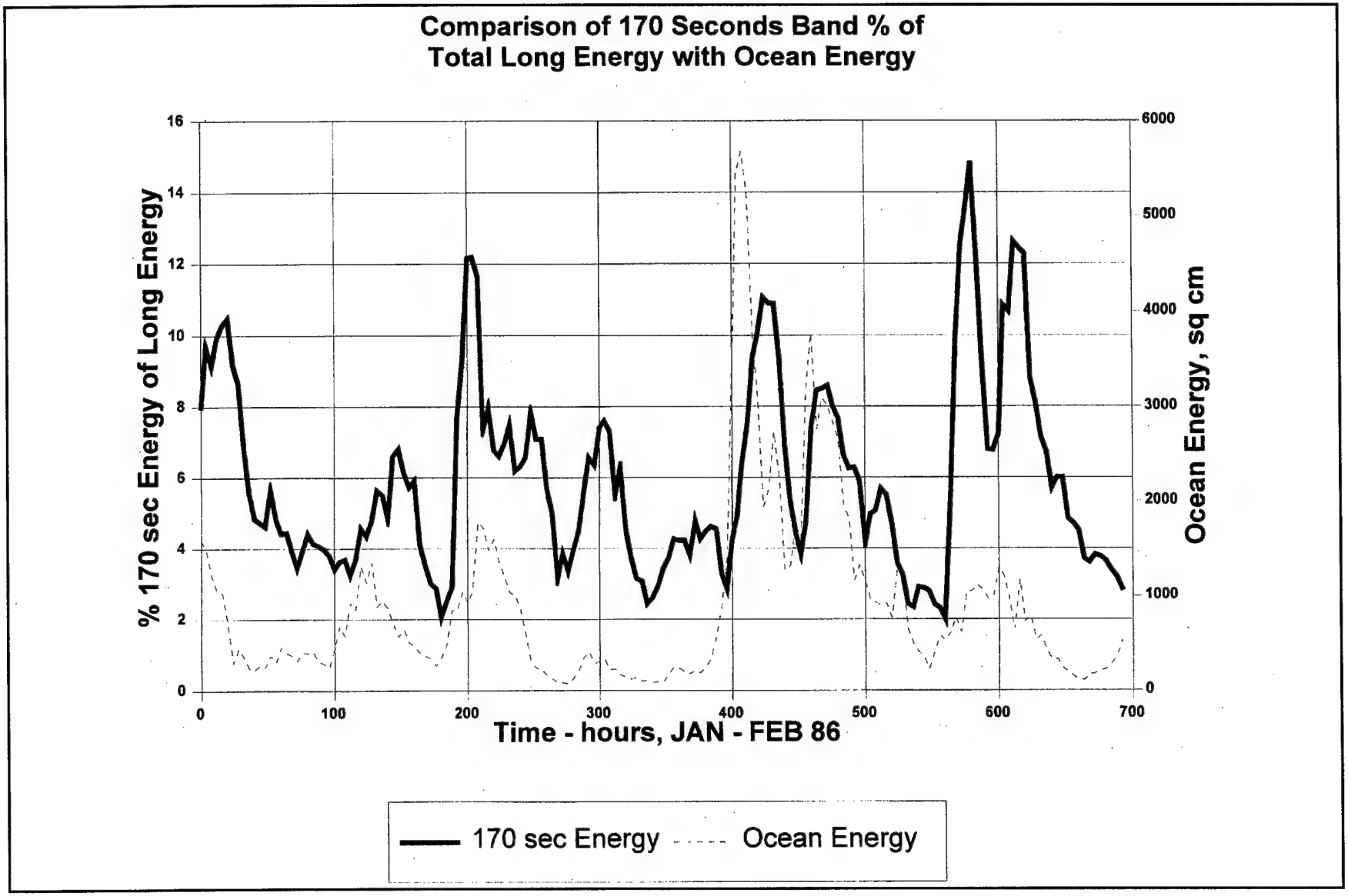
Comparison of 170 Seconds Band % of
Total Long Energy with Ocean Energy
% 170 sec Energy of Long Energy
Ocean Energy, sq cm
Time - hours, JAN - FEB 86
0
2
4
6
8
10
12
14
16
0
1000
2000
3000
4000
5000
6000
0
100
200
300
400
500
600
700
170 sec Energy
Ocean Energy

Plate 57

Plate 58

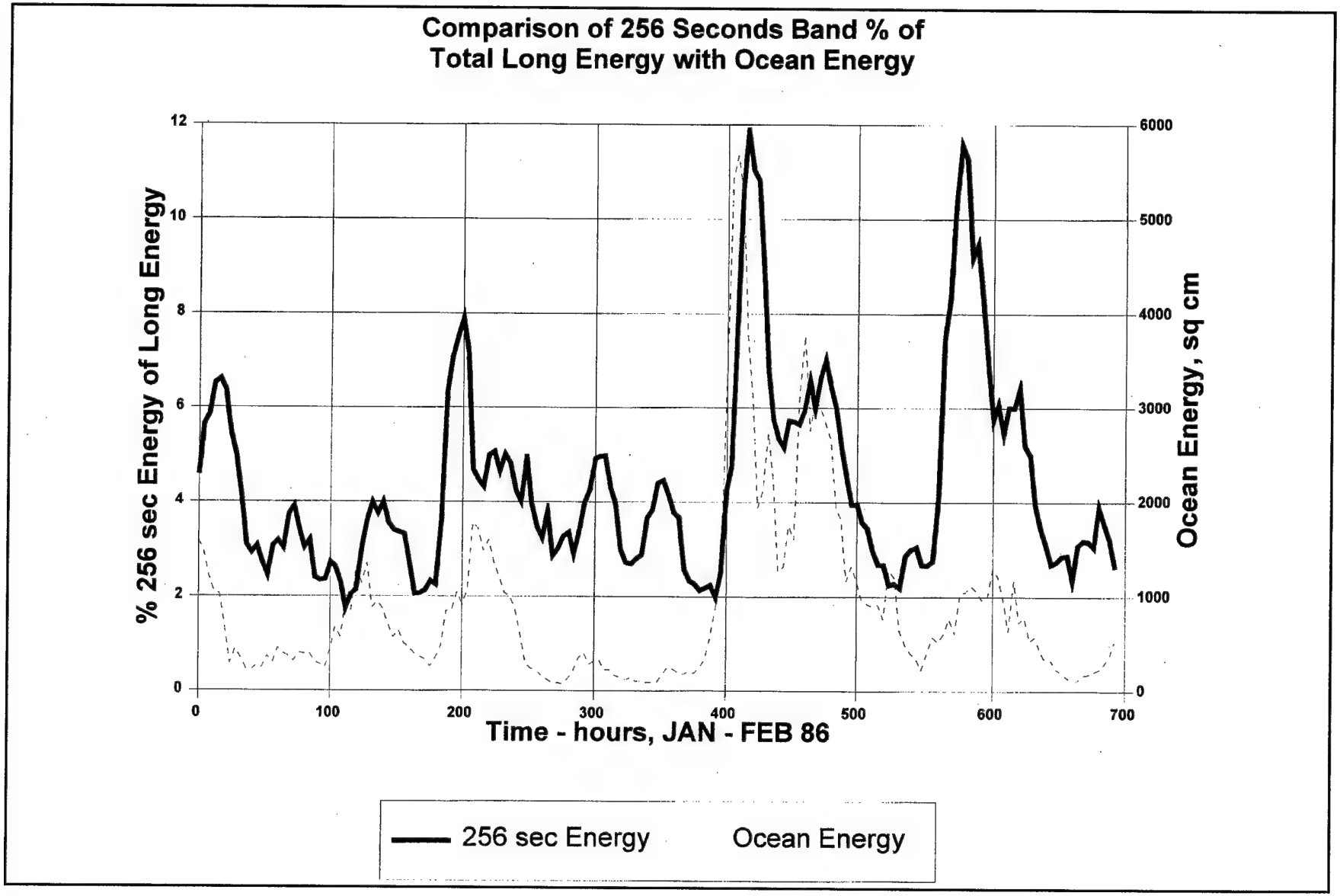
Comparison of 256 Seconds Band % of
Total Long Energy with Ocean Energy
% 256 sec Energy of Long Energy
Ocean Energy, sq cm
Time - hours, JAN - FEB 86
0
2
4
6
8
10
12
0
1000
2000
3000
4000
5000
6000
0
100
200
300
400
500
600
700
256 sec Energy
Ocean Energy

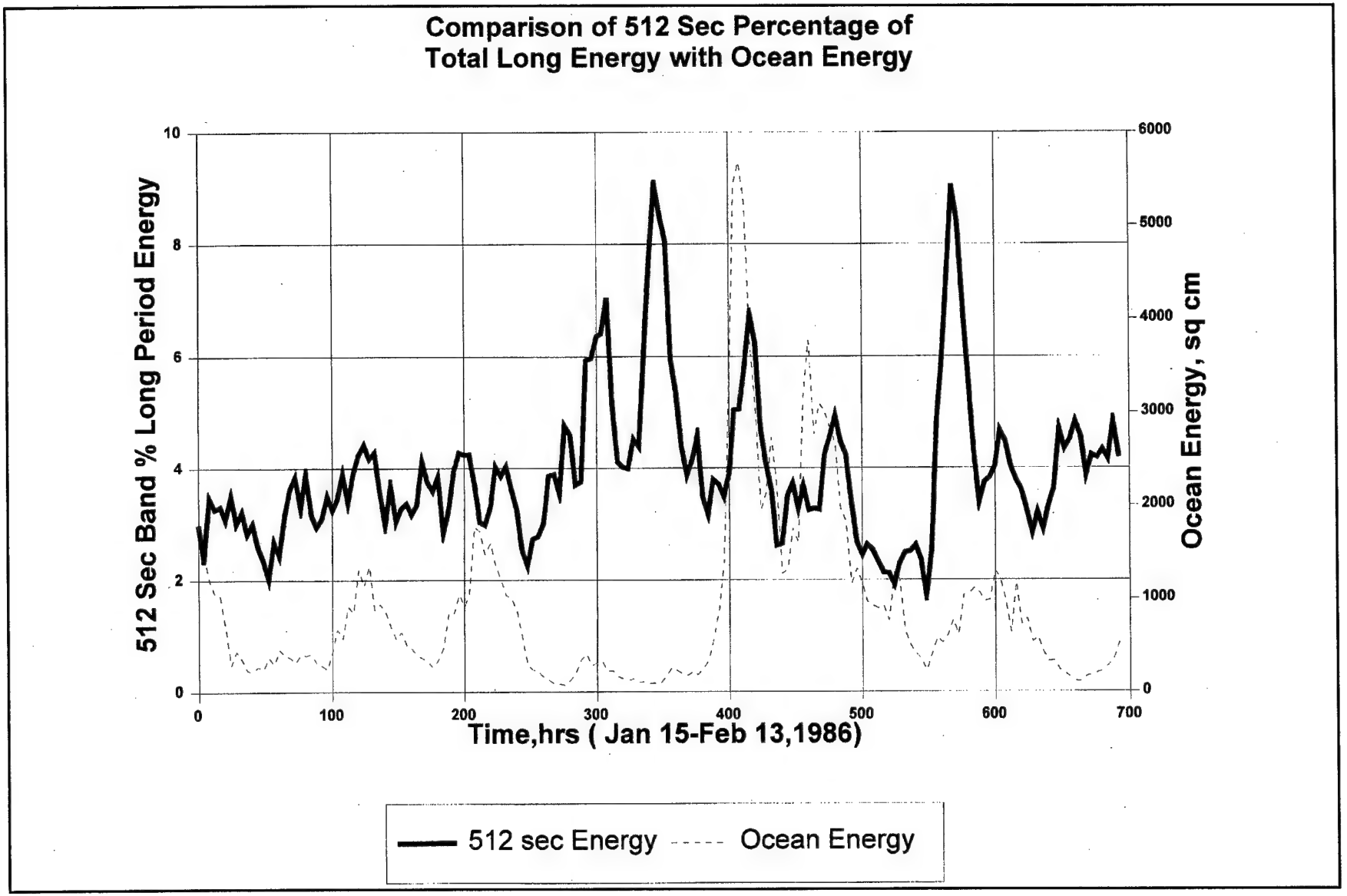
Comparison of 512 Sec Percentage of
Total Long Energy with Ocean Energy
512 Sec Band % Long Period Energy
Ocean Energy, sq cm
Time,hrs (Jan 15-Feb 13,1986)
0
2
4
6
8
10
0
1000
2000
3000
4000
5000
6000
0
100
200
300
400
500
600
700
512 sec Energy
Ocean Energy

Plate 59

Plate 60

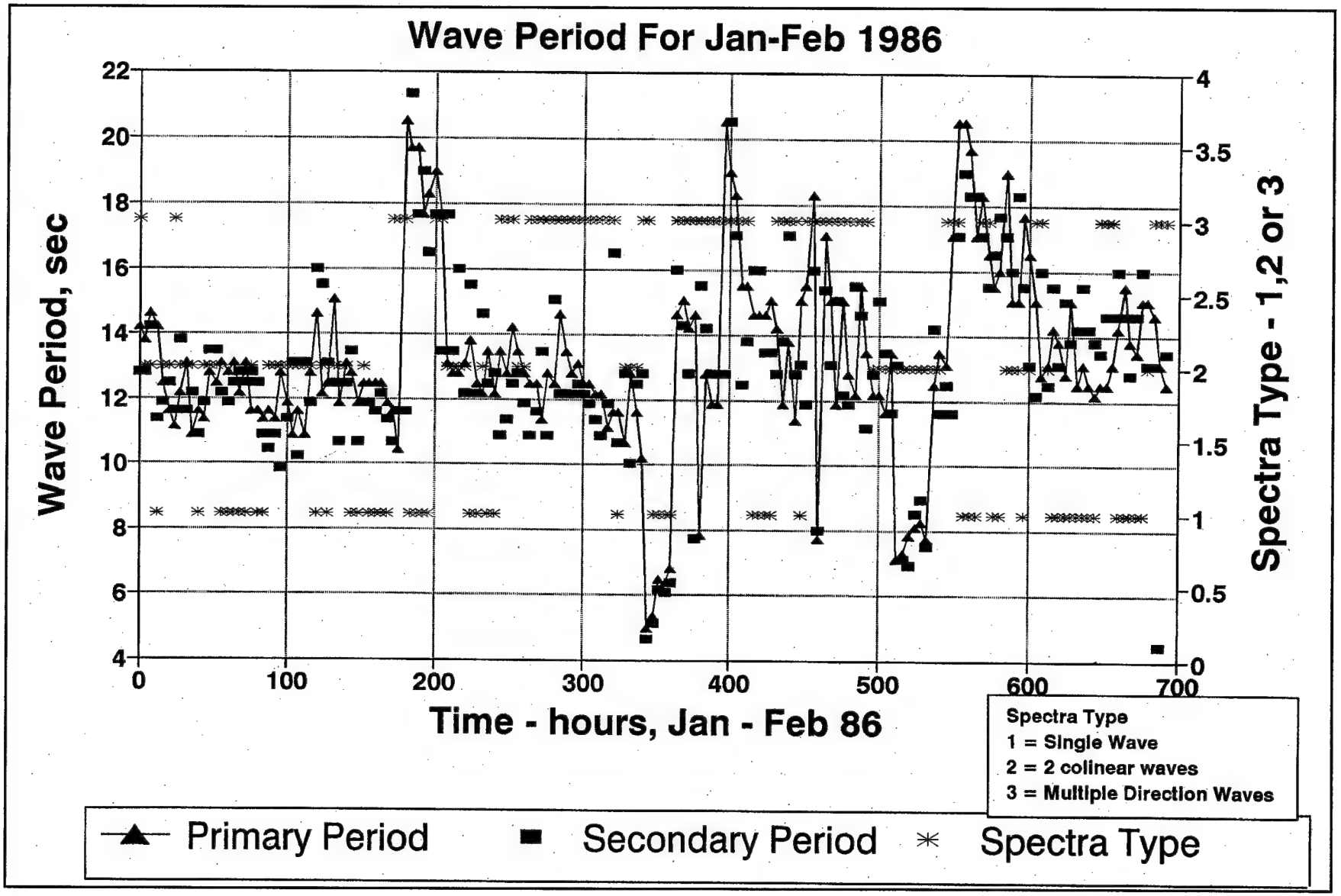
Wave Period For Jan-Feb 1986
Wave Period, sec
Spectra Type - 1,2 or 3
Time - hours, Jan - Feb 86
22
20
18
16
14
12
10
8
6
4
4
3.5
3
2.5
2
1.5
1
0.5
0
0
100
200
300
400
500
600
700
Spectra Type
1 = Single Wave
2 = 2 colinear waves
3 = Multiple Direction Waves
Primary Period
Secondary Period
Spectra Type

87-11-

SHIP MOVEMENT & SURGE RECORD

SHEET 1 OF 1

AGENCY APL

BERTH 126 DATE (FIRST DAY) 11-12-87

SHIP NAME Pres. Washington

DATE & TIME ARRIVED 11-12-87

DATE & TIME DEPARTED AT DOCK

TYPE OF CARGO (CIRCLE ONE)
1. CONTAINERS 3. WET BULK
2. BREAK BULK 4. DRY BULK

DRAFT 36 FT/M. FWD 36 FT/M. AFT

DRAFT ____ FT/M. FWD ____ FT/M. AFT

MOORING CONFIGURATION (CIRCLE ONE)

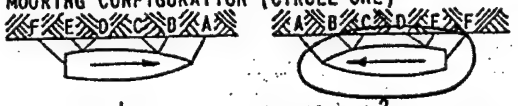

1. 2. 3.

OTHER
SHOW SHIP HEAD WITH ARROW

	LINES	TYPE, NO. & DIAM. (IN.) PLASTIC	MANILA	STEEL	OTHER	NOTE IF LINES ARE— SLACK	TIGHT	HEAVY STRAIN
FWD	A) BOW		13"				✓	
FWD	B) BREAST		2 "				✓	
FWD	C) SPRING		1 "				✓	
AFT	D) SPRING		1 "				✓	
AFT	E) BREAST		1 "				✓	
AFT	F) STERN		1 "				✓	

	SURGE RECORD	00-04	04-08	08-12	12-16	16-20	20-24
1ST DAY	TIME				2pm		
1ST DAY	SURGE & MOVEMENT SYMBOLS				None		
2ND DAY	TIME						
2ND DAY	SURGE & MOVEMENT SYMBOLS						
3RD DAY	TIME						
3RD DAY	SURGE & MOVEMENT SYMBOLS						
4TH DAY	TIME						
4TH DAY	SURGE & MOVEMENT SYMBOLS						

SURGE & MOVEMENT SYMBOLS:

DEGREE OF SURGE: L=LIGHT M=MEDIUM H=HEAVY

TYPE OF MOVEMENT (LIST MAIN TYPE FIRST):
A= LONGITUDINAL (FORE & AFT) B= TRANSVERSE (SIDEWAYS)
C= VERTICAL (UP & DOWN) D= FISHTAIL E= ROLL

CARGO HANDLING DELAYS DUE TO SURGE: CIRCLE ONE AND NOTE DATE & TIME
DIFFICULTIES: (1) NONE 2) SOME 3) CONSIDERABLE 4) STOPPED WORK

REMARKS: UNUSUAL CONDITIONS OR DIFFICULTIES OBSERVED: DAMAGE TO SHIP LINES, AND/OR WHARF, AND SEVERITY: SIGNIFICANT CHANGES IN MOORING CONFIGURATION:
NOTE DATE & TIME:
11-12-87 1400 Hr - ocean calm

	1 ST DAY	2 ND DAY	3 RD DAY	4 TH DAY
0-8		0-8	0-8	0-8
8-16		8-16	8-16	8-16
16-24		16-24	16-24	16-24

SIGNATURES

PORT OF LOS ANGELES
APL WHARFINGER
SAN PEDRO, CALIF.

NOV 12 1987

SAN PEDRO OFFICE
HARBOR/CONSTRUCTION SECTION
PORT OF LOS ANGELES

NOV 13 1987

RECEIVED

SPL FORM FEB 71 578

Ship movement and surge record DISPATCHED

Plate 61

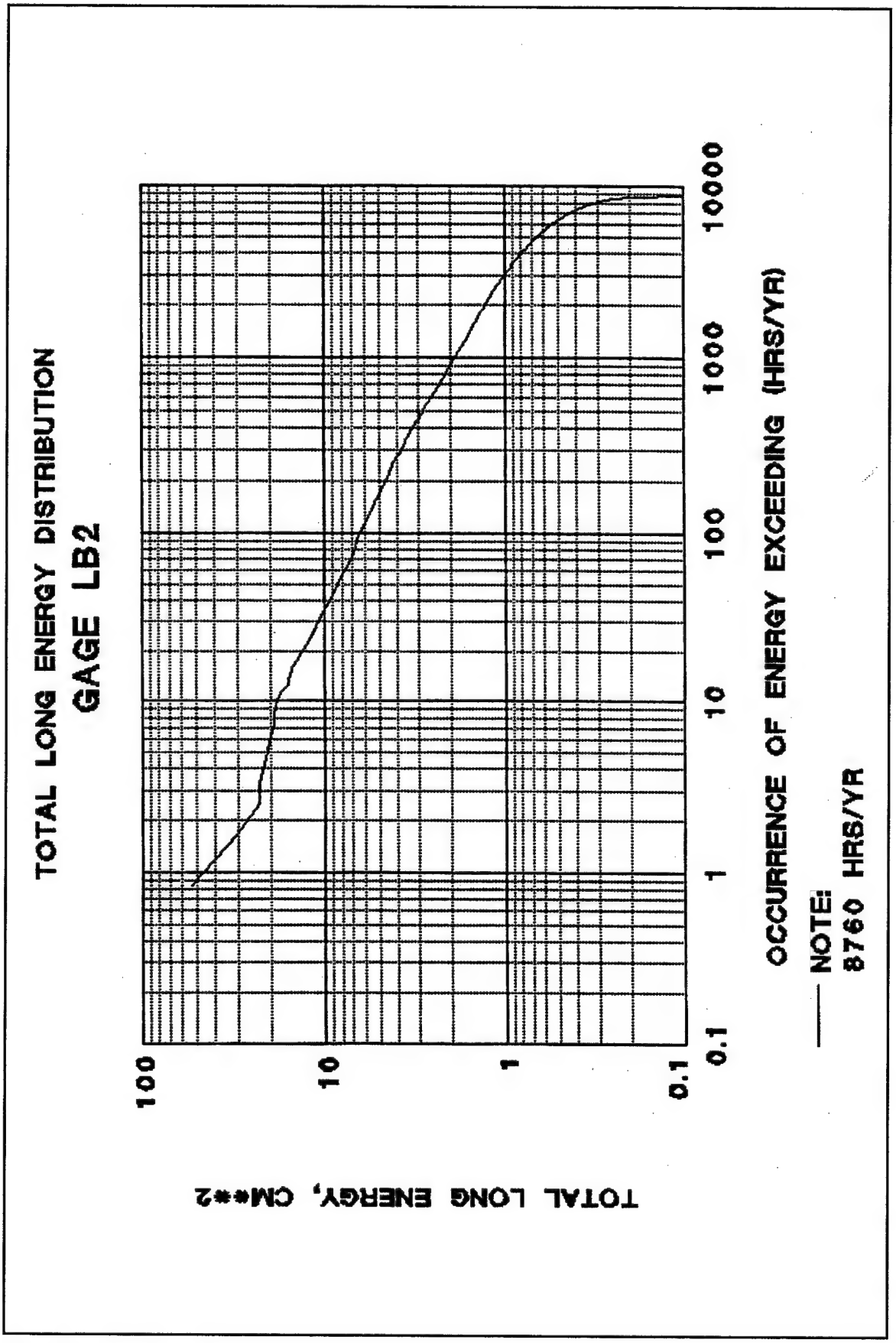
TOTAL LONG ENERGY DISTRIBUTION
GAGE LB2
TOTAL LONG ENERGY, CM**2
100
10
1
0.1
0.1
1
10
100
1000
10000
OCCURRENCE OF ENERGY EXCEEDING (HRS/YR)
NOTE:
8760 HRS/YR

Plate 62

1984-86 Moored Container Ship Movement Observations

BERTH 245

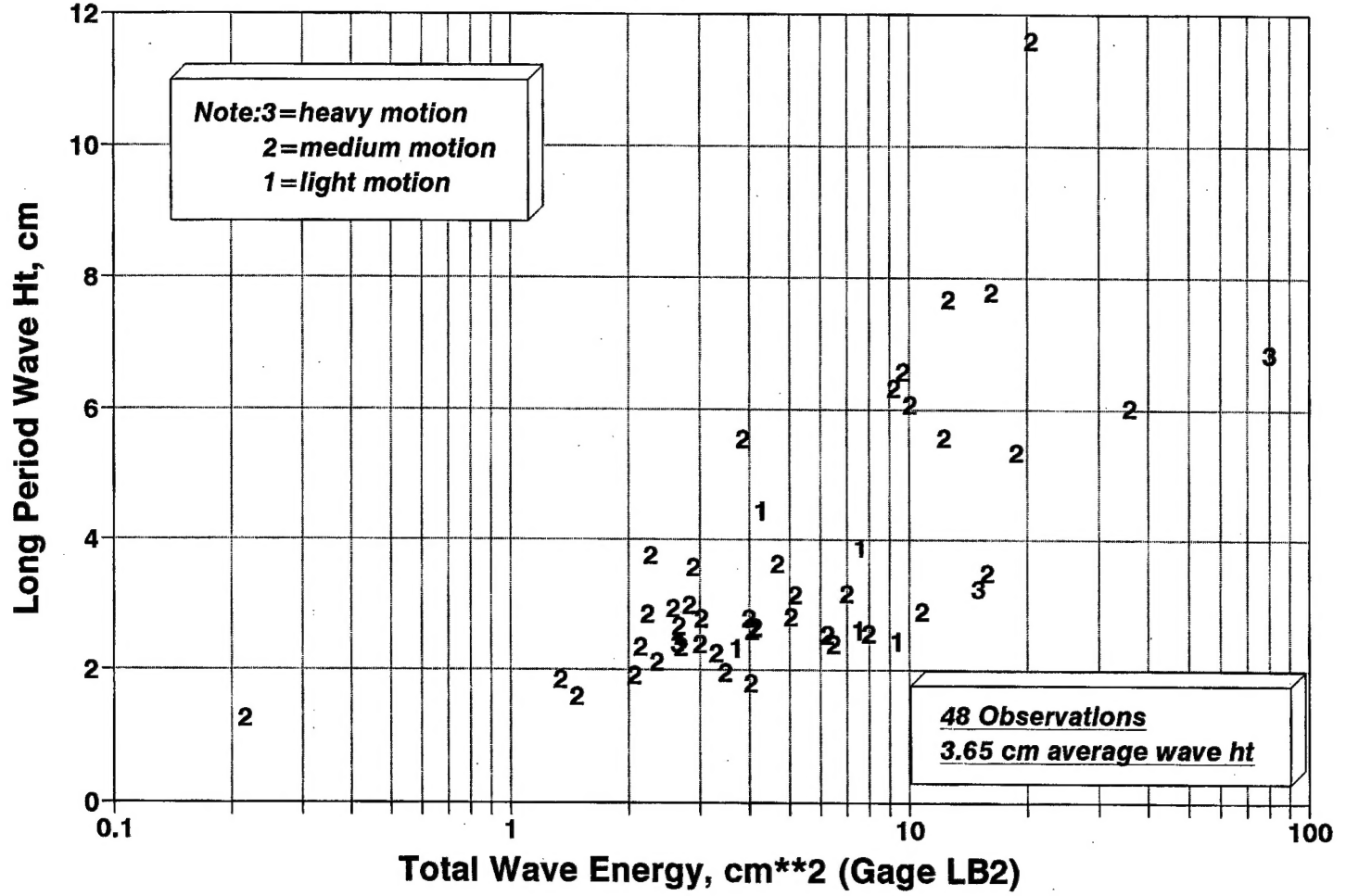

Note: Long Period Wave Height Based On Energy In 41-205 sec Wave Period Range

Plate 63

Plate 64

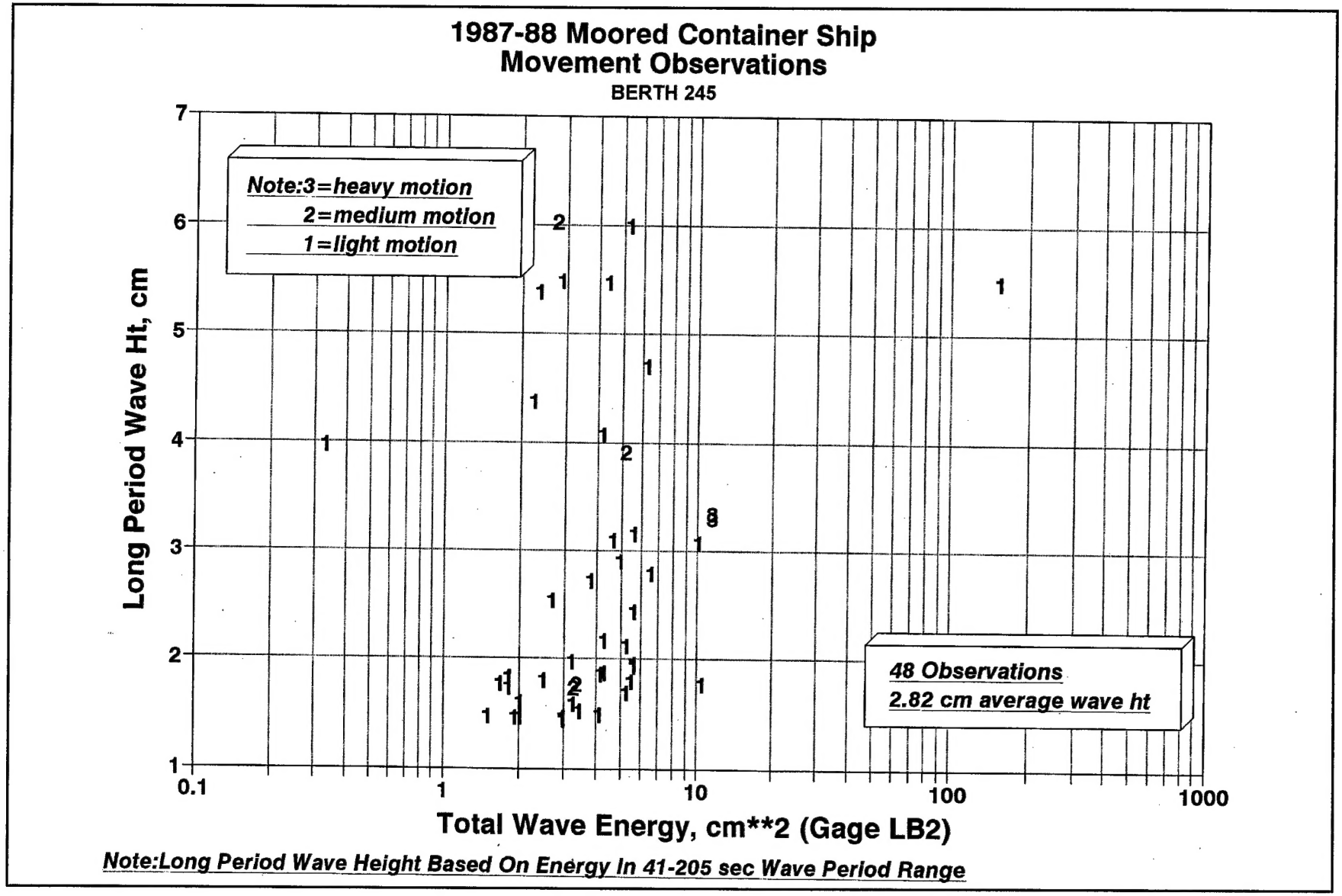
1987-88 Moored Container Ship
Movement Observations
BERTH 245
Note:3=heavy motion
2=medium motion
1=light motion
48 Observations
2.82 cm average wave ht
Long Period Wave Ht, cm
Total Wave Energy, cm**2 (Gage LB2)
0.1
1
10
100
1000
1
2
3
4
5
6
7
Note:Long Period Wave Height Based On Energy In 41-205 sec Wave Period Range

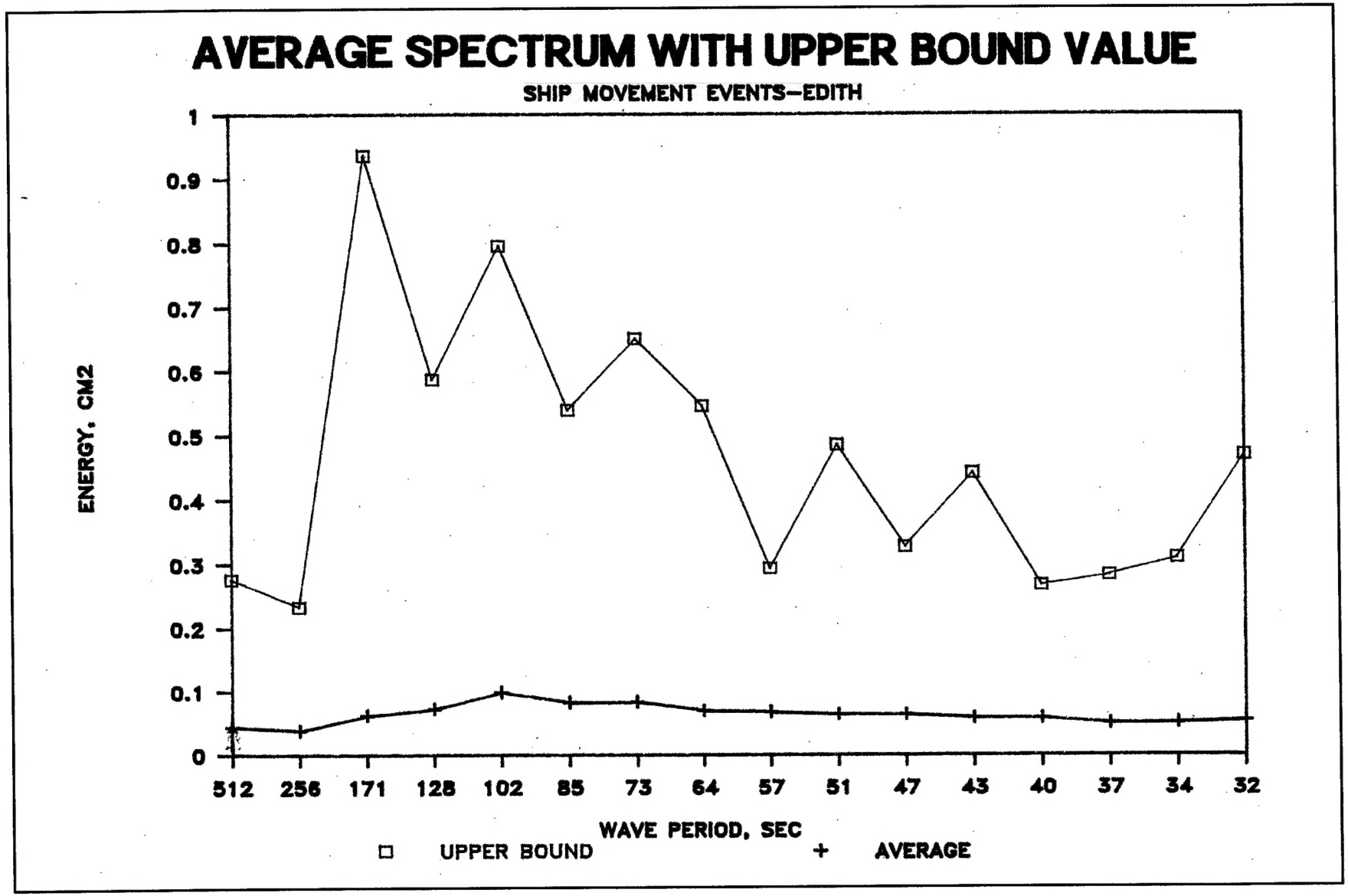
AVERAGE SPECTRUM WITH UPPER BOUND VALUE
SHIP MOVEMENT EVENTS--EDITH
ENERGY, CM2
1
0.9
0.8
0.7
0.6
0.5
0.4
0.3
0.2
0.1
0
512
256
171
128
102
85
73
64
57
51
47
43
40
37
34
32
WAVE PERIOD, SEC
UPPER BOUND
AVERAGE

Plate 65

REPORT DOCUMENTATION PAGE

Form Approved
OMB No. 0704-0188

1. AGENCY USE ONLY *(Leave blank)*	2. REPORT DATE	3. REPORT TYPE AND DATES COVERED
	October 1999	Final report

4. TITLE AND SUBTITLE
Los Angeles and Long Beach Harbors Model Enhancement Program: Long Waves and Harbor Resonance Analysis

5. FUNDING NUMBERS

6. AUTHOR(S)
William C. Seabergh, Leonette J. Thomas

7. PERFORMING ORGANIZATION NAME(S) AND ADDRESS(ES)
U.S. Army Engineer Research and Development Center
Waterways Experiment Station
3909 Halls Ferry Road, Vicksburg, MS 39180-6199

8. PERFORMING ORGANIZATION REPORT NUMBER
Technical Report CHL-99-20

9. SPONSORING/MONITORING AGENCY NAME(S) AND ADDRESS(ES)
U.S. Army Engineer District, Los Angeles, P.O. Box 2711, Los Angeles, CA 90053-2325; Port of Los Angeles, San Pedro, CA 90733-0151; Port of Long Beach, Long Beach, CA 90801-0570

10. SPONSORING/MONITORING AGENCY REPORT NUMBER

11. SUPPLEMENTARY NOTES

12a. DISTRIBUTION/AVAILABILITY STATEMENT
Approved for public release; distribution is unlimited.

12b. DISTRIBUTION CODE

13. ABSTRACT ***(Maximum 200 words)***

Long-period wave data have been collected at an offshore wave gauge and seven harbor gauges for over 8 years in the Los Angeles/Long Beach Harbor region. These data are being used in studies for the design of expansion of the harbors. In particular, the data have been used to select long-period spectra for reproduction in a physical model of the harbors. The analysis of prototype wave data indicated correlation between the long-wave spectrum and the short-wave spectrum. Information was examined to determine the effect of the source of the short-period waves (Southern Hemisphere swell, hurricanes, or winter storms, typically from the west) on the nature of the long-period component of the waves. Relationships between the origin of the wave energy and long-wave period were determined. Wave statistics were used to interpret effects of the energy level on the wave transformation into the harbors and correlate long-wave and short-wave spectra. Examination of a 5- to 22-sec short-wave period and a 30- to 400-sec long-wave period indicated correlation of smaller short-wave periods with smaller long-wave periods, and larger short-wave periods with larger long-wave periods. Observations of moored-ship motion level was correlated to long-wave energy in a harbor basin.

14. SUBJECT TERMS
Harbor resonance
Long Beach Harbor
Long waves
Los Angeles Harbor
Moored ship motion
Seiching

15. NUMBER OF PAGES
131

16. PRICE CODE

17. SECURITY CLASSIFICATION OF REPORT	18. SECURITY CLASSIFICATION OF THIS PAGE	19. SECURITY CLASSIFICATION OF ABSTRACT	20. LIMITATION OF ABSTRACT
UNCLASSIFIED	UNCLASSIFIED		